

**The University of
Nottingham**

**Receptors for the Extraction of the
Hexachloroplatinate Anion**

GEORGE GREEN LIBRARY OF
SCIENCE AND ENGINEERING

Katherine Jane Bell, MSci

Thesis submitted to the University of Nottingham for the
degree of Doctor of Philosophy

April 2008

BEST COPY

AVAILABLE

Variable print quality

Declaration

Except where specific reference has been made to other sources, the work presented in this thesis is the original work of the author. It has not been submitted, in whole or in part, for any other degree.

Signed:  Katherine J. Bell

Date: 22/09/2008

Acknowledgements

I would like to thank the following people:

- Firstly my supervisor, Professor Martin Schröder, for giving me the opportunity to work in his group and for his advice and support.
- Professor Peter Tasker and Dr Arjan Westra at the University of Edinburgh for their opinions and advice on setting up the solvent extractions in Nottingham.
- Dr Claire Wilson and Professor Sandy Blake for their assistance and patience with the crystallographic analyses presented in this work.
- Dr Rebecca Warr for her help in the lab, assistance with the extraction studies and proof-reading of this thesis.
- The undergraduate project students that have worked on this project especially Dan Rawson and Natasha Birkin.
- Professor Antonio Bianchi at the University of Florence for performing the potentiometry experiments presented in this work.
- Dr Scott Young in the School of Environmental Sciences at the University of Nottingham for ICP-MS. Shaz Aslam for recording the ^{195}Pt NMR spectra. Tony and Graham for their assistance with the mass spectrometry experiments. Tong Lui and Stephen Boyer for elemental analysis.
- I would also like to thank all the members of the Schröder group, past and present for making my time in Nottingham memorable. Finally, I would like to thank my family for their love and support.

Declaration.....	i
Acknowledgements.....	ii
Table of Contents.....	iii
Abstract.....	viii
Abbreviations.....	x
Ligand Abbreviations.....	xii
1. Introduction	1
1.1. Background	2
1.1.1. Uses of Platinum	2
1.1.2. Supply and Demand of Platinum	5
1.2. Platinum Refining	6
1.2.1. Overview	6
1.2.2. Mining of Platinum Containing Ores	7
1.2.3. From Ore to Concentrate.....	8
1.2.4. Separation of Platinum from a Concentrate.....	9
1.2.4.1. Classical Precipitation Methods.....	9
1.2.4.2. Solvent Extraction.....	12
1.2.4.2.1. Leaching.....	12
1.2.4.2.2. Extraction	13
1.2.4.2.3. Recovery of Platinum from $[PtCl_6]^{2-}$	22
1.2.4.2.4. Examples of Industrial Solvent Extraction Processes.....	23
1.2.4.2.5. Summary of Solvent Extraction	25
1.2.4.3. Other methods to separate PGMs.....	25
1.2.5. Summary	26
1.3. Anion Binding.....	27
1.3.1. Introduction	27
1.3.2. Receptors for Anions	28
1.3.2.1. Electrostatic Interactions.....	28
1.3.2.2. Using Electrostatics to Bind $[PtCl_6]^{2-}$	32
1.3.2.3. Hydrogen-bonding	33
1.3.2.4. Hydrogen-bond Donor Groups	35
<i>Amides and Sulfonamides</i>	35
<i>Urea and Thiourea</i>	37
<i>Pyrroles and Amidopyrroles</i>	39
1.3.2.5. Using Hydrogen-bonding to Target $[PtCl_6]^{2-}$	40
1.3.2.6. Areas of High Electron Density Surrounding $[PtCl_6]^{2-}$	43
1.3.2.7. Other Methods to bind Anions.....	45
1.3.2.8. Recognition of Anions Using a Combination of Interactions.....	47
1.4. Aims of Project	48
1.5. References	50
2. Design and Synthesis of Tripodal Receptors	60
2.1. Introduction	60
2.2. Receptor Design	60
2.2.1. Electrostatic Attraction	60
2.2.2. Hydrogen-bonding	61
2.2.3. Organic Solubility	62
2.2.4. Synthetic Accessibility.....	63
2.2.5. Receptor Design	63

2.3. Receptor Synthesis	64
2.3.1. TREN-based Sulfonamide Receptors	64
2.3.1.1. Synthesis and Characterisation	65
2.3.1.2. Crystal Structure of L ¹	66
2.3.2. TREN-based Urea Receptors	68
2.3.2.1. Synthesis and Characterisation	69
2.3.2.2. Crystal Structure of L ²	70
2.3.3. TREN-based Thiourea Receptors	72
2.3.3.1. Synthesis and Characterisation	72
2.3.3.2. Crystal Structure of L ⁵	74
2.3.4. TREN-based Amide Receptor	75
2.3.4.1. Synthesis and Characterisation	75
2.3.4.2. Crystal Structure of L ⁸	76
2.3.5. TREN-based Amido Pyrrole Receptor	78
2.3.5.1. Synthesis and Characterisation	78
2.3.5.2. Crystal structure of L ⁹	80
2.4. Complexation Reactions	81
2.4.1. Synthesis of a Sulfonamide Complex	82
2.4.1.1. Synthesis of [(L ¹ H) ₂ PtCl ₆]	82
2.4.1.2. Crystal Structure of [(L ¹ H) ₂ PtCl ₆]	82
2.4.2. Synthesis of Urea Complexes	85
2.4.2.1. Synthesis of [(L ² H) ₂ PtCl ₆]	85
2.4.2.2. Synthesis of [(L ³ H) ₂ PtCl ₆]	87
2.4.2.3. Crystal Structure of [(L ³ H) ₂ PtCl ₆]	87
2.4.2.4. Synthesis of [(L ⁴ H) ₂ PtCl ₆]	92
2.4.3. Synthesis of Thiourea Complexes	92
2.4.4. Synthesis of an Amide Complex	92
2.4.4.1. Synthesis of [(L ⁸ H) ₂ PtCl ₆]	92
2.4.5. Synthesis of an Amido Pyrrole Complex	93
2.4.5.1. Attempted synthesis of [(L ⁹ H) ₂ PtCl ₆]	93
2.5. Summary of Results	94
2.6. Experimental	95
2.6.1. Synthesis of Receptors	95
2.6.2. Synthesis of Complexes	101
2.7. References	104
3. Improving the Solubility of Complexes	109
3.1. Introduction	109
3.2. Design Modifications	110
3.3. Urea Receptors	110
3.3.1. Synthesis and Characterisation	110
3.3.2. Crystal Structure of L ¹¹	111
3.3.3. Crystal Structure of L ¹²	114
3.3.4. Complexation Reactions	116
3.3.5. Synthesis of Other Methoxy Urea Receptors	117
3.3.6. Complexation Reactions	118
3.3.7. Summary	118
3.4. Thiourea Receptors	119
3.4.1. Synthesis and Characterisation	119
3.4.2. Complexation Reactions	119
3.4.3. Summary	120

3.5. Amide Receptors.....	121
3.5.1. Synthesis and Characterisation	121
3.5.2. Crystal structure of L ¹⁹	121
3.5.3. Complexation Reactions	123
3.5.4. Crystal Structure of [(L ¹⁹ H) ₂ PtCl ₆]	125
3.5.5. Summary	128
3.6. Potentiometry	128
3.7. NMR Spectroscopic Titrations.....	130
3.7.1. Experiment Design.....	131
3.7.2. Data Analysis	132
3.7.3. Results	134
3.7.3.1. Receptor Considerations	134
3.7.3.2. Anion Considerations.....	135
3.7.3.3. NMR Titration Results.....	136
3.8. UV/vis Spectroscopic Titrations	137
3.9. Summary of Results	139
3.10. Experimental	140
3.10.1. Receptor Synthesis.....	140
3.10.2. Complexation Reactions	148
3.11. References	152
 4. Solvent Extraction Studies	155
4.1. Principles of Extraction.....	155
4.2. Current Methods Used to Extract [PtCl ₆] ²⁻	156
4.3. Method Development.....	157
4.3.1. Production of [PtCl ₆] ²⁻	157
4.3.2. Choice of Solvent.....	158
4.3.3. Measurement of Pt Extraction.....	158
4.3.4. Mixing Time Studies.....	159
4.3.5. Chloride Selectivity.....	159
4.3.6. pH of Extractions	160
4.3.7. Control Experiments	162
4.3.8. Back Extractions	163
4.3.9. Method of Extraction	164
4.4. Treatment of Results	166
4.4.1. Extraction Graph	166
4.4.2. Confirming the Stoichiometry of the Complex.....	166
4.5. Test Extractions.....	168
4.5.1. Test Extraction Results	168
4.6. Extraction Results	169
4.6.1. TOA	169
4.6.2. Sulfonamide Receptor.....	171
4.6.3. Urea Receptors	171
4.6.4. Amide Receptors.....	174
4.7. Comparisons.....	176
4.7.1. Hydrogen-bond Donor Type.....	176
4.7.2. Comparisons with TOA	178
4.8. Other Experiments	179
4.8.1. Receptor Selectivity	179
4.8.2. Extractions in Toluene	181
4.8.3. Recycling Receptors	183

4.9. Summary of Results	184
4.10. Synthesis	185
4.11. References	186
5. Alternative Tripodal Systems.....	188
5.1. Introduction	188
5.2. Incorporating Halogen-bonding into the Receptor Design	188
5.2.1. Design of Receptors	191
5.2.2. Synthesis of Receptors	192
5.2.2.1. Urea Receptor	192
5.2.2.2. Amide Receptor	193
5.2.3. Complexation Reactions	193
5.2.4. Summary of Results	194
5.3. Extended Tripodal Receptors	194
5.3.1. Design of Receptors	195
5.3.2. Synthesis of Receptors	196
5.3.2.1. Urea Receptors	196
5.3.2.2. Thiourea Receptor.....	196
5.3.2.3. Amide Receptor	197
5.3.3. Complexation Reactions	198
5.3.3.1. Urea Complexes	198
5.3.3.2. Thiourea Complex.....	199
5.3.3.3. Amide Complex	199
5.3.4. Extraction Studies	199
5.3.4.1. Test Extractions.....	199
5.3.4.2. Effect of Hydrogen-bond Donor Group.....	200
5.3.4.3. Effect of Receptor Scaffold.....	202
5.3.5. Summary of Results	203
5.4. Experimental	204
5.4.1. Synthesis of Hydrogen- and Halogen-bonding Receptors and Complexes.....	204
5.4.2. Synthesis of Extended Tripodal Receptors and Complexes	206
5.5. References	212
6. Bipodal and Monopodal Receptors	214
6.1. Introduction	214
6.2. Bipodal Receptors	214
6.2.1. Synthesis of Bipodal Receptors	215
6.2.1.1. Urea Receptors	215
6.2.1.2. Crystal Structure of L ²⁹	216
6.2.1.3. Urea Receptors (part 2).....	219
6.2.1.4. Thiourea Receptors	221
6.2.1.5. Crystal Structure of L ³⁵	221
6.2.1.6. Amide Receptors	223
6.2.2. Potentiometry of Bipodal Receptors	224
6.2.3. Complexation Reactions	226
6.2.3.1. Urea Complexes	226
6.2.3.2. Crystal Structure of [(L ²⁹ H) ₂ PtCl ₆]	227
6.2.3.3. Thiourea Complexes	231
6.2.3.4. Amide Complex	231
6.2.3.5. Crystal Structure of [(L ³⁸ H) ₂ PtCl ₆]	232

6.2.4. Extraction Studies	235
6.2.4.1. Test Extractions.....	235
6.2.4.2. Urea vs Amide	235
6.2.4.3. Tripodal vs Bipodal Receptors.....	238
6.2.4.4. Geometry vs Hydrogen-bonds	240
6.2.4.5. Effect of Spacer Unit.....	241
6.2.4.6. Effect of Alkyl Substituent	243
6.2.4.7. Effect of Hydrogen-bonds.....	245
6.2.5. Summary of Results	247
6.3. Monopodal Receptors	248
6.3.1. Synthesis of Monopodal Receptors.....	249
6.3.2. Complexation Reactions	249
6.3.3. Solvent Extractions	250
6.3.4. Summary of Results	251
6.4. Experimental	252
6.4.1. Receptor Synthesis	252
6.4.2. Complexation Reactions	263
6.5. References	267
7. Conclusions.....	268
7.1. References	275
Appendix A Reagent Preparation and Instrumentation.....	276
Appendix B Crystallographic Information for Chapter 2.....	277
Appendix C Crystallographic Information for Chapter 3.....	280
Appendix D Potentiometry Methodology.....	282
Appendix E Solvent Extraction Methodology.....	283
Appendix F Crystallographic Information for Chapter 6.....	287
Appendix G Publications.....	289

Abstract

This thesis presents research into the binding, extraction and transport of the hexachloroplatinate anion, $[\text{PtCl}_6]^{2-}$, by organic receptors in a solvent extraction process. The target anion is produced during the processing of platinum-containing ores and the aim was to develop reagents that can selectively extract $[\text{PtCl}_6]^{2-}$ to optimise the recovery of platinum.

Chapter One outlines reasons for the interest in $[\text{PtCl}_6]^{2-}$ and provides an overview of the processes and techniques used to refine precious metals. An introduction to anion coordination chemistry relevant to the research project is also presented.

Chapter Two discusses the design features incorporated into organic receptors to enable strong and selective binding of $[\text{PtCl}_6]^{2-}$. These features include a tertiary amine protonation site, hydrogen-bond donor groups and organic solubilising moieties. The synthesis of a series of functionalised tripodal tris(2-aminoethyl)amine based receptors with sulfonamide, amide, urea, thiourea or pyrrole NH hydrogen-bond donor groups are reported. Complexation reactions between the receptors and H_2PtCl_6 to form $[(\text{LH})_2\text{PtCl}_6]$ ion pairs are discussed. Crystallographic analysis of the $[(\text{LH})_2\text{PtCl}_6]$ complexes with TREN-based sulfonamide, urea and amide receptors confirms the presence of hydrogen-bonds between the NH donor groups and the outer-sphere of $[\text{PtCl}_6]^{2-}$. The low organic solubility of the complexes prevented the study of these systems in solvent extractions.

Chapter Three describes the variation of terminal substituents of the tripodal receptors with the aim of improving the organic solubility of the extractants and their $[\text{PtCl}_6]^{2-}$ complexes. In these “second generation” receptors the terminal substituents assessed include 3, 5-dimethylphenyl, 4-*iso*-propylphenyl, 4-*tert*-butylphenyl, 3, 5-dimethoxyphenyl, 3, 4-dimethoxyphenyl and 3, 4, 5-trimethoxyphenyl. Through

reaction of the receptors with H_2PtCl_6 the solubility of the resultant complexes are assessed.

Chapter Four describes the development of an optimised solvent extraction method to study the extractive behaviour receptors. A pH swing mechanism is utilised to control the uptake and release of $[\text{PtCl}_6]^{2-}$. The extraction results for trioctylamine and the soluble tripodal urea and amide receptors are compared. Attempts are also made to confirm the stoichiometry of the complex in solution.

Chapter Five describes the synthesis of tris(2-aminoethyl)amine based receptors with hydrogen- and halogen-bond donor groups with the aim of increasing the strength of the interaction between a receptor and $[\text{PtCl}_6]^{2-}$. Receptors with an extended tripodal scaffold based on a tris(3-aminopropyl)amine with urea and amide moieties are also presented. The results of the complexation reactions and solvent extraction studies with these modified extractants are presented.

Chapter Six presents the design and synthesis of bipodal and monopodal receptors in order to assess the role of the number of hydrogen-bond donor functionalised arms. The results of the solvent extraction studies with these receptors are discussed and comparisons made between tripodal, bipodal and monopodal extractants. The crystallographic analysis of the $[(\text{LH})_2\text{PtCl}_6]$ complexes formed between the bipodal urea and amide receptors is described.

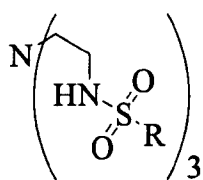
Chapter Seven highlights the important findings from this work. Conclusions are drawn as to the optimum receptor system developed and this is compared to the extractant system thought to be in current use for the extraction and transport of $[\text{PtCl}_6]^{2-}$.

Abbreviations

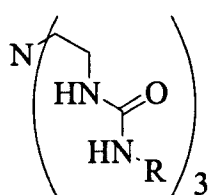
δ	Chemical shift
ϵ	Extinction coefficient
λ_{\max}	Maximum wavelength
ν	Wavenumber
\AA	Angstroms
aq	Aqueous phase
br	Broad (NMR)
Bu	Butyl
d	Days
d	Doublet (NMR)
dmf	N, N'-dimethylformamide
dmso	Dimethylsulfoxide
Et	Ethyl
EtOH	Ethanol
Et ₂ O	Diethyl ether
EtOAc	Ethyl acetate
ES	Electrospray
h	Hours
ICP-MS	Inductively Coupled Plasma Mass Spectrometry
ICP-OES	Inductively Coupled Plasma Optical Emission Spectroscopy
<i>iso</i> -Pr	Iso-Propyl
IR	Infrared
<i>J</i>	Coupling constant
L	Ligand
m	Multiplet (NMR)
Me	Methyl

MeOH	Methanol
mins	Minutes
MS	Mass Spectrometry
NMR	Nuclear Magnetic Resonance
OMe	Methoxy
PGM	Platinum Group Metal
Ph	Phenyl
ppm	Parts per million
ppb	Parts per billion
r.t.	Room temperature
s	Singlet (NMR)
t	Triplet (NMR)
<i>tert</i> -Bu	Tertiary butyl
TOA	Trioctylamine
TREN	Tris(2-aminoethyl)amine
TRPN	Tris(3-aminopropyl)amine
thf	Tetrahydrofuran
Vis	Visible
UV	Ultraviolet

Tripodal TREN-based Receptors

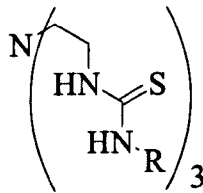


L^1 : R = Ph
 L^{22} : R = Ph(4-OC₈H₁₇)

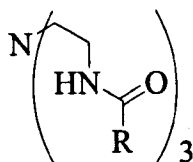


L^2 : R = Ph
 L^3 : R = *tert*-butyl
 L^4 : R = *n*-butyl
 L^{10} : R = Ph(3, 5-Me)
 L^{11} : R = Ph(4-*iso*-propyl)

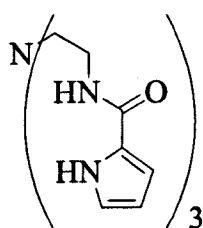
L^{12} : R = Ph(4-*tert*-butyl)
 L^{13} : R = Ph(3, 5-OMe)
 L^{14} : R = Ph(3, 4-OMe)
 L^{15} : R = Ph(3, 4, 5-OMe)
 L^{16} : R = Ph(4-C₈H₁₇)



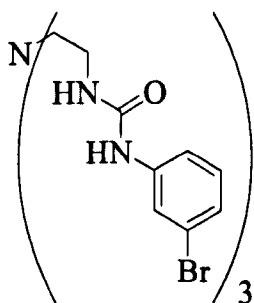
L^5 : R = Ph
 L^6 : R = *tert*-butyl
 L^7 : R = Me
 L^{17} : R = Ph(3, 5-OMe)
 L^{18} : R = Ph(3, 4, 5-OMe)



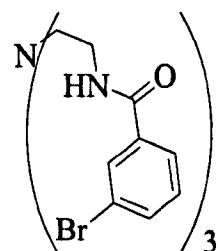
L^8 : R = Ph
 L^{19} : R = Ph(3, 5-OMe)
 L^{20} : R = Ph(3, 4-OMe)
 L^{21} : R = Ph(3, 4, 5-OMe)



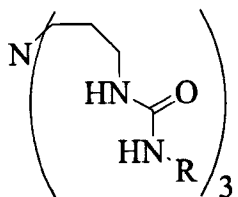
L^9



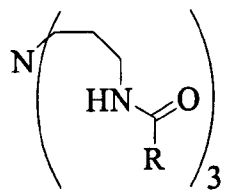
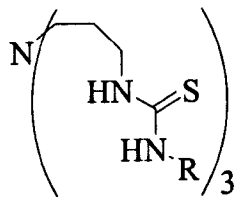
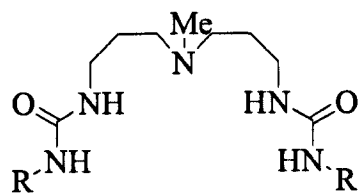
L^{23}



L^{24}

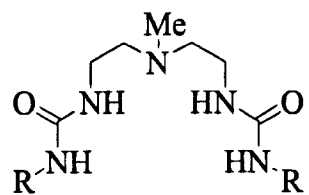
Tripodal TRPN-based Receptors

L^{26} : R = Ph(3, 4, 5-OMe)

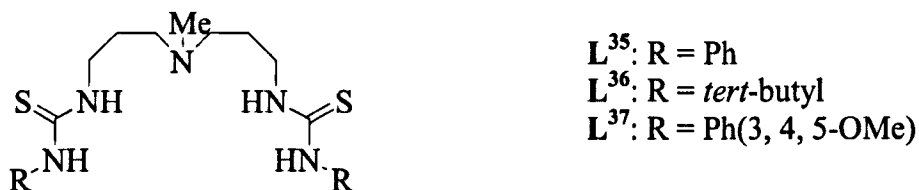
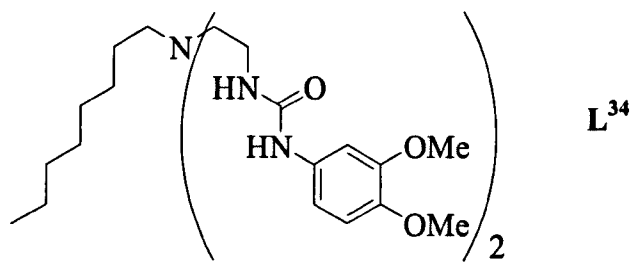
**Bipodal Receptors**

L^{30} : R = *tert*-butyl

L^{31} : R = Ph(3, 4, 5-OMe)



L^{33} : R = Ph(3, 4, 5-OMe)



Monopodal Receptors



1. Introduction

This thesis presents research into the binding, extraction and transport of the hexachloroplatinate anion, $[\text{PtCl}_6]^{2-}$, by organic receptors in a solvent extraction process. The target anion is produced during the processing of Pt-containing ores and the aim was to develop reagents that can selectively extract $[\text{PtCl}_6]^{2-}$ to optimise the recovery of Pt. This Chapter outlines the reasons why our research focussed on $[\text{PtCl}_6]^{2-}$ and provides an overview of the processes used for the refining of the platinum group metals (PGMs). This is followed by a review of anion coordination chemistry that is relevant to the research project.

1.1. Background

The PGMs are platinum (Pt), palladium (Pd), rhodium (Rh), ruthenium (Ru), iridium (Ir) and osmium (Os) and these elements are highlighted in the periodic table in Figure 1.1.

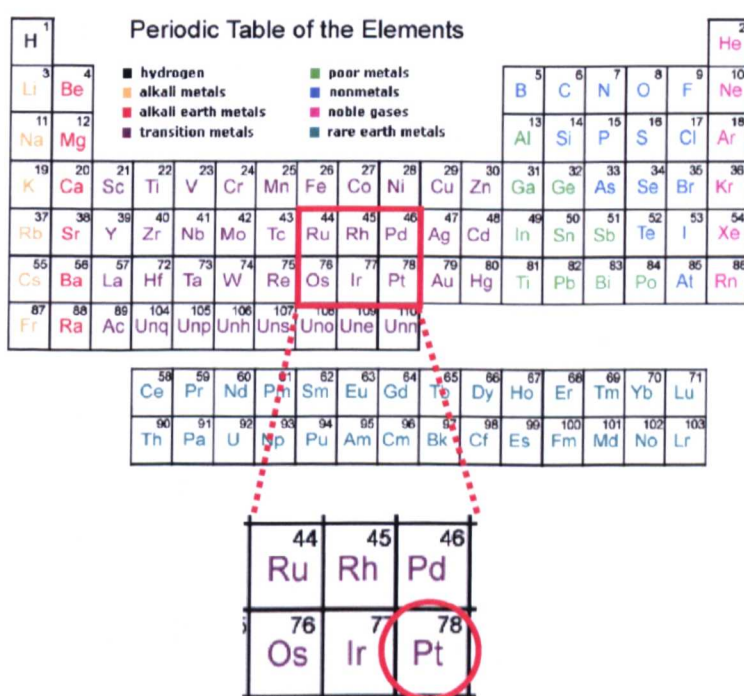


Figure 1.1. Periodic table highlighting the PGMs and platinum.

The PGMs are extremely scarce in comparison to the other precious metals (Au and Ag) due to their low natural abundance and the complex processes required for their extraction and refining. Also, the demand for PGMs relative to other precious metals is high as they find use in a wide range of technologically important applications.

1.1.1. Uses of Platinum

The majority of Pt is used in autocatalysts and jewellery (Figure 1.2).^{1, 2}

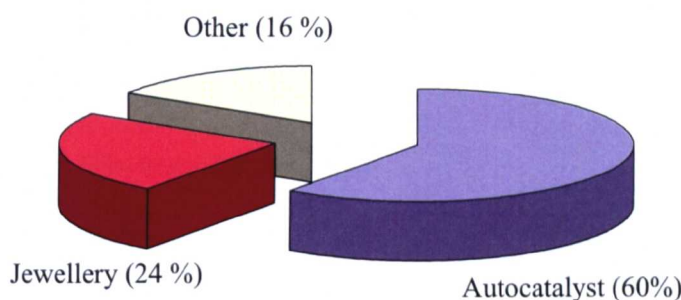


Figure 1.2. Pt use by application in 2006.^{1, 2}

Autocatalysts convert over 90% of harmful emissions into less harmful products. A reduction catalyst uses Pt and Rh to convert nitrogen oxide emissions into N₂ and O₂ and an oxidation catalyst based on Pt and Pd to oxidise hydrocarbons into CO₂ and H₂O and CO (produced from the incomplete combustion of petrol or diesel) into CO₂.^{3, 4} The demand for Pt increased significantly in the 1970's when clean air legislation was introduced in the USA and Japan with many countries introducing similar legislation shortly afterwards.⁵ There are reports on the recovery of PGMs from spent automotive catalysts which highlights the significant demand for the precious metals involved.⁶⁻⁹

Pt is used in jewellery as it is highly valued for its beauty and purity. Its colour, strength, hardness, flexibility and resistance to tarnish are some of the additional advantages of using Pt. The demand for Pt jewellery has increased steadily

for two decades and the world's leading jewellery market is Japan where Pt is very popular and fashionable.¹⁰

The high catalytic activity of PGMs for a wide range of substrates has resulted in their use in industrial synthetic processes.^{11, 12} The PGMs find use as catalysts as the stable oxidation states for these elements have a d⁸ electron configuration and the complexes adopt a square-planar geometry leaving two axial positions vacant. This allows a substrate to bind to the metal, to react and then leave thus freeing the site for a further reaction with another substrate molecule. The stable oxidation states of Pt are Pt(II) and Pt(IV) and this means oxidative addition and reductive elimination processes are possible.¹³⁻¹⁵

Platinum diphosphine complexes containing a trifluoromethyl ligand catalyse the epoxidation of terminal alkenes with hydrogen peroxide (Figure 1.3). The platinum centre performs a bifunctional role in aiding the formation of the hydroperoxide anion and acting as a binding site for the alkene, rendering it more prone to nucleophilic attack.¹⁶⁻²⁰

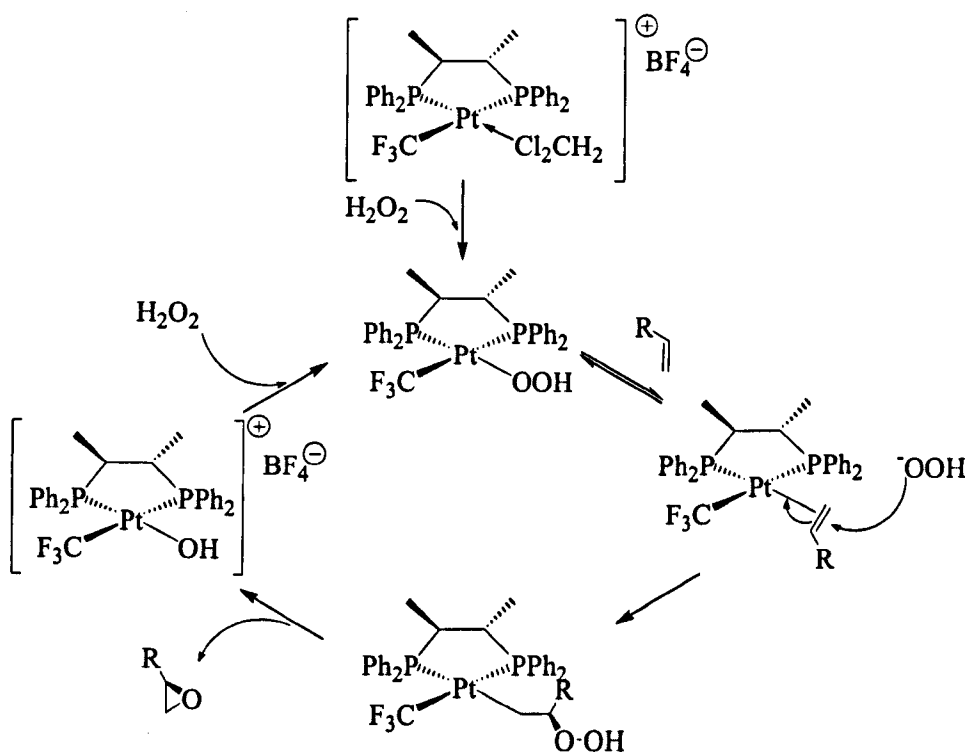


Figure 1.3. An example of using a platinum-based catalyst.¹⁶⁻²⁰

Adams catalyst (PtO_2) is used for hydrogenation reactions. The oxide itself is not an active catalyst but upon exposure to hydrogen it is converted to platinum black which is responsible for catalysing the reaction. An example of a hydrogenation reaction that uses PtO_2 is the reduction of alkenes where the PtO_2 catalyst can be recycled for over 10 cycles without loss of activity (Figure 1.4).²¹⁻²³

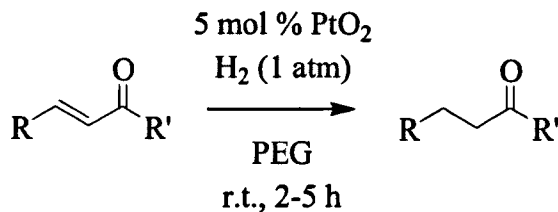


Figure 1.4. An example of a hydrogenation reaction using PtO_2 .²¹⁻²³

Cis-platin, $[\text{cis-PtCl}_2(\text{NH}_3)_2]$, is a platinum-based chemotherapy drug. Following administration *in vivo*, a chloride ligand is substituted by H_2O to form $[\text{PtCl}(\text{H}_2\text{O})(\text{NH}_3)_2]^+$ in which the water ligand is readily displaced allowing *cis*-platin to coordinate to a basic site in DNA. Substitution of both chloride ligands of *cis*-platin leads to the cross-linking of DNA strands which interferes with cell division.²⁴ Other platinum-based pharmaceuticals include triplatin tetranitrate, carboplatin and oxaliplatin (Figure 1.5).²⁵

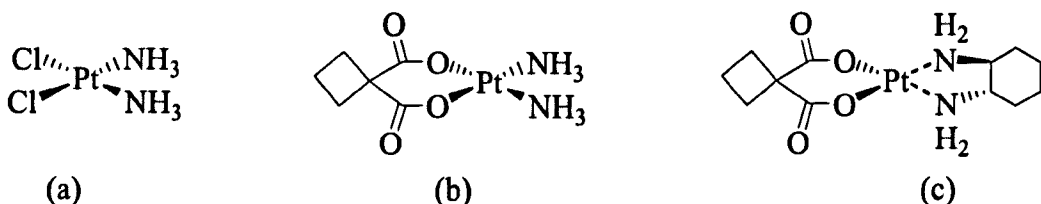


Figure 1.5. Structure of a) *cis*-platin, b) carboplatin and c) oxaliplatin.

The excellent mechanical as well as corrosion- and oxidation-resistant properties of PGMs are particularly pronounced at high temperatures. This has led to a number of applications for PGMs and their alloys in high temperature process industries such as materials for processing extremely corrosive molten glass, nozzles for spinning textiles and coatings for the turbine blades of jet engines.^{26, 27} Due to its

relative scarcity platinum is seen as a good investment with examples including ingots and bullion coins.²⁸

1.1.2. Supply and Demand of Platinum

South Africa and Russia are the two main areas where platinum-containing ores are found (Figure 1.6, a).²⁸ The world-wide production of Pt has increased dramatically over the last century (Figure 1.6, b) reflecting the increase in demand due to the growth in the number of applications. Being able to keep up with the demand for Pt is a major challenge facing mining companies, and there is continual investment in new and improved processes to increase materials balances. Any modifications made to the process that increase the amount of Pt recovered will be of interest as the efficiency of the process will be improved leading to significant gains.

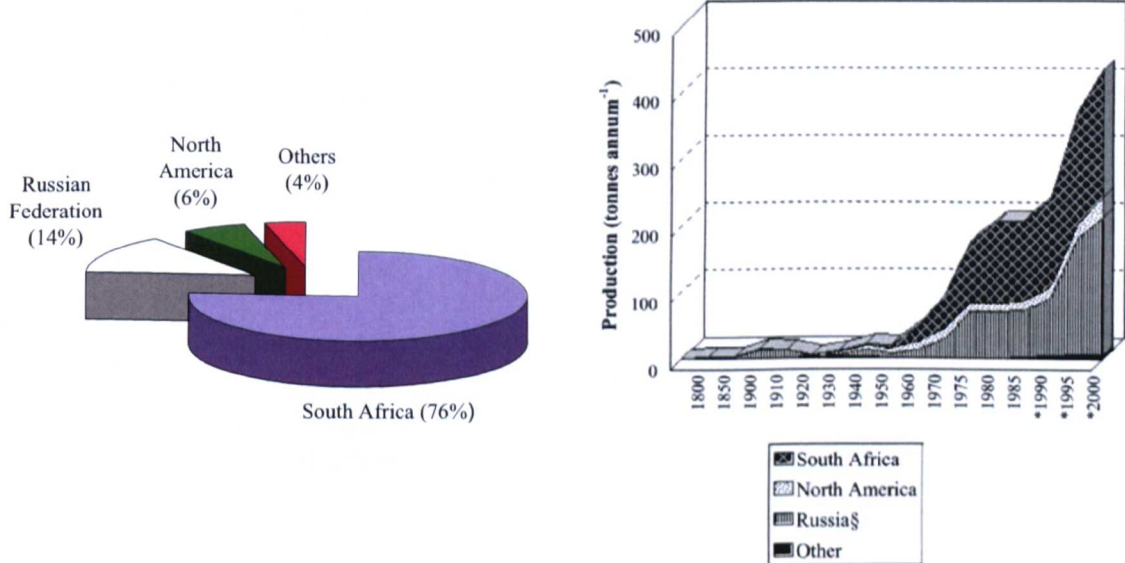


Figure 1.6. a) Pt supply by regions % 2002-2006 and b) worldwide growth in platinum production from 1800-2000.²⁹

1.2. Platinum Refining

1.2.1. Overview

It is estimated that in order to produce a single ounce of Pt a volume of seven to twelve tonnes of ore must be processed. This highlights the low natural abundance of Pt and the complexity of the processes used to obtain pure metal.³⁰ There are three main stages involved in the production of pure platinum metal from its ore (mining, concentration and refining) each of which consists of numerous intricate processes (Figure 1.7). Following the mining of ore the concentration of PGMs is very low and it is necessary to increase their concentrations to enable the latter refining processes to be efficient.

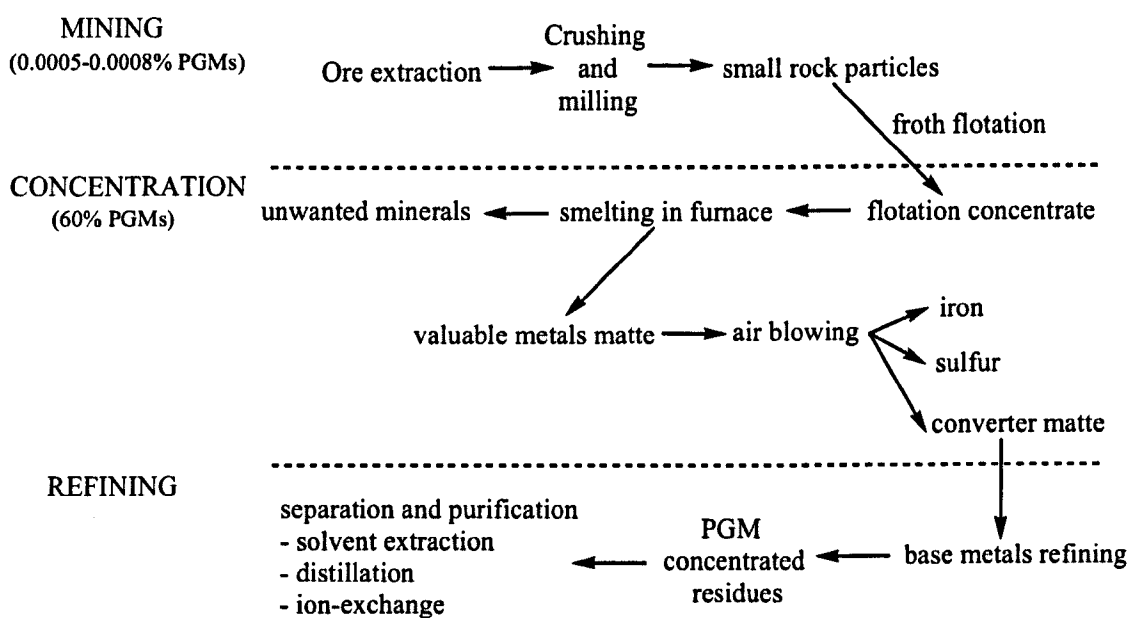


Figure 1.7. Overview of the stages involved in the refining of PGMs.

1.2.2. Mining of Platinum Containing Ores

The ores obtained from mining can contain PGMs alloyed with iron, arsenic, tellurium, antimony, and vanadium. Platinum-palladium sulfide minerals (cooperite and braggite) and mineralised PGMs with copper and nickel sulfide and/or chromite are also known (commonly chalcopyrite, pyrrhotite, pentlandite).³¹ Platinum can be

found as native platinum (in which it is not combined with another element) but these are very small particles which are widely dispersed and hard to recover. Following mining, the ore is crushed and milled to produce smaller sized rock particles meaning that the minerals containing PGMs are exposed.

1.2.3. From Ore to Concentrate

A common technique used to increase the concentration of PGMs is froth flotation in which the crushed rock particles are mixed with H₂O and special flotation agents which attach to the surfaces of the metal ore particles. The flotation agents convert hydrophilic ore particles into hydrophobic materials and examples of such reagents include thiols, alkyl thiocarbonates, dialkyldithiophosphates, fatty carboxylates and hydroxamates (Figure 1.8).³² Air is pumped through the liquid forming bubbles to which the PGM-containing particles adhere and float to the surface. The flotation concentrate is removed as an oil based froth and the unwanted materials are removed as an aqueous slurry from the bottom of the separator.³³

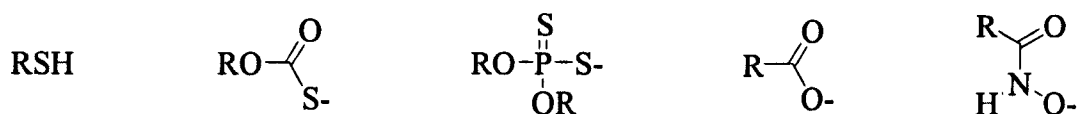


Figure 1.8. Structures of some froth flotation agents.³²

Once dried, the flotation concentrate is smelted in an electric furnace at temperatures over 1500 °C to produce a matte which contains the valuable metals.³³ Air is blown through the matte to remove Fe and S which are lost as gaseous SO₂ and FeO₂. A disadvantage of this process is the production of polluting SO₂ which is a problem that is becoming increasingly significant as environmental regulations become stricter and more difficult to meet.³³ Any Ni, Cu and Co present in the matte are separated from PGMs using electrolytic techniques meaning residues containing

PGMs are concentrated.²⁸ An overview of the processes used in the production of a concentrate from an ore is shown in Figure 1.9.

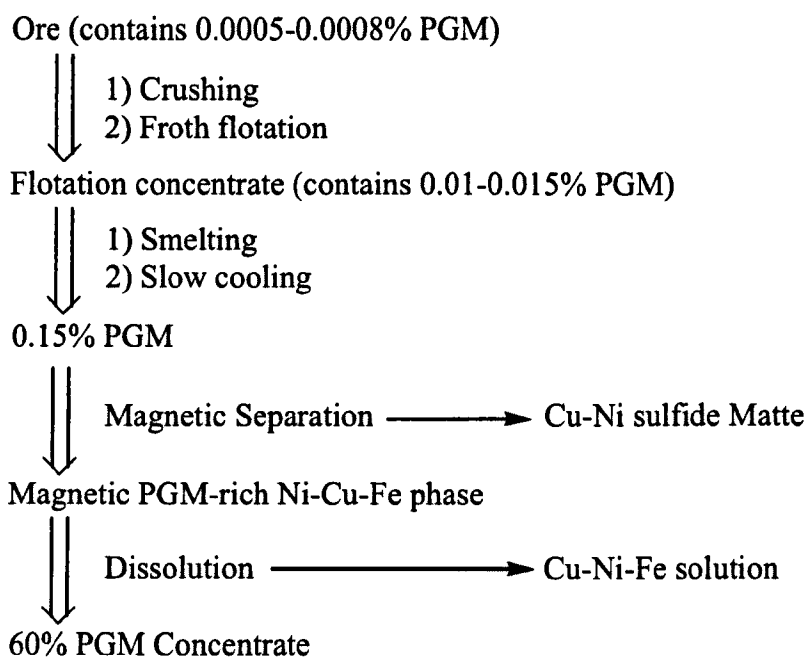


Figure 1.9. Concentration process for PGMs from sulfide ores.²⁶

1.2.4. Separation of Platinum from a Concentrate

The final stage involves separating and purifying the PGMs that are present in the concentrate. This is the most difficult and intricate part of the process and there are two main approaches involving selective precipitation and solvent extraction. The specific details of the reagents that are actually used are shrouded in secrecy due to the commercial sensitivity of these processes.

1.2.4.1. Classical Precipitation Methods

Up until the mid-1970s the separation of PGMs was achieved largely through a series of selective precipitation reactions.²⁹ This involved dissolving the metal concentrate in *aqua regia* thus oxidising and solubilising the PGMs. In practice, Ru, Rh, Ir and Os dissolve more slowly than Au, Ag, Pt and Pd which enables a partial separation between these two groups. By varying the conditions throughout the process the

dissolved metals are selectively precipitated allowing their separation from other metals.^{34, 35}

The hexachlorometallate anions $[\text{PtCl}_6]^{2-}$, $[\text{RuCl}_6]^{2-}$ and $[\text{IrCl}_6]^{2-}$ are separated by precipitation as their ammonium salts via reaction with ammonium chloride (Equation 1).²⁹



Ligand substitution can also be used to separate the PGMs in a concentrate. The reactivity of PGMs towards ligand substitution depends on the nature of the reactant ligands, the oxidation state of the metal and the row of the periodic table in which the metal is found. The most stable PGM complexes contain heavier donor atoms with the approximate overall order of $\text{S} \sim \text{C} > \text{I} > \text{Br} > \text{Cl} > \text{N} > \text{O} > \text{F}$ and this applies particularly to Pt and Pd.³⁶ This trend is directly related to Pearson's hard-soft acid base theory in which species are ranked according to their size, charge and polarisability.³⁷ Hard is used to describe species which are small, have high charge states and are weakly polarisable, whilst the term soft applies to species which are larger, have low charge states and are easily polarisable. Hard acids prefer to combine with hard bases whilst soft acids pair with soft bases. Pt and Pd are soft acids and will thus preferably bind to soft bases such as SCN^- or CO . Sulfur-bonded systems have been used to precipitate Pt and Pd; however, the stripping of the metal from the complex can be difficult due to the strong metal-ligand interaction.³⁸

Metals in their divalent oxidation state are readily susceptible towards substitution by soft donor ligands and rates of substitution can be several orders of magnitude faster than for metals in their higher oxidation states.³⁶ Inertness to substitution varies in the order 3rd row $>$ 2nd row $>$ 1st row for comparable complexes of transition metals and hence a second row PGM is more reactive than a related

third row PGM. This is because the 5d orbitals are spatially larger than the 4d orbitals and give rise to better orbital overlap between the metal and ligand.³⁹

Both Ru and Os form volatile tetroxides under strongly oxidising conditions which enables their separation from the other PGMs by distillation. OsO₄ is more stable than RuO₄ and selective reduction of RuO₄ by dissolution in HCl enables separation of these two metals.²⁹ An outline of the use of selective precipitation to separate the PGMs in a concentrate is illustrated in Figure 1.10.

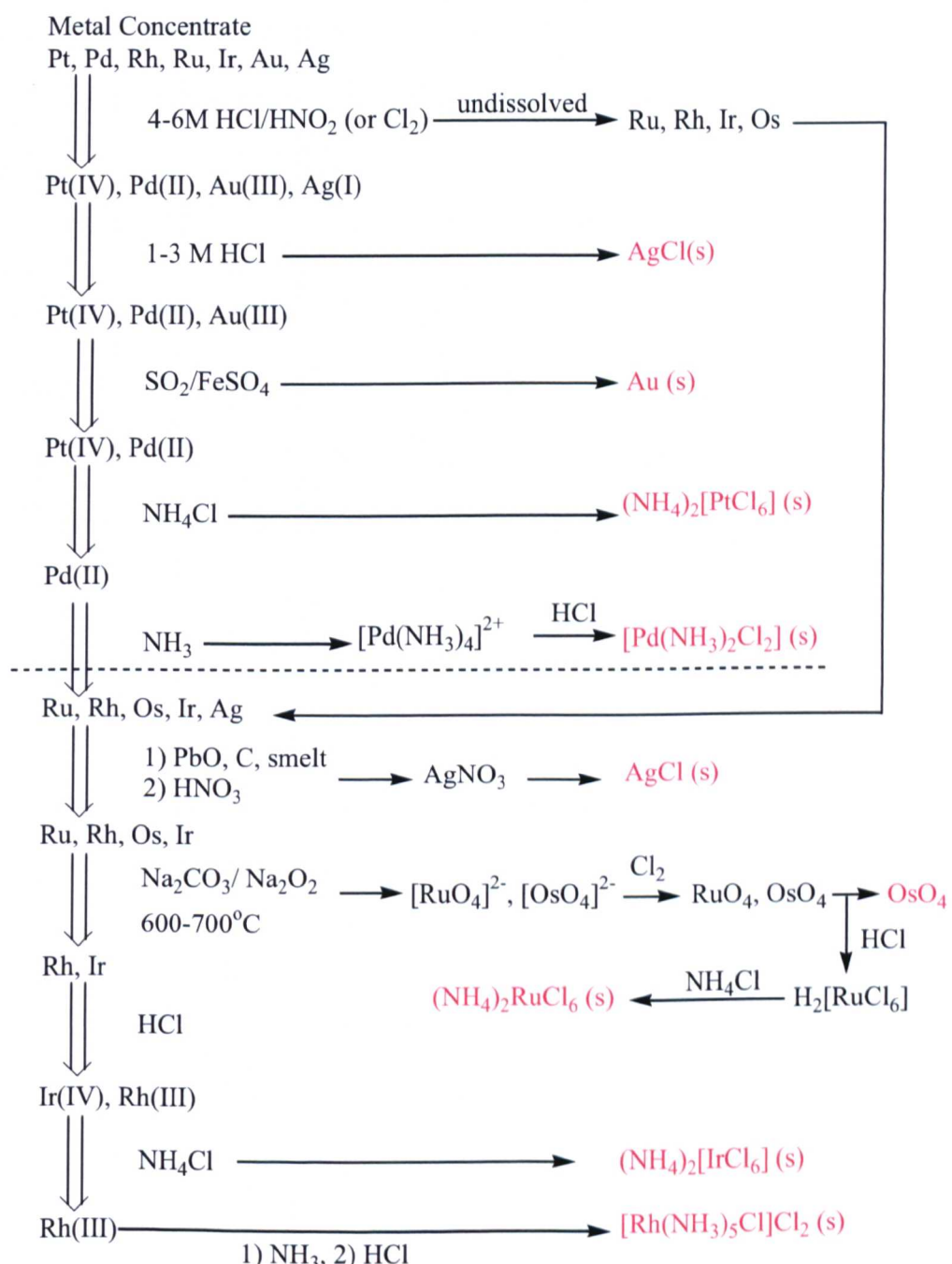


Figure 1.10. Classical refining for the separation of PGMs.²⁹

There are problems associated with using precipitation to refine PGMs as separation can be inefficient due to poor selectivity and interfering precipitation reactions. Filter cakes often contain entrained filtrate and thorough washing of these cakes is difficult to achieve as they often have poor filtration characteristics.³⁸ This means that further purification is required involving re-dissolution and re-precipitation requiring increased recycling and re-treatment. As the primary yields are rather low the numerous unit operations and recycle streams lead to lengthy refining times making the process labour intensive.^{7, 29, 36, 40} In an attempt to improve this situation much effort has been placed on the development of solvent extraction techniques for the separation of PGMs.

1.2.4.2. Solvent Extraction

Solvent extraction can be used as an alternative to classical precipitation methods to separate PGMs. It involves selective transfer of the target metal ion from an aqueous phase into an immiscible organic phase thus facilitating its separation from other species present in the aqueous phase. Solvent extraction can be used to selectively recover small amounts of metal ions from dilute feedstocks and is thus an important technique used in the processing of low grade ores. A solvent extraction has four steps consisting of leaching, extraction, stripping and electrowinning.²⁹

1.2.4.2.1. Leaching

Leaching involves dissolution of the concentrate and typically *aqua regia* is used as a cost-effective medium in which all PGMs can be brought into solution. Simple leaching occurs at atmospheric temperature and pressure whilst pressure leaching involves higher pressures and temperatures to quicken the process.⁴¹ The process of leaching results in the metals being present in solution as chlorometallate species and

the major PGM species encountered in chloride media are shown in Table 1.1.²⁹ With the exception of Ru, which also forms a significant portion of complex multinuclear species, all of the PGMs in their tetravalent oxidation state predominantly form hexachloro complex anions in strong chloride media. The most commonly encountered chloro-species for Pt is the hexachloroplatinate anion, $[\text{PtCl}_6]^{2-}$, and as such research has focussed on targeting this anion. The chlorometallate species listed in Table 1.1 can aquate in weak chloride solutions and H_2O , but this is inhibited in stronger chloride media.³⁸

Table 1.1. PGM species found in aqueous chloride media.²⁹

<i>Ruthenium</i>	<i>Rhodium</i>	<i>Palladium</i>
Ru(III)	Rh(III)	Pd(II)
$[\text{RuCl}_6]^{3-}$	$[\text{RhCl}_6]^{3-}$	$[\text{PdCl}_4]^{2-}$
$[\text{RuCl}_5(\text{H}_2\text{O})]^{2-}$	$[\text{RhCl}_5(\text{H}_2\text{O})]^{2-}$	
$[\text{RuCl}_4(\text{H}_2\text{O})_2]^-$	$[\text{RhCl}_4(\text{H}_2\text{O})_2]^-$	
$[\text{RuCl}_3(\text{H}_2\text{O})_3]$		
Ru(IV)	Rh(IV)	Pd(IV)
$[\text{RuCl}_6]^{2-}$	$[\text{RhCl}_6]^{2-}$	$[\text{PdCl}_6]^{2-}$
$[\text{Ru}_2\text{OCl}_{10}]^{4-}$		
$[\text{Ru}_2\text{OCl}_8(\text{H}_2\text{O})_2]^{2-}$		
<i>Osmium</i>	<i>Iridium</i>	<i>Platinum</i>
Os(IV)	Ir(III)	Pt(II)
$[\text{OsCl}_6]^{2-}$	$[\text{IrCl}_6]^{3-}$	$[\text{PtCl}_4]^{2-}$
	$[\text{IrCl}_5(\text{H}_2\text{O})]^{2-}$	
	$[\text{IrCl}_4(\text{H}_2\text{O})_2]^-$	
	Ir(IV)	Pt(IV)
	$[\text{IrCl}_6]^{2-}$	$[\text{PtCl}_6]^{2-}$

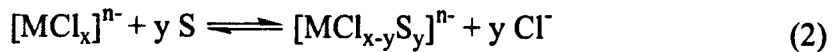
1.2.4.2.2. Extraction

There are two types of liquid-liquid extraction that are frequently encountered.^{42, 43} Firstly, when the receptor and metal ions are both soluble in the aqueous phase but the resulting complex is soluble in the organic phase. Secondly, when the receptor is soluble in the organic phase and the metal ions are soluble in the aqueous phase then extraction and complexation occurs at the inter-phase surface, and the metal species is then transferred into the organic phase.⁴³ For a receptor to be successful there are several criteria that need to be met, including:^{43, 44}

- Sufficiently high binding strength for the metal ion to be extracted
- Selective ion complexation
- High stability against hydrolysis
- Ideally the complex that forms should be neutral and as hydrophobic as possible to enable transfer into the organic phase.
- Reversible complexation allowing for total recovery of the metal without significant ligand destruction

Mechanism of Extraction

The separation of metals that are present in an acidic chloride solution can be achieved by exploiting differences in the outer-sphere electron density of the chlorometallate complexes.^{29, 36, 39} As PGM chlorometallate complexes are predominantly anionic, solvent extraction techniques have been developed to exploit the differences in anion exchange behaviour of the various species with both inner- and outer-sphere coordination mechanisms used.³⁶ The inner-sphere coordination mechanism involves complex formation where the active species in the organic phase acts as a nucleophile and displaces a chloride ligand from the chlorometallate anion to directly coordinate to the metal centre (Equation 2):³⁹



Pd(II) is sufficiently labile to make this approach viable for which coordinating solvents such as dialkyl sulfides⁴⁵ and hydroxyoximes³⁹ can be used (Figure 1.11). Oximes are produced commercially and have high distribution coefficients for Pd(II), but suffer from slow reaction kinetics.³⁸ Using inner-sphere coordination to extract PGMs has limited use because of the relatively slow substitution kinetics leading to long equilibration times which are impractical for large scale, multi-stage separation processes.

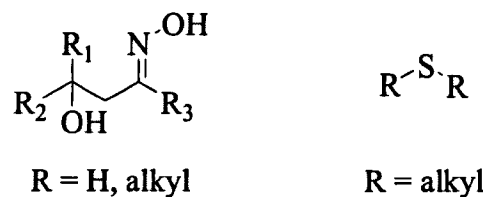
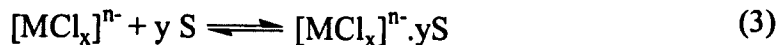


Figure 1.11. Structure of a hydroxyoxime and dialkylsulfide.^{38, 45}

Two types of interaction that utilise outer-sphere coordination are solvating systems and ion-pair formation. Typically solvating systems are either carbon or phosphorus bonded oxygen bearing extractants (such as alcohols, ketones and ethers) which extract by solvating the outer-sphere of a metal complex via a dipole attraction, as shown in Equation 3.³⁹



Examples of reagents that operate through a solvating mechanism include methyl *iso*-butyl ketone and dibutyl-carbitol (Figure 1.12). These extractants have been used to extract Au as $[\text{AuCl}_4]^-$ and as PGMs are not extracted to any appreciable extent by solvating systems, it provides a method of separating Au.^{36, 38}

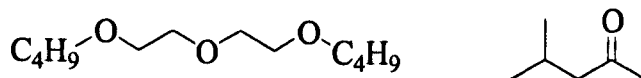
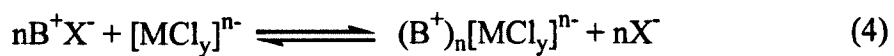


Figure 1.12. Structure of dibutyl-carbitol and methyl *iso*-butyl ketone.

In ion-exchange reactions the active species binds the chlorometallate anion through non-covalent interactions with the outer-sphere of the anion to form a receptor-chlorometallate ion pair.³⁶ The PGM-chloro complexes can undergo anion-exchange reactions with salts of a variety of organic bases (BX) (Equation 4):



Examples of extractants that use an outer-sphere ionic mechanism include tri-*n*-octylamine and tri-*n*-butyl phosphate (Figure 1.13). Tri-*n*-octylamine is a strong base meaning it is protonated more readily than a weak base such as tri-*n*-butyl phosphate.⁴⁶ A strong base can, therefore, be used at relatively low acid concentration whilst weak-base ion-exchangers only protonate significantly at high acid concentrations meaning they can only extract under these conditions.²⁹ Some examples of solvents used for selective metal extraction are listed in Table 1.2.

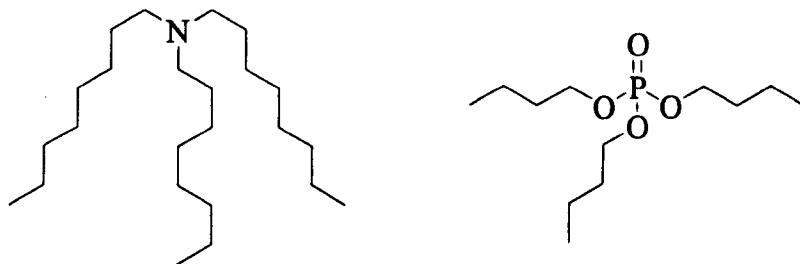


Figure 1.13. Structure of tri-*n*-octylamine and tri-*n*-butyl phosphate.

Table 1.2. Examples of solvent extractants used in PGM refining.²⁹

Metals selectively extracted under process conditions	Mechanism	Solvents	
Pd(II)	Complex Formation	Dialkyl sulfides Hydroxyoximes	
[MCl ₆] ²⁻	Anion Exchange	Strong base	Tri- <i>n</i> -octylamine
[AuCl ₄] ²⁻	Anion Exchange	Weak base	Dibutyl carbitol Isodecanol
[MCl ₆] ²⁻	Anion Exchange	Weak base	Methyl-iso-butyl ketone Tri- <i>n</i> -butyl phosphate

The size and charge of the target metal anion affect the binding in the solvent-metal ion pair. Anions with a high charge density have larger hydration shells leading to a lower coulombic interactions with counter-ions.⁴⁷ Also, the packing in the complex ion-pair is influenced by the stoichiometry required to form a charge-neutral complex.³⁹ Assuming the organic base is monocationic, a $[MCl_6]^{3-}$ anion requires three cations to be charge-neutral, while $[MCl_6]^{2-}$ needs two cations, and $[MCl_4]^-$ only one.

Solvent Extraction to Separate PGMs

Depending on the starting feedstock and process constraints, various schemes have been postulated for separating PGMs using solvent extraction.^{32, 48} An example of how solvent extraction can be used to separate PGMs is shown in Figure 1.15.²⁹

Following the dissolution of the concentrate, Ag is the first metal to be removed and this is typically achieved by the precipitation of AgCl. The rapid and efficient extraction of Au as $[AuCl_4]^-$ is achieved with solvating reagents such as methyl *iso*-butyl ketone or dibutyl carbitol.^{49, 38} Methyl *iso*-butyl ketone has the added advantage of also removing several impurities such as Fe, Te and As. Elimination of these elements at an early stage is desirable as they tend to interfere with other separations. Pd(II) is substitutionally labile meaning that extraction of $[PdCl_4]^{2-}$ can be achieved with long chain alkyl sulfides or hydroxyoximes which can directly coordinate to the metal centre through an inner-sphere substitution mechanism.³⁸ Alternatively, high molecular weight quaternary ammonium cations (such as tetrabutylammonium chloride and decyltrimethylammonium chloride) can be used to extract $[PdCl_4]^{2-}$ in a solvent extraction process.⁵⁰ Pt is the next metal to be separated and can be removed by ion exchange with an amine such as tri-*n*-octylamine under acidic conditions.³⁸ At this stage Rh(III), Ru(III) and Ir(III) remain

in solution. The extraction of Ru and Os chloro species is difficult owing to the complex series of equilibria that exist in solution (Figure 1.14).

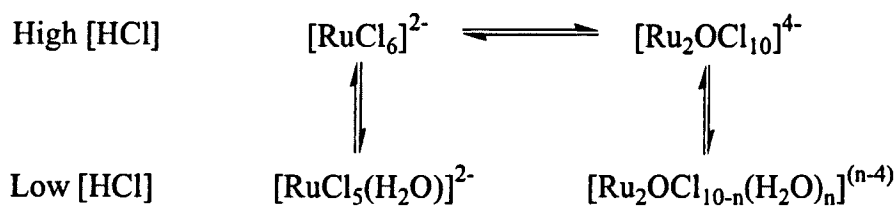


Figure 1.14. Complex equilibria exist for Ru in chloride solution.

The removal of Ru as RuO_4 by distillation has been reported.^{51, 58} There is also work detailing the use of mono-N-substituted amides to separate Ru in a solvent extraction process.^{52, 53, 54} The low stability of $[\text{IrCl}_6]^{3-}$ ion pairs results in Ir(III) being oxidised to Ir(IV) to give $[\text{IrCl}_6]^{2-}$, which can then be extracted using an amine in a similar manner to $[\text{PtCl}_6]^{2-}$. The ability to select Ir extraction by control of the metal oxidation state gives great flexibility in the extraction process.³⁸

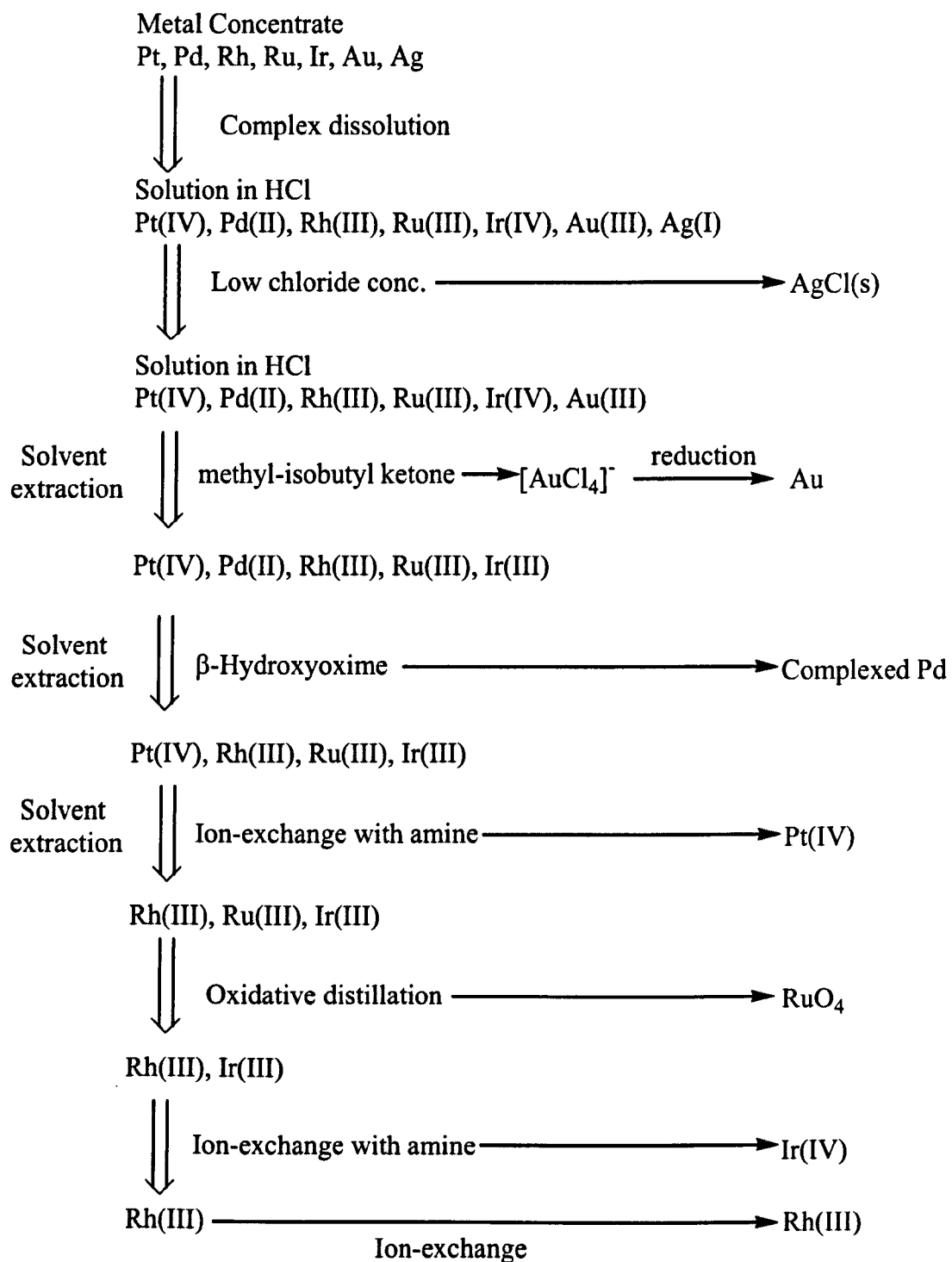


Figure 1.15. Modern refining method incorporating solvent extraction/ion-exchange.^{55,36}

Solvent extraction has been tailored for a range of non-precious metals including Cu and Co.⁵⁶ There is also work showing how solvent extraction can be used for a range of other metals including Ga,^{57,58} Te,⁵⁹ In,⁶⁰ and Sb.⁶¹

Solvent Extraction to Separate $[PtCl_6]^{2-}$

This Section provides more detail of how solvent extraction can be used to selectively extract and transport $[PtCl_6]^{2-}$. The extractants and processes that are used are commercially sensitive and precise details are not published. Platinum can be removed selectively by ion exchange using amine solvents. Secondary and tertiary amines and quaternary ammonium systems generally have acceptable distribution characteristics (Figure 1.16) meaning that the equilibrium in Equation 5 lies well to the right:³⁹

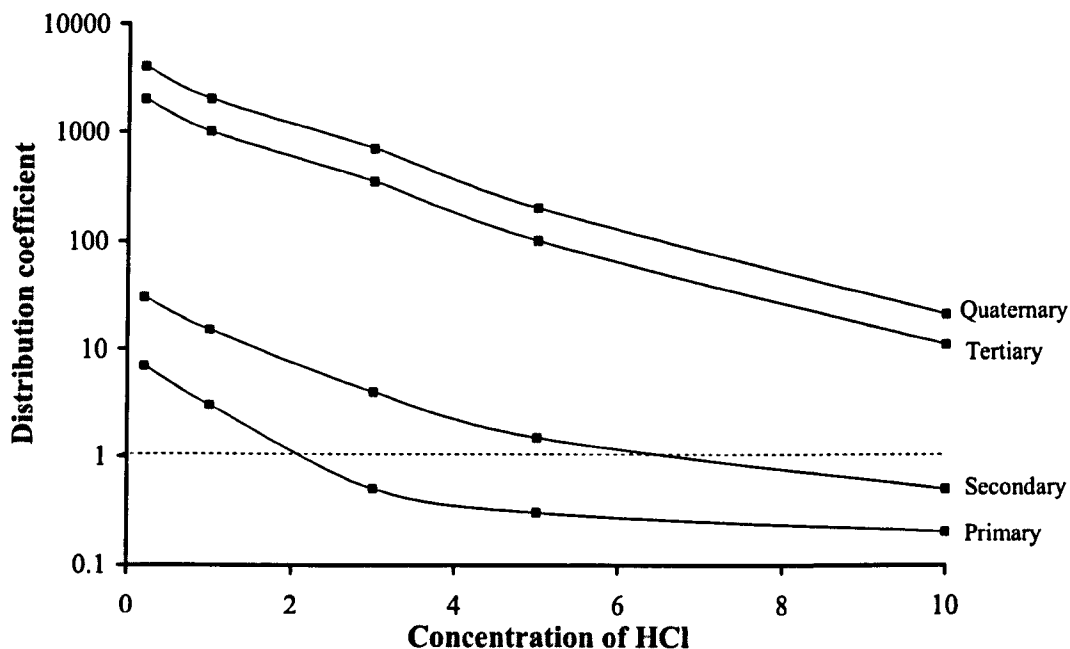
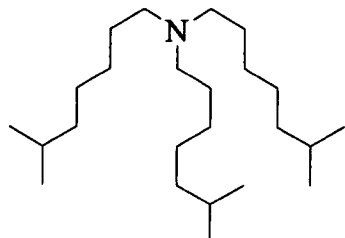


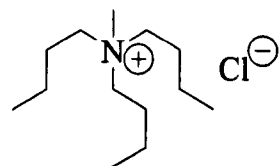
Figure 1.16. Distribution data for the extraction of $[PtCl_6]^{2-}$ by typical amines.³⁹

There is literature evidence suggesting that Alamine or Aliquat type reagents are used to extract $[PtCl_6]^{2-}$.^{32, 62} Alamines have three alkyl substituents bonded to a tertiary amine while Aliquats are amine quaternary salts with the positive charge counter balancing the negative charge of the anion (Figure 1.17). Extraction using Alamines relies on the protonation of the tertiary amine nitrogen to give a monocationic species $[LH]^+$ which can form an ion-pair with $[PtCl_6]^{2-}$. Aliquat extractants

do not require protonation prior to extraction. For both classes of extractant the organic solubility of the receptor and its complex is encouraged by hydrophobic alkyl substituents.



Alamine 308



Aliquat 175

Figure 1.17. Example of Alamine and Aliquat extractants.

There are several literature examples of the use of Alamine type reagents to extract $[\text{PtCl}_6]^{2-}$ in a solvent extraction process (Figure 1.18). Yoshizawa and co-workers studied the extraction and stripping equilibrium of $[\text{PtCl}_6]^{2-}$ between acidic chloride media and trioctylamine (TOA) in toluene.⁶³ Fu and co-workers,⁶⁴⁻⁶⁶ Hasegawa et al⁶⁷ and Mirza⁶⁸ have also studied the extraction of $[\text{PtCl}_6]^{2-}$ with TOA. Solvent extraction of $[\text{PtCl}_6]^{2-}$ using N-n-octylaniline has been described by Anuse⁶⁹,⁷⁰ and using Alamine 304 in xylene was studied by Alguacil and co-workers.⁷¹

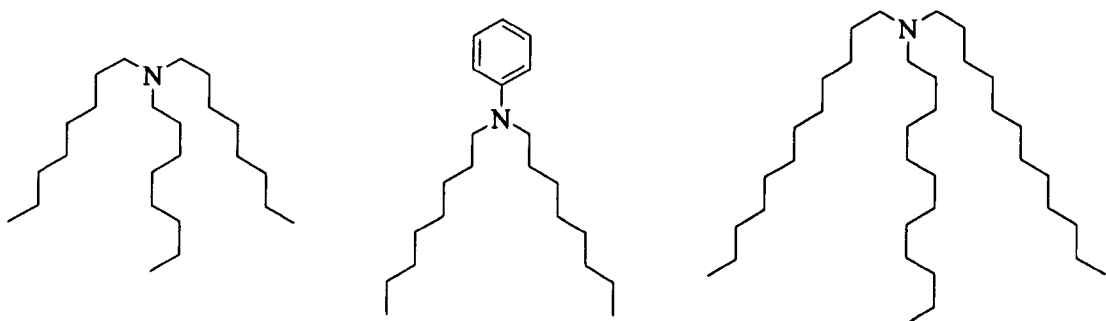


Figure 1.18. Examples of some Alamine based extractants for $[\text{PtCl}_6]^{2-}$ a) TOA; b) N-n-octylaniline and c) Alamine 304.⁶⁴⁻⁷¹

Yamamoto and co-workers have studied the liquid-liquid distribution of ion pairs of $[\text{PtCl}_6]^{2-}$ with quaternary ammonium counter ions.⁷² They found that long chain alkyltrimethylammonium cations were more effective than

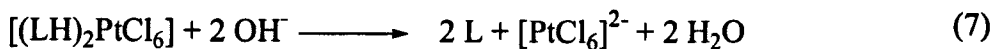
tetraalkylammonium cations for extraction of $[\text{PtCl}_6]^{2-}$ into CHCl_3 . This may be due to the alkyltrimethylammonium cations having less steric bulk enabling closer contacts within the ion-pairs and leading to improved extraction.

1.2.4.2.3. Recovery of Platinum from $[\text{PtCl}_6]^{2-}$

Following the extraction of $[\text{PtCl}_6]^{2-}$ into an organic phase it is necessary to back extract the chlorometallate species to enable the recovery of Pt. This can be accomplished by treating the organic phase with strong acid or alkali. Use of acid (HX) relies on substitution of $[\text{PtCl}_6]^{2-}$ for X^- leading to formation of $[(\text{LH})\text{X}]$ and release of $[\text{PtCl}_6]^{2-}$ (Equation 6):



Strong alkali is more commonly used to achieve stripping, deprotonation of the amine receptor removes the electrostatic attraction causing dissociation of the complex and release of $[\text{PtCl}_6]^{2-}$ (Equation 7):



The use of base has the disadvantage that inner-sphere complexes can be formed in which the amine nitrogen atom coordinates to the metal centre with associated loss of chloride ligands. (Equation 8):³⁹

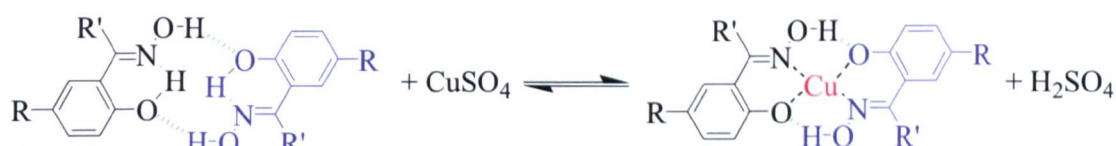


The substitution of chloride ligand for amine generally decreases in the order primary > secondary > tertiary > quaternary amine. This is why tertiary or quaternary amines typically have found use as solvent extractants for $[\text{PtCl}_6]^{2-}$. Quaternary salts are unable to form inner sphere complexes (unless degraded) but have the disadvantage of forming very strong ion-pairs which are difficult to strip.³⁶

Electrowinning can be used to obtain high purity metal from the metal containing species.^{32, 41, 73} It involves the electrodeposition of metals from their associated salts that are present in solution. It can be used on a large scale and is an important technique for the economical and straightforward purification of non-ferrous metals.

1.2.4.2.4. Examples of Industrial Solvent Extraction Processes

An example of an industrial solvent extraction process is the selective extraction of copper by phenolic oxime ligands (Figure 1.19).



(R and R' = monatomic substituents)

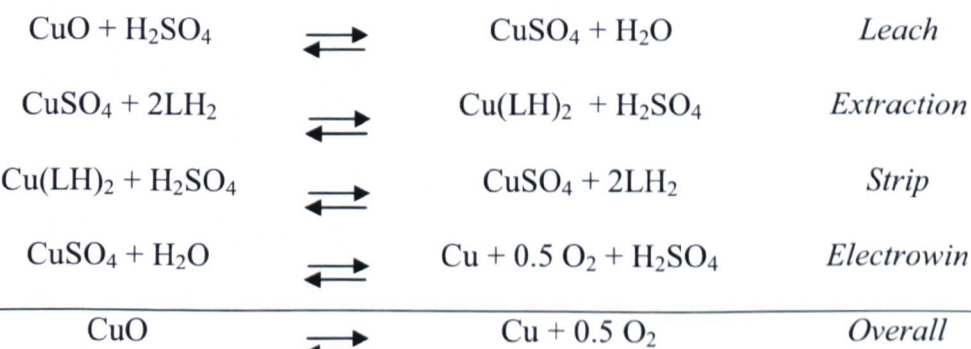


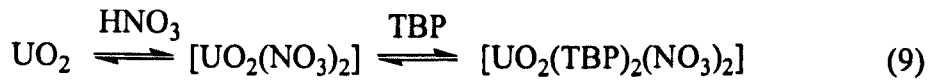
Figure 1.19. Phenolic oxime ligands can extract copper in a solvent extraction process.

In the first step CuO is leached from its ore using H₂SO₄ to give a pregnant leach solution containing a number of metal sulfates. The leached Cu(II) ions are extracted into the organic phase by the hydrophobic ligand (LH₂) to form a charge-neutral complex [Cu(LH)₂]. Following extraction, Cu is stripped from the loaded organic

phase using H_2SO_4 which re-protonates the ligands and releases Cu(II) to form a CuSO_4 solution. Re-protonation of the ligand to form organic soluble LH_2 means it can be recycled and used in further extraction cycles. Electrolysis of the CuSO_4 solution produces pure Cu metal (product) and H_2SO_4 (spent electrolyte) which is fed back into the stripping stage.^{42, 74, 75}

The success of this system depends on the fact that the oxime ligand is pH sensitive with the pH gradient being the driving force for the transport of the Cu(II) across the circuit. Under basic conditions the phenol is deprotonated enabling the formation of a pseudo-macrocyclic Cu(II) complex. The greater stability provided by chelating and macrocyclic ligands makes them better candidates than analogous unidentate or cyclic ligands.⁴³

Another example of an industrial scale process is the PUREX process (plutonium and uranium recovery by extraction) which uses solvent extraction to extract U(VI) and Pu(IV) from spent nuclear fuel. The irradiated fuel is dissolved in HNO_3 and extraction is achieved using tri-*n*-butyl phosphate (TBP) in kerosene. At high concentrations of HNO_3 , U(VI) is extracted to form the organic soluble complex $[\text{UO}_2(\text{TBP})_2(\text{NO}_3)_2]$ (Equation 9 and Figure 1.20). Back extraction is achieved by contact with dilute HNO_3 causing dissociation of the complex releasing $\text{U}(\text{NO}_3)_2$ and TBP. Pu(IV) forms a similar complex to U(VI) but it is possible to strip the Pu by reduction to Pu(III) which does not complex with TBP unless the nitrate concentration is very high.^{76, 77}



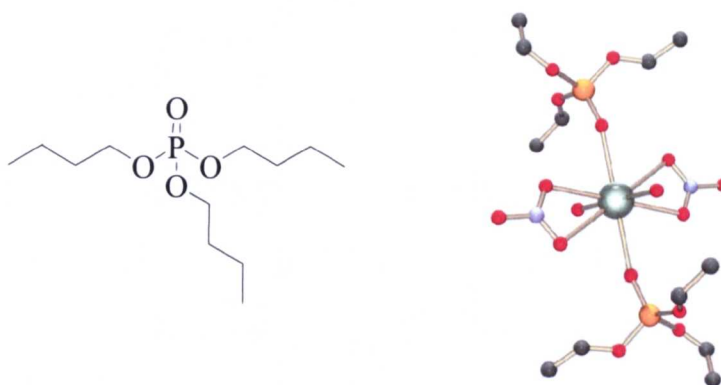


Figure 1.20. Structure of tri-n-butyl phosphate (TBP) and the $[UO_2(TBP)_2(NO_3)_2]$ complex.⁷⁸

1.2.4.2.5. Summary of Solvent Extraction

Solvent extraction offers a number of advantages over the classical precipitation methods. It offers higher selectivity and more complete removal of metals through the use of multi-stage extraction. This reduces the need for excessive recycling, shortens the refining times and lowers production costs and, as such, solvent extraction is being developed as an increasingly sound and diverse technique.²⁹

1.2.4.3. Other methods to separate PGMs

Solid-phase extraction methods can be used as an alternative to solvent extraction and precipitation. Work by Koch and co-workers reports the use of silica-based (poly)amine ion exchangers to selectively extract PGMs (Figure 1.21, a). Extraction experiments showed high selectivity for PGMs and no detectable amounts of transition metals were adsorbed.⁷⁹ Amberlite IRA 400 is another solid-phase extractant that uses anion-exchange (Figure 1.21, b).^{80,81}

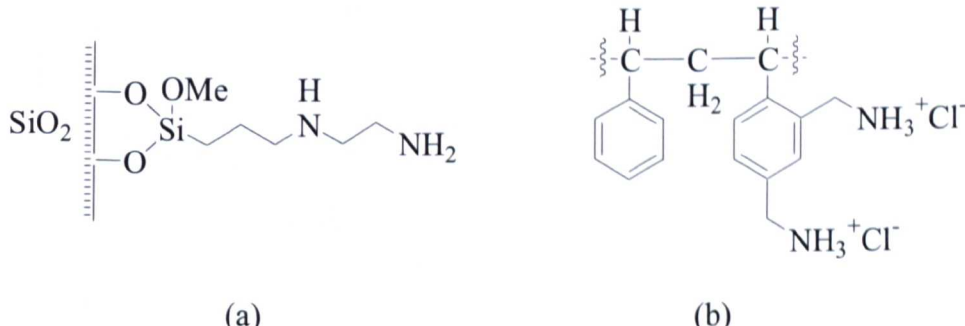


Figure 1.21. a) the structure of a silica based amine containing receptor and b) Amberlite IRA 400.⁷⁹⁻⁸¹

The Superlig® series are proprietary media which are thought to make use of cation and anion selective ligands covalently-bonded to solid supports.⁸² Their selectivity has been attributed to a high level of molecular recognition based on the selective fixation of certain ions as a function of their ionic radii and their chemical preferences. (Figure 1.22).⁸¹

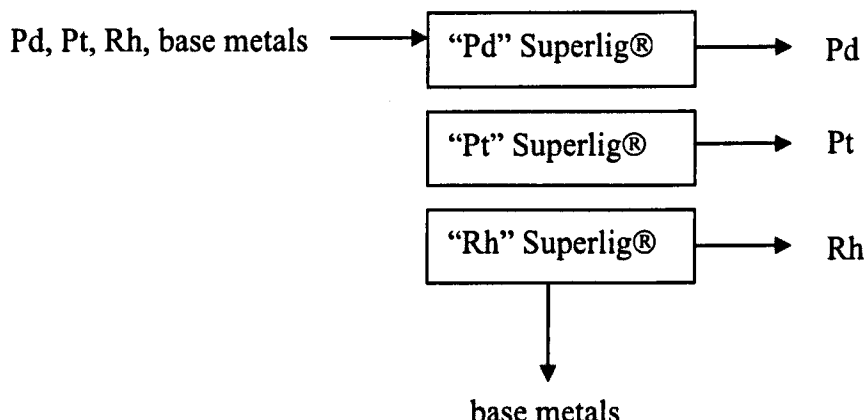


Figure 1.22. Separation of Pd, Pt and Rh from chloride media using Superlig® media.⁸²

Ion-exchange chromatography uses anion-exchange groups on solid supports for the separation of mixtures of PGMs and multiple separations are possible within a relatively short time.^{83, 84} For this reason the scaling up of chromatographic separation has been proposed as an alternative refining technique.⁸⁴ The Toyopearl® range of media are based on neutral polymethacrylates which support hydrophilic alcohols and ethers in addition to having an ester backbone.⁸⁵

1.2.5. Summary

The only cost effective method of bringing PGMs into solution is to dissolve the ore in *aqua regia* to form chlorometallate anions. The predominant Pt species in chloride solution is $[\text{PtCl}_6]^{2-}$ which is therefore the anion that we targeted in this work. As

solvent extraction is currently the preferred method to separate PGMs, the work described in the subsequent chapters has focussed on the design, synthesis and evaluation of organic receptors to selectively extract and transport $[\text{PtCl}_6]^{2-}$ in a solvent extraction process.

1.3. Anion Binding

1.3.1. Introduction

This Section provides an overview of anion coordination chemistry relevant to the project and highlights the key binding features that could be incorporated into the receptors for $[\text{PtCl}_6]^{2-}$. Research into anion binding has increased in the last twenty years and a continuous effort has been applied to the problems inherent in binding anions.⁸⁶⁻⁹³ There are a number of reasons for the increased interest in this field of chemistry. Chemically, anions play important roles in the area of catalysis⁹⁴ and in biology it is estimated that approximately 70% of enzyme substrates are negatively-charged. For example adenosine triphosphate (ATP) is a tetra-anion and deoxyribonucleic acid (DNA) is also a polyanion containing phosphate esters along its ribose backbone.⁹⁵⁻⁹⁷ Environmentally, anions can pose pollution problems. Nitrate anions found in fertilisers can be washed off agricultural land and into the water supply where they can cause problems such as eutrophication of water streams which disrupts aquatic life cycles.⁹⁸⁻¹⁰³

For a receptor to be selective for a particular anionic guest a high degree of design complementarity is required. Therefore, the size, geometry and charge of an anion are features that must be addressed if it is to be strongly bound by a receptor. The $[\text{PtCl}_6]^{2-}$ anion has an octahedral geometry with six chloride ligands bound to a Pt(IV) centre giving the species a net charge of -2 (Figure 1.23). The Cl—Pt—Cl distance across the anion is 4.61 Å.

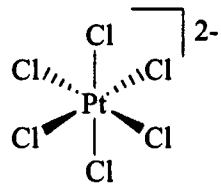


Figure 1.23. The octahedral geometry of the hexachloroplatinate(IV) anion, $[\text{PtCl}_6]^{2-}$.

1.3.2. Receptors for Anions

An anion receptor is a molecule that can bind to an anion via non-covalent interactions. Useful design features to incorporate into such receptors include electrostatic and hydrogen-bonding interactions and Lewis acid coordination.^{86, 90 97, 104-107} Receptors for anions must function within the pH window of their target anion as some anions are stable over a specific pH range and can become protonated at low pH consequently losing their negative charge.^{97, 107}

1.3.2.1. Electrostatic Interactions

The simplest and most obvious way of binding an anion is to use a positive charge to provide a strong electrostatic ion-ion interaction (Figure 1.24). Electrostatic interactions are based on the coulombic interaction between opposite charges. Ion-ion interactions are non-directional whilst ion-dipole interactions must be suitably aligned for optimal binding efficiency. A typical covalent bond has an energy of around 350 kJ mol⁻¹ whilst an ionic bond has a bond energy of 250 kJ mol⁻¹.¹⁰⁸ The high strength of electrostatic interactions makes them a very useful tool for achieving strong binding.

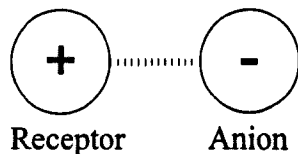


Figure 1.24. Using an electrostatic interaction to bind anions.

If a number of positively-charged groups are built into a receptor, they will tend to repel one another. To overcome this problem the positive charges can be built into a rigid system which has the added advantage of providing a binding pocket. Schmidtchen and co-workers produced a series of receptors that use quaternary ammonium groups arranged in a tetrahedral manner to bind anions inside a cage-like receptor (Figure 1.25, a).¹⁰⁹⁻¹¹² The four quaternary nitrogen atoms give the receptor a net charge of +4 and it forms 1:1 complexes with anionic guests in aqueous solution. By altering the length of the alkyl chain between the four ammonium groups Schmidtchen was able to tune the selectivity of the receptor for particular halides. Thus, for $X = (\text{CH}_2)_6$ the internal diameter is approximately 4.6 Å which provides a good match to the iodide anion which has a diameter of 4.12 Å. The smaller halides, whilst fitting inside the cavity of the receptor are not as strongly bound due to a poorer size complementarity.

A problem with using receptors that have a permanent positive charge is that they have a counter anion associated with them which may compete for the anion binding site. To overcome this limitation Schmidtchen modified the structure of the macrotricyclic receptor to produce a zwitterionic structure which has no net charge and therefore no counter ion (Figure 1.25, b).^{113, 114} It was found that this receptor binds anions more strongly as there is no competition from counter anions.

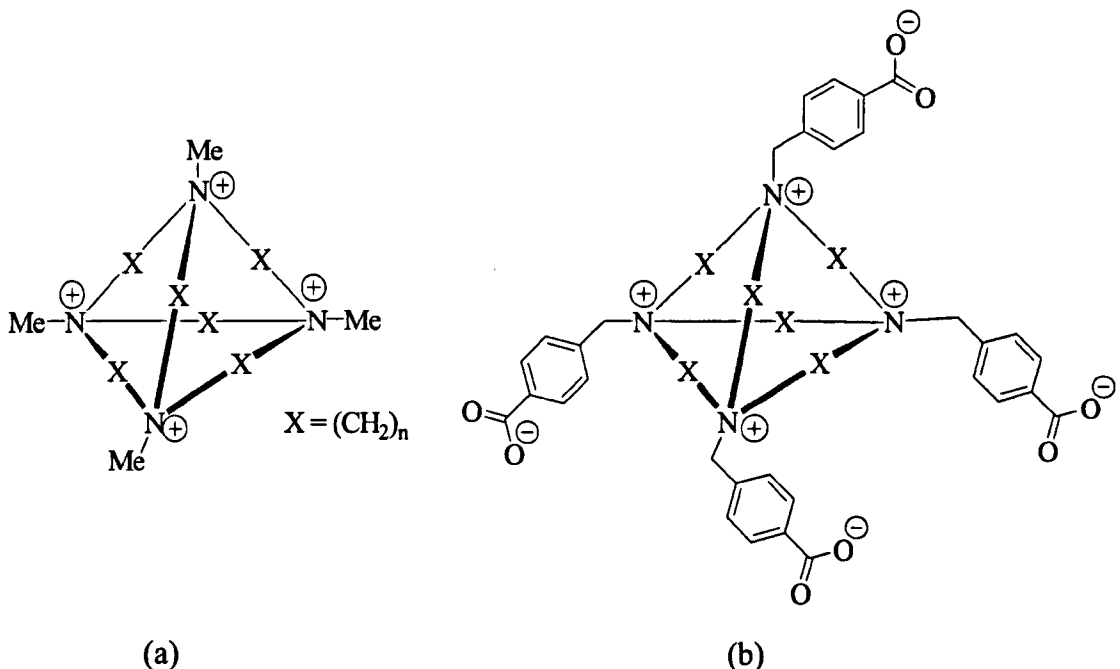


Figure 1.25. Examples of receptors that use electrostatic interactions to interact with an anion.¹⁰⁹⁻¹¹⁴

In addition to anion receptors that utilise a permanent cationic charge it is also possible to use a dipolar bonds to form an electrostatic interaction with an anion. The receptor shown in Figure 1.26 has its dipoles convergently aligned providing a halide binding site below the macrocyclic ring.^{115, 116}

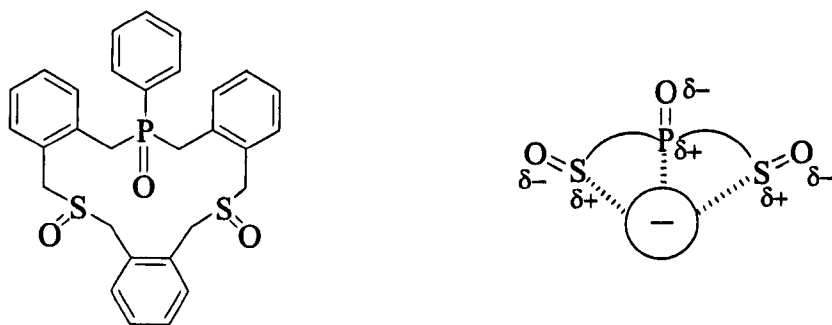


Figure 1.26. Views of a dipolar anion receptor.^{115, 116}

The protonation of a receptor under acidic conditions facilitates anion binding and subsequent treatment of the ion-pair with base deprotonates the receptor reverting it back to its charge-neutral state. Consequently, the anion is decomplexed and the uptake and release of the anion is thus controlled by variation of pH in a so

called “pH swing mechanism”. Appropriate functional groups that can be protonated to form a cationic receptor include amines,^{117, 118} pyridines,¹¹⁹ and imidazoles.¹²⁰

The heteroditopic receptor shown in Figure 1.27 illustrates how the protonation of a tertiary amine facilitates anion binding.¹²¹⁻¹²⁶ The receptor is designed to extract metal sulfates, MSO_4 , and has two binding pockets: one to bind to M^{2+} and one for the SO_4^{2-} counter ion. The receptor itself is neutral and upon coordination of M^{2+} a proton is transferred from each of the two hydroxyl groups to each of the two tertiary amine groups. Thus, it is a zwitterionic form of the ligand that binds the cation and anion at separate binding sites. The hydroxyl groups have a -1 charge to interact with the M^{2+} cation whilst the pendant tertiary amine groups are protonated and bind to the SO_4^{2-} anion.¹²⁴

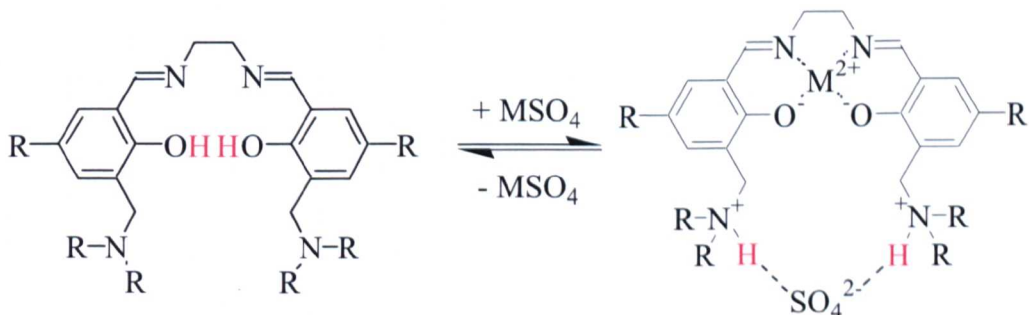


Figure 1.27. Metal(II) sulfate binding by a zwitterionic ligand.¹²⁴

A functionalised thioether receptor capable of simultaneously binding Ag^+ and NO_3^- is known (Figure 1.28).¹²⁷ Anion binding occurs via a switch mechanism whereby coordination of the metal cation breaks internal hydrogen-bonds allowing an anion to bind to the urea hydrogen sites on the attached pendant arms. No anion binding occurs in the absence of a bound metal ion demonstrating that an electrostatic interaction contributes to the binding of NO_3^- by the receptor.

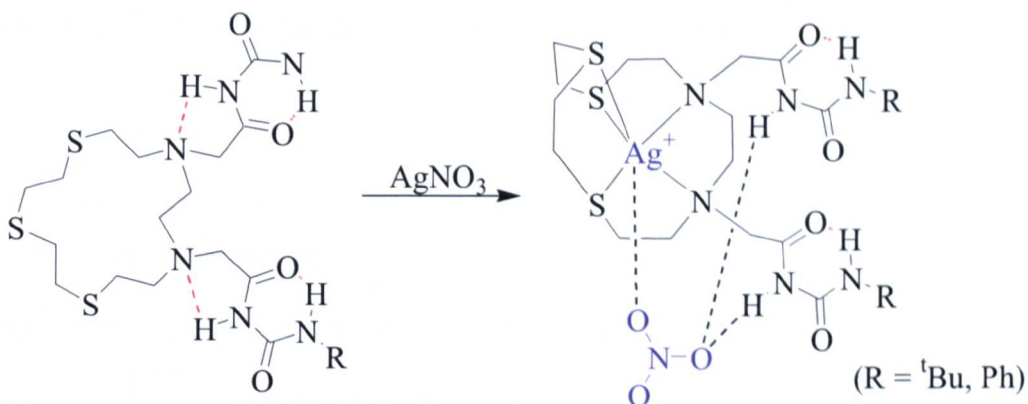


Figure 1.28. Using a ditopic receptor to bind AgNO_3 .¹²⁷

A ditopic receptor capable of binding monovalent salts is shown in Figure 1.29. Various sodium and potassium salts (NaNO_3 , NaNO_2 , KNO_3) can be bound to the receptor by a contact ion pair between the metal cation that is bound to the crown ether ring, and the oxyanion that is hydrogen-bonded to the receptor NH residues.¹²⁸

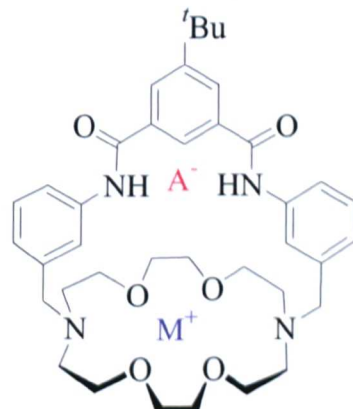


Figure 1.29. Using a ditopic receptor to bind metal salts.¹²⁸

1.3.2.2. Using Electrostatics to Bind $[\text{PtCl}_6]^{2-}$

Alamine and Aliquat reagents use electrostatics to extract $[\text{PtCl}_6]^{2-}$. As protonation of Alamines is required to enable an electrostatic interaction with $[\text{PtCl}_6]^{2-}$, they have the advantage that the uptake and release of the anion can be controlled by a pH swing mechanism. In contrast, the Aliquat extractants are permanently cationic meaning that they can extract without acid but stripping and recovery of the anion

can be difficult. Using electrostatics is a feature to be considered in the design of our receptor systems.

1.3.2.3. Hydrogen-bonding

A hydrogen atom attached to an electronegative element (X = fluorine, oxygen or nitrogen) can be a hydrogen-bond donor. A hydrogen-bond acceptor (A) must have a lone pair of electrons to interact with an X—H bond. As anions have a lone pair of electrons they can behave as hydrogen-bond acceptors and thus the incorporation of hydrogen-bonds into a receptor provides a route to the binding of the target anion (Figure 1.30).

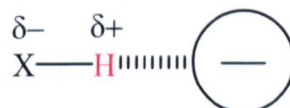


Figure 1.30. Anions can accept hydrogen-bonds.

Hydrogen-bond energies extend from 60-170 kJ mol⁻¹ for strong hydrogen-bonds, 17-60 kJ mol⁻¹ for moderate bonds and 4-17 kJ mol⁻¹ for weak bonds.¹²⁹ The strength of a hydrogen-bond is inversely proportional to the H···A length and a strong hydrogen-bond is often associated with a short H···A distance. Strong hydrogen-bonds are also associated with X—H···A bond angles close to 180° and observed downfield shifts in the ¹H NMR spectrum. In contrast, weak hydrogen-bonds have smaller X—H···A bond angles and a shorter X—H distance than H···A distance (Table 1.3).¹²⁹⁻¹³¹

Table 1.3. Some properties of strong, moderate and weak hydrogen-bonds

	Strong	Moderate	Weak
X—H \cdots A interaction	Mostly covalent	Mostly electrostatic	Electrostatic
Bond lengths	X—H \approx H \cdots A	X—H < H \cdots A	X—H << H \cdots A
$\theta(X—H\cdots A)^\circ$	175–180	130–180	90–150
Bond energy/kJ mol $^{-1}$	60–170	17–60	4–17
Examples	F $^-$ —H \cdots F $^-$	O/N—H \cdots O=C	C—H \cdots O/N
		O—H \cdots O—H	O/N—H \cdots π

Because hydrogen-bonds are long-range interactions, a group X—H can be bonded to more than one acceptor. A bifurcated hydrogen-bond has two acceptors or two donors and a trifurcated hydrogen-bond has three acceptors (Figure 1.31).

**Figure 1.31.** Examples of different types of hydrogen-bonding geometry; a) linear b) bifurcated donor and c) bifurcated acceptor and d) trifurcated.

X-ray diffraction is a useful tool to characterise solid-state hydrogen-bonds and the primary information obtained is the distance and bond angle of the X—H \cdots A moiety. The H \cdots A distance should be shorter than the sum of the van der Waals radii of H and the acceptor.^{130, 132} The limitation of crystallography arises as it only shows the interactions as they are present in the solid state and it may be more suitable to study the interactions in solution using other methods.

NMR spectroscopy can be a useful tool for studying supramolecular interactions in solution. The frequency at which a particular nucleus resonates is dependent on its electronic environment, and, thus any changes to this electronic environment will be seen as a shift in the signal in the NMR spectrum.^{133, 134} Other

techniques that can be used are UV/visible spectroscopy and mass spectrometry. UV/visible can be especially useful for the investigation of π electron systems or transition metals as their spectra can be strongly perturbed on complex formation.¹³⁵ Mass spectrometry can also be used to detect the host-guest complex although it may be observed as its constituent fragments.

1.3.2.4. Hydrogen-bond Donor Groups

Functional groups such as amides,¹³⁷⁻¹⁴⁵ ureas¹⁴⁶ and thioureas¹⁴⁷⁻¹⁵² have acidic NH protons enabling NH...anion hydrogen-bonding (Figure 1.32). To maximise the interaction between a receptor and anion it is generally favourable to incorporate several hydrogen-bond donors into the receptor.¹⁵³

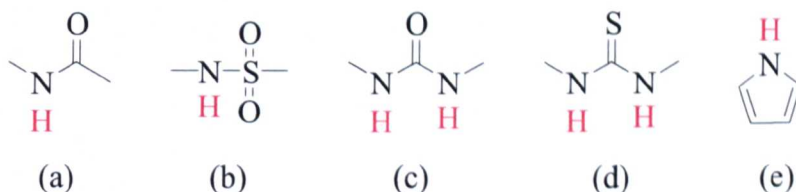


Figure 1.32. Examples of hydrogen-bond donor groups a) Amide b) Sulfonamide c) Urea d) Thiourea e) Pyrrole.

Amides and Sulfonamides

The amide and sulfonamide hydrogen-bond donor groups both have one acidic NH donor per moiety which can hydrogen-bond to an anion.^{137, 154} There are many examples of anion receptors that utilise amide or sulfonamide groups to hydrogen-bond to the target anion some of which are subsequently discussed.

In 1986, Pascal prepared the first amide-based receptor which interacts with the anion solely through NH...anion hydrogen-bonds.¹⁵⁵ This receptor has three amide NH groups pointing into a central cavity (Figure 1.33). The X-ray crystal structure suggested that the dimensions of the cavity were favourable for fluoride binding and subsequent ^1H NMR titrations in $\text{dmso}-d_6$ confirmed this to be the case.

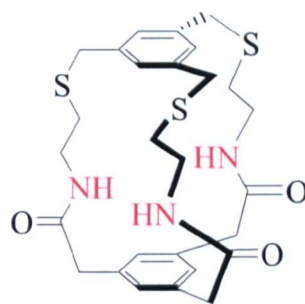


Figure 1.33. Example of an amide hydrogen-bonding receptor.¹⁵⁵

Acyclic tripodal receptors containing amide or sulfonamide units have been used to bind anions. The flexibility of such ligands allows adjustments in the size of the cavity as well as formation of almost linear hydrogen-bonds.¹³³ The C₃ symmetric tripodal amide and sulfonamide receptors (Figure 1.34 a and b, respectively) have been shown to bind tetrahedral anions such as H₂PO₄⁻, HSO₄⁻ and VO₄³⁻ in CHCl₃.¹⁵⁶ Crabtree and co-workers have shown that simple acyclic, non-pre-organised diamide receptors (Figure 1.34, c) can be used to bind Br⁻ in CH₂Cl₂.¹⁵⁷



Figure 1.34. Structures of some amide and sulfonamide anion hosts.^{156, 157}

Amide moieties have also been introduced into macrocyclic anion receptors. For example, the rigid, cyclic peptide shown in Figure 1.35 contains the unnatural amino acid 3-amino-benzoic acid which acts as a rigid element to orient the hydrogen-bond donating amide groups to the centre of the macrocycle.¹⁵⁸ This receptor was found to bind to phosphomonoester ([PO₄R]²⁻) via hydrogen-bonding

interactions between the amide protons on the peptide backbone and the phosphate oxygen atoms. Similar peptide-based receptors for the coordination of anionic species have been reported.¹³⁷⁻¹⁴⁵

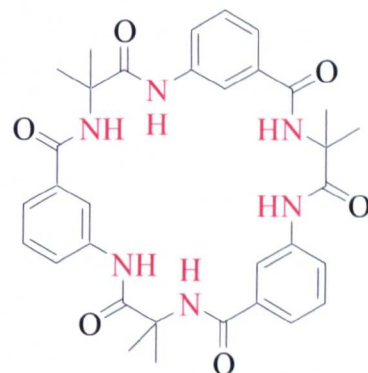


Figure 1.35. An example of a cyclic amide receptor for anions.¹⁵⁸

Urea and Thiourea

Urea and thiourea groups have two acidic NH donors per moiety and find use in receptors for anions owing to their ability to act as hydrogen-bond donors.¹⁵⁹⁻¹⁶² Following the seminal papers by Wilcox¹⁶³ and Hamilton¹⁴³ on urea-anion interactions, a variety of anion receptors have been reported in which one or more urea/thiourea fragments are incorporated into an acyclic, cyclic or polycyclic framework.¹⁶⁴⁻¹⁷⁸

The hydrogen-bond donating tendencies of an NH group are related to its protonic acidity. Thiourea is a stronger acid than urea ($pK_a = 21.1$ and 26.9 , respectively in dmso)¹⁷⁹ and thus it is expected that thiourea containing receptors establish stronger hydrogen-bond interactions with anions than their urea counterparts. Receptors incorporating a urea or thiourea hydrogen-bond unit have been compared by Fabbrizzi and co-workers (Figure 1.36).^{105, 159} The urea and thiourea derivatives both formed 1:1 hydrogen-bonded complexes with various anions including $H_2PO_4^{2-}$, Cl^- and F^- in dmso. In the presence F^- the urea receptor undergoes deprotonation and HF is released to form $[HF_2]^-$. In the case of the

thiourea receptor, because it is more acidic, deprotonation takes place with each of the anions studied.

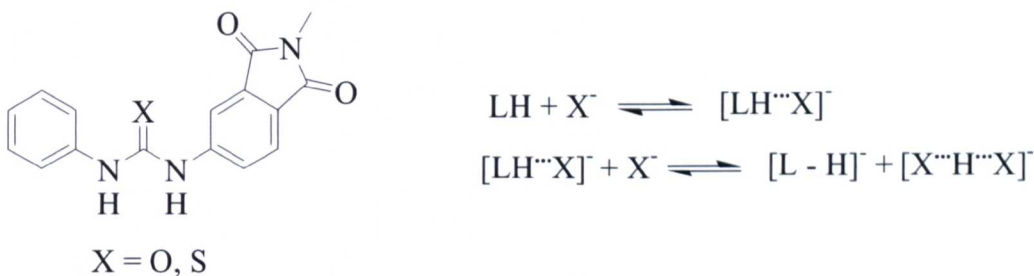


Figure 1.36. Comparison of urea and thiourea hydrogen-bond donor groups.^{105, 159}

Kelly and Kim have reported the synthesis and binding studies of mono-urea and bis-urea ligands.¹⁸⁰ A simple urea-based receptor produced stable complexes with mono-anionic carboxylate, mono- and di-anionic phosphate groups (Figure 1.37, a). The bis-urea was designed to serve as a receptor for dinitro substituted benzenes and it was thought that this receptor might find use as a sensor to detect explosives such as TNT (Figure 1.37, b). However, binding studies confirmed that it had similar binding properties to the mono-ligands with an affinity for di-anionic phosphate groups.

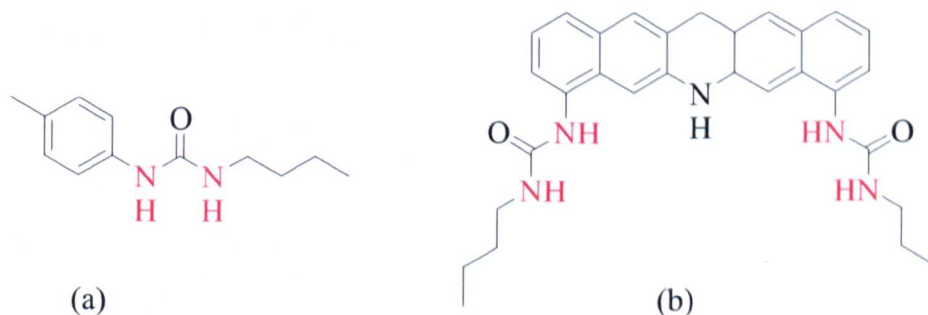


Figure 1.37. Examples of urea based receptors.¹⁸⁰

Cyclic ureas and thioureas have also been synthesised by numerous groups for the selective binding of anions.¹⁴⁶ Reinhoudt and co-workers have described the synthesis of a macrocyclic anion receptor containing four pre-organised urea moieties (Figure 1.38, a).¹⁸¹ A study of the anion binding ability of this receptor with

the tetrabutyl ammonium salt of H_2PO_4^- in dmso showed there to be pronounced effects in the ^1H NMR spectrum. The cyclic thiourea receptor shown in Figure 1.38b was found to have selectivity for H_2PO_4^- over AcO^- , Cl^- , HSO_4^- and Br^- .^{176, 182}

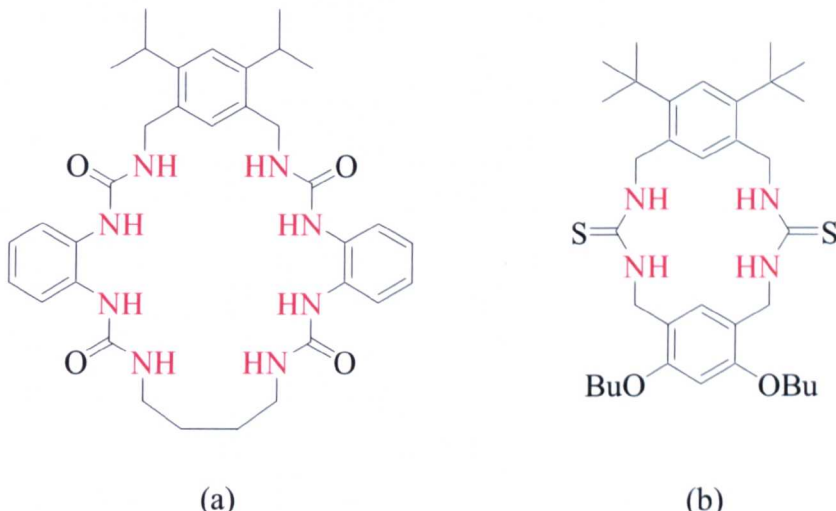


Figure 1.38. Examples of cyclic urea and thiourea-based receptors.^{176, 181, 182}

Pyrroles and Amidopyrroles

Pyrrole moieties can use their NH group to form hydrogen-bonds to anions and in recent years pyrrole-containing entities have emerged as one of the most versatile and useful of anion binding moieties.^{183, 184} Part of the attraction of pyrrole containing receptors unit is that they do not contain a built-in hydrogen-bond acceptor. This means that intraligand $\text{N}-\text{H}\cdots\text{O}=\text{C}$ cannot be formed with pyrroles.¹⁸³

The use of pyrroles has been pioneered by Sessler and co-workers who have incorporated these moieties into macrocycles to bind anions.¹⁸⁵⁻¹⁸⁷ The pyrrole based receptor shown in Figure 1.39 has been shown to bind F^- , Cl^- and H_2PO_4^- in CD_2Cl_2 .

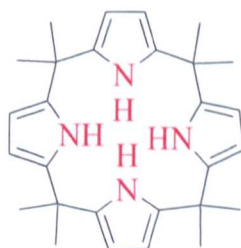


Figure 1.39. The structure of octamethylcalix[4]pyrrole.¹⁸⁵⁻¹⁸⁷

Amidopyrrole containing receptors incorporate two NH donors arranged in a convergent manner that can bind anions (Figure 1.40, a).¹⁸⁸ Gale and co-workers have used the amidopyrrole moiety in a variety of anion receptors, an example of which is shown below (Figure 1.40, b).¹⁸⁹ They found that this receptor was selective for carboxylate oxo-anions and crystallographic analysis of the complex showed the anion to be located in the binding pocket between the two pendant arms.¹⁹⁰

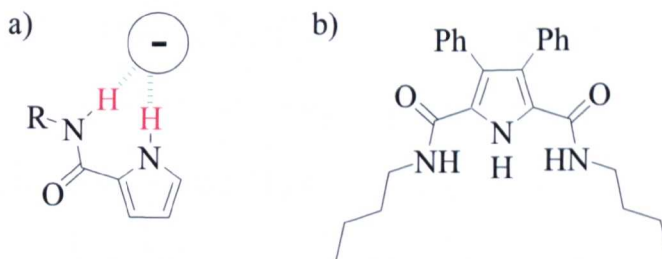


Figure 1.40. a) Amidopyrroles providing convergent hydrogen-bonds to an anion and b) an example of a receptor which uses amidopyrrole to bind anions.^{189, 190}

1.3.2.5. Using Hydrogen-bonding to Target $[\text{PtCl}_6]^{2-}$

Orpen and Brammer have carried out a study to assess the hydrogen-bonding capabilities of the M—Cl unit.¹⁹¹ The Cambridge Structural Database was used to analyse 6624 crystallographically characterised hydrogen-bonds that contain M—Cl, C—Cl or Cl[−] and either NH or OH groups. The objective of this work was to compare the geometry of D—H^{···}Cl interactions and to assess the relative probability of such contacts being formed in these different environments.

The D—H^{···}Cl intermolecular interactions were categorised as short (H^{···}Cl \leq 2.52 Å), intermediate (2.52 – 2.95 Å) and long (2.95 – 3.15 Å) (*cf.* sum of van der Waals radii for H and Cl = 1.2 + 1.75 = 2.95 Å). The percentage of interactions that fall in the various categories (in particular the ‘short’ group) were taken as an indicator of the strength of the interaction. It was found that Cl[−] forms many short Cl[−]H interactions, as does the M—Cl group, whereas C—Cl moieties form almost no short Cl[−]H interactions resulting in the sequence of acceptor strengths being Cl[−]

$> M-Cl \geq C-Cl$. The implication of these observations is that $M-Cl$ containing complexes have the potential to interact with hydrogen-bond donors in both a strong (i.e. short) and anisotropic manner. It is thought that halogens bonded to transition metals are good hydrogen-bond acceptors because of the strongly polarised character of the $M-X$ bond resulting in an enhanced partial negative charge of the halogen.¹⁹²

¹⁹³ The correlation of $D-H\cdots Cl$ angles with $H\cdots Cl$ distances shows a predominance of $D-H\cdots Cl^-$ angles close to 180° at short $H\cdots Cl^-$ separations.¹⁹⁴ In contrast, the preferred angle for $D-H\cdots Cl-M$ interactions was found to be between $90 - 130^\circ$ attributed to the contribution of the axial p orbital to the $M-X$ bonds.^{192, 195, 196}

A subsequent study of metal-assisted hydrogen-bonding was undertaken by Brammer and co-workers who analysed hydrogen-bonds between N—H, O—H and C—H and X—M ($M = F, Cl, Br, I$) moieties.¹⁹⁵ They observed that the length of the $H\cdots X$ interactions increases in the order $F < Cl < Br < I$. Thus, hydrogen-bonds with metal fluorides were found to be markedly shorter than those of their heavier halogen congeners. This is in agreement with the expected trends for the strength of hydrogen-bonds based on the polarity of the $X-M$ bond.

The potential of chlorometallate anions to act as hydrogen-bond acceptors has been confirmed by Orpen and co-workers who observed bifurcated $N-H\cdots Cl-Pt$ hydrogen-bonds between NH^+ pyridinium moieties and $[PtCl_4]^{2-}$ anions (Figure 1.41).¹⁹⁶

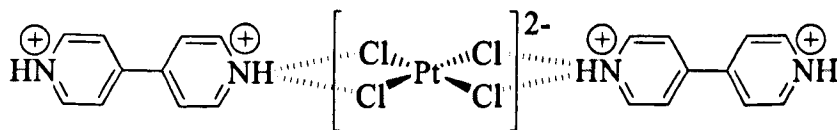


Figure 1.41. Hydrogen-bonds between bipyridinium cations and $[PtCl_4]^{2-}$.¹⁹⁶

Using hydrogen-bonds to target other chlorometallate anions is also known. Heteroditopic azathioether macrocycles incorporating acylurea functionalised

pendant arms can simultaneously bind the cationic and anionic moieties of a metal salt as confirmed by the crystal structure of $[\text{CuCl}(\text{L})_2\text{CuCl}_4$ (Figure 1.42).¹⁹⁷ The asymmetric unit contains two $[\text{CuCl}(\text{L})]^+$ cations and one $[\text{CuCl}_4]^{2-}$ dianion. The $[\text{CuCl}_4]^{2-}$ species is hydrogen-bonded to the acylurea NH of each arm with $\text{N}2 \cdots \text{Cl}6 = 3.29(2)$ Å and $\text{N}5 \cdots \text{Cl}5 = 3.27(2)$ Å.

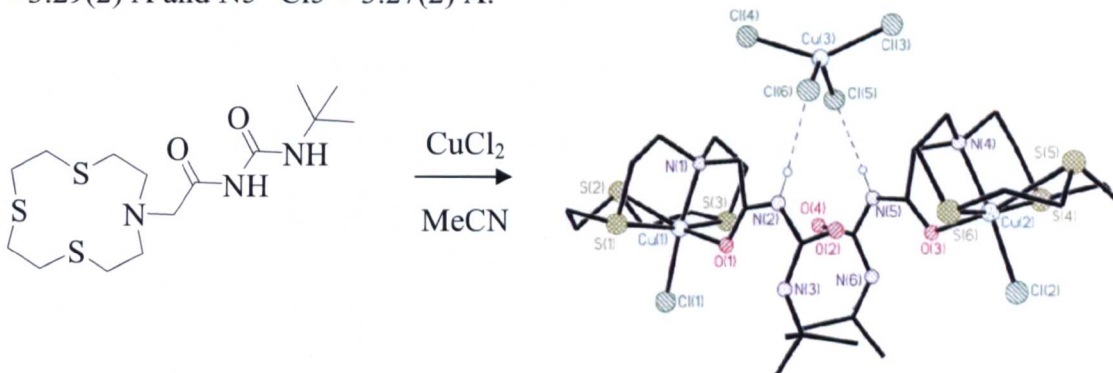


Figure 1.42. View of the structure of $[\text{CuCl}(\text{L})_2\text{CuCl}_4$.¹⁹⁷

There is also work showing the incorporation hydrogen-bonds into receptors for $[\text{PdCl}_4]^{2-}$,¹⁹⁸ $[\text{AuCl}_4]^-$,¹⁹⁸ $[\text{CoCl}_4]^{2-}$,^{199, 200} $[\text{OsCl}_6]^{2-}$,²⁰¹ $[\text{MnCl}_4]^{2-}$,^{199, 202} $[\text{CdCl}_4]^{2-}$,^{199, 202} $[\text{PbCl}_4]^{2-}$,¹⁹⁹ $[\text{FeCl}_5]^{2-}$,²⁰¹ $[\text{ZnCl}_4]^{2-}$,^{199, 202, 203} and $[\text{HgCl}_4]^{2-}$.¹⁹⁹ In these systems a range of supramolecular architectures were observed in which N—H···Cl hydrogen-bonds formed to the outer sphere of the chlorometallate anions. Some examples of which are shown in Figure 1.43.

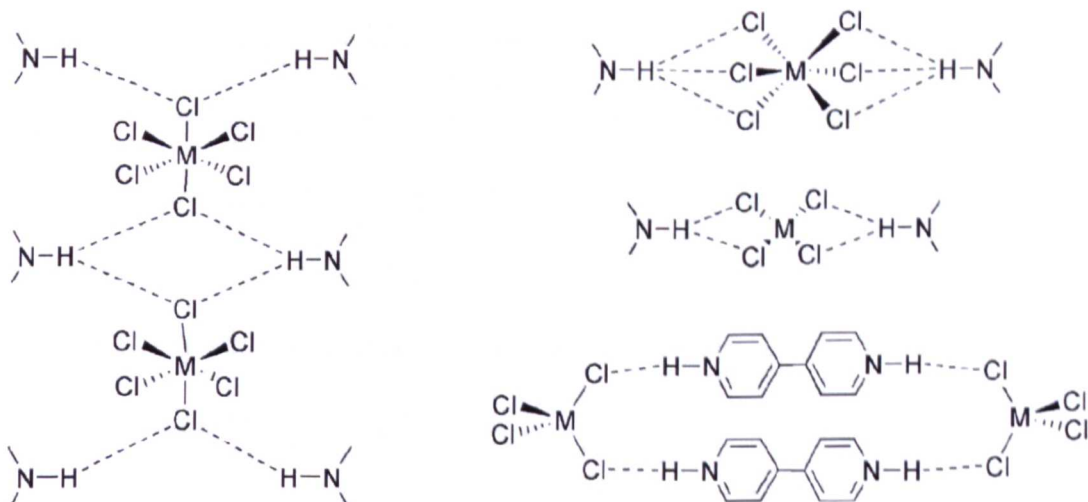


Figure 1.43. Examples of connectivity motifs which use hydrogen-bonds to target chlorometallate anions.

1.3.2.6. Areas of High Electron Density Surrounding $[\text{PtCl}_6]^{2-}$

To enable a strong and selective interaction between a receptor and $[\text{PtCl}_6]^{2-}$, it is important to assess the areas of high electron density around the anion which can be targeted by hydrogen-bonds. The directional preference of hydrogen-bond donors to terminal metal halides is governed by the electrostatic potential around the halide ligand, which can be explained in terms of a simple orbital model of metal-halide bonding (Figure 1.44).²⁰⁴ The area between two chloride ligands is targeted by the NH group as it is electron rich due to the two p orbitals containing lone pairs of electrons.²⁰⁵

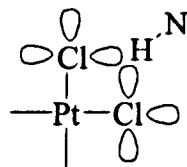


Figure 1.44. The NH group targets the lone pairs of chloride in a $[\text{PtCl}_6]^{2-}$ species.²⁰⁵

In addition to this simple orbital model there are reports of using crystallographic analyses,²⁰⁶ Density Functional Theory (DFT) calculations²⁰⁶⁻²⁰⁹ and ^{195}Pt NMR spectroscopic studies²⁰⁹ to establish the areas of highest electron density surrounding $[\text{PtCl}_6]^{2-}$. Brammer and co-workers analysed structures in the Cambridge Structural Database to identify close contacts between N—H groups and octahedral $[\text{MCl}_6]^{n-}$ anions.²⁰⁶ Although no restriction was placed on charge, dianions were found to be the most common chlorometallate species and the distribution of hydrogen-bond donors in the vicinity of the anion were analysed as population density plots (Figure 1.45). The results show that the edges and faces of the octahedron are targeted by NH groups.

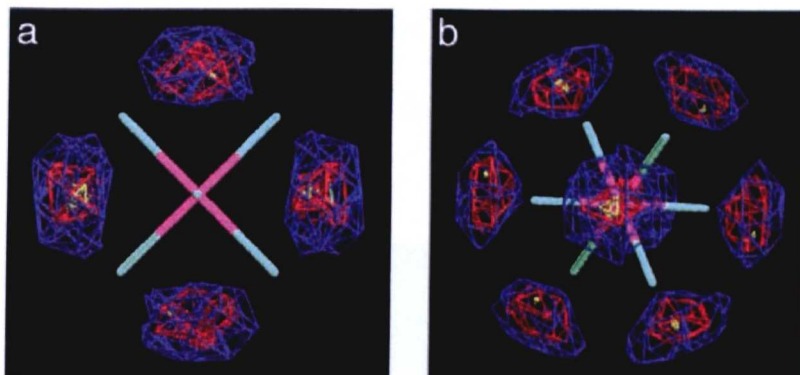


Figure 1.45. The experimental population density of hydrogen atoms from NH groups in the vicinity of octahedral $[MCl_6]^{2-}$ anions obtained from crystal structure data; viewed parallel to a) 4-fold molecular axis and b) 3-fold molecular axis. Contours; blue 35%, red 55%, yellow 80% of maximum population.²⁰⁶

Theoretical methods have also been used to calculate the negative electrostatic potentials of $[PdCl_6]^{2-}$ (Figure 1.46).²⁰⁶ The areas of highest negative electrostatic potential correspond to areas in which there is the highest electron density. These areas are located around each of the six chloride ligands and along the edges and in the faces of the octahedron. These results correlate with the previously described simple orbital model and the results of the crystallographic analyses.

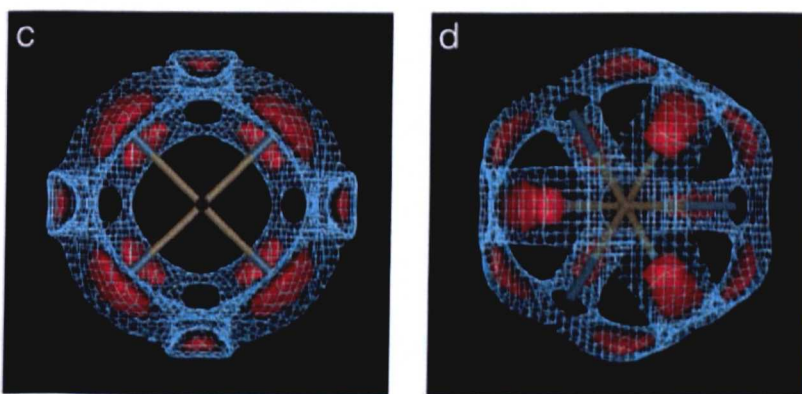


Figure 1.46. Calculated negative electrostatic potential in the vicinity of the $[PdCl_6]^{2-}$ anion; viewed parallel to a) 4-fold molecular axis and d) 3-fold molecular axis. Contours; solid at -196 kcal/mol, mesh at -194 kcal/mol. The areas of highest electron density are shown in red.²⁰⁶

Koch and co-workers have described the use of molecular dynamic calculations alongside ^{195}Pt NMR spectroscopy to reveal well-defined hydration shells around $[PtCl_6]^{2-}$ in H_2O (Figure 1.47). Eight H_2O molecules were found to be

located in close proximity to the anion, with each H_2O molecule hydrogen-bonding to a face defined by three coordinated chloride ligands of the octahedron of the $[\text{PtCl}_6]^{2-}$.²⁰⁹

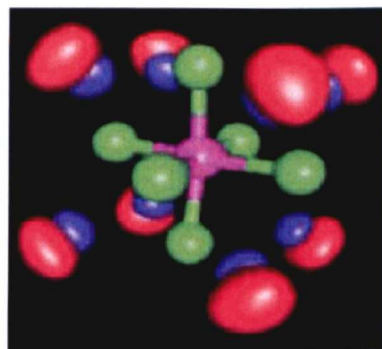


Figure 1.47. The probability density surfaces of O atoms (red) and H atoms (blue) at 100% greater than bulk solvent (H_2O or MeOH) for $[\text{PtCl}_6]^{2-}$.²⁰⁹

Compiling the results of these studies leads to the summary that the areas of highest electron density surrounding a $[\text{PtCl}_6]^{2-}$ anion are located along the 12 edges and within the eight faces of the octahedron. Bifurcated and trifurcated hydrogen-bonds can be used to target these areas (Figure 1.48).

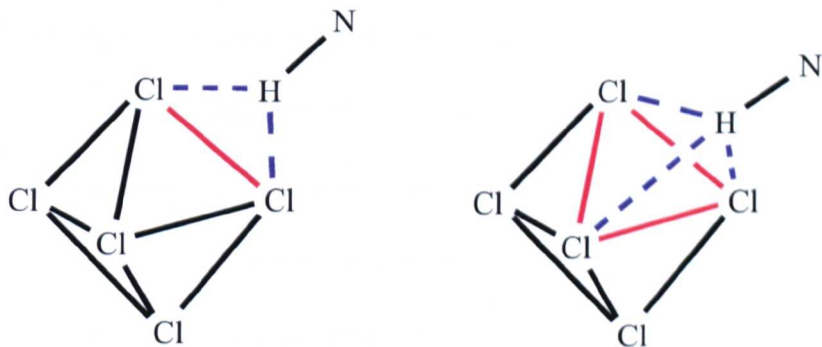


Figure 1.48. Bifurcated and trifurcated hydrogen-bonds can be used to address the edges and faces of $[\text{PtCl}_6]^{2-}$.

1.3.2.7. Other Methods to bind Anions

Lewis-acidic centres can bind anions by an orbital overlap and this has led to the development of anion receptors that contain boron,²¹⁰⁻²¹⁵ mercury,^{216, 217} silicon,^{218, 219} germanium,²²⁰⁻²²³ and tin centres.²²⁴⁻²²⁸ Organoboron compounds have only six valence electrons making them ideal as electron pair acceptors. The first examples of

this type of anion receptor were reported in 1967 by Shriver and Biallis.²²⁹ The chelating receptors illustrated in Figure 1.49 have two terminal BX_2 groups which can accept an electron pair from an anion. When compared with non-chelating, mononuclear BF_3 an overall chelate effect was observed.^{213, 214}

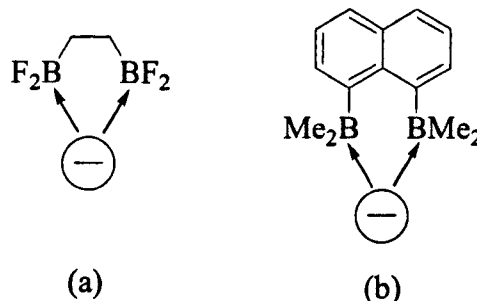


Figure 1.49. a) a chelating boron anion receptor and b) Katz's rigid preorganised chelating ligand for anionic guests.^{213, 214}

Organomercury receptors have also found use as anion receptors. The Hg centre is sp-hybridised and, therefore, contains two unfilled π -orbitals with geometric reorganisation not required to accept electron pairs. An example of a mercury based receptor is shown in Figure 1.50a and a crystal structure confirmed the Cl^- anion to be strongly coordinated to all four atoms of mercury.^{216, 217, 219} Although tetravalent organotin has a full valence shell of eight electrons, it is still capable of accepting additional electron pairs into low-lying unoccupied molecular orbitals. An example is the organotin macrocycle shown in Figure 1.50b which can encapsulate halide anions to form a complex with 1:1 stoichiometry.²³⁰

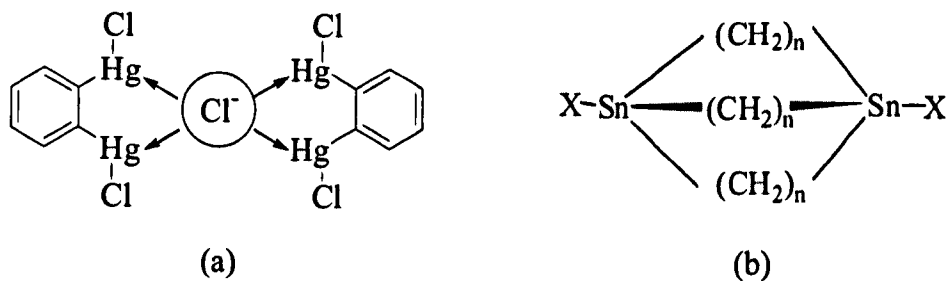


Figure 1.50. Examples of a) mercury and b) tin based anion receptors.^{216, 217, 230}

1.3.2.8. Recognition of Anions Using a Combination of Interactions

To achieve a strong and selective interaction, it is common to use a number of different types of interaction together in one receptor. These binding features can be incorporated onto different scaffolds such as macrocyclic¹⁴⁶ or acyclic ligands such that the chelate and macrocyclic effect will contribute to the stability of the resulting complex.²³²

Gale and co-workers have reported a metal-organic anion receptor containing a urea functionalised iso-quinoline ligand that exhibits strong binding of sulfate (Figure 1.51a).²³³ In this receptor hydrogen-bonds are used in combination with electrostatic interactions to bind the target anion. A cobaltocenium system functionalised with amide moieties binds anions via the cooperative binding forces of mutual electrostatic attraction between the positively-charged guest and amide NH...anion hydrogen-bonding interactions. (Figure 1.51b).^{234, 235} Related receptors that do not contain amide NH donor groups do not complex anions, highlighting the complementarity of the binding moieties. Guanidine is readily protonated to form the guanidinium cation which is stabilised by resonance and charge-delocalisation to provide both electrostatic and hydrogen-bonding interactions (Figure 1.51c).²³⁶⁻²³⁹ Schmidtchen and co-workers have incorporated the guanidinium group into a bicyclic ring and found that these receptors form hydrogen-bonding arrays similar to those present in ureas.²⁴⁰

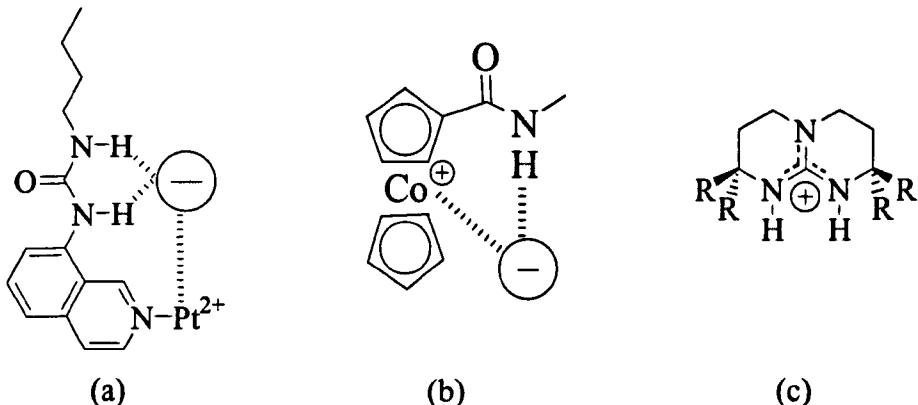


Figure 1.51. a) An example of a receptor that uses a combination of electrostatic attraction and hydrogen-bonds.²³³ b) An amide functionalised cobaltocenium receptor binds anions.^{234, 235} c) Example of a guanidinium anion receptor.²⁴⁰

1.3.4. Summary

To enable the efficient design of a receptor for $[\text{PtCl}_6]^{2-}$ we can draw upon previous research carried out into anion binding. The size, charge and geometry of the anion are factors to consider in the design of a receptor and proven, successful techniques to bind anions include electrostatics, hydrogen-bonds and Lewis acid-base type interactions. The scaffold of the receptor is also important as is the production of a charge-neutral species to aid the dissolution of the complex in organic solvents in a solvent extraction process.

1.4. Aims of Project

The research presented in the following Chapters is aimed at synthesising organic receptors that can extract and transport $[PtCl_6]^{2-}$ from an aqueous phase into an immiscible organic phase in a solvent extraction process. Improvements to the extraction process will lead to increased materials balances and larger amounts of Pt being recovered. The driving force for this research is that Pt is a scarce and costly metal with a wide range of technological applications and an ever increasing demand. Interest in this research arises both from an academic viewpoint as a proof

of concept and also as any advancements made may be of benefit to the companies involved in the refining of Pt-containing ores.

The aims of the work described in this thesis are:

- To design receptors with features that can interact with $[\text{PtCl}_6]^{2-}$
- To synthesise receptors, ideally in the minimum number of synthetic steps and in high yielding reactions from commercially available starting materials
- To evaluate our receptors by forming complexes with $[\text{PtCl}_6]^{2-}$
- Develop a method for testing the extraction efficiency of our receptor systems in a solvent extraction process and carry out solvent extraction studies with our receptors
- Optimise the design of our receptors to achieve maximum extraction

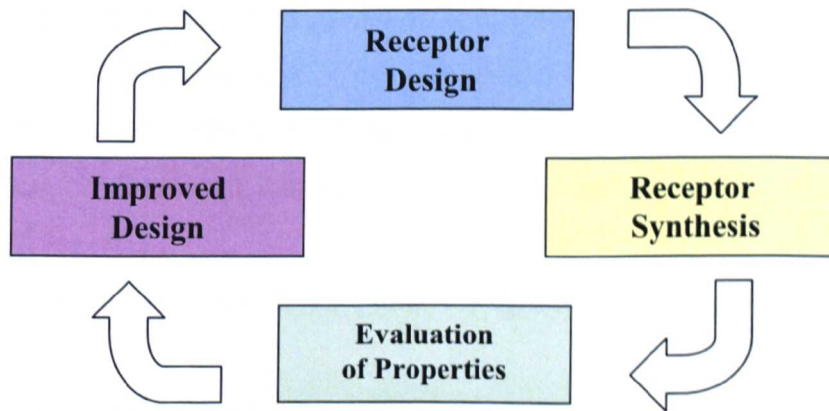


Figure 1.52. Our approach to finding a successful extractant for $[\text{PtCl}_6]^{2-}$.

1.5. References

1. Alam M. S.; Inoue K., *Hydrometallurgy*, 1997, **46**, 373-382.
2. Mhaske A. A.; Dhadke M., *Hydrometallurgy*, 2001, **61**, 143-150.
3. Golunski S. E., *Plat. Met. Rev.*, 2007, **51**, 162.
4. Acres G. J. K., *Plat. Met. Rev.*, 1970, **14**, 2-10.
5. Twigg M. V., *Plat. Met. Rev.*, 1999, **43**, 168-171.
6. Alam M. S.; Inoue K.; Yoshizuka K., *Hydrometallurgy*, 1998, **49**, 213-227.
7. Baba Y.; Fukumoto T., *Chem. Lett.*, 1992, 727-730.
8. Kim C. H.; Woo S. L.; Jeon S. H.; *Ind. Eng. Chem. Res.*, 2000, **39**, 1185-1192.
9. Nowotny C.; Halwachs W.; Schugerl K., *Sep. Purif. Technol.*, 1997, **12**, 135-144.
10. Wright J. C., *Plat. Met. Rev.*, 2002, **46**, 66-72.
11. Clarke M. L., *Polyhedron*, 2001, **20**, 151-164.
12. Kettler P. B., *Org. Proc. Res. Dev.*, 2003, **7**, 342-354.
13. Bond G. C., *J. Mol. Catal. A: Chem.*, 2000, **156**, 1-20.
14. Bond G. C., *Plat. Met. Rev.*, 2000, **44**, 146-155.
15. Okafor V. I.; Coville N. J., *S. Afr. J. Sci.*, 1999, **95**, 503-508.
16. Strukul G.; Michelin R. A., *Chem. Commun.*, 1984, 1538-1539.
17. Strukul G.; Michelin R. A., *J. Am. Chem. Soc.*, 1985, **107**, 7563-7569.
18. Baccin C.; Gusso A.; Pinna F.; Strukul G., *Organometallics*, 1995, **14**, 1161-1167.
19. Zanardo A.; Michelin R.A.; Pinna F.; Strukul G., *Inorg. Chem.*, 1989, **28**, 1648-1653.
20. Strukul G.; Sinigalia R.; Zanardo A.; Pinna F.; Michelin R. A., *Inorg. Chem.*, 1989, **28**, 554-559.
21. Chandrasekhav S.; Prakash S.Y.; Rao C. L., *J. Org. Chem.*, 2006, **71**, 2196-2199.
22. Voorhees V.; Adams R., *J. Am. Chem. Soc.*, 1922, **44**, 1397-1405.
23. Hunt L. B., *Plat. Met. Rev.*, 1962, **6**, 15-152.
24. Alderden R. A.; Hall M. D.; Hambley T. W., *J. Chem. Ed.*, 2006, **83**, 728-735.
25. Wheate N. J.; Collins C. J., *Coord. Chem. Rev.*, 2003, **241**, 133-145.

26. Seymore R. J.; O'Farrelly J. I.; Potter L.C. In *Encyclopaedia of Chemical Technology*; Howe-Grant M. (Ed), Vol. 19, Fourth ed., Wiley, New York, pp 367.
27. Renner H. In *Ullmann's Encyclopaedia of Industrial Chemistry*; Elvers B.; Hawkins S.; Schultz G. (Eds), Vol. A21, Fifth ed., VCH Publishers, 1992, pp 114.
28. www.platinum.matthey.com (accessed October 2007)
29. Bernardis F. L.; Grant R. A.; Sherrington D. C., *React. Funct. Poly.*, 2005, **65**, 205-217.
30. Cawthorn R. G., *S. Afr. J. Sci.*, 1999, **95**, 481-489.
31. www.platinummetalsreview.com (accessed October 2007)
32. Tasker P. A.; Plieger P. G.; West L. C., *Comp. Coord. Chem.* 2, 2004, **9**, 759-808.
33. Galbraith S. G.; Tasker P. A., *Supramol. Chem.*, 2005, **17**, 191-207.
34. Juksing H. G.; McCrindle R. I., *J. Chem. Technol. Biotechnol.*, 2001, **76**, 349-354.
35. Kriek R. J.; Engelbrecht W. J.; Cruywagen J. J.; *J. S. Afr. Inst. Min. Metall.*, 1995, 75-81.
36. Cleare M. J.; Grant R. A.; Charlesworth P., *Extr. Metall.*, 1981, **34**, 34-41.
37. Pearson R. G., *J. Am. Chem. Soc.*, 1963, **85**, 3533-3539.
38. Charlesworth P., *Plat. Met. Rev.*, 1981, **25**, 106-112.
39. Cleare M. J.; Charlesworth P.; Bryson D. J., *J. Chem. Tech. Biotechnol.*, 1979, **29**, 210-224.
40. Leung B. K., Hudson J. M., *Solv. Extr. Ion Exch.*, 1992, **10**, 173-190.
41. Habashi F., *Miner. Eng.*, 1994, **7**, 1209.
42. Galbraith S. G.; Tasker P. A., *Supramol. Chem.*, 2005, **17**, 191-207.
43. Yordanov A. T.; Roundhill D. M., *Coord. Chem. Rev.*, 1998, **170**, 93-124.
44. Deratani A.; Sebille B., *Anal. Chem.*, 1981, **53**, 1742-1746.
45. Preston J. S.; du Preez A. C., *Solv. Extr. Ion Exch.*, 2002, **20**, 359-374.
46. Grant R., In *Proceedings of IPMI Seminar on Precious Metals Recovery and Refining*; L. Manzeik (Ed), Scottsdale, AZ, USA, 1989.
47. Willard H., Merritt L., Dean J., Settle F., In *Instrumental Methods of Analysis*, Wadsworth, California, 1988, pp 636.
48. Al-Bazi S. J.; Chow A., *Talanta*, 1984, **31**, 815-836.
49. Morris D. F. C.; Ali Khan M., *Talanta*, 1968, **15**, 1301-1305.

50. Yamamoto K.; Fujibayashi T.; Motomizu S., *Solv. Extr. Ion Exch.*, 1992, **10**, 459-476.
51. Ali Khan M.; Morris D. F. C.; *Sep. Sci.*, 1967, **2**, 635-644.
52. Grant R. A.; Smith C. S., *Process Metallurgy*, 1990, **7A**, 433-438.
53. Grant R. A.; Burnham R. F.; Collard S., *Process Metallurgy*, 1992, **7A**, 961-966
54. Grant R. A., *Precious Metals and Refining Seminar*, 1990, 7-41.
55. Renner H., In *Ullmann's Encyclopaedia of Industrial Chemistry*; Elvers B. S., Hawkins S., Schulz G. (Eds), Vol. A21, VCH Publishers, 1992, pp 114.
56. Sole K.; Feather A. M.; Cole P. M., *Hydrometallurgy*, 2005, **78**, 52-78.
57. Yamamoto K.; Katoh N., *Anal. Sci.*, 1999, **15**, 1013-1016.
58. Hirayama N.; Horita Y.; Ohima S.; Kubono K.; Kokusen H.; Honjo T., *Talanta*, 2001, **53**, 857-862.
59. Yamamoto K.; Adachi K., *Talanta*, 1998, **47**, 1065-1069.
60. Yamamoto K.; Matsumoto A., *Talanta*, 1997, **44**, 2145-2150.
61. Yamamoto K.; Shimakawa T., *Anal. Sci.*, 2000, **16**, 641-645.
62. Wisniewski M.; Szymanowski J., *Polish. J. App. Chem.*, 1996, **40**, 17-26.
63. Yoshizawa H.; Shiromori K.; Yamada S.; Baba Y.; Kawano Y.; Kondo K.; Ijichi K.; Hatake Y., *Solv. Extr. Res. Devel.*, 1997, **4**, 157-166.
64. Fu J.; Nakamura S.; Akiba K., *Sep. Sci. Technol.*, 1995, **30**, 609-619.
65. Fu J.; Makamura S.; Akiba K., *Anal. Sci.*, 1995, **11**, 149-153.
66. Fu J.; Nakamura S.; Akiba K., *Sep. Sci. Technol.*, 1997, **32**, 1433-1445.
67. Hasegawa Y.; Kobayashi I.; Yoshimoto S., *Solv. Extr. Ion Exch.*, 1991, **9**, 759-768.
68. Mirza M. Y., *Talanta*, 1980, **27**, 101-106.
69. Lokhande T. N.; Anuse M. A.; Chavan M. B., *Talanta*, 1998, **47**, 823-832.
70. Kolekar S. S.; Anuse M. A., *Sep. Sci. Technol.*, 2003, **38**, 2597-2618.
71. Alguacil F. J.; Cobo A.; Coedo A. G.; Dorado M. T.; Sastre A., *Hydrometallurgy*, 1997, **44**, 203-212.
72. Yamamoto K.; Katoh S., *Talanta*, 1996, **43**, 61-66.
73. Szymanowski J., In *Hydroxyoximes and Copper Hydrometallurgy*; CRC Press, Inc. London, 1993.
74. Levin D. (Zeneca Ltd), Eur. Pat. Appl., 584988, 1994.
75. Smith A. G.; Tasker P. A.; White D. J., *Coord. Chem. Rev.*, 2003, **241**, 61-85.

76. Carrott M. J.; Fox O. D.; Maher C. J.; Mason C.; Taylor R. J.; Sinkov S. I.; Choppin G. R. *Solv. Extr. Ion Exch.*, 2007, **25**, 723-745.
77. Bodansky D., *Phys. Today*, 2006, **59**, 80-81.
78. Burns J. H., *Inorg. Chem.*, 1983, **22**, 1174-1178.
79. Kramer J.; Driessen W. L.; Koch K.; Reedijk J., *Hydrometallurgy*, 2002, **64**, 59-68.
80. Floyd L. G., In *2nd International Conference on New Process for Ruthenium, Rhodium and Iridium*, Int. Precious Metals Institute Inc., New York, 1978.
81. Izatt R. M.; Bradshaw J. S.; Bruening R. L.; Izatt N. E.; Krakowiak K. E., In *Metal Separation Technologies Beyond 2000: Integrating Novel Chemistry with Processing*; Liddell K. C.; Chaiko D.J. (Eds), Symposium Proceeding, Hawaii, June 13-18 1999, TMS, 357-370.
82. Bergeron M.; Beaumier M.; Hebert A., *Analyst*, 1991, **116**, 1019-1024.
83. Jones P.; Schwedt G., *Anal. Chim. Acta.*, 1989, **220**, 195-205.
84. Smuckler G., U.S. Patent 4885143, 1999.
85. a) Grant R. A., Taylor Y., US Patent 5,879,644, 1999. b) Sasaki H., Kmiya K., Kato Y., US Patent 4,256,842, 1981.
86. Gale P. A., *Coord. Chem. Rev.*, 2000, **199**, 181-233.
87. a) *Supramolecular Chemistry of Anions*; Bianchi A.; Bowman-James K.; Garcia-Espana E. (Eds), Wiley-VCH, New York, 1997. b) Lehn J. M.; *Pure Appl. Chem.*, 1978, **50**, 871-892.
88. Beer P. D.; Schmitt P., *Curr. Biol. Chem. Biol.*, 1997, **1**, 475-482.
89. Antonisse M. M. G.; Reinhoudt D. N., *Chem. Comm.*, 1998, 443-448.
90. Schmidtchen F. P.; Berger M., *Chem. Rev.*, 1997, **97**, 1609-1646.
91. Dietrich B., *Pure Appl. Chem.*, 1993, **65**, 1457-1464.
92. Scheerder J.; Engbersen J. F. J.; Reinhoudt D. N., *Recl. Trav. Chim. Pays-Bas*, 1996, **115**, 307-320.
93. Beer P. D.; Smith D. K., *Prog. Inorg. Chem.*, 1997, **46**, 1-96.
94. Scheele J.; Timmerman P.; Reinhoudt D. N., *Chem. Commun.*, 1998, 2613-2614.
95. Christianson D. W.; Lipscomb W. N., *Acc. Chem. Res.*, 1989, **22**, 62-69.
96. Lange L. G.; Riordan J. F.; Vallee B. L., *Biochem.*, 1974, **13**, 4361-4370.
97. Beer P. A.; Gale P. A., *Angew. Chem. Int. Ed.*, 2001, **40**, 486-516.
98. Harrison R. M., *Pollution: Causes, Effects and Control*, Royal Society of Chemistry, London, 1983.

99. Moss B., *Chem. Ind.*, 1996, 407-411.
100. Hasler A. D., *Ecology*, 1947, **28**, 383-395.
101. Sfiro A.; Pavoni B., *Environ. Technol.*, 1994, **15**, 1-14.
102. Holloway J. M., Dahlgren R. A.; Hansen B.; Casey W.H., *Nature*, 1998, **395**, 785-788.
103. Glidewell C., *Chem. Br.*, 1990, **26**, 137-140.
104. Scheerder J.; Engbersen J. F. J.; Reinhoudt D. N., *Recl. Trav. Chim. Pays-Bas*, 1996, **115**, 307-320.
105. Amendola V.; Bonizzoni M.; Esteban-Gomez D.; Fabbrizzi L.; Licchelli M.; Sancenon F.; Taglietti A., *Coord. Chem. Rev.*, 2006, **205**, 1451-1470
106. Antonisse M. M. G.; Reinhoudt D. N., *Chem. Commun.*, 1998, 443-448.
107. *Supramolecular Chemistry*; P. D. Beer, P. A. Gale, D. K. Smith (Eds), Oxford University Press, Oxford, 1999.
108. Sanderson R. T.; *Chemical Bonds and Bond Energy*; Academic Press, New York, 1976.
109. Schmidtchen F. P., *Angew. Chem.*, 1977, **89**, 751-752.
110. Schmidtchen F. P., *Chem. Ber.*, 1980, **113**, 864-874.
111. Schmidtchen F. P., *Chem. Ber.*, 1981, **114**, 597-607.
112. Schmidtchen F. P.; Muller G., *Chem. Commun.*, 1984, 1115-1116.
113. Worm K.; Schmidtchen F. P.; Schier A.; Schafer A.; Hesse M., *Angew. Chem. Int. Ed. Engl.*, 1994, **33**, 327-329.
114. Worm K.; Schmidtchen F. P., *Angew. Chem. Int. Ed. Engl.*, 1995, **34**, 65-66.
115. Savage P. B.; Holmgreen S. K.; Gellman S. H., *J. Am. Chem. Soc.*, 1993, **115**, 7900-7901.
116. Savage P. B.; Holmgreen S. K.; Gellman S. H., *J. Am. Chem. Soc.*, 1994, **116**, 4069-4070.
117. Llinares J. M.; Powell D.; Bowman-James K., *Coord. Chem. Rev.*, 2003, **240**, 57-75.
118. Wichmann K.; Antonioli B.; Sohnle T.; Wenzel M.; Gloe K.; Price J. R.; Lindoy L. F.; Blake A. J.; Schröder M., *Coord. Chem. Rev.*, 2006, **250**, 2897-3003.
119. Jeong K. S.; Cho Y. L., *Tet. Lett.*, 1997, **38**, 3279-3282.
120. Yun S.; Ihm H.; Kim H. G.; Lee C. W.; Indrajit B.; Oh K. S.; Gong Y. J.; Lee J. W.; Yoon J.; Lee H. C.; Kim K. S., *J. Org. Chem.*, 2003, **68**, 2467-2470.

121. Galbraith S. G.; Plieger P. G.; Tasker P. A., *Chem. Commun.*, 2002, 2662-2663.
122. Galbraith S. G.; Plieger P. G.; Tasker P. A., *Dalton Trans.*, 2004, 313-318.
123. White D. J.; Laing N.; Miller H.; Parsons S.; Coles S.; Tasker P. A., *Chem. Commun.*, 1999, 2077-2078.
124. Gasperov V.; Galbraith S. G.; Lindoy L. F.; Rumbel B. R.; Skelton B. W.; Tasker P. A.; Whire A. H., *Dalton Trans.*, 2005, 139-145.
125. Coxall R. A.; Lindoy L. F.; Miller H. A. Parkin A.; Parsons S.; Tasker P. A.; White D. J., *Dalton Trans.*, 2003, 55-64.
126. Akkus N.; Campbell J. C.; Davidson J.; Henderson D. K.; Miller H. A.; Parkin A.; Parsons S.; Plieger P. G.; Swart R. M.; Tasker P. A.; West L. C., *Dalton Trans.*, 2003, 1932-1940.
127. Glenny M. W.; Blake A. J.; Schröder M., *J. Chem. Soc., Dalton Trans.*, 2003, 1941-1951.
128. Mahoney J. M., Stucker K. A., Jiang H., Carmichael I., Brinkmann N. R., Beatty A. M., Noll B. C., Smith B. D., *J. Am. Chem. Soc.*, 2005, **127**, 2922-2928.
129. Emsley J., *Chem. Soc. Rev.*, 1980, **9**, 91-124.
130. Jeffrey G. A.; *An Introduction to Hydrogen Bonding*, Oxford University Press, Oxford, 1997, pp 12.
131. Desiraju G. R., Steiner T.; *The Weak Hydrogen Bond*, Oxford University Press, Oxford, 1999.
132. Desiraju G. R.; Steiner T.; *The Weak Hydrogen Bond in Structural Chemistry and Biology*, Oxford University Press, Oxford, 1999.
133. Kavallieratos K.; Bertao C. M.; Crabtree R. H., *J. Org. Chem.*, 1999, **64**, 1675-1683.
134. Blande M. T.; Horner J. H.; Newcomb M., *J. Org. Chem.*, 1989, **54**, 4626-4636.
135. Sessler J. L.; Davis J. M.; Krai V.; Kimbrough T.; Lynch V., *Org. Biomol. Chem.*, 2003, **1**, 4113-4123.
136. Halouani H.; Dumazet-Bonnamour I. D.; Perrin M.; Lamartine R., *J. Org. Chem.*, 2004, **69**, 6521-6527.
137. Bondy C. R.; Loeb S. J., *Coord. Chem. Rev.*, 2003, **240**, 77-99.
138. Beer P. D.; Gale P. A.; Hesek D., *Tet. Lett.*, 1995, **36**, 767-770.

139. Kubik S.; Goddard R.; Kirchner R.; Nolting D.; Seidel J., *Angew. Chem. Int. Ed.*, 2001, **40**, 2648-2651.
140. Chakroborty T. K.; Tapadar S.; Kumar S. K., *Tet. Lett.*, 2002, **43**, 1317-1320.
141. Davies A. P.; Perry J. J.; Williams R. P., *J. Am. Chem. Soc.*, 1997, **119**, 1793-1794.
142. Garcia-Tellado F.; Goswami S.; Chang S. K.; Geib S. J.; Hamilton A. D., *J. Am. Chem. Soc.*, 1990, **112**, 7393-7394.
143. Fan E.; van Arman S. A.; Kincaid S.; Hamilton A. D., *J. Am. Chem. Soc.*, 1993, **115**, 369-370.
144. Bisson A.P.; Lynch V.M.; Monahan M.K.C.; Anslyn E.V., *Angew. Chem. Int. Ed. Engl.*, 1997, **36**, 2340-2342.
145. Chang S.K.; Hamilton A.D., *J. Am. Chem. Soc.*, 1988, **110**, 1318-1319.
146. Choi K.; Hamilton A.D., *Coord. Chem. Rev.*, 2003, **240**, 101-110.
147. Hughes M. P.; Smith B. D., *J. Org. Chem.*, 1997, **62**, 4492-4499.
148. MacBeth C. E.; Larsen P. L.; Sorrell T. N.; Powell D.; Borovik A. S., *Inorg. Chim. Acta*, 2002, **341**, 77-84.
149. Tomapatanaget B.; Tuntulani T.; Wisner J. A.; Beer P. A., *Tet. Lett.*, 2004, **45**, 663-666.
150. Scheerder J.; Fochi M.; Engbersen J. F. J.; Reinhoudt D. N., *J. Org. Chem.*, 1994, **59**, 7815-7820.
151. Raposo C.; Almaraz M.; Martin M.; Weinrich V.; Mussons M. L.; Alcazar V.; Caballero M. C.; Moran J. R., *Chem. Lett.*, 1995, 759-760.
152. Scheerder J.; Engbersen J. F. J.; Casnati A.; Ungaro R.; Reinhoudt D. N., *J.Org. Chem.*, 1996, **60**, 6448-6454
153. Grunwald E.; Steel C., *J. Am. Chem. Soc.*, 1995, **117**, 5687-5692
154. Kang S. O.; Begum R. A.; Bowman-James K., *Angew. Chem. Int. Ed.*, 2006, **45**, 7882-7894.
155. Pascal R. A.; Spergel J.; Engbersen D. V., *Tet. Lett.*, 1986, **27**, 4099-4102.
156. Valiyaveettil J. F. J.; Engbersen J. F. J.; Verboom W.; Reinhoudt D. N., *Angew. Chem. Int. Ed. Engl.*, 1993, **32**, 900-901.
157. Kavallieratos K.; de Gala S. R.; Austin D. J.; Crabtree R. H., *J. Am. Chem. Soc.*, 1997, **119**, 2325-2326.
158. Ishida H.; Suga M.; Donowaki K.; Ohkubo K., *J. Org. Chem.*, 1995, **60**, 5374-5375.

159. Gomez D. E.; Fabbrizzi L.; Licchelli M.; Monzani E., *Org. Biomol. Chem.*, 2005, **3**, 1495-1500.
160. Gale P. A., *Coord. Chem. Rev.*, 2003, **240**, 1-226.
161. Beer P. D.; Gale P. A., *Angew. Chem. Int. Ed.*, 2001, **40**, 486-516.
162. Schmidtchen F. P.; Berger M., *Chem. Rev.*, 1997, **97**, 1609-1646.
163. Smith P. J.; Reddington M.V.; Wilcox C. S., *Tet. Lett.*, 1992, **33**, 6085-6088.
164. Scheerder J.; Engbersen J. F. J.; Casnati A.; Ungaro R.; Reinhoudt D.N., *J. Org. Chem.*, 1995, **60**, 6448-6454.
165. Hughes M. P.; Shang M.; Smith B. D., *J. Org. Chem.*, 1996, **61**, 4510-4511.
166. Hughes M. P.; Smith B. D., *J. Org. Chem.*, 1997, **62**, 4492-4499.
167. Fitzmaurice R. J.; Kyne G. M.; Douheret D.; Kilburn J. D., *J. Chem. Soc. Perkin Trans. I*, 2002, 841-864.
168. Evans A. J.; Matthews S. E.; Cowley A. R.; Beer P. D., *Dalton Trans.*, 2003, 4644-4650.
169. Miyaji H.; Collinson S. R.; Prokes I.; Tucker J. H. R., *Chem. Commun.*, 2003, 64-65.
170. Barboiu M.; Vaughan G.; van der Lee A., *Org. Lett.*, 2003, **5**, 3074-3076.
171. Gunnlaugsson T.; Davis A. P.; Hussey G. M.; Tierney J.; Glynn M., *Org. Biomol. Chem.*, 2004, **2**, 1856-1863.
172. Nishizawa S.; Buhlmann P.; Iwao M.; Umezawa Y., *Tet. Lett.*, 1995, **36**, 6483-6486.
173. Buhlmann P.; Nishizawa S.; Xiao K.P.; Umezawa Y., *Tet. Lett.*, 1997, **53**, 1647-1654.
174. Nie L.; Li Z.; Han J.; Zhang X.; Yang R.; Liu W. X.; Wu F. Y.; Xie J. W.; Zhao Y. F.; Jiang Y. B., *J. Org. Chem.*, 2004, **69**, 6449-6454.
175. Sasaki S.; Mizuno M.; Naemura K.; Tobe Y., *J. Org. Chem.*, 2000, **65**, 275-283.
176. Tobe Y.; Sasaki S.; Mizuno M.; Naemura K., *Chem. Lett.*, 1998, 835-836.
177. Hisaki I.; Sasaki S.; Hirose K.; Tobe Y., *Eur. J. Org. Chem.*, 2007, 607-615.
178. Hay B. P.; Firman T. K.; Moyer B. A., *J. Am. Chem. Soc.*, 2005, **127**, 1810-1819.
179. Bordwell F. G., *Acc. Chem. Res.*, 1988, **21**, 456-463.
180. Kelly T. R.; Kim M. H., *J. Am. Chem. Soc.*, 1994, **116**, 7072-7080.
181. Snellink-Ruel B. H. M.; Antonisse M. M. G.; Engbersen J. F. J.; Timmerman P.; Reinhoudt D. N., *Eur. J. Org. Chem.*, 2000, 165-170.

182. Sasaki S.; Mizuno M.; Naemura K.; Tobe Y., *J. Org. Chem.*, 2000, **65**, 275-283,
183. Gale P. A.; Camiolo S.; Sessler J. L., In *The Encyclopaedia of Supramolecular Chemistry*; Atwood J. L.; Steed J. W. (Eds), Marcel Dekker, 2004.
184. Sessler J. L.; Camiolo S.; Gale P. A., *Coord. Chem. Rev.*, 2003, **240**, 17-55.
185. Sessler J. L.; Cyr M. J.; Lynch V.; McGhee E.; Ibers J. A., *J. Am. Chem. Soc.*, 1990, **112**, 2810-2813.
186. Sessler J. L.; Burrell A. K., *Top. Curr. Chem.*, 1991, **161**, 177-273.
187. Sessler J. L.; Cyr M.; Furuta H.; Kral V.; Mody T.; Morishima T.; Shionoya M.; Weghorn S.J., *Pure Appl. Chem.*, 1993, **65**, 393-398.
188. Gale P.A., *Chem. Commun.*, 2005, 3761-3772
189. Gale P. A.; Camiolo S.; Tizzard G. J.; Chapman C. J.; Light M. E.; Coles S. J.; Hursthouse M. B., *J. Org. Chem.*, 2001, **66**, 7849-7853.
190. Camiolo S.; Gale P. A.; Hursthouse M. B.; Light M. E., *Tet. Lett.*, 2002, **43**, 6995-6996.
191. Aullon G.; Bellamy D.; Brammer L.; Bruton E. A.; Orpen A. G., *Chem. Commun.*, 1998, 653-654.
192. Kovacs A.; Varga Z., *Coord. Chem. Rev.*, 2006, **250**, 710-727.
193. Neve F.; Crispini A., *Cryst. Growth Des.*, 2001, 387-393.
194. Taylor R.; Kennard O., *Acc. Chem. Res.*, 1984, **17**, 320-326.
195. Brammer L.; Bruton E. A.; Sherwood P., *New J. Chem.*, 1999, **23**, 965-968.
196. Adams C. J.; Angeloni A.; Orpen A. G.; Podesta T. J.; Shore B., *Cryst. Growth Des.*, 2006, **6**, 411-422.
197. Love J. B.; Vere J. M.; Glenny M. W.; Blake A. J.; Schröder M., *Chem. Commun.*, 2001, 2678-2679.
198. Kiriyama H.; Matsushita N.; Yamagata Y., *Acta Cryst. Sec. C.*, 1986, **42**, 277-280.
199. Gillon A. M.; Lewis G. R.; Orpen G.; Rotter S.; Starbuck J.; Wang X. M.; Rodriguez-Martin; Ruiz-Perez C., *J. Chem. Soc., Dalton Trans.*, 2000, 3897-3905.
200. Barbour L. J.; MacGillivray L. R.; Atwood J. L., *Supramol. Chem.*, 1996, **7**, 167-169.
201. Dolling B.; Orpen A. G.; Starbuck J.; Wang X. M., *Chem. Commun.*, 2001, 567-568.

202. Gillon A. M.; Orpen A. G.; Starbuck J.; Wang X. M.; Rodriguez-Martin Y.; Ruiz-Perez C., *Chem. Commun.*, 1999, 2287-2288.
203. Zhu M.; Yang P.; Lu L., *Acta Cryst. Sec. E.*, 2003, **E59**, m91-m94.
204. Brammer L.; Bruton E. A.; Sherwood P., *Cryst. Growth Des.*, 2001, **1**, 277-290.
205. Yap G. P. A.; Rheingold A. L.; Das P.; Crabtree R. H., *Inorg. Chem.*, 1995, **34**, 3474-3476.
206. Brammer L.; Swearingen J. K.; Bruton E. A.; Sherwood P., *Proc. Nat. Acad. Sci.*, 2002, **99**, 4956-4961.
207. Lienke A.; Klatt G.; Robinson D. J.; Koch K. R.; Naidoo K. J., *Inorg. Chem.*, 2001, **40**, 2352-2357.
208. Naidoo K. J.; Klatt G.; Koch K. R.; Robinson D. J., *Inorg. Chem.*, 2002, **41**, 1845-1849.
209. Koch K. R.; Burger M. R.; Kramer J.; Westra A. N., *Dalton Trans.*, 2006, 3277-3284
210. Katz H. E., *J. Org. Chem.*, 1989, **54**, 2179-2183.
211. Katz H. E., *J. Am. Chem. Soc.*, 1986, **108**, 7640-7645.
212. Shriver D. F.; Biallis M. J., *J. Am. Chem. Soc.*, 1967, **89**, 1078-1081.
213. Katz H. E., *J. Am. Chem. Soc.*, 1985, **107**, 1420-1421.
214. Katz H. E., *J. Org. Chem.*, 1985, **50**, 5027-5032.
215. Katz H. E., *Organometallics*, 1987, **6**, 1134-1136.
216. Wuest J. D.; Zacharic B., *Organometallics*, 1985, **4**, 410-411.
217. Wuest J. D., Zacharaic B., *J. Am. Chem. Soc.*, 1987, **109**, 4714-4715.
218. Jung M. E.; Xia H., *Tet. Lett.*, 1988, **443**, C19-C21.
219. Beauchamp A. L.; Olivier M. J.; Wuest J. D.; Zachariac B., *J. Am. Chem. Soc.*, 1986, **108**, 73-77.
220. Aoyagi S.; Ogawa K.; Tanaka K.; Takeuchi Y., *J. Chem. Soc. Perkin Trans 2*, 1995, 355-358.
221. Ogawa K.; Aoyagi S.; Takeuchi Y., *J. Chem. Soc. Perkin Trans. 2*, 1993, 2389-2392.
222. Aoyagi S.; Tanaka K.; Zicmane I.; Takeuchi Y., *J. Chem. Soc. Perkin Trans 2*, 1991, 2217-2220.
223. Aoyagi S.; Tanaka K.; Takeuchi Y., *J. Chem. Soc. Perkin Trans 2*, 1994, 1549-1553.
224. Kuivila H. G.; Karol T. J.; Swami K., *Organometallics*, 1983, **2**, 909-914.

225. Karol T. J.; Hutchinson J. P.; Kuivila H. G.; Zubieta J. A., *Organometallics*, 1983, **2**, 106-114.
226. Swami K.; Hutchinson J. P.; Kuivila H. G.; Zubieta J. A., *Organometallics*, 1984, **3**, 1687-1694.
227. Jurkschat K.; Ruhleman A.; Tzschach A., *J. Organomet. Chem.*, 1990, **381**, C53-C56.
228. Jurkschat K.; Kuivila H. G.; Liu S.; Zubieta J. A., *Organometallics*, 1989, **8**, 2755-2759.
229. Shriver D. F.; Biallis M. J., *J. Am. Chem. Soc.*, 1967, **89**, 1078-1081.
230. Azuma Y.; Newcomb M., *Organometallics*, 1984, **3**, 9-14.
231. Cabbiness D. K.; Margerum D. W., *J. Am. Chem. Soc.*, 1970, **92**, 2151-2153.
232. Gale P. A., *Acc. Chem. Res.*, 2006, **39**, 465-475.
233. Bondy C. R.; Gale P. A.; Loeb S. J., *J. Am. Chem. Soc.*, 2004, **126**, 5030-5031.
234. Beer P. D.; Hazlewood C.; Hesek D.; Hoadacova J.; Stokes S. E., *J. Chem. Soc. Dalton Trans.*, 1993, 1327-1332.
235. Beer P. D.; Drew M. G. B.; Hazlewood C.; Hesek D.; Hodacova J.; Stokes S. E., *Chem. Commun.*, 1993, 229-230.
236. Tobey S. L.; Anslyn E.V., *J. Am. Chem. Soc.*, 2003, **125**, 14, 807-815.
237. Tobey S. L.; Jones B. D.; Anslyn E.V., *J. Am. Chem. Soc.*, 2003, **125**, 4026-4027.
238. Wiskur S. L.; Floriano P. N.; Anslyn E.V.; McDevitt J. T., *Angew. Chem. Int. Ed.*, 2003, **42**, 2070-2072.
239. Best M. D.; Tobey S. L.; Anslyn E. V., *Coord. Chem. Rev.*, 2003, **240**, 3-15.
240. Muller G.; Riede J.; Schmidtchen F. P., *Angew. Chem. Int. Ed. Engl.*, 1988, **27**, 1516-1518.

2. Design and Synthesis of Tripodal Receptors

2.1. Introduction

In this Chapter the design of receptors for the extraction and transport of $[\text{PtCl}_6]^{2-}$ is discussed. The synthesis and characterisation of a series of receptors that meet our design criteria are presented, followed by a description of the methods used to form complexes between these ionophores and $[\text{PtCl}_6]^{2-}$.

As discussed previously in Chapter 1, current methods used to extract $[\text{PtCl}_6]^{2-}$ in a solvent extraction process are thought to revolve around the use of long chain alkyl amines such as TOA.¹⁻⁶ Our aims were to develop a receptor that has improved extraction efficiency for $[\text{PtCl}_6]^{2-}$ over current methods leading to an improved materials balance. By introducing specific receptor features into our design, it was argued that stronger interactions between ionophores and $[\text{PtCl}_6]^{2-}$ would lead to potential improvements in extraction.

2.2. Receptor Design

2.2.1. Electrostatic Attraction

An electrostatic attraction was introduced into the design by incorporating a tertiary amine group that can act as a protonation site in the receptor (L).⁷ At low pH the amine will be protonated to form an alkylammonium cation (LH^+)⁸ thus enforcing an electrostatic ion-ion attraction with $[\text{PtCl}_6]^{2-}$. It was envisaged that two protonated receptor molecules would be required to form an organic soluble, charge-neutral complex with $[\text{PtCl}_6]^{2-}$ (Scheme 2.1).⁹



Scheme 2.1. Protonation of a tertiary amine gives a charge-neutral complex when in a 2:1 L: $[\text{PtCl}_6]^{2-}$ ratio.

A second advantage of having a protonation site is that the uptake and release of $[\text{PtCl}_6]^{2-}$ can be controlled by a pH swing mechanism in a solvent extraction process. Thus, under acidic conditions the receptor is protonated to give a charge-neutral ion-pair complex $[(\text{LH})_2\text{PtCl}_6]$. Ideally, this complex would be soluble in an organic solvent that is immiscible with H_2O to facilitate the separation of $[\text{PtCl}_6]^{2-}$ from other species that may be present in the aqueous feed (X^-). Treatment of the organic phase containing $[(\text{LH})_2\text{PtCl}_6]$ with base causes deprotonation of the receptor and dissociation of the complex releasing $[\text{PtCl}_6]^{2-}$ into the aqueous phase with the free ionophore remaining in the organic phase. Thus, the overall solubility of $[\text{PtCl}_6]^{2-}$ is controlled by varying the pH in the aqueous and organic phase (Figure 2.2)

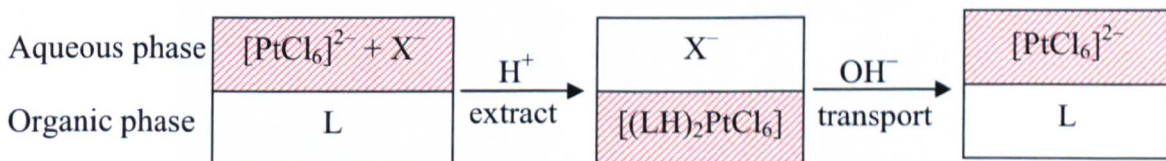


Figure 2.2. Separation of $[\text{PtCl}_6]^{2-}$ from other species (X^-) by formation of an organic soluble complex $[(\text{LH})_2\text{PtCl}_6]$ in a solvent extraction process.

If only electrostatics were used to bind $[\text{PtCl}_6]^{2-}$ we argued that any anionic species present in the aqueous feed might be extracted.¹⁰ To increase the strength and selectivity of the extraction process, additional recognition elements were introduced into the receptor design in the form of hydrogen-bond donor groups.

2.2.2. Hydrogen-bonding

The introduction of hydrogen-bond donor groups to locations complementary to the areas of highest electron density in $[\text{PtCl}_6]^{2-}$ will enhance the interaction between the receptor and metalloanion. The $[\text{PtCl}_6]^{2-}$ anion is a known hydrogen-bond acceptor

^{11, 12} and thus, incorporation of suitable hydrogen-bond donor groups into the ionophore will potentially enhance the interaction with the outer-sphere of $[\text{PtCl}_6]^{2-}$.

Several methods have been used to determine the areas of highest electron density in the outer sphere of $[\text{PtCl}_6]^{2-}$ and these were discussed in detail in Chapter 1.^{13, 14, 15} These confirm that the areas of $[\text{MCl}_6]^{2-}$ that are targeted by NH groups are located along the 12 edges and eight faces of the octahedron (Figure 2.3).¹⁶ Our aim, therefore, was to target these areas of electron density with suitable hydrogen-bond donor groups. A variety of NH hydrogen-bond donor groups have been synthesised and studied to enable the optimum donor group(s) to be found. These groups include sulfonamide,¹⁷ urea,¹⁸ thiourea,^{19, 20} amide²¹ and pyrrole²² moieties.

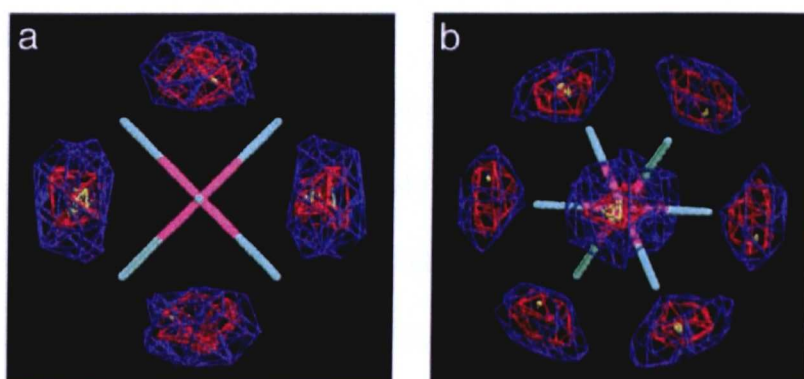


Figure 2.3. The experimental population density of hydrogen atoms from N-H groups in the vicinity of octahedral $[\text{PtCl}_6]^{2-}$ anions obtained from crystal structure data; viewed parallel to a) 4-fold molecular axis and b) 3-fold molecular axis. Contours; blue 35%, red 55%, yellow 80% of maximum population.¹⁶

2.2.3. Organic Solubility

It is important that the extractant and its complex $[(\text{LH})_2\text{PtCl}_6]$ are soluble in an organic solvent that is immiscible with H_2O because, if the systems are selective, this provides a route to the separation of $[\text{PtCl}_6]^{2-}$ from other species present in an aqueous feed.^{9, 23, 24} Thus, organic-solubilising groups were included in the design to maximise the organic solubility of both the receptor and its complex. The organic-

solubilising groups are designed to be located in an area of the receptor such that they do not hinder the interaction of the receptor with $[\text{PtCl}_6]^{2-}$.

2.2.4. Synthetic Accessibility

For a species to find use as a commercial extractant it needs to be synthetically accessible on large scales and be cost-effective. The facile synthesis of a receptor from commercially-available, cheap starting materials, produced in a high yield in a minimum number of synthetic steps, would be a major advantage and is a target of this work.²⁵

2.2.5. Receptor Design

Our approach was to combine the features described above into the design of a receptor system. Ideally, the features would complement each other to form a strong and selective extractant for the extraction and transport of $[\text{PtCl}_6]^{2-}$. All of the ligands described in this Chapter use the commercially-available tripodal amine tris(2-aminoethyl)amine (TREN) as a scaffold (Figure 2.4).

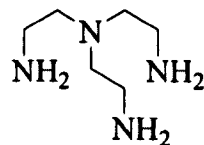


Figure 2.4. Tris(2-aminoethyl)amine (TREN).

TREN has three pendant arms linked to a tertiary amine bridgehead nitrogen and the protonation of this position can be used to provide an electrostatic ion-ion interaction with the anion which can be utilised in a pH swing mechanism. A 2:1 receptor: $[\text{PtCl}_6]^{2-}$ complex will be charge-neutral and, therefore, organic soluble allowing the $[\text{PtCl}_6]^{2-}$ anion to be separated from other species. TREN also has three

ethylamine groups which can be functionalised to introduce additional binding and solubilising features. Recently, TREN-based ligands have been used to recognise anionic species, their coordination ability depending on the binding moieties appended to the TREN unit.^{8, 22, 26-45}

The functionalisation of the three arms of TREN with hydrogen-bond donor groups affords receptors that have four possible sites to interact with $[\text{PtCl}_6]^{2-}$ (three hydrogen-bond donor moieties and one protonation site). Each of these binding sites could address one of the eight faces of the octahedral metalloanion and thus two receptors are needed to optimise the interaction. The C_3 geometry of the tripodal TREN based receptors would thus present neutral hydrogen-bond donors to the edges and/or faces of the hexachloro octahedron (Figure 2.5).

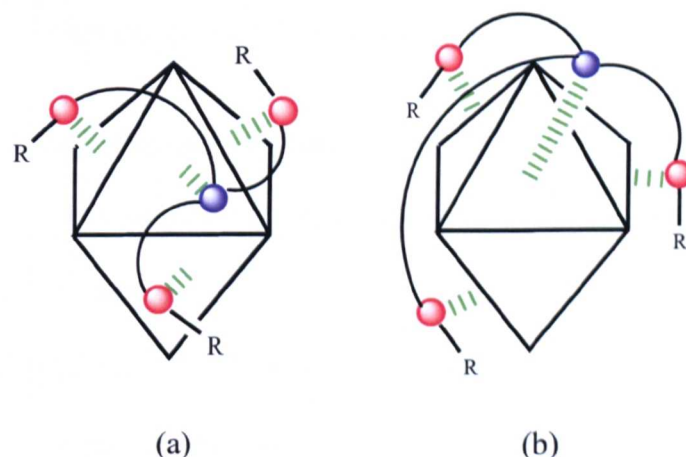


Figure 2.5. Schematic representation showing the interaction of a tripodal receptor with $[\text{PtCl}_6]^{2-}$; a) hydrogen-bond donors targeting the faces of the anion and b) hydrogen-bond donors targeting the edges of the anion. The hydrogen-bond donor sites shown in red, the protonation site shown in blue and the organic solubilising moieties as R. For clarity, just one molecule of receptor is shown, however, a 2:1 receptor: $[\text{PtCl}_6]^{2-}$ complex is required for the overall complex to be charge-neutral.

2.3. Receptor Synthesis

2.3.1. TREN-based Sulfonamide Receptors

The sulfonamide group consists of a SO_2 moiety bonded to an NH group which acts as a hydrogen-bond donor due to its acidity induced from the electron withdrawing

SO_2 group. The pK_a of the sulfonamide group when bonded to a phenyl substituent is 16.1; thus, the NH group is relatively acidic and thus a good hydrogen-bond donor group.⁴⁶ The treatment of sulfonyl chlorides with ammonia or amines is a common route to sulfonamides. The reaction proceeds via a nucleophilic substitution mechanism in which the nucleophilic NH_2 group attacks the sulfur atom of the SO_2 group, with HCl generated as a by-product (Figure 2.6). It is thought that the reaction proceeds via an $\text{S}_{\text{N}}2$ mechanism with the formation of a trigonal bipyramidal transition state.⁴⁷

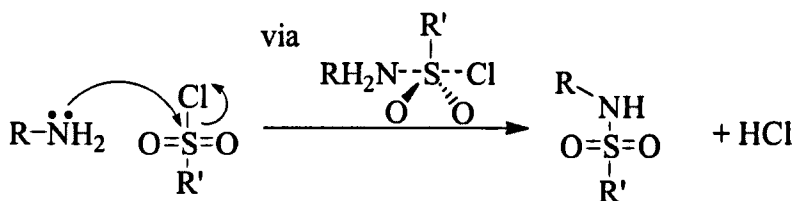
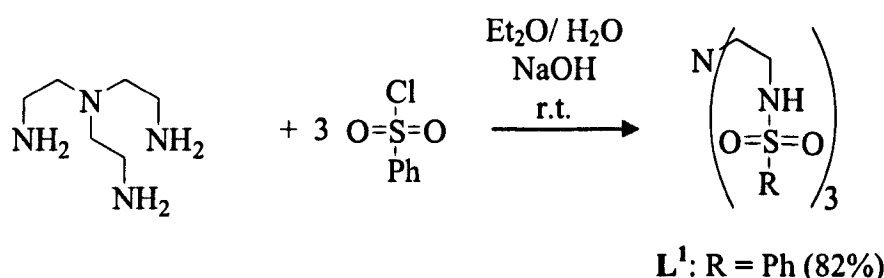


Figure 2.6. Mechanism of the reaction to form a sulfonamide moiety.

2.3.1.1. Synthesis and Characterisation

The receptor L^1 was synthesised by the reaction of one equivalent of TREN with three equivalents of benzene sulfonyl chloride under basic conditions in a biphasic reaction system (Scheme 2.2).⁴⁸ Basic conditions are required to neutralise the generated HCl and to prevent the formation of the HCl salt of the amine which would be unreactive towards electrophiles. Separation of the organic layer and removal of solvent yielded L^1 as a colourless solid. Recrystallisation of this solid from MeOH gave an analytically pure compound as colourless needles in 82% yield. Although L^1 is a new ligand similar TREN-based sulfonamide ligands having different terminal groups have been previously reported for use as anion receptors.^{30, 45, 49}



Scheme 2.2. Synthesis of L¹.

L¹ was characterised by ¹H NMR, ¹³C NMR and IR spectroscopy, mass spectrometry and elemental analysis. The ¹H NMR spectrum of L¹ in CDCl₃ shows the NH proton of the sulfonamide group as a broad signal at 6.02 ppm consistent with C₃ geometry for the molecule in solution. Confirmation that this was indeed the NH signal was afforded by addition of one drop of D₂O to a solution of L¹ in CDCl₃ leading to exchange and the disappearance of the NH signal. The electrospray mass spectrum showed peaks at *m/z* 567 and at *m/z* 590 assigned to [M+H]⁺ and [M+Na]⁺, respectively and the formation of L¹ was further supported by the presence of SO₂ stretching vibrations at 1150 cm⁻¹ and 1350 cm⁻¹ in the IR spectrum.

2.3.1.2. Crystal Structure of L¹

Single crystals of L¹ suitable for X-ray crystal structure analysis were grown by diffusion of *n*-hexane into a concentrated solution of the product in MeOH. L¹ crystallises in the orthorhombic space group *Pbca* with eight molecules in the unit cell. The molecular structure (Figure 2.7) shows intra-molecular hydrogen-bonding between N4—H4A···O2 (H···A = 2.279 Å), which encourages the three arms to be orientated in a tripodal, rather than a splayed, geometry with a regular spacing between each arm. Disorder in the phenyl group C19–C24 was modelled over two half-occupied sites for each atom, distance restraints were applied and the structure was refined with isotropic displacement parameters for the disordered region.

In the extended structure there are inter-molecular hydrogen-bonds between the sulfonamide moieties on adjacent molecules of L¹ between N2—H2A^{···}O3 (H^{···}A = 2.597 Å) and these interactions lead to a chain of alternating molecules of L¹ linked by hydrogen-bonds (Figure 2.8). The details of all hydrogen-bonds are given in Table 2.1 and the crystallographic data and structure refinement details are given in Appendix B.

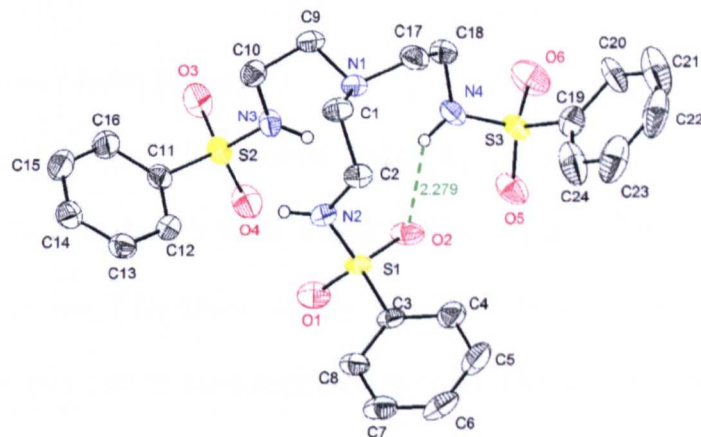


Figure 2.7. Molecular structure of L¹ showing intra-molecular hydrogen-bonds. All hydrogen atoms (except NH) are omitted for clarity. Ellipsoids set at 50% probability. The intra-molecular hydrogen-bond is shown in green and the NH^{···}O distance is measured in Å.

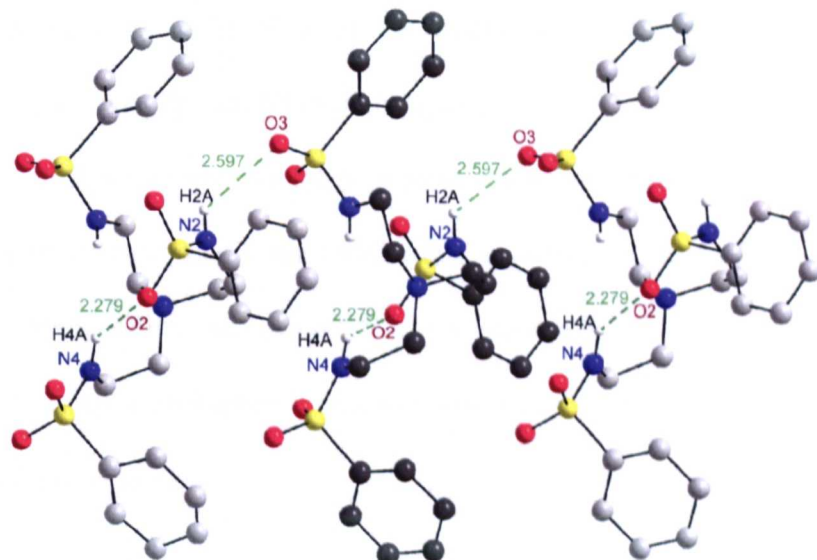


Figure 2.8. View of the structure of L¹ showing the intra- and inter-molecular hydrogen-bonds present in the extended structure. All hydrogen atoms (except NH) are omitted for clarity. Hydrogen-bonds are shown in green and the NH^{···}O distances are measured in Å. For clarity, the carbon atoms belonging to the adjacent L¹ molecules are in alternating shades of light and dark grey.

Table 2.1. Intra- and inter-molecular hydrogen-bonds D—H^{···}A in L¹ (D = donor atom, A = acceptor atom, d = distance).

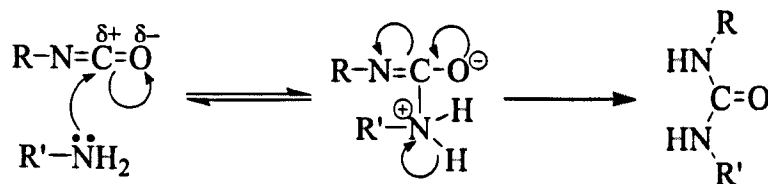
D—H ^{···} A	d(D—H)/ Å	d(H ^{···} A)/ Å	d(D ^{···} A)/ Å	<(DHA)/ °	Symmetry Code
N4—H4A ^{···} O2	0.88	2.279	2.988	138	
N2—H2A ^{···} O3	0.88	2.597	3.081	116	-x+1/2, y-1/2, z

* N4—H4A^{···}O2 is an intra-molecular hydrogen bond whilst N2—H2A^{···}O3 is an inter-molecular hydrogen-bond.

2.3.2. TREN-based Urea Receptors

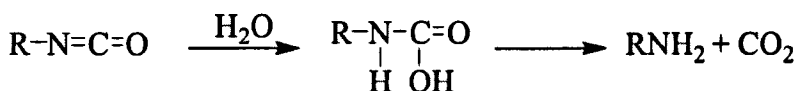
The urea group has two NH moieties linked by a carbonyl group and typically behaves as a two hydrogen-bond donor. It is a particularly effective neutral hydrogen-bonding motif for anion coordination⁵⁰ and there are many examples in the literature where urea groups have been shown to interact with anions in a strong and selective manner, some of which were discussed in Chapter 1. It was, therefore, decided that introducing urea functionality onto the TREN scaffold may prove useful for targeting the [PtCl₆]²⁻ anion. The pKa of the urea group is 26.9 in dmso⁵¹ making the NH groups less acidic than in the sulfonamide receptor (pKa 16.1)⁴⁶ and potentially a poorer hydrogen-bond donor group.

The synthesis of urea moieties is most commonly achieved by the reaction of an amine with an isocyanate, the mechanism of which is shown below in Scheme 2.3.⁵² The nucleophilic amine attacks the positively polarised carbon of the isocyanate to form a zwitterionic intermediate and a proton shift then leads to the formation of a urea moiety.



Scheme 2.3. Mechanism of the reaction to form a urea moiety.

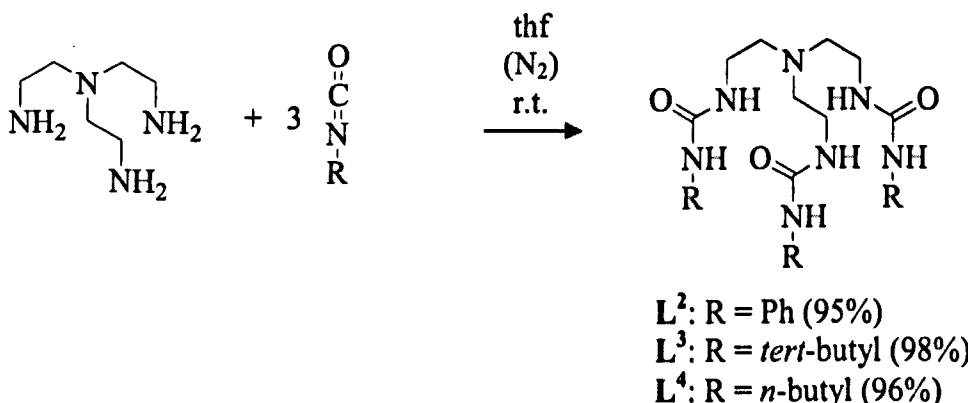
During the synthesis of ureas and thioureas it is important to eliminate H₂O from the reaction to avoid the production of amines via hydrolysis of isocyanates or isothiocyanates. The addition of H₂O to the carbon-nitrogen double bond of the cyanate gives an N-substituted carbamic acid which is unstable and breaks down to give CO₂ (or COS in the case of isothiocyanates) and amine (Scheme 2.4).⁵³ All syntheses of urea or thiourea derivatives were performed using dry solvent and under N₂ to reduce the possibility of unwanted hydrolysis.



Scheme 2.4. Hydrolysis of isocyanates.

2.3.2.1. Synthesis and Characterisation

A series of urea containing receptors were synthesised following the method published by Borovik and co-workers.⁵⁴ Thus, reaction of TREN with three equivalents of the appropriate isocyanate in dry thf and under a N₂ atmosphere yielded the urea receptors L²-L⁴ as colourless solids in yields in excess of 95% (Scheme 2.5).⁵⁵⁻⁶³ It was found that L³ and L⁴, which incorporate terminal *tert*-butyl or *n*-butyl groups on each of the three arms were more soluble in organic solvents than the phenyl analogue.



Scheme 2.5. Synthesis L²-L⁴.

The purity of L^2-L^4 was confirmed by 1H NMR, ^{13}C NMR and IR spectroscopy, mass spectrometry and elemental analysis. The 1H NMR spectrum of L^2 in CD_3OD showed no NH signals due to H-D exchange whilst the mass spectrum showed a parent ion peak at m/z 504 assigned to $[M+H]^+$ and the IR spectrum showed a characteristic C=O stretching vibration at 1650 cm^{-1} . The 1H NMR spectra of L^3 and L^4 were recorded in $CDCl_3$ and both spectra were consistent with a C_3 geometry for the molecules in solution with two resonances observed for the urea NH groups. The IR spectra of L^3 and L^4 showed characteristic C=O stretches at 1650 cm^{-1} and 1652 cm^{-1} , respectively, and the electrospray mass spectra and elemental analytical data further confirmed formation of the desired products.

2.3.2.2. Crystal Structure of L^2

Single crystals of L^2 suitable for X-ray crystal structure analysis were obtained as colourless laths by vapour diffusion of diethyl ether into a solution of the compound in MeOH. L^2 crystallises in the monoclinic space group $P2_1/c$ with four molecules in the unit cell. The molecular structure of L^2 (Figure 2.9) shows an intra-molecular, bifurcated hydrogen-bond between the urea moieties on adjacent arms of L^2 between $N2-H2A\cdots O2$ ($H\cdots A = 2.123\text{ \AA}$) and $N3-H3A\cdots O2$ ($H\cdots A = 2.059\text{ \AA}$). The extended structure reveals that there are bifurcated inter-molecular hydrogen-bonds between the urea moieties on adjacent molecules of L^2 between $N4-H4A\cdots O3$ and $N5-H5A\cdots O3$, and also between $N6-H6A\cdots O1$ and $N7-H7A\cdots O1$ which leads to a chain of L^2 molecules linked by hydrogen-bonds (Figure 2.10). The details of the hydrogen-bonds in L^2 are given in Table 2.2 and the crystallographic data and structure refinement details are given in Appendix B.

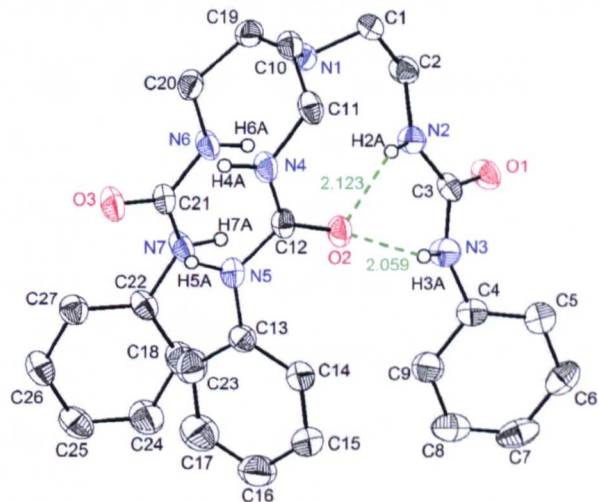


Figure 2.9. Molecular structure of receptor L^2 showing intra-molecular hydrogen-bonds. All hydrogen atoms (except NH) are omitted for clarity. Ellipsoids set at 50% probability. The intra-molecular hydrogen-bonds are shown in green and the $\text{NH}\cdots\text{O}$ distances are measured in Å.

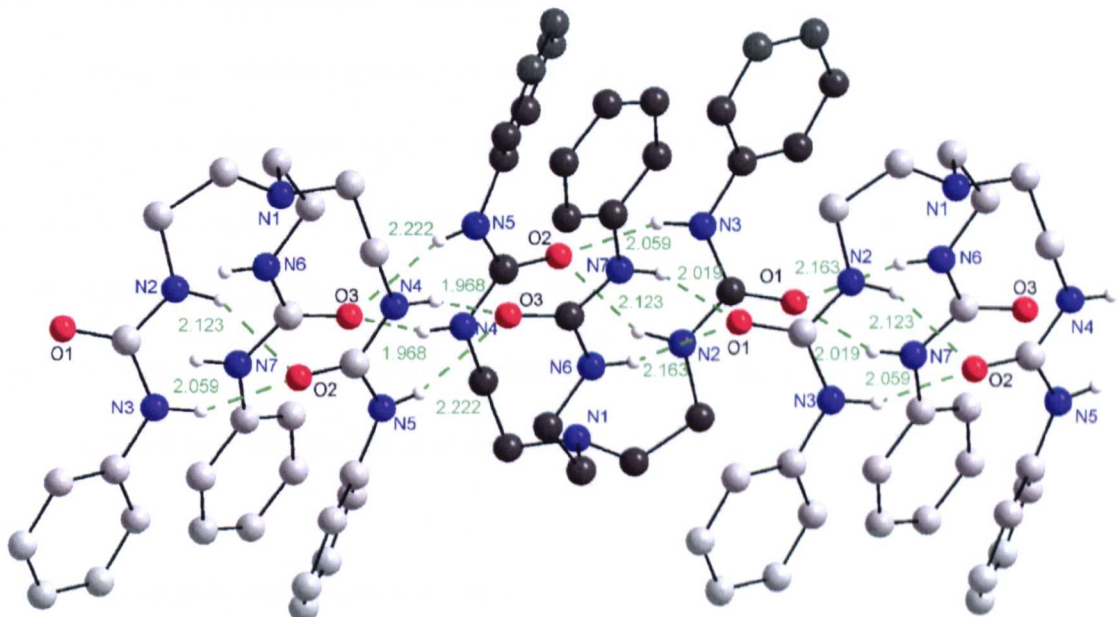


Figure 2.10. View of the structure of L^2 showing the intra- and inter-molecular hydrogen-bonds in the extended structure. All hydrogen atoms (except NH) are omitted for clarity. Hydrogen-bonds are shown in green and the $\text{NH}\cdots\text{O}$ distances are measured in Å. For clarity, the carbon atoms of adjacent molecules of L^2 are in alternating shades of light and dark grey.

Table 2.2. Intra- and inter-molecular hydrogen-bonds D—H^{···}A in L² (D = donor, A = acceptor, d = distance).

D—H ^{···} A	d(D—H)/ Å	d(H ^{···} A)/ Å	d(D ^{···} A)/ Å	<(DHA)/ °	Symmetry code
N2—H2A ^{···} O2	0.88	2.123	2.901(2)	147	
N3—H3A ^{···} O2	0.88	2.059	2.837(2)	147	
N4—H4A ^{···} O3	0.88	1.968	2.808(2)	159	-x+1, -y+1, -z+2
N5—H5A ^{···} O3	0.88	2.222	2.999(2)	147	-x+1, -y+1, -z+2
N6—H6A ^{···} O1	0.88	2.163	2.924(2)	145	-x, -y+1, -z+1
N7—H7A ^{···} O1	0.88	2.019	2.846(2)	156	-x, -y+1, -z+1

*N2—H2A^{···}O2 and N3—H3A^{···}O2 are intra-molecular hydrogen bonds, all others are inter-molecular hydrogen-bonds.

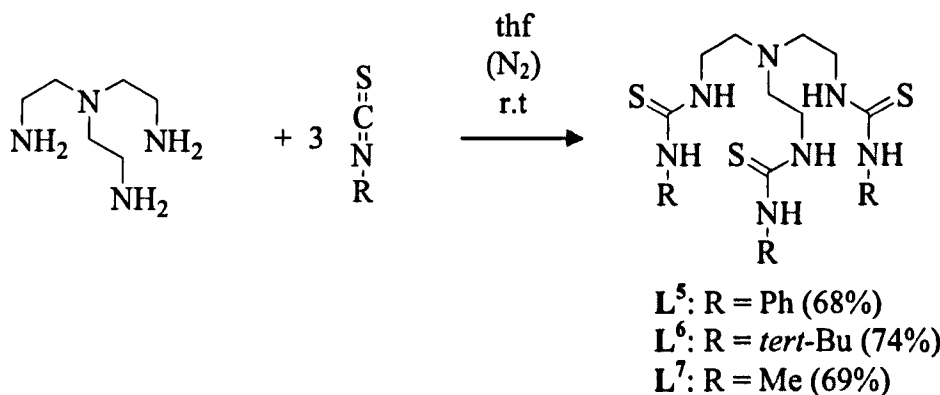
2.3.3. TREN-based Thiourea Receptors

The hydrogen-bond donor properties are related to its protonic acidity and thiourea is a stronger acid than urea ($pK_A = 21.1$ and 26.9 , respectively in dmso).⁶⁴ It was therefore expected that thiourea-containing receptors might establish stronger hydrogen-bond interactions and form more stable complexes with anions than their urea counterparts.⁶⁵ Also, thiourea derivatives can be compared with the analogous urea receptors to probe the effect of the nature of the heteroatom (C=X) in the group.

2.3.3.1. Synthesis and Characterisation

Thiourea moieties are synthesised by the reaction of amines with isothiocyanates in an analogous manner to the synthesis of ureas.⁵⁴ As the route used for the synthesis of urea receptors was found to be reliable, an analogous procedure was used for the preparation of thiourea systems. The receptors L⁵–L⁷ were synthesised by the reaction of one equivalent of TREN with three equivalents of a substituted isothiocyanate in dry thf under N₂ (Scheme 2.6).⁵⁴ Phenyl, *tert*-butyl and methyl

isothiocyanates were used in order to assess the effect of varying the terminal substituents on solubility. As methyl substituents are smaller than phenyl or *tert*-butyl groups it was thought that the NH donor groups may be less sterically hindered allowing shorter and stronger hydrogen-bond interactions. The ligand L⁵ has been synthesised previously and has been used as a phosphate and sulfate receptor.⁵⁵ The perchlorate salt of L⁷ has been reported to bind lithium⁶⁶ and L⁶ has been used as a ligand for copper.⁶⁷



Scheme 2.6. Synthesis of L⁵–L⁷.

The successful formation of L⁵–L⁷ was confirmed by ¹H NMR, ¹³C NMR and IR spectroscopy, mass spectrometry and elemental analysis. The ¹H NMR spectrum of L⁵, in CDCl₃ showed the thiourea NH signals as broad single resonances at 8.25 and 6.90 ppm consistent with C₃ symmetry of the tripodal receptor in solution. The IR spectrum showed a C=S stretching vibration at 1551 cm⁻¹, while the electrospray mass spectrum showed peaks at *m/z* 552 and *m/z* 574 assigned to [M+H]⁺ and [M+Na]⁺, respectively.

The ¹H NMR spectrum of L⁶ in CDCl₃ showed signals for the two different thiourea NH environments at 6.48 and 6.33 ppm. Electrospray mass spectrometry supported the formation of L⁶ with a peak at *m/z* 492 assigned to [M+H]⁺ and the ¹³C NMR spectrum along with the IR spectrum and analytical data further confirmed the formation of the desired product.

L^7 was obtained as an oil while L^5 and L^6 were obtained as colourless solids. Characterisation of the oil confirmed the formation of the desired product. The 1H NMR spectrum showed broad signals at 6.88 ppm and 6.73 ppm assigned to the two thiourea NH protons while electrospray mass spectrometry showed a peak at m/z 366 assigned to $[M+H]^+$.

2.3.3.2. Crystal Structure of L^5

The receptor with terminal phenyl substituents proved to crystallise more readily than the other derivatives. A single crystal of L^5 was obtained as a colourless block by diffusion of *n*-hexane into a concentrated solution of L^5 in MeOH. L^5 crystallises in the monoclinic space group $C2/c$ with eight molecules in the unit cell. The crystal structure shows no apparent intra-molecular or inter-molecular hydrogen-bonding and the molecular structure is shown in Figure 2.10. Crystallographic data and structure refinement details are given in Appendix B.

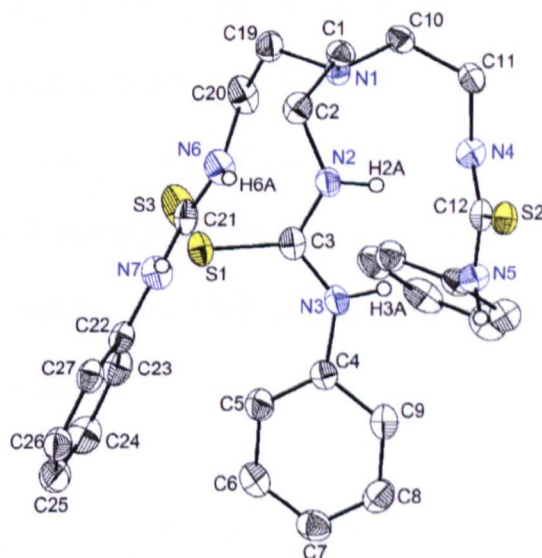


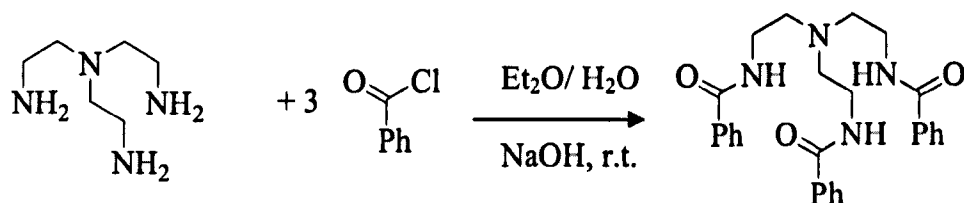
Figure 2.10. Molecular structure of L^5 . All hydrogen atoms (except NH) are omitted for clarity. Ellipsoids set at 50% probability.

2.3.4. TREN-based Amide Receptor

The amide moiety has an acidic NH proton available to act as a hydrogen-bond donor group and there are many examples of anion receptors that utilise this.^{68, 69} For this reason the amide group was incorporated onto the TREN scaffold with the hope it would hydrogen-bond to the $[\text{PtCl}_6]^{2-}$ anion. The pKa of the amide group is 23.3⁵¹ which means it is slightly more acidic than the analogous urea system and might be expected to form stronger hydrogen-bonds. Comparison of urea- and amide-containing receptors would give an important assessment of how the number of NH hydrogen-bond donor groups effects extraction efficiency.

2.3.4.1. Synthesis and Characterisation

L^8 was synthesised by the reaction of one equivalent of TREN with three equivalents of benzoyl chloride in a biphasic reaction (Scheme 2.7).^{48, 45} An off-white precipitate was formed which was collected by filtration, washed with diethyl ether and dried *in vacuo* to give the product in 74% yield. The synthesis and crystal structure of L^8 has been previously reported by Goldcamp and co-workers⁷⁰ who prepared the product via reaction of TREN with benzoyl chloride in the presence of triethylamine. They were interested in the ligand as it incorporates amide moieties for the stabilisation of high valent metal centres and also a tripodal geometry to enforce trigonal pyramidal geometry on metal complexes.



Scheme 2.7. Synthesis of L^8 .^{48, 45}

L^8 (74%)

L^8 was characterised by 1H NMR, ^{13}C NMR and IR spectroscopy, mass spectrometry and elemental analysis. The 1H NMR spectrum of L^8 in $CDCl_3$ shows three signals in the aromatic region at 7.18, 7.33 and 7.60 ppm corresponding to the three different proton environments on the phenyl ring, with the NH resonance observed as a broad signal at 7.18 ppm consistent with C_3 symmetry of the molecule in solution. The electrospray mass spectrum shows a peak at m/z 459 assigned to $[M+H]^+$ and ^{13}C NMR and IR spectroscopy alongside elemental analytical data further confirmed the purity of the product.

2.3.4.2. Crystal Structure of L^8

A single crystal of L^8 was grown by solvent diffusion of *n*-hexane into a concentrated solution of the ligand in MeOH. The crystal structure obtained was the same as a structure previously reported by Goldcamp and co-workers.⁷⁰ However the structure in Figure 2.11 has been re-numbered to enable ease of comparison between this and our other tripodal systems. The molecular structure of L^8 shows an intra-molecular hydrogen-bond between the amide moieties on adjacent arms of L^2 between N2—H1 \cdots O2 ($H\cdots A = 2.157 \text{ \AA}$) encouraging the tripodal geometry of the receptor in which the three pendant arms are orientated in the same direction (Figure 2.11). The extended structure of L^8 also reveals two inter-molecular hydrogen bonds N3—H2 \cdots O3 ($H\cdots A = 2.150 \text{ \AA}$) and N4—H3 \cdots O1 ($H\cdots A = 2.128 \text{ \AA}$) forming linear chains along the c axis (Figure 2.12). The full details of the hydrogen-bonds present in the structure of L^8 are shown in Table 2.3 and the crystallographic data and structure refinement details are given in Appendix B.

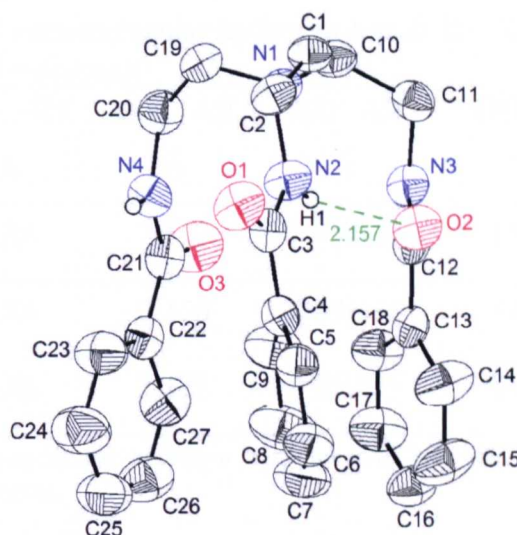


Figure 2.11. Molecular structure of receptor L^8 showing the intra-molecular hydrogen-bond. All hydrogen atoms (except NH) are omitted for clarity. Ellipsoids set at 50% probability. The intra-molecular hydrogen-bond is shown in green and the $\text{NH}\cdots\text{O}$ distance measured in \AA .^{70*}

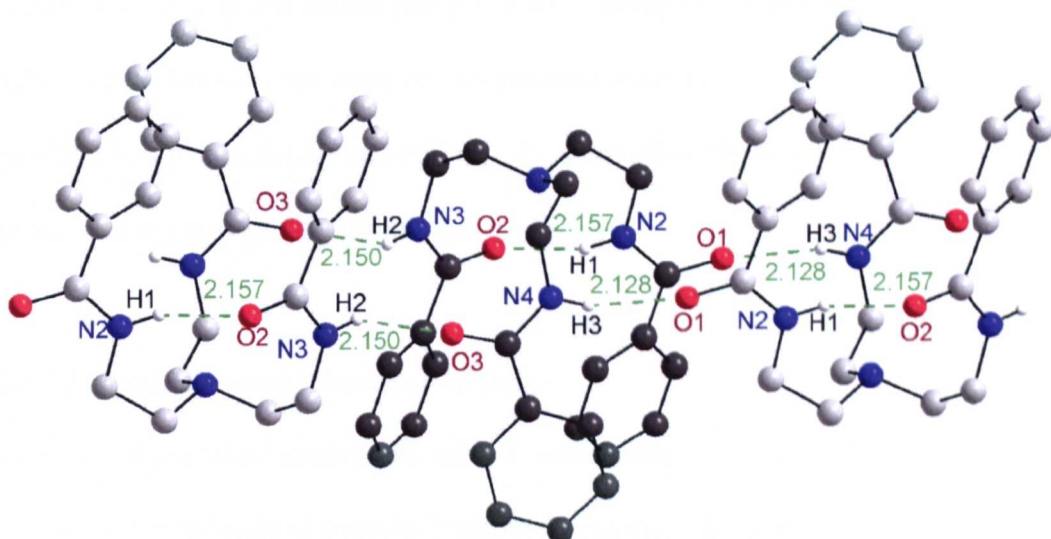


Figure 2.12. View of the structure of L^8 showing intra- and inter-molecular hydrogen-bonds present in the extended structure. All hydrogen atoms (except NH) omitted for clarity. The hydrogen-bonds are shown in green and measured in \AA . For clarity, the carbon atoms of each L^8 molecule are in alternating shades of light and dark grey.

* The structure in Figure 2.11 has been renumbered compared with the published structure to enable ease of comparison between the crystal structures of TREN receptors presented in this thesis.

Table 2.3. Intra- and inter-molecular hydrogen-bonds D—H \cdots A present in L⁸ (D = donor, A = acceptor, d = distance).

D—H \cdots A	d(D—H)/ Å	d(H \cdots A)/ Å	d(D \cdots A)/ Å	\angle (DHA)/ °	Symmetry Codes
N2—H1 \cdots O2	0.86	2.157	2.932(3)	150	
N3—H2 \cdots O3	0.86	2.150	2.896(3)	145	1-x, -y, -z
N4—H3 \cdots O1	0.86	2.128	2.950(3)	160	1-x, -y, 1-z

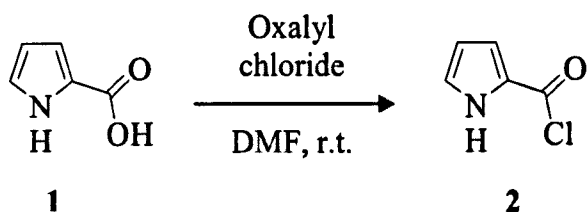
*N2—H1 \cdots O2 is an intra-molecular hydrogen bond whereas N3—H2 \cdots O3 and N4—H3 \cdots O1 are inter-molecular hydrogen-bonds.

2.3.5. TREN-based Amido Pyrrole Receptor

Pyrroles are known hydrogen-bond donor groups with many recent reports of their use as anion receptor motifs.⁷¹ The pKa of the NH proton of pyrrole in dmso is 23.0⁷² which is similar to the amide group (23.3).⁵¹ Receptors with amido pyrrole moieties have two NH donors on each of the pendant arms to give a total of six hydrogen-bond donors per molecule of receptor. By comparison with urea receptors the effect of the spacer between NH groups can be found.

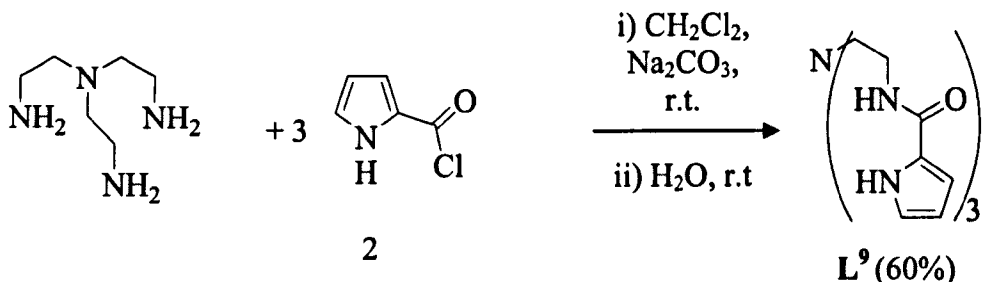
2.3.5.1. Synthesis and Characterisation

Reaction of pyrrole-2-carboxylic acid, 1, with oxalyl chloride and a catalytic amount of dmf under N₂ yielded pyrrole-2-carbonyl chloride, 2, as an off-white solid in 96% yield (Scheme 2.8).^{73, 74, 75} The ¹H NMR spectrum of 2 in CDCl₃ shows a broad signal at 9.58 ppm, assigned to the NH proton and the aromatic protons are observed in the 7.24–7.15 ppm region consistent with the data reported in the literature for this compound.



Scheme 2.8. Synthesis of pyrrole-2-carbonyl chloride, **2**.

Reaction of TREN with three equivalents of **2** in the presence of sodium carbonate in CH_2Cl_2 gave **L**⁹ in moderate yield as an off-white solid (Scheme 2.9). Work published by Sessler and co-workers reports this synthesis together with a crystal structure of **L**⁹.⁷⁶



Scheme 2.9. Synthesis of **L**⁹.

L⁹ was characterised by ^1H NMR, ^{13}C NMR and IR spectroscopy, mass spectrometry and elemental analysis. The ^1H NMR spectrum of **L**⁹ in $\text{dmso}-d_6$ shows the NH protons in the three pyrrole rings resonating at 11.44 ppm and the three NH amide protons were observed as a triplet at 7.95 ppm. The electrospray mass spectrum of the product showed a peak at m/z 426 assigned to $[\text{M}+\text{H}]^+$ and elemental analytical data further confirmed the purity of the product. Unfortunately, at the concentrations required for solvent extractions, the product is not very soluble in organic solvents thus hindering its use as a receptor in solvent extractions.

2.3.5.2. Crystal structure of L⁹

Single crystals of L⁹ were obtained as pale yellow needles by the solvent diffusion of *n*-hexane into a concentrated solution of the product in MeOH. L⁹ crystallised in the triclinic space group *P*-1 with two molecules in the unit cell. The structure analysis shows the presence of an intra-molecular hydrogen-bond between the amide moieties on adjacent arms of the molecule N4—H4A···O3 (H···A = 2.260 Å) encouraging a tripodal geometry in the structure in which the three arms are orientated in the same direction (Figure 2.13).

In addition, there are inter-molecular hydrogen-bonds present between the amide and pyrrolic moieties from adjacent molecules with N3—H3A···O2 (H···A = 1.993 Å), N5—H5A···O1 (H···A = 2.044 Å) and N6—H6A···O1 (H···A = 2.111 Å) (Figure 2.14). This leads to the formation of a hydrogen-bonded network of L⁹ molecules in which the receptors have alternating orientation. The full details of the hydrogen-bonds present in L⁹ are given in Table 2.4 and crystallographic data and structure refinement details are given in Appendix B.

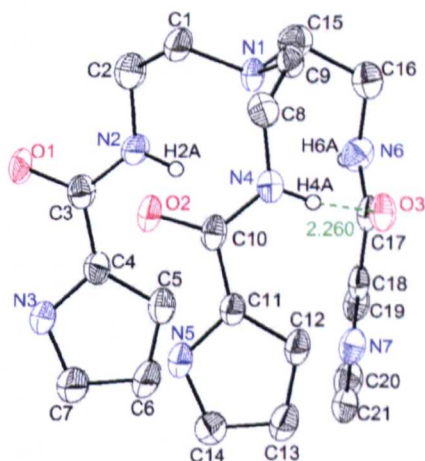


Figure 2.13. Molecular structure of receptor L⁹ showing intra-molecular hydrogen-bonds. All hydrogen atoms (except NH) are omitted for clarity. Ellipsoids set at 50% probability. The intra-molecular hydrogen-bond is shown in green and the NH···O distance is measured in Å.

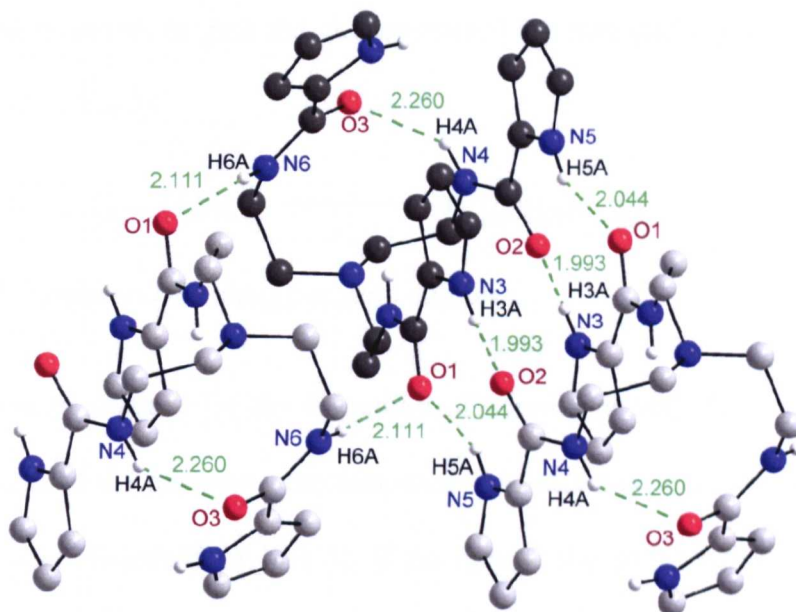


Figure 2.14. View of the structure of L^9 showing the intra- and inter-molecular hydrogen-bonding in the extended structure. All hydrogen atoms (except NH) are omitted for clarity. The hydrogen-bonds are shown in green and the $\text{NH} \cdots \text{O}$ distances are measured in Å. For clarity, the carbon atoms of each molecule are in alternate different shades of light and dark grey.

Table 2.4. Intra- and inter-molecular hydrogen-bonds $D-\text{H} \cdots \text{A}$ in L^9 (D = donor, A = acceptor, d = distance).

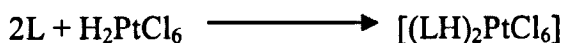
$D-\text{H} \cdots \text{A}$	$d(D-\text{H})$ / Å	$d(\text{H} \cdots \text{A})$ / Å	$d(D \cdots \text{A})$ / Å	$\angle(D\text{H}\text{A})$ / °	Symmetry Codes
N4—H4A···O3	0.86	2.260	2.935(3)	135	
N3—H3A···O2	0.86	1.993	2.796(3)	155	$-x+1, -y+1, -z+1$
N5—H5A···O1	0.86	2.044	2.853(3)	156	$-x+1, -y+1, -z+1$
N6—H6A···O1	0.86	2.111	2.919(3)	156	$-x+2, -y+1, -z+1$

*N4—H4A···O3 is an intra-molecular hydrogen bond whereas N3—H3A···O2, N5—H5A···O1 and N6—H6A···O1 are inter-molecular hydrogen-bonds.

2.4. Complexation Reactions

Following the synthesis of receptors complexation reactions were performed. Hexachloroplatinic acid (H_2PtCl_6) was used throughout this work as a source of the $[\text{PtCl}_6]^{2-}$ anion. It was chosen because it is commercially available and is soluble in MeCN, H_2O and acetone. Also, by using H_2PtCl_6 the two protons can protonate two

TREN-based receptors to give the charge-neutral ion-pair $[(\text{LH})_2\text{PtCl}_6]$ with no by-products. (Scheme 2.9).



Scheme 2.9. Synthesis of a charge-neutral complex.

A general method for the formation of complexes was developed in which two equivalents of the receptor were dissolved in MeCN and added to one equivalent of H_2PtCl_6 , also dissolved in MeCN. If necessary, the solutions of ligands were gently heated to aid dissolution. The complexation reactions that were carried out with the receptors L^1 – L^9 are now discussed in turn and the evidence for the formation of complex products presented.

2.4.1. Synthesis of a Sulfonamide Complex

2.4.1.1. Synthesis of $[(\text{L}^1\text{H})_2\text{PtCl}_6]$

Two equivalents of L^1 were added to one equivalent of H_2PtCl_6 in MeCN. The receptor L^1 was only partially soluble in MeCN which hindered the complexation reaction. No precipitate formed in this reaction although not all of the receptor was soluble which prevented analysis of the resulting solution by ^1H NMR spectroscopy.

2.4.1.2. Crystal Structure of $[(\text{L}^1\text{H})_2\text{PtCl}_6]$

The complex $[(\text{L}^1\text{H})_2\text{PtCl}_6]$ crystallised as pale yellow laths following the mixing of an aqueous HCl solution containing K_2PtCl_6 with a solution of two equivalents of L^1 in MeOH. The structure determination of $[(\text{L}^1\text{H})_2\text{PtCl}_6]$ revealed one $[\text{PtCl}_6]^{2-}$ anion lying on a centre of inversion with both sulfonamide receptors protonated at their bridgehead nitrogen atom (N1) to give an overall charge-neutral complex (Figure

2.15). Disorder involving the atoms C3–C8 in a terminal phenyl ring was modelled by allowing two half-occupied sites for each atom. Distance restraints were applied and the structure refined with isotropic atomic displacement parameters for the disordered region.

The definition of what constitutes a hydrogen-bond is based upon the distance between the hydrogen-bond donor and acceptor atoms which should be less than or equal to the sum of the van der Waals radii for these two atoms. In the case of hydrogen-bonds of the type N—H \cdots Cl—Pt the H \cdots Cl distance should be less than 2.95 Å, and this general criterion has been used in all structures of complexes that are presented throughout this thesis.

Each [L¹H⁺] cation is involved in three hydrogen-bonds to two separate [PtCl₆]²⁻ anions with a bifurcated interaction to one [PtCl₆]²⁻ anion and a single hydrogen-bond to another [PtCl₆]²⁻ anion. Figure 2.15 shows the bifurcated hydrogen-bonding interactions N4—H4B \cdots Cl3 (H \cdots A = 2.609 Å) and N4—H4B \cdots Cl2 (H \cdots A = 2.889 Å) between two [L¹H⁺] receptors and a central [PtCl₆]²⁻ anion. The extended structure (Figure 2.16) reveals that, in addition to the bifurcated interaction shown in Figure 2.15, a second arm of each tripod interacts with a different [PtCl₆]²⁻ unit N2—H2C \cdots Cl3 (H \cdots A = 2.790 Å).

The areas of [PtCl₆]²⁻ that are bound by the NH donor groups are highlighted in Figure 2.17. The hydrogen-bond donor group H4B forms a bifurcated hydrogen-bond with Cl2 and Cl3 and is located slightly out of the triangular plane defined by Pt1, Cl2 and Cl3. The H2C donor is located in the plane defined by Pt1, Cl2 and Cl3. Although H2C is located between Cl2 and Cl3 there is only a hydrogen-bond to Cl2 as the H2C \cdots Cl3 distance is too long.

The extended structure reveals N—H···O, N—H···N and N—H···S hydrogen-bonds however, for clarity, these interactions have been omitted from Figure 2.16. The details of all the hydrogen-bonds present in the structure are given in Table 2.5 and the crystallographic data and structure refinement details for the $[(L^1H)_2PtCl_6]$ complex are given in Appendix B.

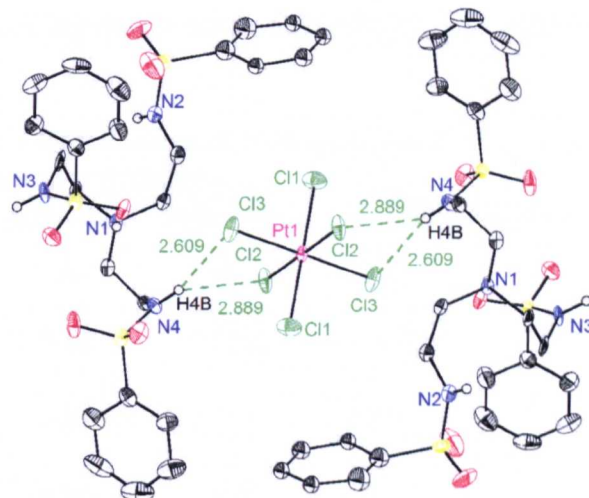


Figure 2.15. Molecular structure of $[(L^1H)_2PtCl_6]$ showing hydrogen-bonding between the receptors and $[PtCl_6]^{2-}$ anions. All hydrogen atoms (except NH) omitted for clarity. Ellipsoids set at 50% probability. Hydrogen-bonds are shown in green and the $NH \cdots Cl$ distances are measured in Å. One of the disorder components has been omitted for clarity.

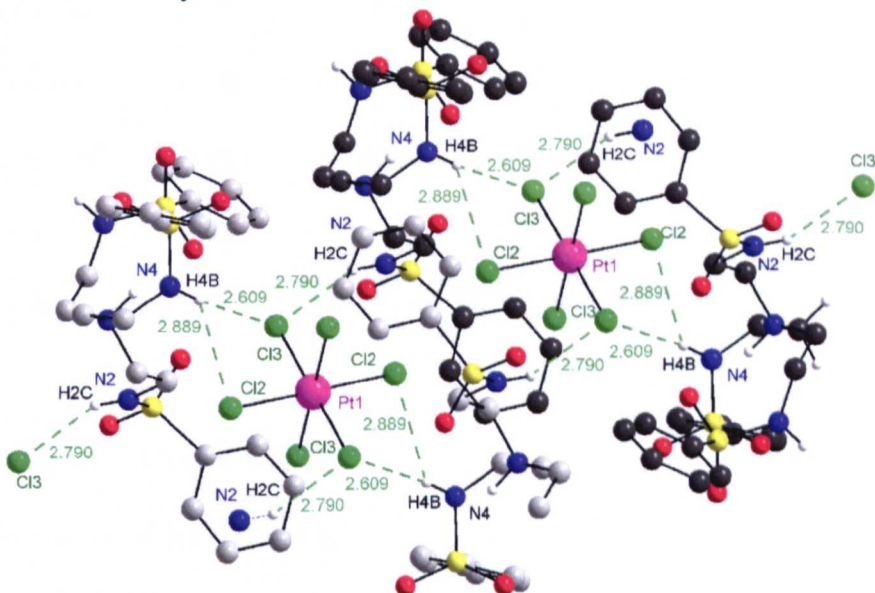


Figure 2.16. View of the structure of $[(L^1H)_2PtCl_6]$ showing the hydrogen-bonds between L^1 and $[PtCl_6]^{2-}$ in the extended structure. All hydrogen atoms (except NH) are omitted for clarity. Hydrogen-bonds are shown in green and the $NH \cdots Cl$ distances are measured in Å. For clarity, the carbon atoms of each $[(L^1H)_2PtCl_6]$ unit are shown in different shades of grey.

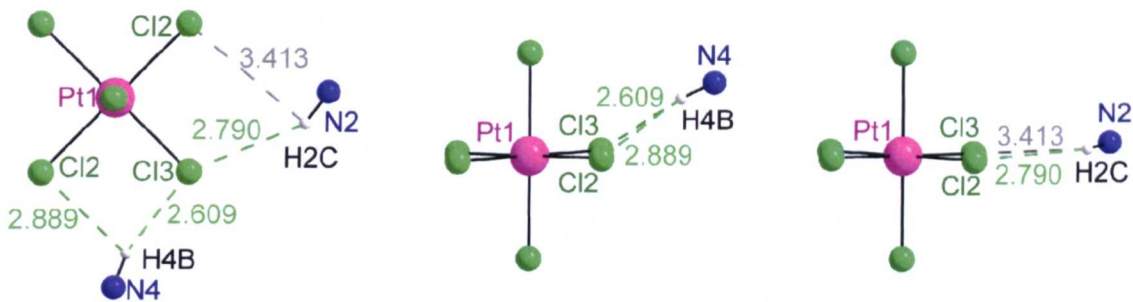


Figure 2.17. Highlighting the location of the NH groups relative to $[\text{PtCl}_6]^{2-}$.

Table 2.5. Intra- and inter-molecular hydrogen-bonds D—H \cdots A in $[(\text{L}^1\text{H})_2\text{PtCl}_6]$ (D = donor, A = acceptor, d = distance).

D—H \cdots A	d(D—H)/ Å	d(H \cdots A)/ Å	d(D \cdots A)/ Å	$\angle(\text{DHA})/$ °	Symmetry Codes
N2—H2C \cdots Cl3*	0.88	2.790	3.570	148	x, y+1, z
N4—H4B \cdots Cl3*	0.88	2.609	3.460	163	
N4—H4B \cdots Cl2*	0.88	2.889	3.422	121	-x, -y, -z
N1—H1C \cdots O3#	0.93	2.082	2.957	156	
N1—H1C \cdots N3#	0.93	2.530	2.991	111	
N1—H1C \cdots S2#	0.93	2.789	3.584	114	
N3—H3A \cdots O5#	0.88	2.490	3.190	137	-x, y+1/2, -z+1/2
N3—H3A \cdots O4#	0.88	2.600	3.214	128	-x, y+1/2, -z+1/2
N3—H3A \cdots S3#	0.88	2.989	3.627	131	-x, y+1/2, -z+1/2

*hydrogen-bonds between L^1 and $[\text{PtCl}_6]^{2-}$ # hydrogen-bonds between L^1 molecules

2.4.2. Synthesis of Urea Complexes

2.4.2.1. Synthesis of $[(\text{L}^2\text{H})_2\text{PtCl}_6]$

Two equivalents of L^2 were added to MeCN and heated to aid dissolution of L^2 . The solution was mixed with one equivalent of H_2PtCl_6 , also dissolved in MeCN, and a yellow precipitate formed immediately which was collected by filtration and dried *in*

vacuo. The ^1H NMR spectrum of the product in $\text{dmso}-d_6$ shows a signal which integrates in a 1:3 ratio with each of the two NH urea resonances (H_c and H_d in Figure 2.18) at 9.65 ppm and is assigned to the protonated tertiary amine position ($\text{N}^+\underline{\text{H}}\text{R}_3$). Also, a downfield shift is observed for both NH resonances; thus, in the free receptor the NH resonances occur at 6.20 and 8.52 ppm, whereas in the complex they are observed at 6.45 and 8.80 ppm. These shifts indicate that hydrogen-bonding interactions are present between the urea NH groups of L^2 and $[\text{PtCl}_6]^{2-}$. When a hydrogen-bond is formed it has an electron-withdrawing effect on the donor proton, and the associated signal in the NMR spectrum often shifts downfield.⁷⁷ It is significant that the effects of hydrogen-bonding are apparent in this spectrum since it was recorded in $\text{dmso}-d_6$, which is a highly competitive hydrogen-bonding solvent.

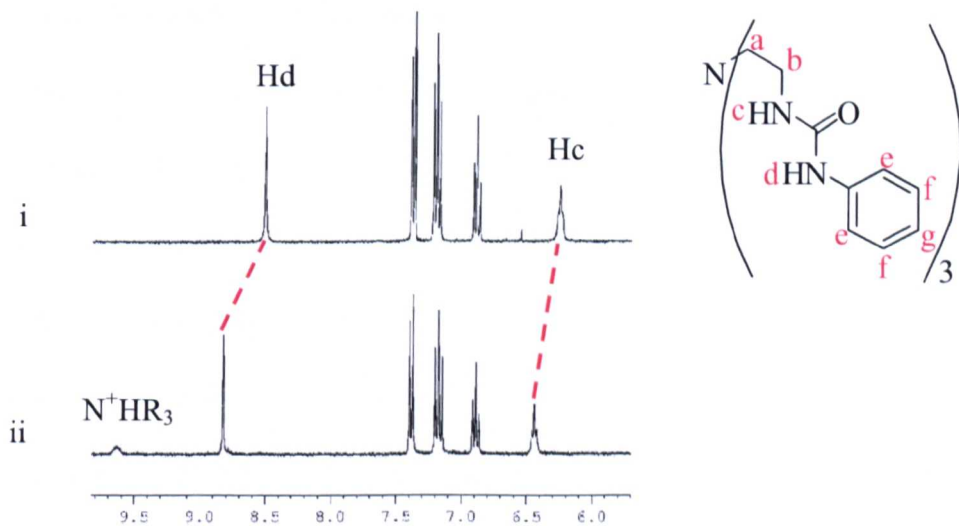


Figure 2.18. ^1H NMR spectra [$\text{dmso}-d_6$, 300 MHz] of i) L^2 and ii) $[(\text{L}^2\text{H})_2\text{PtCl}_6]$.

Elemental analysis of the precipitate further confirmed the formation of the expected product, and IR spectroscopy showed a carbonyl stretching vibration at 1650 cm^{-1} . Both L^2 and $[(\text{L}^2\text{H})_2\text{PtCl}_6]$ have low solubilities in organic solvents and consequently the use of L^2 as a receptor in solvent extraction studies was limited. The work carried out to improve the organic solubility of urea receptors and their complexes is presented in Chapter 3.

2.4.2.2. Synthesis of $[(L^3H)_2PtCl_6]$

Two equivalents of L^3 were dissolved in MeCN and added to one equivalent of H_2PtCl_6 in MeCN. When the two solutions were mixed, a precipitate formed which was collected by filtration and dried *in vacuo*. The 1H NMR spectrum of the product showed a signal at 10.05 ppm assigned to N^+HR_3 and the IR spectrum showed a characteristic carbonyl stretching vibration at 1632 cm^{-1} . Elemental analytical data for the product confirmed the 2:1 $(LH)^+:[PtCl_6]^{2-}$ stoichiometry. Although L^3 with terminal *tert*-butyl substituents is more soluble than the analogous phenyl receptor L^2 , it still forms a complex that is only soluble in dmso preventing the use of the receptor in solvent extraction studies.

2.4.2.3. Crystal Structure of $[(L^3H)_2PtCl_6]$

Single crystals of the complex $[(L^3H)_2PtCl_6]$ suitable for X-ray diffraction were grown by repeating the reaction above with lower concentrations of reactants. Slow evaporation of the resulting solution for 2 days led to the formation of crystals as yellow tablets. The complex crystallised in the triclinic space group *P*-1 with one $[(L^3H)_2PtCl_6]$ species in the unit cell, the $[PtCl_6]^{2-}$ anion lies on a centre of inversion and the two receptor cations are related by the inversion centre. Both urea receptors are protonated at their bridgehead position (N1) to give a $[L^3H^+]$ cation resulting in the complex having a net charge of zero (Figure 2.19). There is significant hydrogen-bonding between $[PtCl_6]^{2-}$ and the urea moieties in $[L^3H^+]$. A bifurcated hydrogen-bond is observed between N2—H2A \cdots Cl1 ($H\cdots A = 2.805\text{ \AA}$) and N2—H2A \cdots Cl3 ($H\cdots A = 2.799\text{ \AA}$) and with additional bonding between N2—H3A \cdots Cl3 ($H\cdots A = 2.664\text{ \AA}$) and N4—H4A \cdots Cl2 ($H\cdots A = 2.791\text{ \AA}$). Figures 2.20 and 2.21 highlight the location of the urea NH groups that hydrogen-bond to $[PtCl_6]^{2-}$.

The extended crystal structure shows that there is a hydrogen-bonded chain arrangement of the type $\cdots\{[L^3H^+]\cdots[PtCl_6]^{2-}\cdots[L^3H^+]\}\cdots\{[L^3H^+]\cdots[PtCl_6]^{2-}\cdots[L^3H^+]\}\cdots$ (Figure 2.22) with each $[L^3H^+]$ cation using two arms to interact with $[PtCl_6]^{2-}$ and the third arm to interact with another $[L^3H^+]$ cation through a bifurcated hydrogen-bond. The structure reveals that although two pendant arms of the receptor hydrogen-bond to $[PtCl_6]^{2-}$, the anion is not encapsulated as proposed from the receptor design. This is thought to be because the oxygen atoms of the urea moieties are competitive for the NH donor groups and, thus, there are interactions of the type N—H \cdots O alongside the desired N—H \cdots Cl interactions in the solid state. The details of all the hydrogen-bonding interactions in $[(L^3H)_2PtCl_6]$ are shown in Table 2.6 and crystallographic data and structure refinement details for the complex are given in Appendix B.

Comparison of the crystal structures of $[(L^1H)_2PtCl_6]$ with $[(L^3H)_2PtCl_6]$ shows that there are more hydrogen-bonds present between the urea receptor molecules and $[PtCl_6]^{2-}$ than with the sulfonamide receptors. If the number of hydrogen-bonds determines the strength of the interaction between a receptor and anion then this infers a stronger interaction between urea receptors and $[PtCl_6]^{2-}$. This is interesting as the sulfonamide NH donor groups are more acidic and it was, therefore, predicted they would form a stronger interaction. This suggests that the number of hydrogen-bond donor groups is perhaps more significant than the acidity of individual NH donor groups.

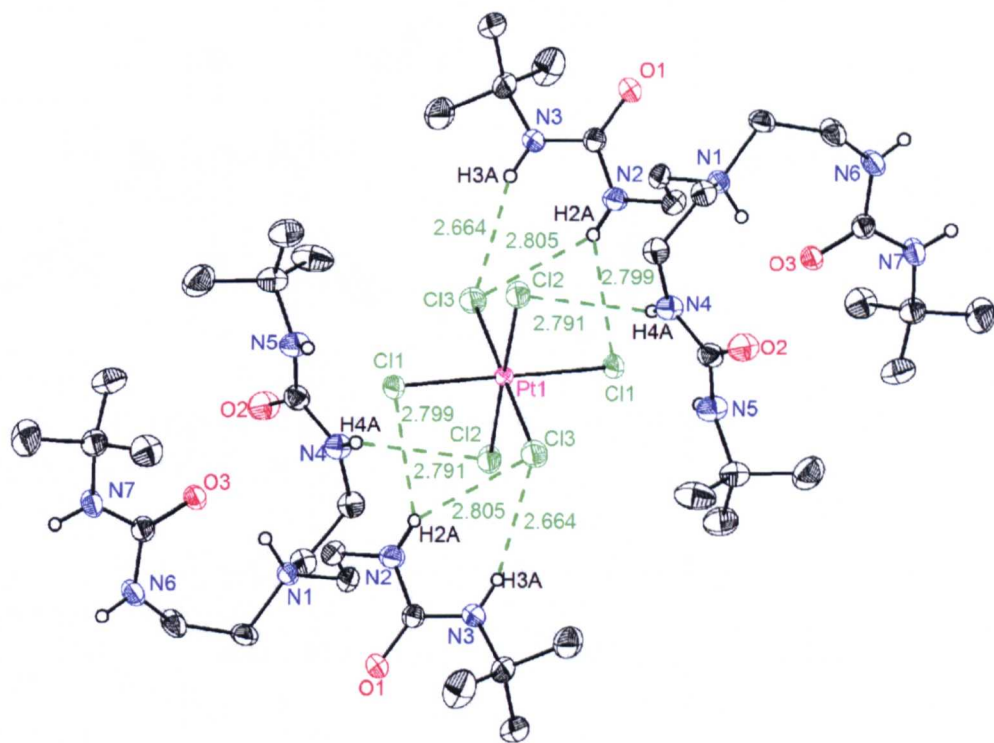


Figure 2.19. Molecular structure of $[(L^3)_2PtCl_6]$ showing hydrogen-bonds between L^3 and $[PtCl_6]^{2-}$. All hydrogen atoms (except NH) omitted for clarity. Ellipsoids set at 50% probability. Hydrogen-bonds are shown in green and the $NH \cdots Cl$ distances are measured in Å.

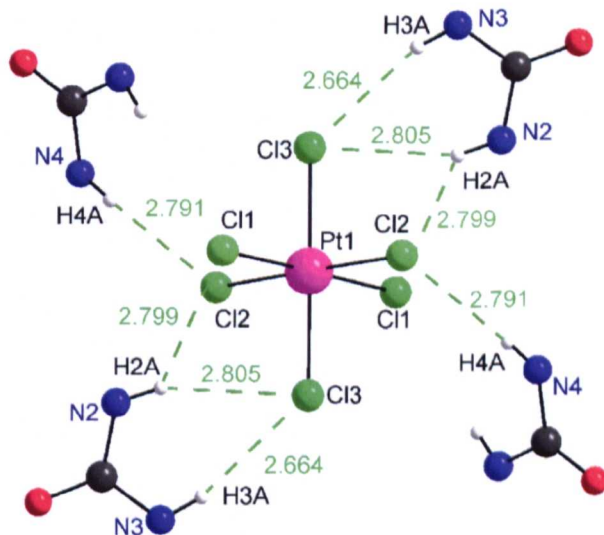


Figure 2.20. Highlighting how four urea groups are orientated around $[PtCl_6]^{2-}$.

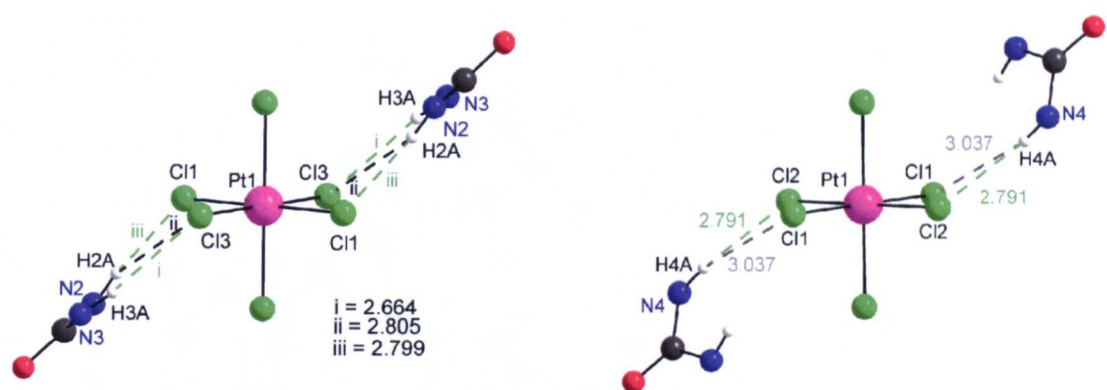


Figure 2.21. Highlighting the location of NH hydrogen-bond donor groups in relation to the $[\text{PtCl}_6]^{2-}$ anion.

Table 2.6. Hydrogen-bonds D—H \cdots A present in $[(\text{L}^{\text{3}}\text{H})_2\text{PtCl}_6]$ (D = donor, A = acceptor, d = distance).

D—H \cdots A	d(D—H)/ Å	d(H \cdots A)/ Å	d(D \cdots A)/ Å	$\angle(\text{DHA})/$ °	Symmetry Code
N2—H2A \cdots Cl1	0.86	2.799	3.4390	132	
N2—H2A \cdots Cl3	0.86	2.805	3.5778	150	
N3—H3A \cdots Cl3	0.86	2.664	3.4951	163	
N4—H4A \cdots Cl2	0.86	2.791	3.3629	125	
N6—H6A \cdots O1	0.86	2.096	2.832	143	-x+1, -y+1, -z
N7—H7A \cdots O1	0.86	2.180	2.951	149	-x+1, -y+1, -z

* Interactions between $[\text{L}^{\text{3}}\text{H}^+]$ and $[\text{PtCl}_6]^{2-}$ are shown above the horizontal line whilst interligand hydrogen-bonds are below the line.

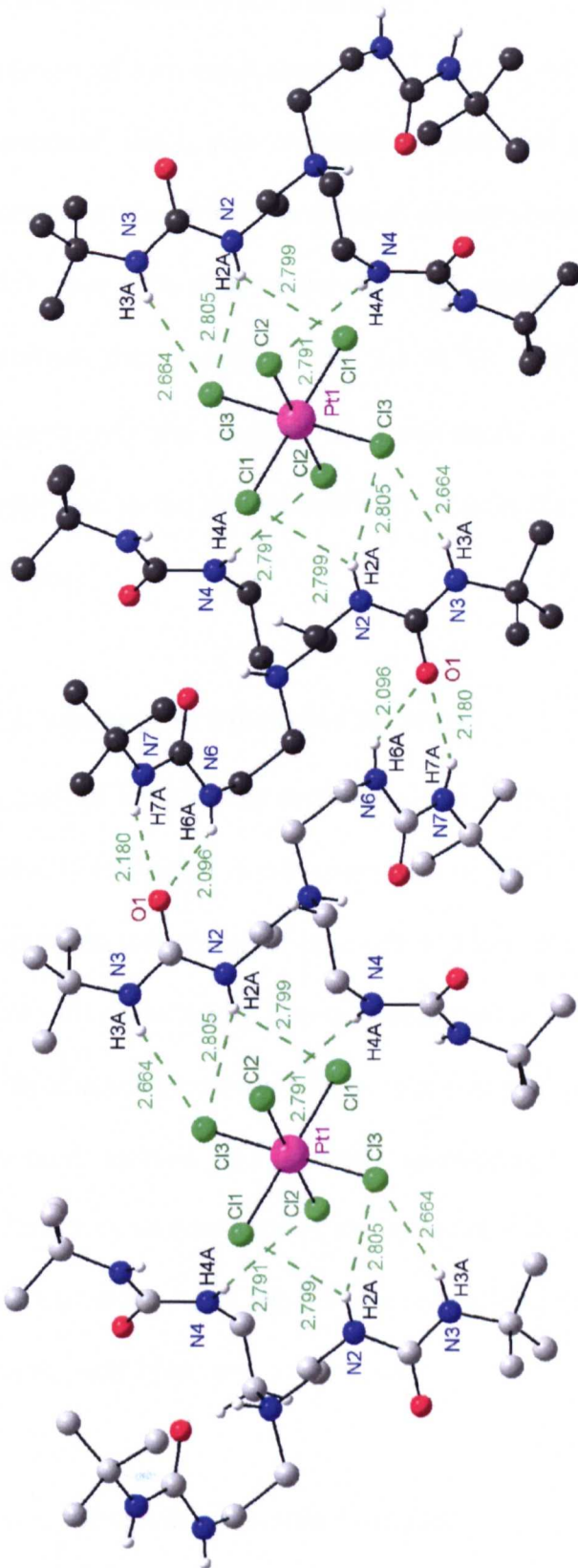


Figure 2.22. View of the structure of $[(L^3H)_2PtCl_6]$ showing the hydrogen-bonds present in the extended structure. All hydrogen atoms (except NH) omitted for clarity. Hydrogen-bonds are shown in green and measured in Å. The carbon atoms for each entity of $[(L^3H)_2PtCl_6]$ are shown in different shades of grey.

2.4.2.4. Synthesis of $[(L^4H)_2PtCl_6]$

Reaction of two equivalents of L^4 with H_2PtCl_6 in MeCN gave a yellow-orange precipitate which was collected by filtration and dried *in vacuo*. The 1H NMR spectrum of the product in $dmso-d_6$ shows a broad signal at 10.07 ppm, integrating in a 1:3 ratio with each of the urea NH signals, and assigned to N^+HR_3 . Elemental analytical data confirmed the 2:1 $(L^4H)^+:[PtCl_6]^{2-}$ stoichiometry of the product. Unfortunately the receptor L^4 is not useful as an extractant in solvent extraction studies due to the limited solubility of both the receptor and its complex in organic solvents.

2.4.3. Synthesis of Thiourea Complexes

For each of the thiourea receptors (L^5-L^7) two equivalents of ligand were dissolved in MeCN and added to one equivalent of H_2PtCl_6 also dissolved in MeCN. For each receptor, on the mixing of reactants a yellow-orange precipitate formed immediately which was collected by filtration and dried *in vacuo*. Unfortunately, each product of the three complexation reactions was completely insoluble, even in $dmso$, and this prevented analysis by 1H NMR spectroscopy but elemental analytical data did confirm the stoichiometry of the complexes as $[(LH)_2PtCl_6]$. The infrared spectrum of each product shows signals characteristic of the N—H and C=S groups at around 3200cm^{-1} and 1560 cm^{-1} , respectively.

2.4.4. Synthesis of an Amide Complex

2.4.4.1. Synthesis of $[(L^8H)_2PtCl_6]$

Two equivalents of L^8 were dissolved in MeCN and added to H_2PtCl_6 in MeCN. A yellow precipitate was formed and this was collected by filtration and dried *in vacuo*. The 1H NMR spectrum of the product in $dmso-d_6$ shows a signal which integrates in

a 1:3 ratio with the amide NH signal at 9.87 ppm assigned to the $\text{N}^+\underline{\text{H}}\text{R}_3$ proton (Figure 2.23). Upon complexation there is a downfield shift of the urea NH signal (Hc) indicating the presence of hydrogen-bonding interactions between L^8H^+ and $[\text{PtCl}_6]^{2-}$.⁷⁷ The IR spectrum of the product showed characteristic N—H bands at 3371 cm^{-1} , 3221 cm^{-1} and C=O 1637 cm^{-1} , respectively while elemental analytical data confirmed the 2:1 $(\text{L}^8\text{H})^+:[\text{PtCl}_6]^{2-}$ stoichiometry of the complex.

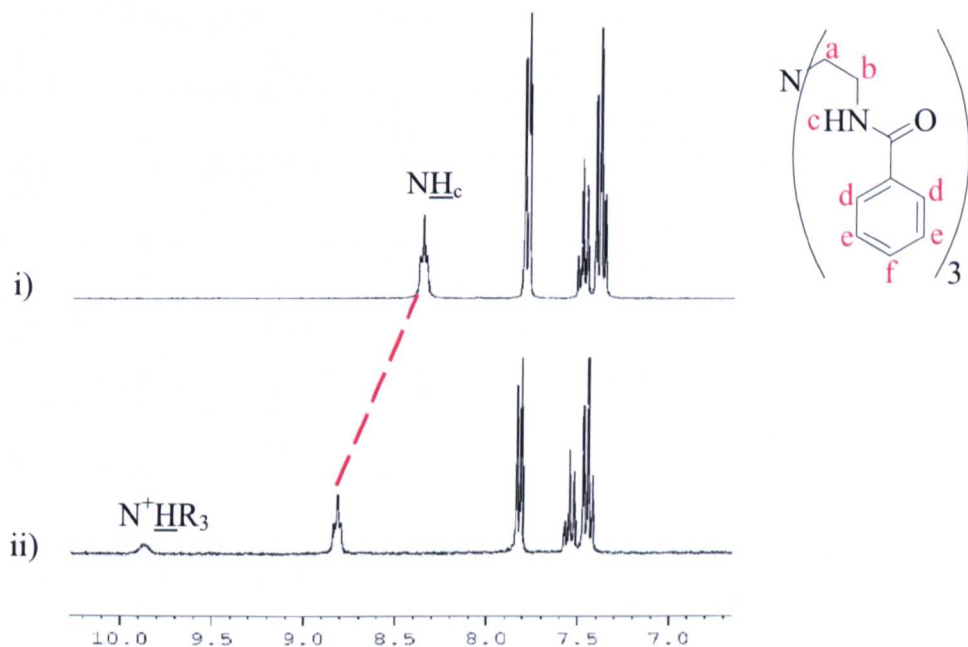


Figure 2.23. ^1H NMR spectra [$\text{dmso}-d_6$, 300 MHz] of i) L^8 and ii) $[(\text{L}^8\text{H})_2\text{PtCl}_6]$.

2.4.5. Synthesis of an Amido Pyrrole Complex

2.4.5.1. Attempted synthesis of $[(\text{L}^9\text{H})_2\text{PtCl}_6]$

The pyrrole-containing receptor L^9 was found to be insoluble in MeCN, even when heated. However, reaction of a suspension of L^9 with H_2PtCl_6 in MeCN afforded an insoluble yellow solid. As the receptor was not completely soluble, it proved difficult to separate the two solids (undissolved receptor and the complex product). The reaction was also attempted in acetone but L^9 remained insoluble and the same observation was made. Characterisation of a pure product was thus not possible in this case.

2.5. Summary of Results

The key design features for the target receptors described in this Chapter are i) a tripodal geometry, ii) a protonation site, iii) hydrogen-bond donor groups, iv) organic solubilising groups and v) synthetic accessibility. A series of TREN-based receptors have been successfully synthesised incorporating sulfonamide, urea, thiourea, amide or pyrrole hydrogen-bond donor moieties and phenyl, *tert*-butyl, *n*-butyl or methyl organic solubilising groups. In most cases the target receptor was synthesised in one synthetic step. Full characterisation of these products by ^1H NMR, ^{13}C NMR and IR spectroscopy, mass spectrometry and elemental analytical data confirmed their formation and purity. Crystals of those receptors containing terminal phenyl groups (L^1 , L^2 , L^5 , L^8 and L^9) were successfully obtained and in each case (except for the thiourea ligand L^5) both intra- and inter-molecular hydrogen-bonds were observed to give interesting chain-type structures.

Reaction of two equivalents of a receptor with one equivalent of H_2PtCl_6 in MeCN gave, in most cases, a yellow precipitate. Generally, these products were found to have low solubility, but, where possible, ^1H NMR spectra were recorded which confirmed the protonation of the bridgehead N-centre in the receptor. Elemental analytical data for the products confirmed the 2:1 $(\text{LH})^+:\text{[PtCl}_6]^{2-}$ stoichiometry of the complexes. Single crystal X-ray structures were obtained for $[(\text{L}^1\text{H})_2\text{PtCl}_6]$ and $[(\text{L}^3\text{H})_2\text{PtCl}_6]$ which showed that the bridgehead nitrogen position was indeed protonated and that the two protonated receptor molecules interact with $[\text{PtCl}_6]^{2-}$ through hydrogen-bonding interactions thus confirming our basic design strategy.

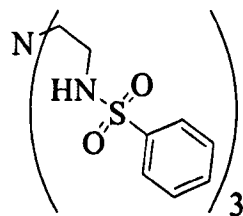
The low solubility of the receptors and complexes synthesised in this Chapter means that they have limited use in solvent extractions. However, the complexes do provide us with very useful information about how these receptors interact with

$[\text{PtCl}_6]^{2-}$. The next step was to modify the receptor design by improving the solubility of the complexes in organic solvents, and this is discussed in Chapter Three.

2.6. Experimental

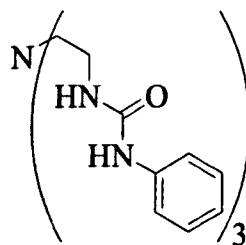
2.6.1. Synthesis of Receptors

2.6.1.1. Synthesis of N,N',N''-(nitrilotri-2,1-ethanediyl)tris-benzenesulfonamide, L¹.^{45, 48}



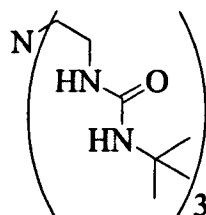
Benzene sulfonyl chloride (4.10 cm^3 , 32 mmol) was dissolved in Et_2O (15 cm^3) and added dropwise to a solution of TREN (1.50 cm^3 , 10 mmol) in H_2O (20 cm^3) containing NaOH (1.28 g, 32 mmol). The reaction was stirred for 2 h and then allowed to stand for 2 h. The reaction mixture was filtered by gravity and the solid collected and recrystallised from MeOH to give L¹ as a colourless, crystalline solid. Yield: 4.65 g, 82%. ¹H NMR (300 MHz, CDCl_3): δ/ppm 7.92 (m, 6H, H_{Ar}), 7.90–7.51 (m, 9H, H_{Ar}), 6.02 (br, 3H, NH), 2.97 (br, 6H, NCH₂), 2.66 (br, 6H, NCH₂). ¹³C NMR (68 MHz, CDCl_3): δ/ppm 140, 133, 129, 127, 54, 41. MS (ES⁺): m/z 567 [M+H]⁺, 590 [M+Na]⁺. IR (KBr, cm^{-1}): 3297 ($\nu_{(\text{NH})}$), 1619 ($\nu_{(\text{C-C, Ar})}$), 1350 ($\nu_{(\text{SO}_2)}$), 1150 ($\nu_{(\text{SO}_2)}$). Anal. calc. for $\text{C}_{24}\text{H}_{30}\text{N}_4\text{O}_6\text{S}_3$: C, 50.87; H, 5.34; N, 9.89. Found: C, 50.85; H, 5.34; N, 9.73%.

2.6.1.2. Synthesis of N,N',N''-(nitrilotri-2,1-ethanediyl)tris[N'-phenylurea], L².⁵⁴



Phenyl isocyanate (0.46 cm^3 , 4.20 mmol) was added dropwise to a solution of TREN (0.20 cm^3 , 1.35 mmol) in dry thf (30 cm^3) under N_2 . The reaction was stirred at room temperature for 2 h during which time a colourless precipitate formed which was collected by filtration and dried *in vacuo*. No further purification was required. Yield: 0.65 g, 95%. ^1H NMR (270 MHz, CD_3OD): δ/ppm 7.26 (d, 6H, $^3J_{\text{HH}} = 8 \text{ Hz}$, $\underline{\text{H}_{\text{Ar}}}$), 7.21–7.16 (m, 6H, $\underline{\text{H}_{\text{Ar}}}$), 6.95 (t, 3H, $^3J_{\text{HH}} = 8 \text{ Hz}$, $\underline{\text{H}_{\text{Ar}}}$), 3.54–3.48 (m, 6H, $\underline{\text{CH}_2}$), 2.68 (t, 6H, $^3J_{\text{HH}} = 5 \text{ Hz}$, $\underline{\text{CH}_2}$). ^{13}C NMR (68 MHz, $\text{dmso}-d_6$): δ/ppm 156, 141, 129, 122, 118, 55, 37. MS (ES $^+$): m/z 504 [$\text{M}+\text{H}]^+$, 526 [$\text{M}+\text{Na}]^+$. IR (KBr, cm^{-1}): 3334 ($\nu_{(\text{NH})}$), 1650 ($\nu_{(\text{C=O})}$). Anal. calc. for $\text{C}_{27}\text{H}_{33}\text{N}_7\text{O}_3$: C, 64.40; H, 6.60; N, 19.47. Found: C, 64.29; H, 6.78; N, 19.11%.

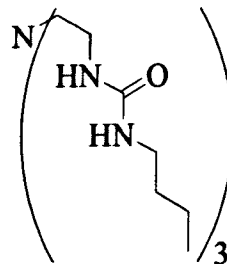
2.6.1.3. Synthesis of N,N',N''-(nitrilotri-2,1-ethanediyl)tris[N'-*tert*-butylurea], L³.⁵⁴



L³ was prepared in an analogous way to L² by the reaction of TREN with *tert*-butylisocyanate to give a colourless solid. Yield: 0.58 g, 98%. ^1H NMR (300 MHz, CDCl_3): δ/ppm 5.79 (br, 3H, $\underline{\text{NH}}$), 5.15–5.13 (m, 3H, $\underline{\text{NH}}$), 3.13 (br, 6H, $\underline{\text{CH}_2}$), 2.46 (br, 6H, $\underline{\text{CH}_2}$), 1.33 (s, 27H, ^1Bu). ^{13}C NMR (68 MHz, CDCl_3): δ/ppm 160, 56, 50,

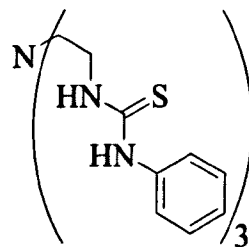
49, 30. MS (ES⁺): 444 [M+H]⁺, 467 [M+Na]⁺. IR (KBr, cm⁻¹): 3350 ($\nu_{(N-H)}$), 1650 ($\nu_{(C=O)}$). Anal. calc. for C₂₁H₄₅N₇O₃: C, 56.86; H, 10.22; N, 22.10. Found: C, 56.50; H, 10.24; N, 20.58%.

2.6.1.4. Synthesis of N,N',N''-(nitrilotri-2,1-ethanediyl)tris[N'-butylurea], L⁴⁵⁴



L⁴ was prepared in an analogous way to L² by the reaction of TREN with butylisocyanate to give a colourless solid. Yield: 0.57 g, 96%. ¹H NMR (300 MHz, CDCl₃): δ /ppm 6.00 (br, 3H, NH), 5.54 (br, 3H, NH), 3.17–3.10 (m, 6H, CH₂), 2.53 (br, 6H, CH₂), 1.98 (br, 6H, CH₂), 1.53–1.30 (m, 12H, CH₂), 0.92 (t, 9H, $^3J_{HH}$ = 7 Hz, CH₃). ¹³C NMR (68 MHz, CDCl₃): δ /ppm 160, 55, 40, 39, 33, 21, 14. MS (ES⁺): m/z 444 [M+H]⁺. IR (KBr, cm⁻¹): 3354 ($\nu_{(N-H)}$), 1652 ($\nu_{(C=O)}$). Anal. calc. for C₂₁H₄₅N₇O₃: C, 56.86; H, 10.22; N, 22.10. Found: C, 56.77; H, 10.22; N, 21.96%.

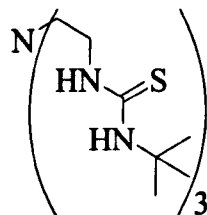
2.6.1.5. Synthesis of N,N',N''-(nitrilotri-2,1 -ethanediyl)tris[N'-phenylthiourea], L⁵⁵⁴



Phenyl isothiocyanate (0.49 cm³, 4.15 mmol) was added to a solution of TREN (0.20 cm³, 1.34 mmol) in dry thf (30 cm³) under N₂. The reaction stirred at room temperature for 16 h following which the solvent was removed *in vacuo* to give an

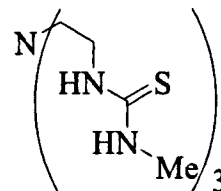
off-white solid which was recrystallised from MeOH to give the receptor as a colourless crystalline solid. Yield: 0.50 g, 68%. ^1H NMR (270 MHz, CDCl_3): δ/ppm 8.25 (s, 3H, NH), 7.32–7.15 (m, 15H, H_{Ar}), 6.90 (br, 3H, NH), 3.81–3.78 (m, 6H, CH_2), 2.73 (t, 6H, $^3J_{\text{HH}} = 6$ Hz, CH_2). ^{13}C (75 MHz, $\text{dmso}-d_6$): δ/ppm 181, 140, 129, 126, 124, 53, 43. MS (ES $^+$): m/z 552 [$\text{M}+\text{H}]^+$, 574 [$\text{M}+\text{Na}]^+$. IR (solid, cm^{-1}): 3345 ($\nu_{(\text{NH})}$), 3286 ($\nu_{(\text{NH})}$), 1551 ($\nu_{(\text{C=S})}$). Anal. calc. for $\text{C}_{27}\text{H}_{33}\text{N}_7\text{S}_3$: C, 58.86; H, 6.04; N, 17.79. Found: C, 58.54; H, 6.00; N, 17.56%.

2.6.1.6. Synthesis of N,N',N''-(nitrilotri-2,1-ethanediyl)tris[N'-tertbutylthiourea] L⁶.⁵⁴



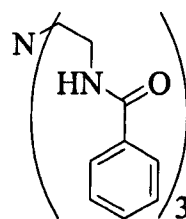
L^6 was prepared in an analogous manner to L^5 by the reaction of TREN with *tert*-butyl isothiocyanate to give a colourless solid. Yield: 0.48 g, 74%. ^1H NMR (270 MHz, CDCl_3): δ/ppm 6.48 (br, 3H, NH), 6.33 (br, 3H, NH), 3.58–3.54 (m, 6H, CH_2), 2.66 (t, 6H, $^3J_{\text{HH}} = 6$ Hz, CH_2), 1.42 (s, 27H, ^1Bu). ^{13}C (68 MHz, CDCl_3): δ/ppm 181, 54, 53, 43, 30. MS (ES $^+$): m/z 492 [$\text{M}+\text{H}]^+$. IR (solid, cm^{-1}): 3300 ($\nu_{(\text{NH})}$), 1650 ($\nu_{(\text{C=S})}$). Anal. calc for $\text{C}_{21}\text{H}_{45}\text{N}_7\text{S}_3$: C, 51.28; H, 9.22 ; N, 19.94. Found: C, 51.23; H, 9.07; N, 18.94%.

2.6.1.7. Synthesis of N,N',N''-(nitrilotri-2,1-ethanediyl)tris[N'-methylthiourea], L⁷.⁵⁴



L⁷ was prepared in a similar manner to L⁵ by the reaction of TREN with methyl isothiocyanate to give a colourless oil. Yield: 0.34 g, 69%. ¹H NMR (300 MHz, CDCl₃): δ/ppm 6.88 (br, 3H, NH), 6.73 (br, 3H, NH), 3.72–3.69 (m, 6H, CH₂), 3.05 (d, 9H, ³J_{HH} = 4 Hz, CH₃), 2.64 (t, 6H, ³J_{HH} = 5 Hz, CH₂). ¹³C NMR (68 MHz, CDCl₃): δ/ppm 172, 68, 53, 26. MS (ES⁺): found m/z 366.1556, calc. m/z 366.1563 for [M+H]⁺. Anal. calc. for C₁₂H₂₇N₇S₃: C, 39.42; H, 7.44; N, 26.82. Found: C, 42.06; H, 7.47; N, 23.85%.

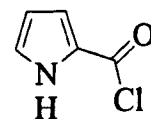
2.6.1.8. Synthesis of N,N',N''-(nitrilotri-2,1-ethanediyl)tris-benzamide, L⁸.^{45, 48}



Benzoyl chloride (0.90 cm³, 7.66 mmol) dissolved in diethyl ether (10 cm³) was added slowly to TREN (0.40 cm³, 2.70 mmol) in H₂O (20 cm³) containing NaOH (0.33 g, 8.25 mmol). The reaction stirred at room temperature for 48 h and then the off-white solid that had formed was collected by filtration, washed with a portion of diethyl ether (10 cm³) and dried *in vacuo* to give a colourless solid. Yield: 0.92 g, 74%. ¹H NMR (300 MHz, CDCl₃): δ/ppm 7.60 (d, 3H, ³J_{HH} = 6 Hz, H_{Ar}), 7.33–7.30 (m, 6H, H_{Ar}), 7.18 (br, 3H, NH), 7.07 (t, 6H, ³J_{HH} = 9 Hz, H_{Ar}), 3.60–3.55 (m, 6H, CH₂), 2.76 (t, 6H, ³J_{HH} = 6 Hz, CH₂). ¹³C NMR (68 MHz, CDCl₃): δ/ppm 168, 134,

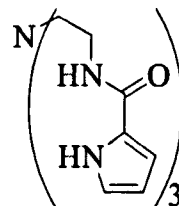
131, 128, 127, 54, 38. MS (ES^+): m/z 459 $[\text{M}+\text{H}]^+$. IR (solid, cm^{-1}): 3345 ($\nu_{(\text{NH})}$), 3286 ($\nu_{(\text{NH})}$), 1536 ($\nu_{(\text{C=O})}$). Anal. calc. for $\text{C}_{27}\text{H}_{30}\text{N}_4\text{O}_3$: C, 70.72; H, 6.59; N, 12.22. Found: C, 70.86; H, 6.61; N, 12.24%.

2.6.1.9. Synthesis of pyrrole-2-carbonyl chloride.⁷³⁻⁷⁵



An excess of oxalyl chloride (0.60 cm^3) was added to pyrrole-2-carboxylic acid (0.70 g, 6.30 mmol) in benzene (30 cm^3) under N_2 . To this mixture was added two drops of dmf to catalyse the reaction. The reaction was stirred at room temperature for 16 h during which time all the starting material dissolved to give a colourless solution. The solvent was then removed *in vacuo* to give the product as a pale yellow powder. Yield: 0.78 g, 96% yield. ^1H NMR (270 MHz, CDCl_3): δ/ppm 9.58 (br, 1H, NH), 7.24–7.15 (m, 2H, $2 \times \text{CH}$), 6.40–6.32 (m, 1H, CH). ^{13}C NMR (68 MHz, CDCl_3): δ/ppm 170, 131, 128, 123, 112.

2.6.1.10. Synthesis of $\text{N},\text{N}',\text{N}''$ -(nitrilotri-2,1-ethanediyl)tris-pyrrole, L⁹.⁷⁶



TREN (0.07 cm^3 , 0.51 mmol) was dissolved in CH_2Cl_2 (20 cm^3) and Na_2CO_3 was added to give a basic solution. Pyrrole-2-carbonyl chloride (0.20 g, 1.54 mmol) was added to the stirring solution and a precipitate was formed in an exothermic reaction. The reaction mixture was stirred at room temperature for 3 h and H_2O (10 cm^3) was added to dissolve the Na_2CO_3 and form a biphasic system. The precipitate was

insoluble in both the organic and aqueous layers and was collected by filtration and washed with a portion of diethyl ether (10 cm^3) to give the product as an off-white solid which was dried *in vacuo*. Yield: 0.13 g, 60%. ^1H NMR (270 MHz, dmso- d_6): δ/ppm 11.44 (br, 3H, NH), 7.95 (br, 3H, NH), 6.85 (br, 3H, H_{Ar}), 6.74 (br, 3H, H_{Ar}), 6.07 (br, 3H, H_{Ar}), 3.33–3.18 (m, 6H, CH₂), 2.68 (t, 6H, $^3J_{\text{HH}} = 7\text{ Hz}$, CH₂). ^{13}C NMR (68 MHz, dmso- d_6): δ/ppm 161, 127, 122, 111, 110, 54, 47. MS (ES $^+$); found *m/z* 426.2262, calc. *m/z* 426.2253 for [M+H] $^+$. IR (solid, cm^{-1}): 3221 ($\nu_{(\text{N-H})}$), 1602 ($\nu_{(\text{C=O})}$), 1570 ($\nu_{(\text{C=C, Ar})}$). Anal. calc. for C₂₁H₂₇N₇O₃: C, 59.28; H, 6.40; N, 23.04. Found: C, 59.37, 6.40, 22.93%.

2.6.2. Synthesis of Complexes

2.6.2.1. Attempted Synthesis of [(L¹H)₂PtCl₆]

L¹ was insoluble in MeCN, even when heated, which prevented the reaction with H₂PtCl₆.

2.6.2.2. Synthesis of [(L²H)₂PtCl₆]

L² (0.02 g, 0.04 mmol) in MeCN (2 cm^3) was added to H₂PtCl₆ (0.01 g, 0.02 mmol) in MeCN (1 cm^3). An orange precipitate formed immediately which was collected by filtration and dried *in vacuo*. ^1H NMR (300 MHz, dmso- d_6): δ/ppm 9.61 (br, 1H, NH $^+$), 8.80 (s, 3H, NH), 7.40 (d, 6H, $^3J_{\text{HH}} = 8\text{ Hz}$, H_{Ar}), 7.19–7.14 (m, 6H, H_{Ar}), 6.92 (t, 3H, $^3J_{\text{HH}} = 8\text{ Hz}$, H_{Ar}), 6.45 (t, 3H, $^3J_{\text{HH}} = 6\text{ Hz}$, NH), 3.51 (m, 6H, CH₂), 3.37 (m, 6H, CH₂). IR (solid, cm^{-1}): 3358 ($\nu_{(\text{N-H})}$), 1650 ($\nu_{(\text{C=O})}$). Anal. calc. for C₅₄H₆₈Cl₆N₁₄O₆Pt + 1.4 H₂O: C, 44.97; H, 4.95; N, 13.60. Found: C, 44.97; H, 4.71; N, 13.56%.

2.6.2.3. Synthesis of $[(L^3H)_2PtCl_6]$

This compound was prepared in a similar manner to $[(L^2H)_2PtCl_6]$ and precipitated as a yellow solid. 1H NMR (270 MHz, dmso- d_6): δ /ppm 10.05 (br, 1H, NH $^+$), 6.05 (br, 3H, NH), 4.31 (br, 3H, NH), 3.31 (br, 6H, CH $_2$), 3.20 (br, 6H, CH $_2$), 1.25 (s, 27H, 'Bu). IR (solid, cm $^{-1}$): 3342 ($\nu_{(N-H)}$), 1632 ($\nu_{(C=O)}$). Anal. calc. for C $_{42}H_{92}Cl_6N_{14}O_6Pt$: C, 38.89; H, 7.15; N, 15.12. Found: C, 38.82; H, 7.09; N, 15.03%.

2.6.2.4. Synthesis of $[(L^4H)_2PtCl_6]$

This compound was prepared in a similar manner to $[(L^2H)_2PtCl_6]$ and precipitated as a yellow powder. 1H NMR (270 MHz, dmso- d_6): δ /ppm 10.07 (br, 1H, NH $^+$), 6.26 (t, 3H, $^3J_{HH} = 5$ Hz, NH), 6.18 (t, 3H, $^3J_{HH} = 5$ Hz, NH), 3.32 (br, 6H, CH $_2$), 3.23 (br, 6H, CH $_2$), 1.41–1.20 (m, 18H, CH $_2$), 0.88 (t, 9H, $^3J_{HH} = 7.0$ Hz, CH $_3$). Anal. calc. for C $_{42}H_{92}Cl_6N_{14}O_6Pt$: C, 38.89; H, 7.15; N, 15.12. Found: C, 38.94; H, 6.94; N, 14.97%.

2.6.2.5. Synthesis of $[(L^5H)_2PtCl_6]$

This compound was prepared in a similar manner to $[(L^2H)_2PtCl_6]$ and precipitated as a yellow powder. The product was completely insoluble hence no 1H NMR spectrum could be recorded. IR (solid, cm $^{-1}$): 3175 ($\nu_{(N-H)}$), 1562 ($\nu_{(C=S)}$). Anal. calc. for C $_{54}H_{68}Cl_6N_{14}PtS_6$: C, 42.86; H, 4.53; N, 12.96. Found: C, 42.69; H, 4.51; N, 12.89%.

2.6.2.6. Synthesis of $[(L^6H)_2PtCl_6]$

This compound was prepared in a similar manner to $[(L^2H)_2PtCl_6]$ and precipitated as a yellow powder. The product was completely insoluble hence no 1H NMR spectrum could be recorded. IR (solid, cm^{-1}): 3227 ($\nu_{(N-H)}$), 1566 ($\nu_{(C=S)}$). Anal. calc. for $C_{42}H_{92}Cl_6N_{14}PtS_6$: C, 36.20; H, 6.65; N, 14.07. Found: C, 35.80; H, 6.51; N, 13.89%.

2.6.2.7. Synthesis of $[(L^7H)_2PtCl_6]$

This compound was prepared in a similar manner to $[(L^2H)_2PtCl_6]$ and precipitated as a yellow powder. The product was completely insoluble hence no 1H NMR spectrum could be recorded. IR (solid, cm^{-1}): 3211 ($\nu_{(N-H)}$), 1594 ($\nu_{(C=S)}$). Anal. calc. for $C_{24}H_{56}Cl_6N_{14}PtS_6$: C, 25.26; H, 4.95; N, 17.19. Found: C, 25.16; H, 4.82; N, 17.03%.

2.6.2.8. Synthesis of $[(L^8H)_2PtCl_6]$

This compound was prepared in a similar manner to that described for $[(L^2H)_2PtCl_6]$ and precipitated as a yellow powder. 1H NMR (300 MHz, $dmso-d_6$): δ /ppm 9.87 (br, 1H, NH^+), 8.81 (t, 3H, $^3J_{HH} = 5$ Hz, NH), 7.81 (d, 6H, $^3J_{HH} = 7.10$ Hz, H_{Ar}), 7.54 (t, 3H, $^3J_{HH} = 7.3$ Hz, H_{Ar}), 7.47–7.41 (m, 6H, H_{Ar}), 3.72 (d, 6H, $^3J_{HH} = 5$ Hz, CH_2), other CH_2 obscured by H_2O signal. IR (solid, cm^{-1}): 3371 ($\nu_{(N-H)}$), 3221 ($\nu_{(N-H)}$), 1637 ($\nu_{(C=O)}$). Anal. calc. for $C_{54}H_{62}Cl_6N_8O_6Pt$: C, 48.88; H, 4.71; N, 8.44. Found: C, 49.15; H, 4.63; N, 8.37%.

2.6.2.9. Attempted Synthesis of $[(L^9H)_2PtCl_6]$

L^9 was insoluble in MeCN, even when heated, which prevented the reaction with H_2PtCl_6 .

2.7. References

1. Yoshizawa H.; Shiomori K.; Yamada S.; Baba Y.; Kawano Y.; Kondo K.; Ijichi K.; Hatake Y., *Solv. Extr. Res. Dev.*, Japan, 1997, **4**, 157-166.
2. Fu J.; Nakamura S.; Akiba K., *Sep. Sci. Technol.*, 1995, **30**, 609-619.
3. Fu J.; Nakamura S.; Akiba K., *Anal. Sci.*, 1995, **11**, 149-153.
4. Fu J.; Nakamura S.; Akiba K., *Sep. Sci. Technol.*, 1997, **32**, 1433-1445.
5. Hasegawa Y.; Kobayashi I.; Yoshimoto S., *Solv. Extr. Ion Exch.*, 1991, **9**, 759-768.
6. Mirza M. Y., *Talanta*, 1980, **27**, 101-106.
7. Dietrich B.; Hosseini M. W.; Lehn J. M.; Sessions R. B., *J. Am. Chem. Soc.*, 1981, **103**, 1282.
8. Llinares J. M.; Powell D.; Bowman-Jones K., *Coord. Chem. Rev.*, 2003, **240**, 57-75.
9. Rosenqvist T., *Principles of Extractive Metallurgy*, McGraw-Hill, Tokyo, 1983.
10. Bowman-James K., *Acc. Chem. Res.*, 2005, **38**, 671-678.
11. Aullon G.; Bellamy D.; Brammer L.; Bruton E. A.; Orpen G., *Chem. Commun.*, 1998, 653-654.
12. Kovacs A.; Varga Z., *Coord. Chem. Rev.*, 2006, **250**, 710-727.
13. Koch K. R.; Burger M. R.; Kramer J.; Westra A. J., *Dalton Trans.*, 2006, 3277-3284.
14. Naidoo K. J.; Klatt G.; Koch K. R.; Robinson D. J., *Inorg. Chem.*, 2002, **41**, 1845-1849.
15. Lienke A.; Klatt G.; Robison D. J.; Koch K.; Naidoo K. J., *Inorg. Chem.*, 2001, **40**, 2352-2357.
16. Brammer L.; Swearingen J. K.; Bruton E. A.; Sherwood P., *Proc. Nat. Acad. Sci (USA)*, 2002, **99**, 4956-4961.
17. Middleton Boon J.; Lambert T. N.; Smith B. D.; Beatty A. M.; Ugrinova V.; Brown S. N., *J. Org. Chem.*, 2002, **67**, 2168-2174.
18. Amendola V.; Bonizzoni M.; Esteban-Gomez D.; Fabbrizzi L.; Licchelli M.; Sancenon F.; Taglietti A., *Coord. Chem. Rev.*, 2006, **250**, 1451-1470.
19. Amendola V.; Bonizzoni M.; Esteban-Gomez D.; Fabbrizzi L.; Licchelli M.; Sancenon F.; Taglietti A., *Coord. Chem. Rev.*, 2006, **250**, 1451-1470.
20. Hisaki I.; Sasaki S.; Hirose K.; Tobe Y., *Eur. J. Org. Chem.*, 2007, 607-615.

21. Bondy C. R.; Loeb S. J., *Coord. Chem. Rev.*, 2003, **240**, 77-99.
22. Sessler J. L.; Camiolo S.; Gale P. A., *Coord. Chem. Rev.*, 2003, **240**, 17-55.
23. Galbraith S. G.; Tasker P.A., *Supramol. Chem.*, 2005, **17**, 191-207.
24. Yordanov A. T.; Roundhill D. M., *Coord. Chem. Rev.*, 1998, **170**, 93-124.
25. Koch K. R., *Coord. Chem. Rev.*, 2001, **216-217**, 473-488.
26. Bazzicalupi C.; Bencini A.; Borsari L.; Giorgi C.; Valtancoli B., *J. Org. Chem.*, 2005, **70**, 4257-4266.
27. Hossain Md. A.; Liljegren J.A.; Powell D.; Bowman-James K., *Inorg. Chem.*, 2004, **43**, 3751-3755.
28. Kang S. O.; Llinares J. M.; Powell D.; Vandervelde D.; Bowman-James K.; *J. Am. Chem. Soc.*, 2003, **125**, 10152-10153.
29. Hay B.P.; Gutowski M.; Dixon D.A.; Garza J.; Vargas R.; Moyer B.A., *J. Am. Chem. Soc.*, 2004, **126**, 7925-7934.
30. Ilioudis C. A.; Tocher D. A.; Steed J. W., *J. Am. Chem. Soc.*, 2004, **126**, 12395-12402.
31. Turner D. R.; Pastor A.; Alajarin M.; Steed J. W., *Struct. Bonding*, 2004, **108**, 97-168.
32. Alajarin M.; Pastor A.; Orenes R. A.; Steed J. W.; Arakawa R., *Chem. Eur. J.*, 2004, **10**, 1383-1397.
33. Best M. D.; Tobey S. L.; Anslyn E.V., *Coord. Chem. Rev.*, 2003, **240**, 3-15.
34. Albeda M. T.; Frias J. C.; Garcia-Espana E.; Luis S.V., *Org. Biomol. Chem.*, 2004, **2**, 816-820.
35. Miranda C.; Escarti F.; Yunta M. J. R.; Navarro P.; Garcia Espana E.; Jimeno M. L., *J. Am. Chem. Soc.*, 2004, **126**, 823-833.
36. Lamarque L.; Navarro P.; Miranda C.; Aran V.J.; Ochoa C.; Escarti F.; Garcia-Espana. E.; Latorre J.; Luis S.V.; Miravet J. F., *J. Am. Chem. Soc.*, 2001, **123**, 10560-10570.
37. Sessler J. L.; Katayev E.; Pantos G. D.; Ustynyuk Y. A., *Chem. Commun.*, 2004, 1276-1277.
38. Sessler J. L.; Seidel D., *Angew. Chem. Int. Ed.*, 2003, **42**, 5134-5175.
39. Haj-Zaroubi M.; Mitzel N. W.; Schmidtchen F. P.; *Angew. Chem. Int. Ed.*, 2002, **41**, 104-107.
40. Nelson J.; Nieuwenhuyzen M.; Pal I.; Town R. M., *Dalton Trans.*, 2004, 2303-2308.

41. Nelson J.; Nieuwenhuyzen M.; Pal I.; Town R. M., *Dalton Trans.*, 2004, 229-235.
42. McKee V.; Nelson J.; Town R. M. *Chem. Soc. Rev.*, 2003, **32**, 309-325.
43. Gale, P. A., *Coord. Chem. Rev.*, 2003, **240**, 191-221.
44. Beer P. D.; Hopkins P. K.; McKinney J. D. *Chem. Commun.*, 1999, 1253-1254.
45. Valiyaveettil S. K.; Engbersen J. F. J.; Verboom W.; Reinhoud D. N., *Angew. Chem., Int. Ed.*, 1993, **32**, 900-902.
46. Bordwell F. G.; Fried H. E.; Hughes D. L.; Lynch T. Y.; Satish A. V.; Whang Y. E., *J.Org. Chem.*, 1990, **55**, 3330-3336.
47. Marsh J., *Advanced Organic Chemistry: Reactions, Mechanisms and Structure*, John Wiley and Sons, 4th Edition, pp 499.
48. Geraldes C. F. G. C.; Brucher E.; Cortes S.; Koenig S. H.; Sherry A. D.; *J. Chem. Soc., Dalton Trans.*, 1992, 2517-2522.
49. Albelda M.; Garcia-Espana E.; Jimenez H.R.; Llinares J. M.; Soriana C.; Sornosa-Ten A.; Begona V., *Dalton Trans.*, 2006, **37**, 4474-4481.
50. Choi K.; Hamilton A. D, *Coord. Chem. Rev.*, 2003, **240**, 101-110.
51. Bordwell F. G.; Ji G. Z., *J. Am. Chem. Soc.*, 1991, **113**, 8398-8401.
52. Castro E. A., Moodie R. B., Sansom P. J., *J. Chem. Soc., Perkin Trans. 2*, 1985, 737-742.
53. Marsh J., *Advanced Organic Chemistry: Reactions, Mechanisms and Structure*, John Wiley and Sons, 4th Edition, pp 886
54. Zart M. K.; Sorrell T. N.; Powell D.; Borovik A. S., *Dalton Trans.*, 2003, 1986-1992.
55. Raposo C.; Almaraz M.; Martin M.; Weinrich V.; Mussons M. L.; Alcazar V.; Caballero M. C.; Moran J. R, *Chem. Lett.*, 1995, **9**, 759-760.
56. Budria J. G.; Raugei S.; Cavallo L.; *Inorg. Chem.*, 2006, **45**, 1732-1738.
57. MacBeth C. E.; Larsen P. L.; Sorrell T. N.; Powell D.; Borovik A. S., *Inorg. Chim. Acta*, 2002, **341**, 77-84.
58. Gupta R.; Zhang Z. H.; Powell D.; Hendrich M. P.; Borovik A.S., *Inorg. Chem.*, 2002, **41**, 5100-5106.
59. MacBeth C. E.; Hammes B. S.; Young V. G.; Borovik A. S., *Inorg. Chem.*, 2001, **40**, 4733-4741.

60. Hammes B. S.; Young V. G.; Borovik A. S., *Angew. Chem. Int. Ed.*, 1999, **38**, 666-669.
61. Gupta R.; MacBeth C. E.; Young V. G.; Borovik A. S., *J. Am. Chem. Soc.*, 2002, **124**, 1136-1137.
62. Shirin Z.; Hammes B. S.; Young V. G.; Borovik A. S., *J. Am. Chem. Soc.*, 2000, **122**, 1836-1837.
63. De Loos M.; Ligtenbarg A. G.; Van Esch J.; Kooijman H.; Spek A. L.; Hage R.; Kellogg R. M.; Feringa B. L.; *Eur. J. Org. Chem.*, 2000, **22**, 3675-3678.
64. Bordwell F. G., *Acc. Chem. Res.*, 1988, **21**, 456- 463.
65. Gómez D. E.; Fabbrizzi L.; Licchelli M.; Monzani E., *Org. Biomol. Chem.*, 2005, **3**, 1495-1500.
66. Liao C.; Lai J.; Chen J.; Chen H.; Cheng G.; Su J.; Wang Y.; Lee G.; Leung M., *J. Org. Chem.*, 2001, **66**, 2566-2571.
67. Gupta R.; Zhang Z.; Powell D.; Hendrich M. P.; Borovik A. S., *Inorg. Chem.*, 2002, **41**, 5100-5106.
68. Khang S.; Begum R.A.; Bowman-James K., *Angew. Chem. Int. Ed.*, 2006, **45**, 7882-7894.
69. Bondy C.; Loeb S. J.; *Coord. Chem. Rev.*, 2003, **240**, 77-99.
70. Goldcamp, M. J.; Krause Bauer J. A.; Baldwin M. J., *Acta Cryst.*, 2000, **e56**, e602-e603.
71. For a review see Sessler J. L.; Camiolo S.; Gale P. A., *Coord. Chem. Rev.*, 2003, **240**, 17-55.
72. Bordwell F. G.; Drucker G. E.; Fried H. E., *J. Org. Chem.*, 1981, **46**, 632-635.
73. Alajarín M.; Pastor A.; Orenes R. A.; Steed J. W., *J. Org. Chem.*, 2002, **67**, 20, 7091-7095.
74. Boatman R. J.; Whitlock H. W., *J. Org. Chem.*, 1976, **41**, 18, 3050-3051.
75. Stein D.; Anderson G. T.; Chase C. E.; Koh Y.; Weinreb S. M., *J. Am. Chem. Soc.*, 1999, **121**, 9574-9579.
76. Sessler J. L.; Berthon-Gelloz G.; Gale P. A.; Camiolo S.; Anslyn E. V.; Anzenbacher P.; Furuta H.; Kirkovits G. J.; Lynch V. M.; Maeda H.; Morosini P.; Scherer M.; Shriver J.; Zimmerman R. S., *Polyhedron*, 2003, **22**, 2963-2983.

77. Jeffrey G. A., *An Introduction to Hydrogen Bonding*, Oxford University Press, Oxford, 1997, 9th edition, pp 228.

3. Improving the Solubility of Complexes

3.1. Introduction

It is a key requirement of this work that both the receptor and its complex are soluble in an organic phase that is immiscible with H₂O to facilitate the separation of [PtCl₆]²⁻ from other species present in the aqueous feed.¹ The receptors in Chapter 2 that have terminal phenyl substituents display low solubility in organic solvents. Receptors with *tert*-butyl terminal groups were, in general, more soluble; however, their complexes [(LH)₂PtCl₆] were either completely insoluble or only soluble in dmso. This Chapter describes the attempts that were made to increase the organic solubility of the receptors and of their corresponding [PtCl₆]²⁻ complexes.

3.2. Design Modifications

The receptors discussed in this Chapter have a TREN scaffold functionalised with hydrogen-bond donor groups to allow both electrostatic and hydrogen-bonding between the receptor and [PtCl₆]²⁻. The previous results presented in Chapter 2 confirm this approach to be successful in targeting [PtCl₆]²⁻. To improve and optimise the organic solubility of the receptors and their complexes the terminal R groups on each of the three arms of the receptor were varied. This approach was chosen as it allowed the key binding sites of the receptor to remain unaffected.

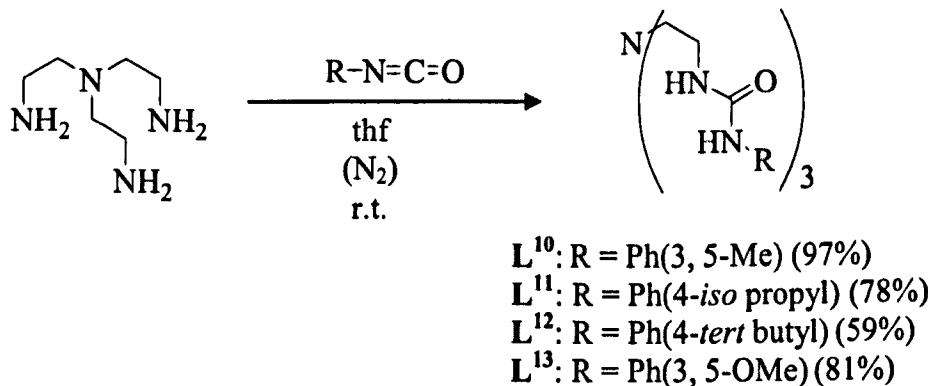
More specifically, the phenyl group was chosen as a starting point for these “second generation” receptors for two reasons. Firstly, the phenyl group is a stronger electron withdrawing group than an alkyl group such as *tert*-butyl, *n*-butyl or methyl.² This means that NH moieties bonded to phenyl groups are more acidic than their alkyl counterparts and consequently may be better hydrogen-bond donors leading to stronger hydrogen-bonds being formed and potential improvements in extraction. Secondly, the introduction of varying substituents onto the aromatic ring

at ortho, meta and para positions is a synthetically accessible and thus a convenient route to improve solubility. The receptors presented in this Chapter have terminal phenyl groups with alkyl or methoxy substituents of varying number and ring positions and, in the first instance, this approach was applied to TREN-based receptors containing urea, thiourea or amide hydrogen-bonding moieties.

3.3. Urea Receptors

3.3.1. Synthesis and Characterisation

Second generation TREN-based urea receptors were prepared from a range of commercially-available substituted phenyl isocyanates including 3, 5-dimethylphenyl, 4-*tert*-butylphenyl, 4-*iso*-propylphenyl and 3, 5-dimethoxyphenyl isocyanate. In each case TREN was reacted with three equivalents of the appropriate isocyanate to give the receptors L¹⁰–L¹³ as colourless precipitates in good yields (Scheme 3.1).³ The products were characterised by ¹H NMR, ¹³C NMR and IR spectroscopy, mass spectrometry and elemental analysis which confirmed the formation of analytically pure compounds. The ¹H NMR spectrum of each receptor shows two signals due to the urea NH protons thus confirming C₃ symmetry in solution. No previous reports of the synthesis of L¹⁰–L¹³ were found although structures with 4-nitrophenyl, azobenzene, 3, 4-dichlorophenyl and 4-cyanophenyl terminal groups have been prepared.^{4–7}



Scheme 3.1. Synthesis of L¹⁰–L¹³.

3.3.2. Crystal Structure of L¹¹

Single crystals of L¹¹ were obtained by the slow evaporation of a concentrated solution of the product in MeOH. L¹¹ crystallises in the orthorhombic space group *Pbca* with 8 molecules in the unit cell. The molecular structure shows intra-molecular, bifurcated hydrogen-bonding between N4—H4'···O1 ($H\cdots A = 2.032 \text{ \AA}$) and N5—H5A···O1 ($H\cdots A = 2.027 \text{ \AA}$) stabilising a tripodal conformation (Figure 3.1). Disorder in the *iso*-propyl group C10–C12 was modelled over two sites with an occupancy of 0.57/ 0.43 and refined with isotropic absorption displacement parameters. The H6A and H5A protons were geometrically placed and the other hydrogen atoms of the NH groups were defined by the difference map.

The extended structure of L¹¹ shows that there are also inter-molecular hydrogen-bonds present between the urea moieties of adjacent molecules (Figure 3.2). There are inter-molecular, bifurcated hydrogen-bonds between N2'—H2···O3 ($H\cdots A = 1.964 \text{ \AA}$) and N3—H3···O3 ($H\cdots A = 2.003 \text{ \AA}$), N6—H6A···O2 ($H\cdots A = 2.334 \text{ \AA}$) and N7—H7A···O2 ($H\cdots A = 2.233 \text{ \AA}$) leading to a chain of L¹¹ molecules. One of the three pendant arms use their urea NH hydrogen-bond donor groups in intra-molecular hydrogen-bonds with the remaining two arms participating in inter-molecular hydrogen-bonding thus, every urea moiety in each receptor participates in hydrogen-bonding interactions. The full details of all of the hydrogen-bonds present in the structure of L¹¹ are shown in Table 3.1 and the crystallographic data and structure refinement details are given in Appendix C.

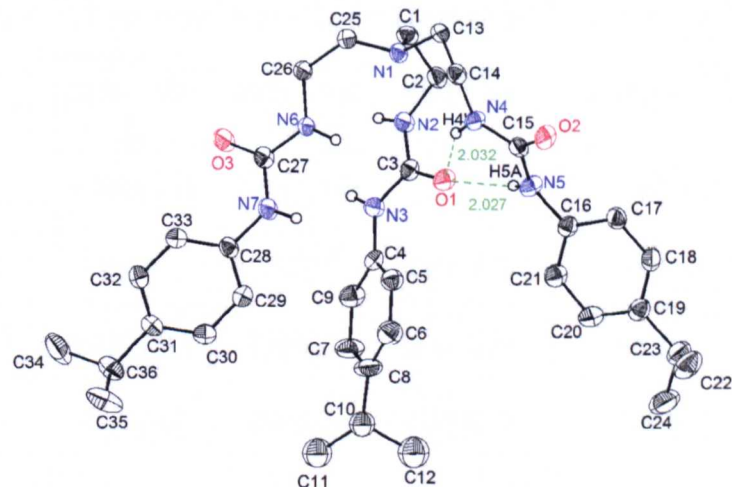


Figure 3.1. Molecular structure of L¹¹ showing the intra-molecular hydrogen-bonds. All hydrogen atoms (except NH) are omitted for clarity. Ellipsoids set at 50% probability. The intra-molecular NH···O hydrogen-bonds are shown in green and measured in Å. One of the disorder components has been removed and C10–C12 remain isotropic.

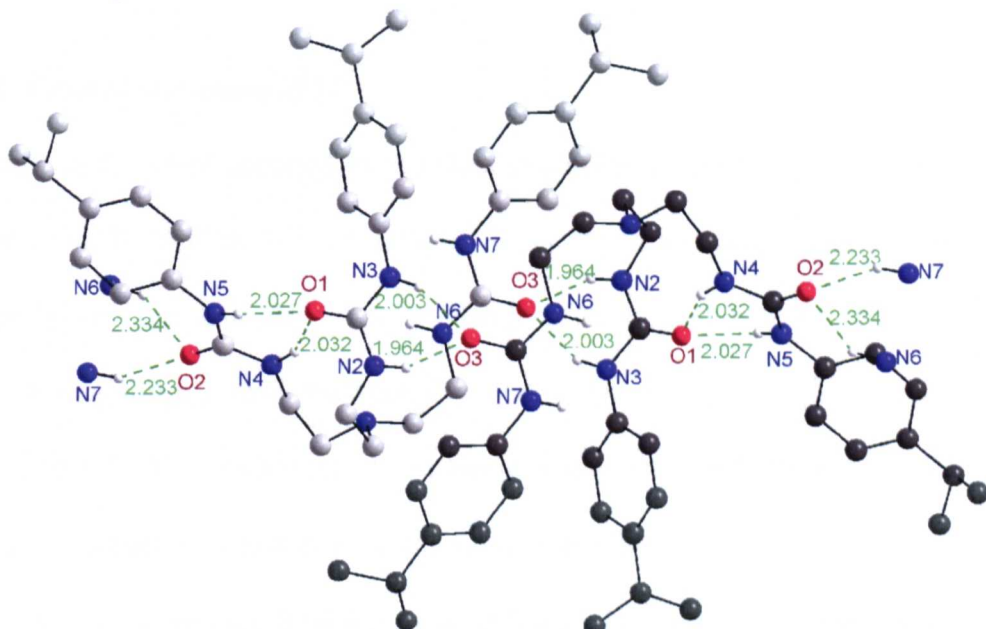


Figure 3.2. View of the structure of L¹¹ showing the intra- and inter-molecular hydrogen-bonds present in the extended structure. All hydrogen atoms (except NH) are omitted for clarity. Hydrogen-bonds are shown in green and measured in Å. For clarity, the carbon atoms of each L¹¹ molecule are shown in different shades of light and dark grey. The interactions between N7—H7···O2 and N6—H6A···O2 are indicated but the complete molecule is not shown.

Table 3.1. Intra- and inter-molecular hydrogen-bonds D—H \cdots A in L¹¹ (D = donor, A = acceptor, d = distance).

D—H \cdots A	d(D—H)/ Å	d(H \cdots A)/ Å	d(D \cdots A)/ Å	\angle (DHA)/ °	Symmetry Codes
N4—H4 \cdots O1	0.900(19)	2.032(19)	2.867(2)	154(2)	
N5—H5A \cdots O1	0.88	2.027	2.817(2)	149	
N2—H2 \cdots O3	0.912(19)	1.96(2)	2.817(2)	155(2)	-x, -y, -z
N3—H3 \cdots O3	0.92(2)	2.00(2)	2.859(2)	154(2)	-x, -y, -z
N6—H6A \cdots O2	0.88	2.334	3.031(2)	136	-x, -y+1, -z
N7—H7 \cdots O2	0.816(18)	2.232(19)	2.939(2)	145(2)	-x, -y+1, -z

*N4—H4 \cdots O1 and N5—H5A \cdots O1 are intra-molecular hydrogen-bonds whilst all other hydrogen-bonds are inter-molecular hydrogen-bonds.

3.3.3. Crystal Structure of L¹²

Crystals of L¹² were obtained by the slow evaporation of a concentrated solution of the product in MeOH. L¹² crystallised in the triclinic space group P-1 with two molecules in the unit cell. The molecular structure shows an intra-molecular, bifurcated hydrogen-bond between N6—H6A \cdots O2 (H \cdots A = 2.206 Å) and N7—H7A \cdots O2 (H \cdots A = 2.033 Å) encouraging a tripodal conformation (Figure 3.3). Disorder present in a terminal *tert*-butyl group C36–C39 was modelled over two sites with an occupancy 0.64/0.36 and refined with isotropic atomic displacement parameters.

The extended structure of L¹² shows two bifurcated inter-molecular hydrogen-bonds between the urea moieties on adjacent molecules N2—H2A \cdots O3 (H \cdots A = 2.463 Å) and N3—H3A \cdots O3 (H \cdots A = 2.092 Å), N4—H4A \cdots O1 (H \cdots A = 2.052 Å) and N5—H5A \cdots O1 (H \cdots A = 2.071 Å) giving rise to a chain of L¹² molecules (Figure 3.4). One of the three arms participates in intra-molecular hydrogen-bonding whilst the other two arms are involved in inter-molecular

hydrogen-bonding. The details of the hydrogen-bonds present in the structure of L¹² are shown in Table 3.2 and the crystallographic data and structure refinement details are given in Appendix C.

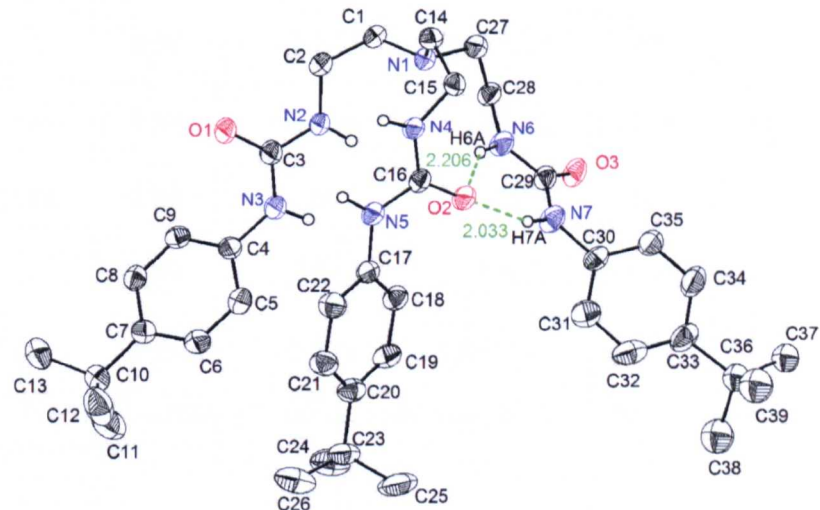


Figure 3.3. Molecular structure of L¹² showing intra-molecular hydrogen-bonds. All hydrogen atoms (except NH) are omitted for clarity. Ellipsoids set at 50% probability. The intra-molecular hydrogen-bonds are shown in green and the NH···O distances are measured in Å. One of the disorder components has been removed and thus C36–C39 remain isotropic.

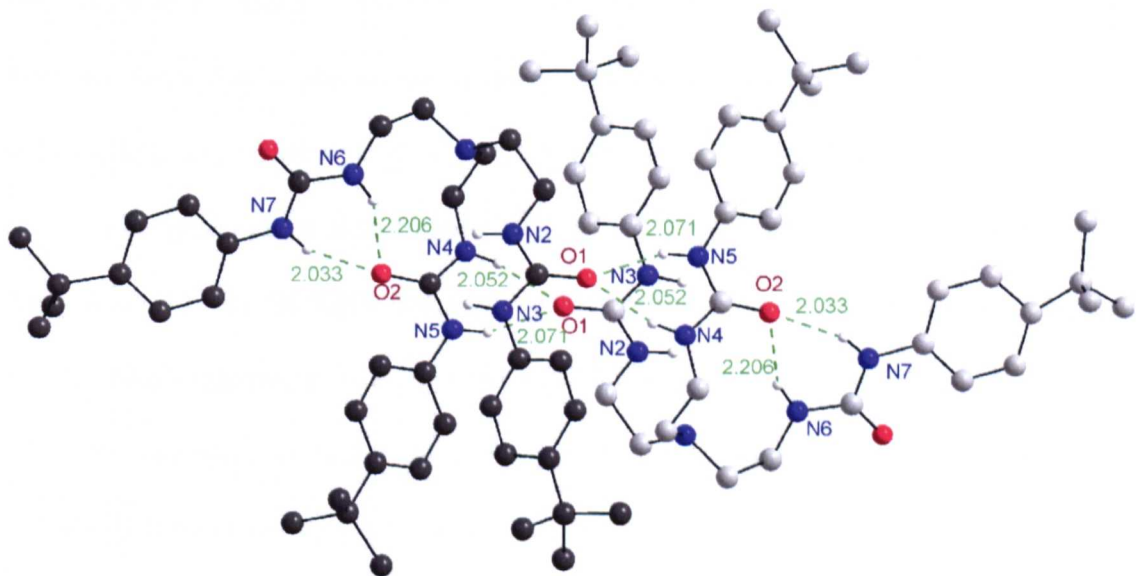


Figure 3.4. View of the structure of L¹² showing the intra- and inter-molecular hydrogen-bonds present in the extended structure. All hydrogen atoms (except NH) are omitted for clarity. Hydrogen-bonds are shown in green and measured in Å. The carbon atoms of the two molecules of L¹² are in different shades of grey.

Table 3.2. Intra- and inter-molecular hydrogen-bonds D—H \cdots A in L¹² (D = donor, A = acceptor, d = distance).

D—H \cdots A	d(D—H)/ Å	d(H \cdots A)/ Å	d(D \cdots A)/ Å	\angle (DHA)/ °	Symmetry Codes
N6—H6A \cdots O2	0.88	2.206	3.005(2)	151	
N7—H7A \cdots O2	0.88	2.033	2.873(2)	159	
N2—H2A \cdots O3	0.88	2.463	3.173(2)	138	-x+1, -y+1, -z+1
N3—H3A \cdots O3	0.88	2.092	2.917(2)	157	-x+1, -y+1, -z+1
N4—H4A \cdots O1	0.88	2.052	2.850(2)	150	-x, -y+2, -z+1
N5—H5A \cdots O1	0.88	2.071	2.888(2)	154	-x, -y+2, -z+1

*N6—H6A \cdots O2 and N7—H7A \cdots O2 are intra-molecular hydrogen-bonds, all others are hydrogen-bonds are inter-molecular.

3.3.4. Complexation Reactions

Two equivalents of each of the urea receptors L¹⁰–L¹³ were reacted with one equivalent of H₂PtCl₆ in MeCN. Yellow precipitates formed immediately for the reaction with L¹⁰ and L¹¹, but with L¹², containing 4-*tert*-butylphenyl groups, it took over 16 hours for a precipitate to form and for L¹³, with 3, 5-dimethoxyphenyl substituents, no precipitation was observed even after several days.

The precipitates that formed with L¹⁰–L¹² were collected by filtration and dried *in vacuo*. The ¹H NMR spectrum of each product, recorded in dmso-*d*₆, showed a peak which integrated in a 1:3 ratio with the urea NH signals in the region 9.50–9.75 ppm and was assigned to the protonated bridgehead nitrogen position N⁺HR₃. A downfield shift of the urea NH signals was also observed consistent with hydrogen-bonding interactions between the receptors and [PtCl₆]²⁻.^{8,9} Elemental analytical data on each of the products confirmed the formation of a 2:1 (LH)⁺:[PtCl₆]²⁻ complex while IR spectroscopy showed characteristic NH and C=O stretches in the regions 3333–3365 cm⁻¹ and 1651–1673 cm⁻¹, respectively.

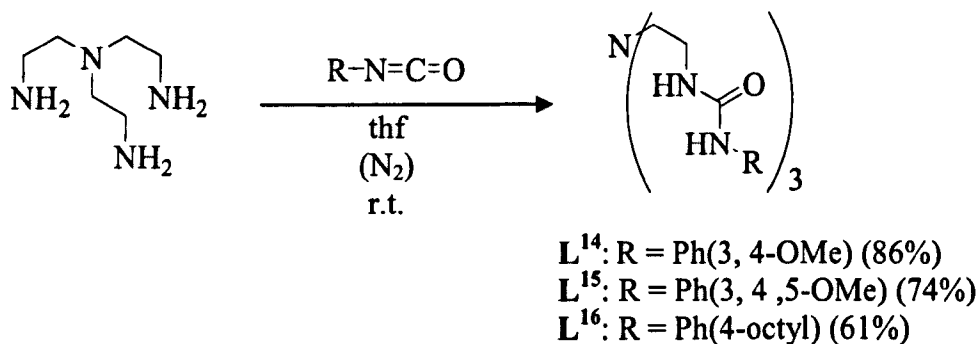
The reaction of L^{13} with H_2PtCl_6 formed a clear yellow solution and after several days at room temperature there was still no precipitate. To confirm the formation of the soluble complex $[(L^{13}H)_2PtCl_6]$ the reaction was repeated in MeCN- d_3 and the 1H NMR spectrum of the resulting solution recorded. A signal was observed at 9.25 ppm assigned to the protonated bridgehead nitrogen position, N^+HR_3 and there was a downfield shift of each of the urea NH protons indicating hydrogen-bonding interactions had formed.^{8,9} Positive electrospray mass spectrometry of the reaction solution showed a peak at m/z 684 assigned to $[L^{13}H]^+$. The negative electrospray spectrum showed a peak at m/z 718 due to $[L^{13}+Cl]^-$. Most significantly a peak was also observed at m/z 1772 assigned to $[L^{13}(L^{13}H)PtCl_6]^-$ suggesting the presence of the desired 2:1 $(L^{13}H)^+:[PtCl_6]^{2-}$ complex. Peaks were also observed at m/z 981 and 1089 assigned to $[(L^{13}-2H)PtCl_3]^-$ and $[(L^{13}H)PtCl_6]^-$, respectively, in which other chloroplatinate species are observed.

The results of the 1H NMR spectroscopy and mass spectrometry experiments confirm that the MeCN solution resulting from the mixing of L^{13} with H_2PtCl_6 does contain the desired complex $[(L^{13}H)_2PtCl_6]$. Therefore, by incorporating 3, 5-dimethoxyphenyl groups into the receptor the organic solubility of the complex had been established. This allowed the extraction efficiency of L^{13} to be assessed in solvent extraction experiments the results of which are discussed in Chapter 4.

3.3.5. Synthesis of Other Methoxy Urea Receptors

To assess if other methoxyphenyl moieties could be used to increase organic solubility two new TREN-based urea receptors were prepared. L^{14} and L^{15} were synthesised by the reaction of TREN with 3, 4-dimethoxyphenyl isocyanate and 3, 4, 5-trimethoxyphenyl isocyanate, respectively (Scheme 3.2).³ L^{14} formed as a colourless precipitate and was collected by filtration and dried *in vacuo* to give the

product in 86% yield. L^{15} did not precipitate from the reaction solution but removal of the solvent *in vacuo* and column chromatography (3% MeOH, 97% CHCl_3) gave analytically pure L^{15} . By comparing the extraction results for L^{13} , L^{14} and L^{15} the effects of the substitution pattern and number of methoxy groups on extraction ability can be assessed. To probe the effect of alkyl chain length on solubility a receptor with octylphenyl substituents was synthesised. Thus, TREN was reacted with 4-octylphenyl isocyanate to give L^{16} in moderate yield (Scheme 3.2).



Scheme 3.2. Synthesis of L^{14} – L^{16} .

3.3.6. Complexation Reactions

Two equivalents of L^{14} and L^{15} were reacted with H_2PtCl_6 in MeCN and no precipitate formed in either reaction indicating the formation of soluble products. The reactions were repeated in $\text{MeCN-}d_3$ and the ^1H NMR spectrum of each of the resulting solutions recorded. In both cases a signal in the range 9.65–9.87 ppm was observed assigned to the protonated bridgehead nitrogen (NH^+R_3). No complexation reaction was performed with L^{16} as there was only a limited amount of the product and it was decided it would be of more interest to use it in solvent extraction studies.

The ^{195}Pt NMR spectrum of $[(L^{14}\text{H})_2\text{PtCl}_6]$ in $\text{MeCN-}d_3$ shows one signal at 247 ppm confirming only one Pt environment in solution. This is a downfield shift of 23 ppm compared to the signal observed for H_2PtCl_6 (224 ppm) indicating that the environment of Pt changes upon complexation. ^{195}Pt signals observed are very sensitive to changes in conditions and so both spectra were recorded at the same

temperature, concentration and frequency and in the same solvent.¹⁰ This suggests that the shift is due to a change in the outer coordination sphere of $[\text{PtCl}_6]^{2-}$ resulting from the interaction with the receptor molecules.

3.3.7. Summary

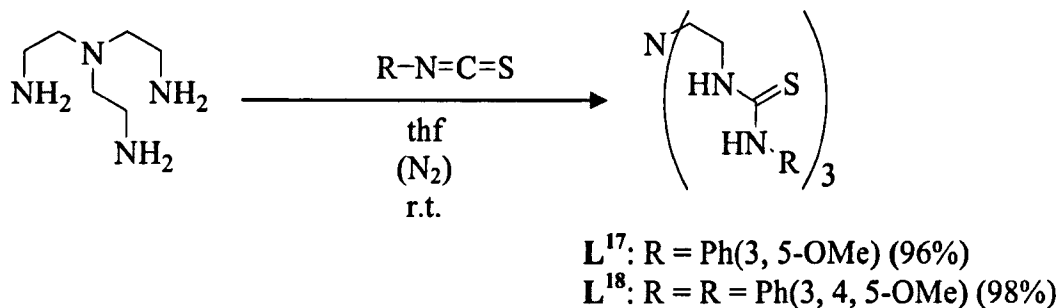
The required solubility of the urea complexes has been achieved by incorporating methoxy substituents onto the terminal phenyl groups of the receptors, and characterisation of the products revealed the expected 2:1 $(\text{LH})^+:[\text{PtCl}_6]^{2-}$ complex stoichiometry. The three TREN-based urea receptors L^{13} , L^{14} , and L^{15} formed MeCN-soluble complexes and these were then assessed in test extraction experiments to determine if they could be used as practical extractants for $[\text{PtCl}_6]^{2-}$.

The results of these experiments are described and discussed in Chapter 4.

3.4. Thiourea Receptors

3.4.1. Synthesis and Characterisation

Since the organic solubility of urea receptors was increased by introducing methoxyphenyl terminal substituents a similar route was chosen in an attempt to improve the solubility of thiourea receptors and their complexes. The ligands L^{17} and L^{18} were synthesised by the reaction of TREN with three equivalents of 3, 5-dimethoxyphenyl or 3, 4, 5-trimethoxyphenyl isothiocyanate, respectively (Scheme 3.3).³ Both products formed as colourless precipitates in high yields and were characterised by ^1H NMR, ^{13}C NMR and IR spectroscopy, mass spectrometry and elemental analysis.



Scheme 3.3. Synthesis of L¹⁷ and L¹⁸

3.4.2. Complexation Reactions

The reaction of L¹⁷ and L¹⁸ with H₂PtCl₆ in MeCN afforded, in both cases, insoluble orange products which prevented characterisation by ¹H NMR spectroscopy. Elemental analytical data confirmed the formation of the desired 2: 1 (LH)⁺: [PtCl₆]²⁻ complexes and the IR spectra showed characteristic N-H bands in the region 3231–3287 cm⁻¹ and C=S stretching vibrations at 1596 cm⁻¹.

For the thiourea receptors, incorporation of methoxyphenyl substituents did not lead to improved solubility of the complexes. This means that these thiourea systems could not be studied in solvent extraction studies and comparisons between urea and thiourea moieties could not be made. The insolubility of the complexes may arise from sulfur having a strong affinity for Pt-centres with direct coordination of the S-donors of thiourea to the metal centre. There are examples in the literature of the Cl⁻ ligands of [PtCl₆]²⁻ being substituted for sulfur atoms from thiourea moieties.^{11, 12} For example, the reaction of K₂PtCl₆ in HCl with a solution of thiourea (tu) in MeOH leads to the formation of a series complexes Pt(tu)₄Cl₂ type (Figure 3.6).¹³ Work published by Koch and co-workers shows that the direct coordination of thiourea S-donors has been used in platinum extraction.¹⁴⁻²³

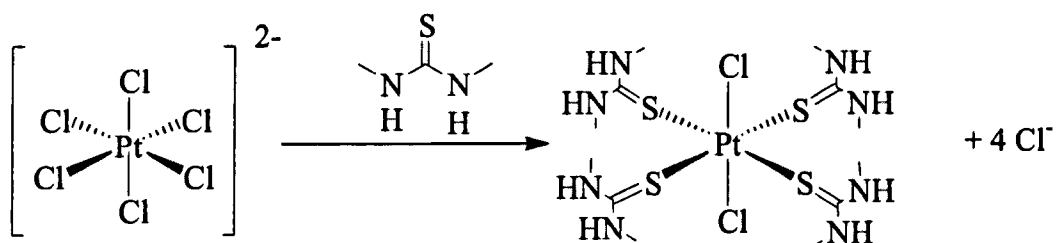


Figure 3.6. Thiourea moieties directly coordinated to a platinum centre.¹³

3.4.3. Summary

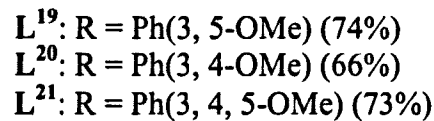
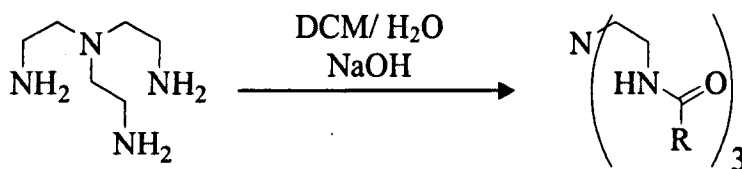
The thiourea receptors were initially studied as it was thought that they would be good hydrogen-bond donors and form strong hydrogen-bonds to $[\text{PtCl}_6]^{2-}$ leading to high extraction efficiency.²⁴ Although introducing methoxyphenyl substituents improved the solubility of the receptors L¹⁷ and L¹⁸ the complexes they form with H_2PtCl_6 remain insoluble. The use of these thioureas in solvent extraction studies was not possible and no further work was carried out to improve the solubility of these systems.

3.5. Amide Receptors

3.5.1. Synthesis and Characterisation

When the TREN-based amide receptor, L⁸, was reacted with H_2PtCl_6 a precipitate formed which was only soluble in dmso. As introducing methoxyphenyl substituents into the urea receptors improved the organic solubility of their H_2PtCl_6 complexes the same approach was applied to amide receptors. The receptors L¹⁹–L²¹ were synthesised by reaction of TREN with three equivalents of the 3, 5-dimethoxy, 3, 4-dimethoxy or 3, 4, 5-trimethoxy benzoyl chloride, respectively (Scheme 3.4).²⁵ Each product was obtained as a colourless powder and was characterised by ^1H NMR, ^{13}C NMR and IR spectroscopy, mass spectrometry and elemental analysis, which showed them to be analytically pure. Similar 2, 3, 4-trimethoxyphenyl substituted amides have been previously synthesised by Raymond and co-workers via reaction of TREN

with a 2-mercaptopthiazoline derivative of 2, 3, 4-trimethoxybenzoic acid.²⁶ L¹⁹ is a new ligand but there are reports of both L²⁰ and L²¹ in the literature.^{27, 28}



Scheme 3.4. Synthesis of L¹⁹–L²¹.

3.5.2. Crystal structure of L¹⁹

Single crystals of L¹⁹ suitable for X-ray diffraction were obtained by the slow evaporation of a concentrated solution containing the product in MeOH. L¹⁹ crystallises in the triclinic space group *P*-1 with two receptors in the unit cell. The structure has intra-molecular hydrogen-bonds between amide moieties on adjacent arms of the tripod N2—H2A···O7 (H···A = 2.040 Å) (Figure 3.5). The extended structure shows that there are also inter-molecular hydrogen-bonds present in the structure between N3—H3A···O1 (H···A = 2.250 Å) giving a chain-like structure of L¹⁹ molecules (Figure 3.6). The full details of the two types of hydrogen-bonds present in the structure are given in Table 3.3 and the crystallographic data and structure refinement details are given in Appendix C.

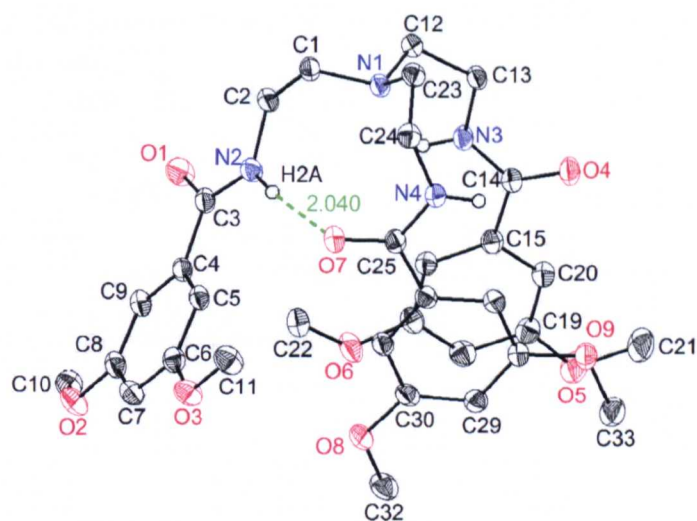


Figure 3.5. Molecular structure of L^{19} showing intra-molecular hydrogen-bonds. All hydrogen atoms (except NH) are omitted for clarity. Ellipsoids set at 50% probability. The intra-molecular hydrogen-bond is shown in green and the $NH \cdots O$ distance is measured in Å.

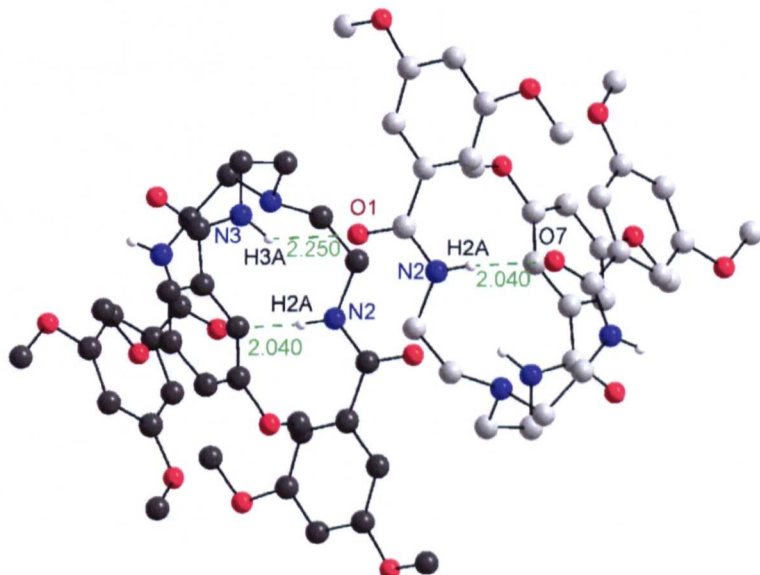


Figure 3.6. View of the structure of L^{19} showing the intra- and inter-molecular hydrogen-bonds present in the extended structure. All hydrogen atoms (except NH) are omitted for clarity. Hydrogen-bonds are shown in green and the $NH \cdots O$ distances are measured in Å. The carbon atoms of the two molecules of L^{19} are shown in different shades of grey.

Table 3.3. Intra- and inter-molecular hydrogen-bonds D—H \cdots A in L¹⁹ (D = donor, A = acceptor, d = distance).

D—H \cdots A	d(D—H)/ Å	d(H \cdots A)/ Å	d(D \cdots A)/ Å	\angle (DHA)/ °	Symmetry Codes
N2—H2A \cdots O7	0.88	2.040	2.910(2)	170	
N3—H3A \cdots O1	0.88	2.250	2.913(2)	132	-x, -y+1, -z+1

*N2—H2A \cdots O7 is an intra-molecular hydrogen-bond whereas N3—H3A \cdots O1 is an inter-molecular hydrogen-bond.

3.5.3. Complexation Reactions

Reaction of L²⁰—L²¹ with H₂PtCl₆ in MeCN afforded soluble products. To confirm the formation of the desired complexes in solution the reactions were repeated in MeCN-*d*₃ and the ¹H NMR spectrum of each solution recorded. Both spectra showed a signal due to the protonated bridgehead position (NH⁺R₃) which integrated in a 1:3 ratio with each of the urea NH signals. The ¹³C NMR spectrum of [(L²¹H)₂PtCl₆] was recorded to monitor the effect of complexation on the carbon environments of L²¹. A small downfield shift for the carbonyl signal (C=O) was observed consistent with the adjacent amide NH moiety participating in hydrogen-bonding interactions. A shift in the signal assigned to carbon atoms adjacent to the bridgehead nitrogen (N(CH₂)₃) was also observed corresponding with protonation of the bridgehead nitrogen.

After mixing L¹⁹ with H₂PtCl₆ in MeCN yellow crystals formed and these were collected by filtration and dried *in vacuo* (see Section 3.5.4.). The ¹H NMR spectrum of the crystals dissolved in dmso-*d*₆ showed a resonance at 9.68 ppm which integrated in a 1:3 ratio with the amide NH signal and was assigned to the protonated bridgehead nitrogen N⁺HR₃. Elemental analytical data confirmed the formation of the complex [(L¹⁹H)₂PtCl₆]. The negative electrospray mass spectrum on the remaining solution showed a peak at *m/z* 673 assigned to [L¹⁹+Cl]⁻ and, more interestingly, peaks were also observed at *m/z* 936, 972, 1044, 1378 and 1682 with

the correct isotope distribution for $[(L^{19}-2H)PtCl_3]^-$, $[(L^{19}-H)PtCl_4]^-$, $[(L^{19}H)PtCl_6]^-$, $[(L^{19}H)(PtCl_5)_2]^-$ and $[L^{19}(L^{19}H)PtCl_6]^-$, respectively. The peak at m/z 1682 is of particular interest as it suggests the formation of a 2:1 $(L^{19}H)^+:[PtCl_6]^{2-}$ complex. Fragmentation of the $[PtCl_6]^{2-}$ anion is also observed in these mass spectrometry experiments and other complexed chloroplatinate species are evident in the spectrum such as $[Pt(IV)Cl_3]^+$, $[Pt(IV)Cl_4]$ and $[Pt(IV)Cl_5]^-$.

The ^{195}Pt NMR spectrum of L^{20} and H_2PtCl_6 in $MeCN-d_3$ shows one signal at 244 ppm indicating that there is a single platinum environment present in solution. The $^{35}Cl/^{37}Cl$ isotopomer distribution characteristic of the ^{195}Pt resonance in $[PtCl_6]^{2-}$ species (Figure 3.7) is preserved confirming that Cl^- substitution by $MeCN$ solvent molecules does not take place during the experiment on the NMR timescale.¹⁰ For comparison, the ^{195}Pt NMR spectrum of H_2PtCl_6 in $MeCN-d_3$ was also recorded and one signal at 224 ppm observed. These results show that on formation of the complex there is a downfield shift of 20 ppm indicating that the environment of the platinum centre of $[PtCl_6]^{2-}$ changes when it is complexed with $(L^{20}H)^+$.

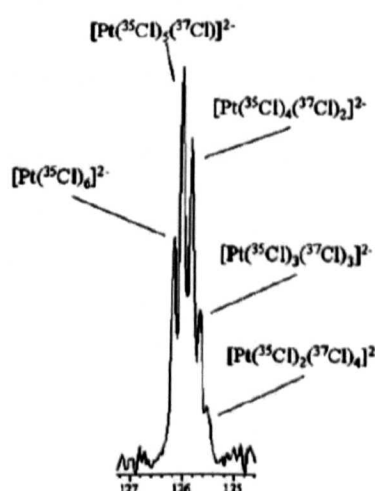


Figure 3.7. ^{195}Pt NMR spectrum of $H_2PtCl_6 \cdot H_2O$ (recorded at 303 K at 600 MHz in ethylene glycol- d_6) illustrating the resolution of the ^{35}Cl and ^{37}Cl isotopomers.²⁹

3.5.4. Crystal Structure of $[(L^{19}H)_2PtCl_6]$

Crystals of $[(L^{19}H)_2PtCl_6]$ suitable for X-ray diffraction were obtained within 30 minutes of mixing an MeCN solution containing two equivalents of L^{19} with an MeCN solution containing one equivalent of H_2PtCl_6 . The structure determination of $[(L^{19}H)_2PtCl_6]$ revealed one $[PtCl_6]^{2-}$ anion lying on a centre of inversion and two receptor cations related by the inversion centre (Figure 3.8). Both amide receptors are protonated at their bridgehead nitrogen atom (N1) to give an overall charge-neutral complex. One of three amide NH donors of $(L^{19}H)^+$ hydrogen-bonds to $[PtCl_6]^{2-}$ forming a bifurcated interaction N2—H2A \cdots Cl1 ($H\cdots A = 2.952 \text{ \AA}$) and N2—H2A \cdots Cl2 ($H\cdots A = 2.832 \text{ \AA}$).

In addition to these $NH\cdots Cl$ hydrogen-bonds there is an intra-ligand hydrogen-bond N3—H3A \cdots O1 ($H\cdots A = 2.128 \text{ \AA}$) and an inter-ligand hydrogen-bond N4—H4A \cdots O4 ($H\cdots A = 2.151 \text{ \AA}$). Each $(L^{19}H^+)$ cation uses one of its amide moieties to hydrogen-bond to one $[PtCl_6]^{2-}$ anion while the remaining two amide groups hydrogen-bond to another $(L^{19}H^+)$ cation to give a chain arrangement $\cdots((L^{19}H^+)\cdots[PtCl_6]^{2-}\cdots(L^{19}H^+))\cdots((L^{19}H^+)\cdots[PtCl_6]^{2-}\cdots(L^{19}H^+))\cdots$ (Figure 3.9).

The structure also contains two molecules of MeCN which are disordered over two sites with an 0.65/ 0.35 occupancy and refined with isotropic displacement parameters. The details of the hydrogen-bonds present in the structure of $[(L^{19}H)_2PtCl_6]$ are given in Table 3.4 and the crystallographic data and structure refinement details are given in Appendix C.

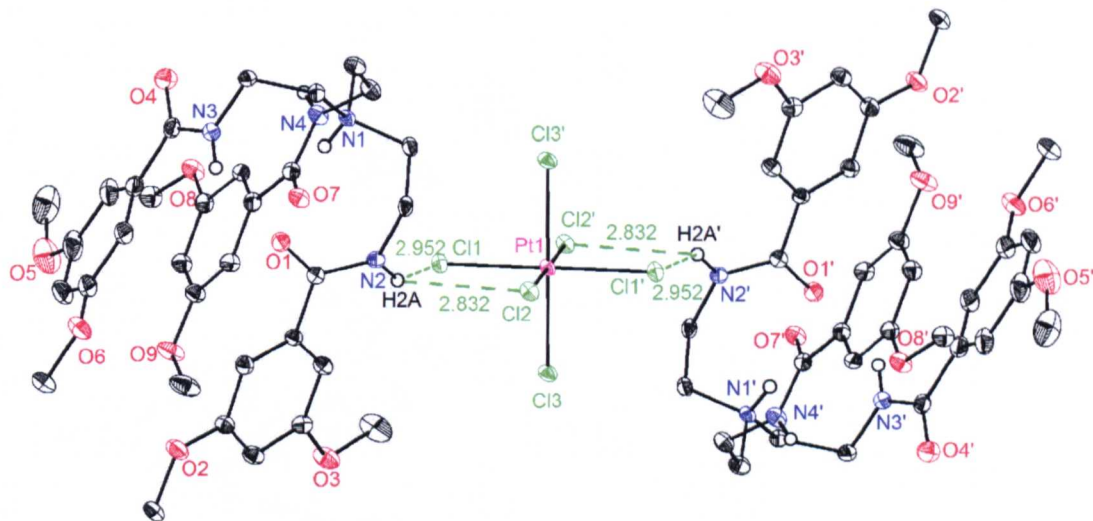


Figure 3.8. View of the structure of $[(\text{L}^{19}\text{H})_2\text{PtCl}_6]$ showing the intra- and inter-molecular hydrogen-bonds present. All hydrogen atoms (except NH) are omitted for clarity. Ellipsoids set at 50% probability. The hydrogen-bonds between $(\text{L}^{19}\text{H}^+)$ and $[\text{PtCl}_6]^{2-}$ are shown in green and the $\text{NH} \cdots \text{Cl}$ distances are measured in Å.

Table 3.4. Intra- and inter-molecular hydrogen-bonds in $[(\text{L}^{19}\text{H})_2\text{PtCl}_6]$ (D = donor, A = acceptor, d = distance).

D—H \cdots A	d(D—H)/ Å	d(H \cdots A)/ Å	d(D \cdots A)/ Å	$\angle(\text{DHA})/^\circ$	Symmetry Codes
N2—H2A...Cl2	0.86	2.832	3.438(3)	128.90	
N2—H2A...Cl1	0.86	2.952	3.618(3)	135.70	
N3—H3A...O1	0.86	2.128	2.868(4)	143.80	
N4—H4A...O4	0.86	2.151	2.950(4)	154.80	-x+1, -y, -z+1

*N3—H3A \cdots O1 is an intra-ligand hydrogen-bond whilst N4—H4A \cdots O4 is an inter-ligand hydrogen-bond.

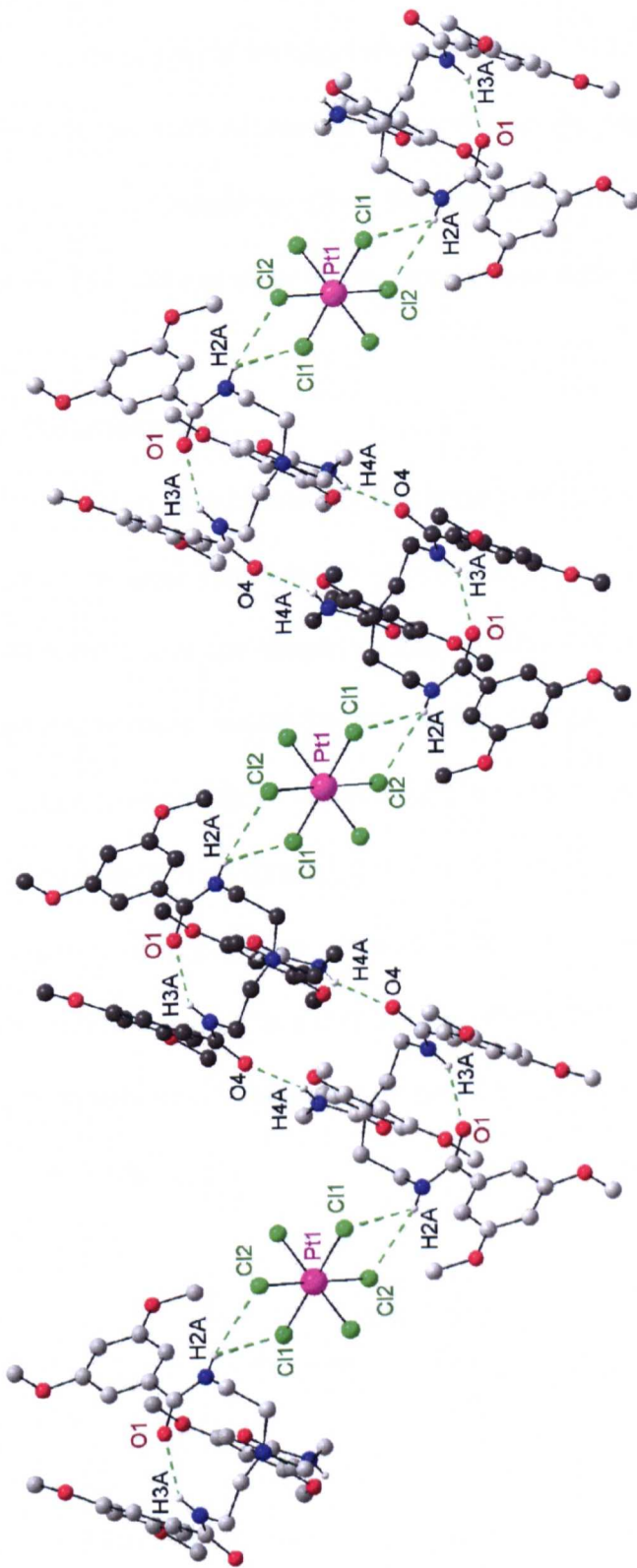


Figure 3.9. View of the structure of $[(L^{19}H)_2PtCl_6]$ showing the hydrogen-bonds present between L^{19} and $[PtCl_6]^{2-}$ in the extended structure. All hydrogen atoms (except NH) are omitted for clarity. Hydrogen-bonds are shown in green and measured in Å. The carbon atoms of each $[(L^{19}H)_2PtCl_6]$ unit are shown in alternating shades of light and dark grey.

3.5.5. Summary

The incorporation of terminal methoxyphenyl substituents into TREN-based amide receptors has been successful in improving the organic solubility of receptors and their $[\text{PtCl}_6]^{2-}$ complexes. Once the solubility of the complexes had been increased it was then possible to carry out test extractions with these amide receptors.

3.6. Potentiometry*

To provide an insight into the mechanism of extraction, it is important to know the number of sites that can be protonated in the receptor molecules under acidic conditions. From the design of the receptors it was expected that the bridgehead nitrogen position would be protonated to form a mono-cationic species. Indeed, evidence from the three complex crystal structures indicates the bridgehead tertiary amine position is protonated and, therefore, two molecules of receptor are required to generate a charge-neutral complex. Under the acidic conditions used in a solvent extraction process there exists the possibility that the urea or amide moieties within the receptors could become protonated to give a multiply charged cationic receptor (Figure 3.10).

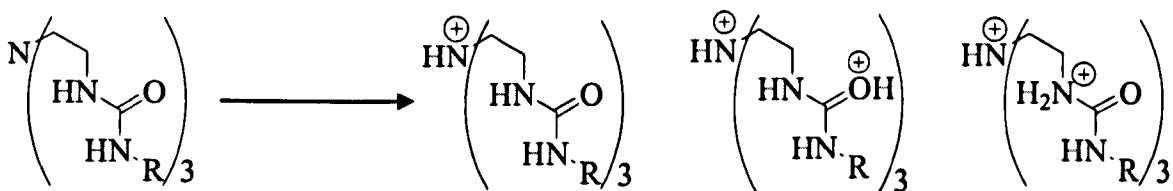


Figure 3.10. Possible protonation sites of a urea receptor under acidic conditions.

To determine the number of protonation sites in the receptors and the pH at which they become protonated potentiometry experiments were performed as

* The potentiometry experiments presented here were carried out by Professor Antonio Bianchi and his group at the University of Florence, Italy.

described in Appendix D.³⁰ The protonation equilibria were determined for the urea receptor L¹⁴ and the amide receptors L²⁰ and L²¹ (Table 3.5).

Table 3.5. Protonation constants determined in MeCN/H₂O 50:50 (v/v) (0.1 M NMe₄Cl, 298.1 ± 0.1 K).

Receptor	L ¹⁴	L ²⁰	L ²¹
Equilibrium	$L + H^+ = LH^+$	$L + H^+ = LH^+$	$L + H^+ = LH^+$
pKa	6.43(7)*	5.94(2)*	5.93(5)*

* Values in parentheses are the standard deviations on the last significant figure.

These results confirm that there is only one protonation site for each receptor represented by the equilibrium $L + H^+ = LH^+$ and the pKa values obtained are consistent with the tertiary amine bridgehead nitrogen position being protonated.³¹ Thus, our receptors are monobasic over the pH range studied and will form a charge-neutral complex will form when the $(LH)^+:[PtCl_6]^{2-}$ ratio is 2:1. This is an excellent result for our receptor design and is also consistent with the previously discussed spectroscopic and crystallographic results.

By comparing the potentiometry results for L¹⁴, L²⁰ and L²¹ it was possible to assess whether the type of hydrogen-bond donor and the number of methoxy substituents has an effect on the basicity of the amine nitrogen. The receptor L¹⁴ contains urea moieties while L²⁰ incorporates amides with both ligands having 3, 4-dimethoxyphenyl substituents. The pKa values differ by 0.5 indicating that the type of hydrogen-bond donor group has relatively little effect on the basicity of the bridgehead nitrogen.

The receptors L²⁰ and L²¹ both have amide hydrogen-bond groups but contain a different number of methoxy substituents. The pKa values for these two receptors are very similar (5.94 and 5.93, respectively) indicating that the number of methoxy substituents on the terminal phenyl group does not affect the basicity of the bridgehead nitrogen.

3.7. NMR Spectroscopic Titrations

NMR spectroscopic titrations can be used to determine the binding constant and binding stoichiometry between a receptor (host) and anion (guest).³²⁻³⁷ The frequency at which a particular nucleus resonates in an NMR spectrum is dependant on its electronic environment and therefore NMR spectroscopy is a sensitive technique for monitoring the interactions between molecules.

In an NMR titration the spectrum of the receptor is recorded and aliquots of the anion added. The NMR spectrum is recorded after each aliquot has been added meaning that resonances of the receptor are monitored as a function of anion concentration.³² If there is an interaction between receptor and anion the environment of the NH protons in the receptor will be perturbed and a shift of the corresponding resonance in the NMR spectra will be observed. Protons which form specific hydrogen-bonds to the anion or are in close contact with the anion will have their resonances most strongly perturbed which will give information on where the hydrogen-bonding is occurring.³⁴

The choice of deuterated solvent used in the titrations is an important factor to consider as the signal(s) of the receptor needs to be clear and in a region that is free from residual solvent resonances. It is also important to use a non-competitive solvent as the solvent should not compete with the anion for hydrogen-bonding to the

receptor. This is necessary to ensure that any shifts in the resonances of the receptor are due to interactions with the anion rather than a solvent effect.

3.7.1. Experiment Design

There are different methods to perform NMR titrations depending on whether or not the concentration of the receptor affects the observed chemical shift. If the receptor has hydrogen-bond donor and acceptor groups then intra- and/or inter-ligand hydrogen-bonds may form and variation in the receptor concentration will affect the observed chemical shifts of the NH resonances. Two methods that can be used for NMR titrations are discussed below;

*Method A:*³² This method can be used if the concentration of the receptor has no effect on the observed chemical shift. A stock solution containing a known concentration of the host and a stock solution of the guest are prepared in a non-competitive deuterated solvent. A ^1H NMR spectrum of the host stock solution is recorded and as there is no guest present the signals observed in the spectrum are the start point of the experiment. A series of NMR tubes containing successively decreasing volumes of host are prepared from the stock solution. Increasing volumes of guest are added keeping the total volume in each of the NMR tubes constant. A typical experimental set-up is shown below (Table 3.6).

Table 3.6. NMR titration experimental design, method A.

	Host Volume/ μL	Guest Volume/ μL	[Host]/ mM	[Guest]/ mM
A	500	0	5.0	0.0
B	450	50	4.5	0.5
C	400	100	4.0	1.0
D	350	150	3.5	1.5
E	300	200	3.0	2.0
F	250	250	2.5	2.5
G	200	300	2.0	3.0
H	100	400	1.0	4.0
I	50	450	0.5	4.5

Method B:³² This method is used when the concentration of the receptor does effect the observed chemical shift meaning it is crucial that the concentration of receptor is constant in each of the ¹H NMR spectra recorded. A series of NMR tubes containing the same volume of host are prepared. To these solutions varying amounts of the anion solution are added. The total volume in each NMR tube is made equal by addition of solvent. An example of an experimental design is shown below in Table 3.7.

Table 3.7. NMR titration experimental design, method B.

	Host Volume/ μl	Guest Volume/ μl	Solvent added/ μl	[Host]/ mM	[Guest]/ mM
A	200	30	370	2	0.3
B	200	60	340	2	0.6
C	200	100	300	2	1.0
D	200	150	250	2	1.5
E	200	200	200	2	2.0
F	200	250	150	2	2.5
G	200	300	100	2	3
H	200	400	0	2	4

3.7.2. Data Analysis

After the ¹H NMR spectra have been recorded a titration curve can be plotted which is a plot of the concentration of the guest versus the change in the observed chemical shift (Figure 3.10).³⁵ In the example below, the graph shows a plateau indicating that the maximum shift for the host system has been attained and that there is no more binding of the guest to further perturb the signal.

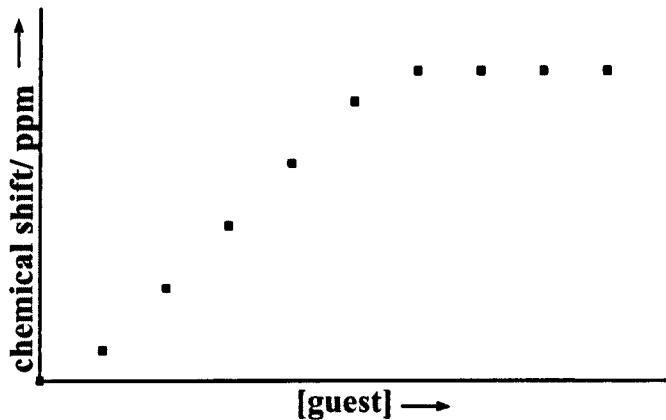


Figure 3.13. Theoretical shape of a titration curve.

The stoichiometry of the complex can be determined from a Job plot which is a graph of the mole fraction against the concentration of the complex.³²

The mole fraction is found from Equation 1;

$$\text{mole fraction} = \text{volume of host} / (\text{volume of host} + \text{volume of guest}) \quad (1)$$

The concentration of complex is calculated using Equation 2;

$$[C] = [R] \times (\delta_{\text{obs}} - \delta_0) / (\delta_E - \delta_0) \quad (2)$$

Where:

[C] Concentration of complex

[R] Concentration of the receptor (in mM)

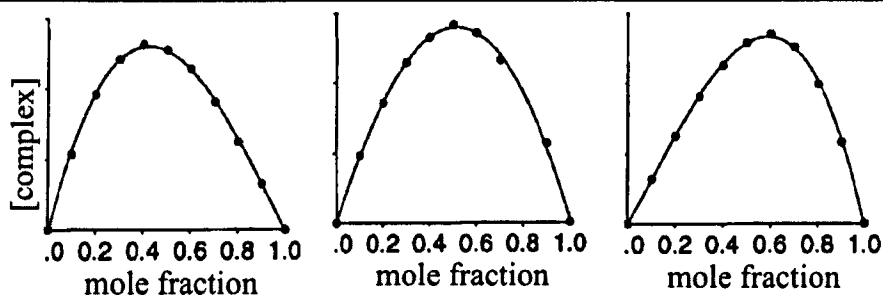
δ_{obs} Observed chemical shift

δ_0 Chemical shift when there is no guest present

δ_E Chemical shift when there is a large excess of guest present

The method of continuous variation is used in Job's method. In this method equal concentration solutions of two species, A and B, are mixed in varying ratios

and a property characteristic of the complex formed is measured. Because the total concentration, $[A] + [B]$, is constant in all solutions, the concentration of an AB complex will reach a maximum value when $[A] = [B]$. The concentration of an A₂B complex will reach a maximum when $[A] = 2[B]$. Thus, a plot of the concentration of complex as a function of the mole fraction of A in solution can be constructed. The maximum of the graph corresponds to the mole fraction of A in the complex which indicates the complex stoichiometry (Figure 3.11).³⁶



Maximum of Job Plot	0.33	0.50	0.66
Complex stoichiometry	1 H: 2 G	1 H: 1 G	2 H: 1 G

Figure 3.11. The maxima of a Job plot indicates complex stoichiometry (H = host, G = guest).³⁶

Once the stoichiometry of the complex has been determined then a computer program can be used to obtain a value for the binding constant. Examples of such programs that can be used for this purpose include EqNMR³⁸ and HypNMR.^{39, 40}

3.7.3. Results

3.7.3.1. Receptor Considerations

The TREN-based urea, thiourea and amide receptors contain hydrogen-bond donor and acceptor sites. The solid state structures show intra-molecular and inter-molecular hydrogen-bonding and it is possible that similar interactions occur in solution (Figure 3.12). The self-association of receptor molecules is concentration

dependant, that is, the more concentrated the solution of the receptor, the greater degree of interaction occurring between molecules.

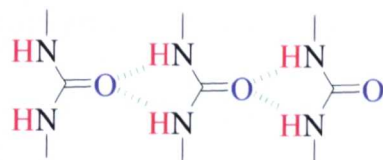


Figure 3.12. Example of the self-association that may occur between urea moieties. (The hydrogen-bond donor groups are shown in red and the hydrogen-bond acceptor groups in blue).

To assess how the concentration of receptor affects the observed NH shift(s) in ^1H NMR spectra a series of NMR experiments were performed. The TREN-based urea receptor L^{10} and the amide receptor L^{19} were both studied and the ^1H NMR spectrum of each receptor at concentrations of 2 mM, 3 mM, 4 mM, 5 mM and 10 mM in CDCl_3 was recorded. For both L^{10} and L^{19} there was a downfield shift in the NH resonance(s) as the concentration of the receptor increased suggesting the formation of intra- or inter-ligand hydrogen-bonds. Therefore in the subsequent NMR titrations the concentration of the receptor was kept constant.

3.7.3.2. Anion Considerations

H_2PtCl_6 is a source of $[\text{PtCl}_6]^{2-}$ along with two protons which can protonate the bridgehead nitrogen atoms of two receptors to give a charge-neutral product $[(\text{LH})_2\text{PtCl}_6]$. Ideally, H_2PtCl_6 would be used as the source of $[\text{PtCl}_6]^{2-}$ in NMR titrations as it is an accurate representation of the complexation reaction. The problem arises as H_2PtCl_6 is commercially obtained as $\text{H}_2\text{PtCl}_6 \cdot x\text{H}_2\text{O}$ and the presence of H_2O molecules broadens the NH signal(s) of the receptor in the ^1H NMR spectrum. It is also hygroscopic and as the number of H_2O molecules associated with H_2PtCl_6 is unknown the precise concentration of the guest solution cannot be calculated. To enable the stoichiometry to be determined it is necessary to know the

number of equivalents of anion added in each experiment to obtain a value for the binding constant.

Alternative sources of $[\text{PtCl}_6]^{2-}$ were considered. K_2PtCl_6 is only soluble in D_2O and is not suitable for use in ^1H NMR titrations as it causes the NH signal of the receptor to be very broad. To improve the organic solubility of K_2PtCl_6 it was reacted with $(\text{Bu}_4\text{N})\text{HSO}_4$ to form $(\text{Bu}_4\text{N})_2\text{PtCl}_6$ ⁴¹ which was soluble in both CH_2Cl_2 and MeCN. If $(\text{Bu}_4\text{N})_2\text{PtCl}_6$ is used there are no protons available and the receptors remain charge-neutral. Protons could be introduced into the solution through addition of acid (HX) however, the counter-anion of the acid (X^-) will then be competitive for the receptor meaning an accurate binding constant may not be obtained.

3.7.3.3. NMR Titration Results

An NMR titration of L^{19} with $(\text{Bu}_4\text{N})_2\text{PtCl}_6$ in CD_2Cl_2 was performed following Method B (Section 3.7.1). The amide NH signal of the receptor showed the largest shift indicating it is this group which forms hydrogen-bonds with $[\text{PtCl}_6]^{2-}$ which correlates with the complex crystal structure $[(\text{L}^{19}\text{H})_2\text{PtCl}_6]$. The ^1H NMR titration plot for the experiment is shown in Figure 3.13. As the concentration of $[\text{PtCl}_6]^{2-}$ increases there is a downfield shift in the NH signal although the graph does not show a plateau as expected. This may be because the bridgehead nitrogen positions are not protonated and the 2:1 receptor-to-anion stoichiometry is not enforced by charge. As the Job plot gave no clear value for the complex stoichiometry no equilibrium constant could be found (Figure 3.14).

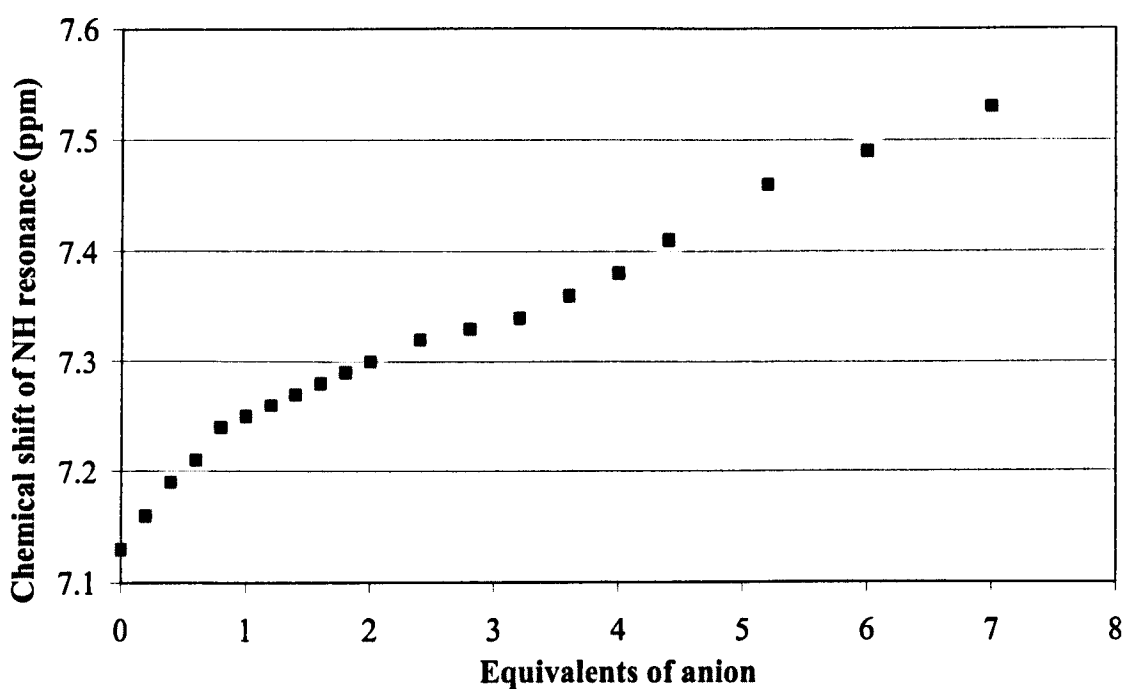


Figure 3.13. ^1H NMR titration curve for L^{19} with $(\text{Bu}_4\text{N})_2\text{PtCl}_6$ in CD_2Cl_2 .

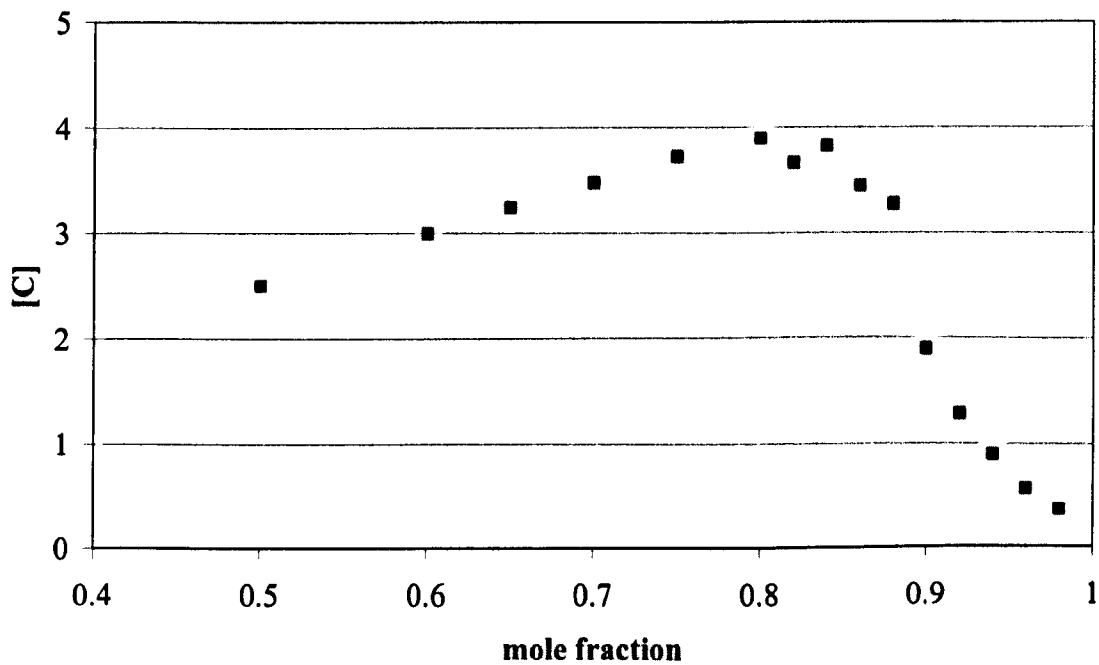


Figure 3.14. Job plot for the titration of L^{19} with $(\text{Bu}_4\text{N})_2\text{PtCl}_6$ in CD_2Cl_2 .

3.8. UV-vis Spectroscopic Titrations

There are several examples in the literature where UV-vis spectroscopy has been used as an alternative to ^1H NMR spectroscopy to probe host-guest interactions.⁴²⁻⁴⁴

It was thought that UV/vis spectroscopy might be a useful tool to assess the interactions taking place between the receptors and $[\text{PtCl}_6]^{2-}$. If significant changes are observed between the spectra of the receptor, $[\text{PtCl}_6]^{2-}$ and a solution resulting from their mixing then UV/vis titrations could be performed enabling an assessment of the strength of interaction between receptor and anion.

The UV/vis spectra of H_2PtCl_6 , the receptor L^{17} and the solution resulting from the mixing of L^{17} with H_2PtCl_6 were recorded in MeCN in the range 190 – 900 nm at 298 K (Figure 3.15). The receptor has $\lambda_{\max} = 219$ and 257 ($\epsilon = 573834$ and 169316, respectively), H_2PtCl_6 has $\lambda_{\max} = 221$ ($\epsilon = 25148$), the complex has $\lambda_{\max} = 220$ and 260 ($\epsilon = 573834$ and 284333, respectively). The spectra of the ligand and the complex are fairly similar indicating the transitions are ligand based (rather than metal based), presumably due to $\pi-\pi^*$ and $n-\pi^*$ transitions due to the aromatic groups present in the receptor. The difference between these two spectra possibly arises from the fact that the receptor solution is colourless whereas the complex solution is yellow.

The changes seen on the formation of the complex are not indicative of the interaction occurring between the receptor and $[\text{PtCl}_6]^{2-}$ and it was therefore not possible to use UV/vis as a tool to probe this interaction. No further use of UV/vis spectroscopy was made.

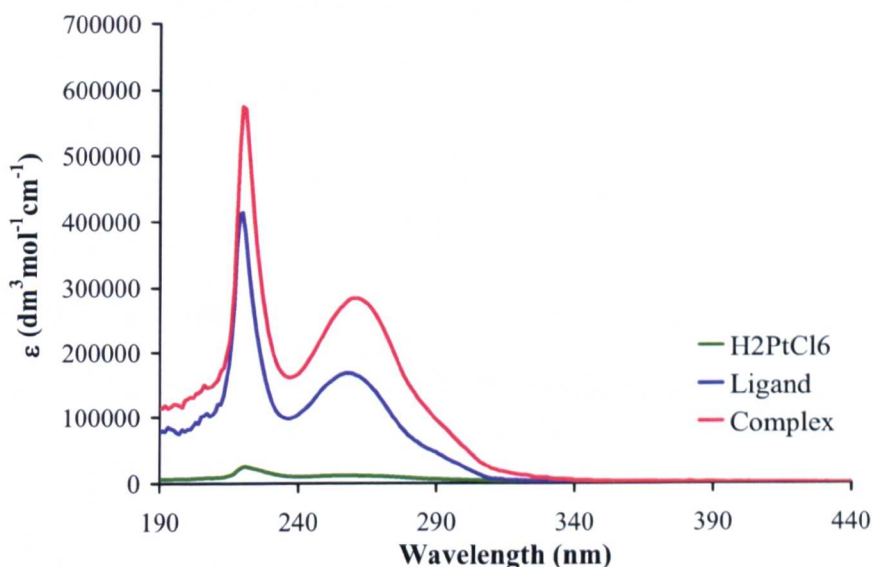


Figure 3.15. Uv-vis spectra of H_2PtCl_6 , L^{17} and $[(\text{L}^{17}\text{H})_2\text{PtCl}_6]$.

3.9. Summary of Results

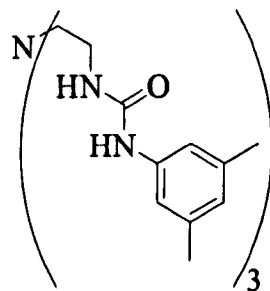
This Chapter presents the work undertaken to increase the organic solubility of receptors and their complexes $[(\text{LH})_2\text{PtCl}_6]$ in CHCl_3 . Various substituted terminal phenyl groups were assessed and it was found that by incorporating methoxyphenyl or octylphenyl groups into TREN-based urea and amide receptors organic soluble complexes formed allowing the study of these systems in solvent extraction experiments. Characterisation of the complexes by ^1H NMR and IR spectroscopy, mass spectrometry and crystallographic analysis further confirmed the success of our approach and the crystal structure of $[(\text{L}^{19}\text{H})_2\text{PtCl}_6]$ provides an insight into the interactions in the solid state. Unfortunately, the introduction of methoxyphenyl groups did not improve the solubility of the TREN-based thiourea complexes and insoluble complexes still formed in the complexation reactions. Potentiometric experiments on TREN-based urea and amide receptors showed they were monobasic and under acidic conditions the bridgehead nitrogen position is protonated which is consistent with spectroscopic and crystallographic observations. The use of ^1H NMR

and UV/vis spectroscopic titrations to assess the receptor-anion interaction were attempted but the results were of little use.

3.10. Experimental

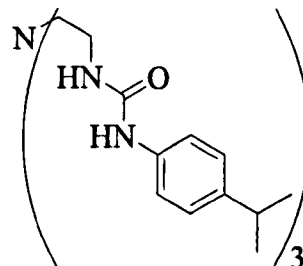
3.10.1. Receptor Synthesis

3.10.1.1. Synthesis of N,N',N''-(nitrilotri-2,1-ethanediyl)tris[N'-3,5-dimethylphenyl urea], L^{10.3}



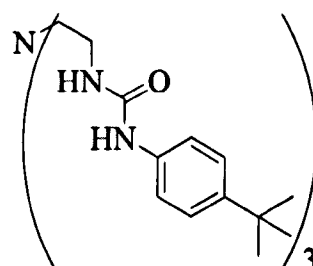
To TREN (0.20 cm^3 , 1.34 mmol) in dry THF (30 cm^3) was added 3, 5-dimethylphenyl isocyanate (0.56 cm^3 , 4.00 mmol) under a N_2 atmosphere. The reaction was stirred at room temperature for 3 h during which time a colourless precipitate formed which was collected by filtration and dried *in vacuo* to give a colourless powder. No further purification was carried out. Yield: 0.76 g, 97%. ^1H NMR (300 MHz, CDCl_3): δ/ppm 7.15 (br, 3H, NH), 6.70 (s, 6H, H_{Ar}), 6.60 (s, 3H, H_{Ar}), 5.98 (br, 3H, NH), 3.22 (br, 6H, CH₂), 2.35 (br, 6H, CH₂), 2.13 (s, 18H, CH₃). ^{13}C (68 MHz, $\text{dmsO}-d_6$): δ/ppm 156, 141, 138, 124, 116, 67, 55, 21. MS (ES $^+$): m/z 588.36 [M+H] $^+$. IR (solid, cm^{-1}): 3302 ($\nu_{(\text{N-H})}$), 1654 ($\nu_{(\text{C=C})}$), 1645 ($\nu_{(\text{C=O})}$). Anal. calc. for $\text{C}_{33}\text{H}_{45}\text{N}_7\text{O}_3$: C, 67.44; H, 7.72; N, 16.68. Found: C, 67.18; H, 8.08; N, 14.91%.

3.10.1.2. Synthesis of N,N',N''-(nitrilotri-2,1-ethanediyl)tris[N'-4-*iso*-propylphenyl ureal], L¹¹.³



This was prepared in a similar manner to L¹⁰ by the reaction of TREN with 4-*iso*-propylphenyl isocyanate to give the product as a colourless powder. Yield: 0.58 g, 69%. ¹H NMR (300 MHz, CDCl₃): δ/ppm 7.43 (s, 3H, NH), 6.97 (s, 12H, H_{Ar}), 6.10 (br t, 3H, NH), 3.13 (br, 6H, CH₂), 2.80 (septet, 3H, ³J_{HH} = 7 Hz, ⁱPrCH₂), 2.23 (br, 6H, CH₂), 1.19 (d, 18H, ³J_{HH} = 7 Hz, ⁱPrCH₃). ¹³C NMR (75 MHz, CDCl₃): δ/ppm 156, 142, 139, 123, 119, 55, 48, 44, 25. MS (ES⁺): m/z 630.41 [M+H]⁺. IR (solid, cm⁻¹): 3100 (v_(N-H)), 1640 (v_(C=O)), 1601 (v_(C=C)). Anal. calc. for C₃₆H₅₁N₇O₃: C, 68.65; H, 8.16; N, 15.57. Found: C, 68.05; H, 8.11; N, 15.43%.

3.10.1.3. Synthesis of N,N',N''-(nitrilotri-2,1-ethanediyl)tris[N'-4-*tert*-butylphenyl ureal], L¹².³

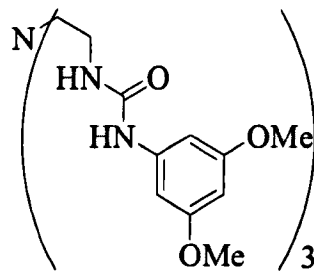


This was prepared in a similar manner to L¹⁰ by the reaction of TREN with 4-*tert*-butylphenyl isocyanate. Yield: 0.53 g, 59%. ¹H NMR (300 MHz, CDCl₃): δ/ppm 7.56 (br, 3H, NH), 7.14 (d, 6H, ³J_{HH} = 8 Hz, H_{Ar}), 7.03 (d, 6H, ³J_{HH} = 8 Hz, H_{Ar}), 6.18 (br, 3H, NH), 3.16 (br, 6H, CH₂), 2.27 (br, 6H, CH₂), 1.25 (s, 27H, ^tBu). ¹³C NMR (75 MHz, dmso-d₆): δ/ppm 156, 144, 138, 126, 117, 54, 48, 34, 32. MS (ES⁺):

m/z 672.46 [M+H]⁺. IR (solid, cm⁻¹): 2997 ($\nu_{(N-H)}$), 1640 ($\nu_{(C=O)}$), 1590 ($\nu_{(C=C, Ar)}$).

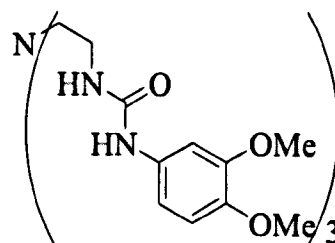
Anal. calc. for C₃₉H₅₇N₇O₃: C, 69.71; H, 8.55; N, 14.59. Found: C, 69.23; H, 8.47; N, 14.35%.

3.10.1.4. Synthesis of N,N',N''-(nitrilotri-2,1-ethanediyl)tris[N'-3,5-dimethoxyphenyl urea], L¹³.³



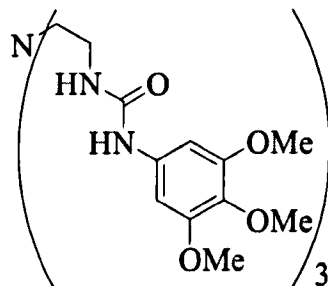
This was prepared in a similar manner to L¹⁰ by the reaction of TREN with 3, 5-dimethoxyphenyl isocyanate to give the product as a colourless solid. Yield: 0.74 g, 81%. ¹H NMR (300 MHz, CDCl₃): δ /ppm 7.39 (s, 3H, NH), 6.44 (s, 6H, H_{Ar}), 6.10 (br t, 3H, NH), 6.06 (s, 3H, H_{Ar}), 3.64 (s, 18H, OMe), 3.22 (br, 6H, CH₂), 2.38 (br, 6H, CH₂). ¹³C NMR (75 MHz, CDCl₃): δ /ppm 162, 156, 142, 96, 93, 56, 55, 48. MS (ES⁺): *m/z* 684.34 [M+H]⁺. IR (solid, cm⁻¹): 3333 ($\nu_{(N-H)}$), 2942 ($\nu_{(C-H)}$), 2836 ($\nu_{(C-H)}$), 1647 ($\nu_{(C=O)}$), 1148 ($\nu_{(C-O)}$). Anal. calc. for C₃₃H₄₅N₇O₉: C, 57.97; H, 6.63; N, 14.34. Found: C, 57.74; H, 6.61; N, 14.10%.

3.10.1.5. Synthesis of N,N',N''-(nitrilotri-2,1-ethanediyl)tris[N'-3,4-dimethoxyphenyl urea], L¹⁴.³



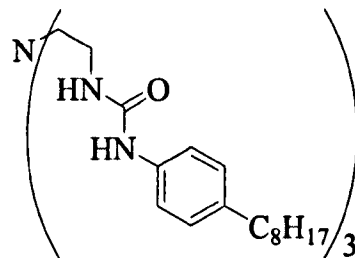
This was prepared in a similar manner to L¹⁰ by the reaction of TREN with 3, 4-dimethoxyphenyl isocyanate to give the product as a colourless solid. Yield: 0.79 g, 86%. ¹H NMR (300 MHz, CDCl₃): δ/ppm 7.50 (s, 3H, NH), 6.91 (s, 3H, H_{Ar}), 6.57 (d, 3H, ³J_{HH} = 9 Hz, H_{Ar}), 6.49 (d, 3H, ³J_{HH} = 9 Hz, H_{Ar}), 6.14 (br t, 3H, NH), 3.76 (s, 9H, OMe), 3.68 (s, 9H, OMe), 3.08 (br, 6H, CH₂), 2.35 (br, 6H, CH₂). ¹³C NMR (68 MHz, dmsO-d₆): δ/ppm 156, 149, 144, 135, 113, 110, 104, 56, 55, 54, 37. MS (ES⁺): m/z 684.33 [M+H]⁺. IR (solid, cm⁻¹): 3299 (ν_(N-H)), 2935 (ν_(C-H)), 2834 (ν_(C-H)), 1627 (ν_(C=O)), 1205 (ν_(C-O)). Anal. calc. for C₃₃H₄₅N₇O₉: C, 57.97; H, 6.63; N, 14.34. Found: C, 58.07; H, 6.69; N, 14.36%.

3.10.1.6. Synthesis of N,N',N''-(Nitrilotri-2,1-ethanediyl)tris(N'-3,4,5-trimethoxyphenyl urea) L¹⁵.³



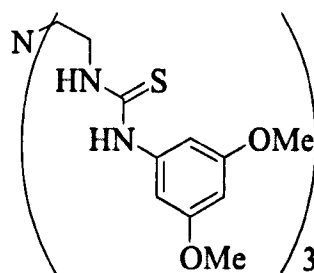
This was prepared in a similar manner to L¹⁰ by the reaction of TREN with 3, 4, 5-trimethoxyphenyl isocyanate and purified by column chromatography on silica gel using 7% MeOH, 93 % CHCl₃ to give the product as a colourless solid. Yield: 0.77 g, 74%. ¹H NMR (300 MHz, dmsO-d₆): δ/ppm 8.50 (s, 3H, NH), 6.72 (s, 6H, H_{Ar}), 6.12 (br t, 3H, NH), 3.68 (s, 18H, OMe), 3.57 (s, 9H, OMe), 3.18–3.16 (m, 6H, CH₂), 2.57 (br, 6H, CH₂). ¹³C NMR (75 MHz, dmsO-d₆): 156, 154, 138, 133, 96, 61, 56, 54, 37. IR (solid, cm⁻¹): 3336 (ν_(N-H)), 1650 (ν_(C=O)), 1603 (ν_(C=C), Ar), 1122 (ν_(C-O)). MS (ES⁺): m/z 774 [M+H]⁺.

3.10.1.7. Synthesis of N,N',N''-(Nitrilotri-2,1-ethanediyl)tris(N'-4-octylphenyl urea), L¹⁶.³



This was prepared in a similar manner to L¹⁰ by the reaction of TREN with 4-octylphenyl isocyanate to give the product as a colourless solid. Yield: 0.56 g, 61%.
¹H NMR (270 MHz, CDCl₃): δ/ppm 7.40 (s, 3H, NH), 6.93 (d, 6H, ³J_{HH} = 6 Hz, H_{Ar}), 6.51 (d, 6H, ³J_{HH} = 6 Hz, H_{Ar}), 6.00 (br t, 6H, NH), 3.13 (br, 6H, CH₂), 3.00 (br, 6H, CH₂), 2.48 (t, 6H, ³J_{HH} = 7 Hz, CH₂), 2.24 (br, 6H, CH₂), 1.28 (br, 30H, CH₂), 0.87 (d, 9H, ³J_{HH} = 6.2 Hz, Me). ¹³C NMR (68 MHz, dmso-d₆): δ/ppm 157, 138, 137, 129, 120, 55, 38, 36, 32, 31, 30, 29, 28, 25, 15. MS (ES⁺): m/z 840.65 [M+H]⁺. IR (solid, cm⁻¹): 3316 (v_(N-H)), 1640 (v_(C=O)), 1597 (v_(C=C, Ar)). Anal. calc. for C₃₃H₄₅N₇O₉: C, 72.88; H, 9.73; N, 11.67. Found: C, 72.88; H, 9.68; N, 11.48%.

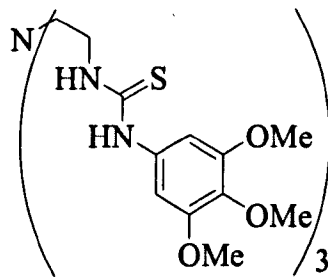
3.10.1.8. N,N',N''-(nitrilotri-2,1-ethanediyl)tris[N'-3,5-dimethoxyphenyl thiourea], L¹⁷.³



To TREN (0.20 cm³, 1.34 mmol) in dry thf (30 cm³) was added 3, 5-dimethoxyphenyl isothiocyanate (0.78 g, 4.00 mmol) under a N₂ atmosphere. The reaction was stirred at room temperature for 18 h and the colourless solid that formed was collected by filtration and dried *in vacuo*. Yield: 0.94 g, 96 %. ¹H NMR (270

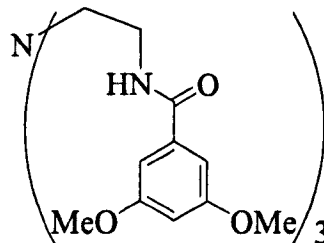
MHz, CDCl₃): δ/ppm 8.28 (br, 3H, NH), 6.82 (br, 3H, NH), 6.40 (s, 6H, H_{Ar}), 6.24 (s, 3H, H_{Ar}), 3.70 (s, 18H, OMe), 3.62 (br, 6H, CH₂), 2.67 (br, 6H, CH₂). ¹³C NMR (68 MHz, dmso-d₆): δ/ppm 180, 161, 141, 101, 97, 67, 56, 25. MS (ES⁺): *m/z* 732.26 [M+H]⁺. IR (solid, cm⁻¹): 3231 (v_(N-H)), 2936 (v_(C-H)), 2836 (v_(C-H)), 1596 (v_(C=S)), 1148 (v_(C-O)). Anal. calc. for C₃₃H₄₆N₇O₆S₃: C, 54.15; H, 6.20; N, 13.40. Found: C, 54.24; H, 6.28; N, 13.48%.

3.10.1.9. Synthesis of N,N',N''-(nitrilotri-2,1-ethanediyil)tris[N'-3,4,5-trimethoxyphenyl thiourea], L¹⁸.³



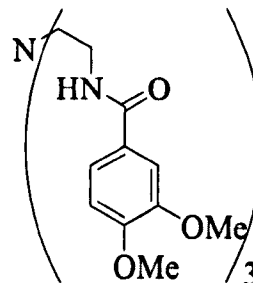
This was prepared in a similar manner to L²⁰ by the reaction of TREN with 3, 4, 5-trimethoxyphenyl isothiocyanate to give the product as a colourless solid. Yield: 1.08g, 98%. ¹H NMR (270 MHz, CDCl₃): δ/ppm 8.33 (br, 3H, NH), 6.74 (br, 3H, NH), 6.52 (s, 6H, H_{Ar}), 3.79 (s, 18H, OMe), 3.78 (s, 9H, OMe), 3.57 (br, 6H, CH₂), 2.65 (br, 6H, CH₂). ¹³C NMR (68 MHz, CDCl₃): δ/ppm 181, 154, 136, 133, 103, 68, 61, 56, 26. MS (ES⁺): *m/z* 822.30 [M+H]⁺. IR (solid, cm⁻¹): 3287 (v_(N-H)), 2937 (v_(C-H)), 1596 (v_(C=O)), 1121 (v_(C-O)). Anal. calc. for C₃₆H₅₁N₇O₉S₃: C, 52.60; H, 6.25; N, 11.93. Found: C, 52.71; H, 6.27; N, 11.95%.

3.10.1.10 N,N',N''-(nitrilotri-2,1-ethanediyl)tris-3,5-dimethoxybenzamide, L¹⁹.²⁵



TREN (0.40 cm³, 2.70 mmol) was dissolved in H₂O (20 cm³) containing NaOH (0.33 g, 8.25 mmol). 3, 5-Dimethoxybenzoyl chloride (1.53 g, 7.66 mmol) dissolved in Et₂O (10 cm³) was added slowly and the reaction stirred at room temperature for 2 days. The off-white solid that formed was collected by filtration, washed with a portion of Et₂O (10 cm³) and dried *in vacuo*. Yield: 1.27 g, 74%. ¹H NMR (270 MHz, CDCl₃): δ/ppm 7.57 (br t, 3H, NH), 6.87 (s, 6H, H_{Ar}), 6.38 (s, 3H, H_{Ar}), 3.63 (s, 18H, OMe), 3.47–3.44 (m, 6H, CH₂), 2.66 (t, 6H, ³J_{HH} = 5 Hz, CH₂). ¹³C NMR (68 MHz, CDCl₃): δ/ppm 168, 161, 159, 105, 103, 55, 54, 39. MS (ES⁺): *m/z* 639.30 [M+H]⁺. IR (solid, cm⁻¹): 3304 (v_(N-H)), 2938 (v_(C-H)), 2837 (v_(C-H)), 1637 (v_(C=O)), 1151 (v_(C-O)). Anal. calc. for C₃₃H₄₂N₄O₉: C, 62.06; H, 6.63; N, 8.77. Found: C, 61.98; H, 6.81; N, 8.59%.

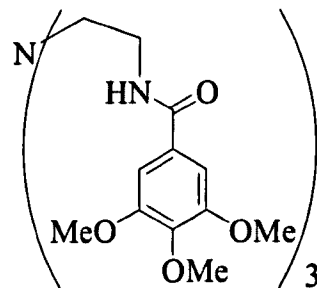
3.10.1.11. Synthesis of N,N',N''-(nitrilotri-2,1-ethanediyl)tris-3,4-dimethoxybenzamide, L²⁰.²⁵



This was prepared in a similar manner to L¹⁷ by the reaction of TREN with 3, 4-dimethoxybenzoyl chloride to give the product as a colourless solid. Yield: 1.14 g, 66%. ¹H NMR (270 MHz, CDCl₃): δ/ppm 7.37 (br, 3H, NH), 7.28 (s, 3H, H_{Ar}), 7.12

(d, 3H, $^3J_{\text{HH}} = 8$ Hz, $\underline{\text{H}}_{\text{Ar}}$), 6.31 (d, 3H, $^3J_{\text{HH}} = 8$ Hz, $\underline{\text{H}}_{\text{Ar}}$), 3.81 (s, 9H, OMe), 3.79 (s, 9H, OMe), 3.60–3.58 (m, 6H, CH₂), 2.77 (t, 6H, $^3J_{\text{HH}} = 5$ Hz, CH₂). ^{13}C NMR (68 MHz, CDCl_3): δ/ppm 168, 155, 153, 147, 126, 120, 110, 109, 56, 54, 39. MS (ES $^+$): m/z 639.30 [M+H] $^+$. IR (solid, cm^{-1}): 3291 ($\nu_{(\text{N-H})}$), 2936 ($\nu_{(\text{C-H})}$), 2836 ($\nu_{(\text{C-H})}$), 1628 ($\nu_{(\text{C=O})}$), 1264 ($\nu_{(\text{C-O})}$). Anal. calc. for $\text{C}_{33}\text{H}_{42}\text{N}_4\text{O}_9$: C, 62.06; H, 6.63; N, 8.77. Found: C, 61.85; H, 6.23; N, 8.26%.

3.10.1.12. Synthesis of $\text{N,N}',\text{N}''$ -(nitrilotri-2,1-ethanediyl)tris-3,4,5-trimethoxybenzamide, L^{21, 25}



This was prepared in a similar manner to L¹⁷ by the reaction of TREN with 3, 4, 5-trimethoxybenzoyl chloride to give the product as a colourless solid. Yield: 1.43 g, 73%. ^1H NMR (270 MHz, CDCl_3): δ/ppm 7.77 (br t, 3H, NH), 7.00 (s, 6H, $\underline{\text{H}}_{\text{Ar}}$), 3.78 (s, 9H, OMe), 3.63 (s, 18H, OMe), 3.44 (br, 6H, CH₂), 2.61 (br, 6H, CH₂). ^{13}C NMR (68 MHz, CDCl_3): δ/ppm 168, 153, 141, 129, 105, 61, 56, 55, 39. MS (ES $^+$): m/z 729.33 [M+H] $^+$. IR (solid, cm^{-1}): 3304 ($\nu_{(\text{N-H})}$), 2939 ($\nu_{(\text{C-H})}$), 2836 ($\nu_{(\text{C-H})}$), 1636 ($\nu_{(\text{C=O})}$), 1120 ($\nu_{(\text{C-O})}$). Anal. calc. for $\text{C}_{36}\text{H}_{48}\text{N}_4\text{O}_{12}$: C, 59.33; H, 6.64; N, 7.69. Found: C, 59.21; H, 6.58; N, 7.71%.

3.10.2. Complexation Reactions

3.10.2.1. Synthesis of $[(L^{10}H)_2PtCl_6]$

Two equivalents of L^{10} were dissolved in MeCN (2 cm^3) to which one equivalent of H_2PtCl_6 also dissolved in MeCN (2 cm^3) was added. A yellow precipitate formed which was collected by filtration and dried *in vacuo*. ^1H NMR (270 MHz, dmso- d_6): δ/ppm 9.54 (br, 1H, NH^+), 8.65 (s, 3H, NH), 7.03 (s, 6H, H_{Ar}), 6.58 (s, 3H, H_{Ar}), 6.43 (br t, 3H, NH), 3.46 (t, 6H, ${}^3J_{HH} = 6\text{ Hz}$, CH_2), 3.37 (br, 6H, CH_2), 2.20 (s, 18H, CH_3). IR (solid, cm^{-1}): 3365 ($\nu_{(N-H)}$), 1673 ($\nu_{(C=O)}$). Anal. calc. for $C_{66}H_{92}N_{14}O_6PtCl_6$: C, 50.00; H, 5.85; N, 12.37. Found: C, 49.78; H, 5.82; N, 12.39%

3.10.2.2. Synthesis of $[(L^{11}H)_2PtCl_6]$

This compound was prepared in a similar manner to that described for $[(L^{10}H)_2PtCl_6]$ and precipitated as a yellow powder. ^1H NMR (270 MHz, dmso- d_6): δ/ppm 9.71 (br, 1H, NH^+), 8.72 (s, 3H, NH), 7.30 (d, 6H, ${}^3J_{HH} = 8\text{ Hz}$, H_{Ar}), 7.04 (d, 2H, ${}^3J_{HH} = 8\text{ Hz}$, H_{Ar}), 6.43 (br t, 3H, NH), 3.52 (br, 6H, CH_2), 2.80 (m, 3H, ${}^1\text{Pr}CH_2$), 2.30 (br, 6H, CH_2), (1.18 (d, 6H, ${}^1\text{Pr}CH_3$). IR (solid, cm^{-1}): 3347 ($\nu_{(N-H)}$), 1660 ($\nu_{(C=O)}$). Anal. calc. for $C_{72}H_{104}Cl_6N_{14}O_6Pt$: C, 51.80; H, 6.28; N, 11.75. Found: C, 51.80; H, 6.17; N, 11.71%.

3.10.2.3. Synthesis of $[(L^{12}H)_2PtCl_6]$

This compound was prepared in a similar manner to that described for $[(L^{10}H)_2PtCl_6]$ and precipitated as a yellow powder. ^1H NMR (270 MHz, dmso- d_6): δ/ppm 9.74 (br, 1H, NH^+), 8.74 (s, 3H, NH), 7.30 (d, 6H, ${}^3J_{HH} = 9\text{ Hz}$, H_{Ar}), 7.19 (d, 6H, ${}^3J_{HH} = 9\text{ Hz}$, H_{Ar}), 6.44 (br t, 3H, NH), 3.51 (br, 6H, CH_2), 3.46 (br, 6H, CH_2), 1.24 (s, 27H, ${}^1\text{Bu}$). IR (solid, cm^{-1}): 3333 ($\nu_{(N-H)}$), 1651 ($\nu_{(C=O)}$). Anal. calc. for $C_{78}H_{116}Cl_6N_{14}O_6Pt$: C, 53.42; H, 6.67; N, 11.18. Found: C, 53.32; H, 6.53; N, 11.08%.

3.10.2.4. Synthesis of $[(L^{13}H)_2PtCl_6]$

This compound was prepared in a similar manner to that described for $[(L^{10}H)_2PtCl_6]$ but no precipitate was seen to form and the reaction was repeated in MeCN- d_3 . 1H NMR (270 MHz, MeCN- d_3): δ /ppm 9.12 (br, 1H, NH $^+$), 6.56 (s, 6H, H_{Ar}), 6.15 (s, 3H, H_{Ar}), 3.67 (br, 18H, OMe), 3.55 (br, 6H, CH₂), other CH₂ under broad H₂O signal, NH signals not observed. MS (ES $^+$): *m/z* 684 [L¹³H] $^+$. MS (ES $^-$): *m/z* 718 [L¹³+Cl] $^-$, 981 [(L¹³-2H)PtCl₃] $^-$, 1089 [(L¹³H)PtCl₆] $^-$, 1772 [L¹³(L¹³H)PtCl₆] $^-$.

3.10.2.5. Synthesis of $[(L^{14}H)_2PtCl_6]$

This compound was prepared in a similar manner to that described for $[(L^{10}H)_2PtCl_6]$ but no precipitate was seen to form and the reaction was repeated in MeCN- d_3 . 1H NMR (270 MHz, MeCN- d_3): δ /ppm 9.65 (br, 1H, NH $^+$), 7.73 (s, 3H, NH), 6.93 (s, 3H, H_{Ar}), 6.83 (br, 3H, H_{Ar}), 6.59 (br, 3H, H_{Ar}), 6.19 (br t, 3H, NH), 3.65 (s, 18H, OMe), 3.56 (br, 6H, CH₂), 3.40 (br, 6H, CH₂). ^{195}Pt NMR (500 MHz, MeCN- d_3): δ /ppm 247.

3.10.2.6. Synthesis of $[(L^{15}H)_2PtCl_6]$

This compound was prepared in a similar manner to that described for $[(L^{10}H)_2PtCl_6]$ but no precipitate was seen to form and the reaction was repeated in MeCN- d_3 . 1H NMR (300 MHz, MeCN- d_3): δ /ppm 9.87 (br, 1H, NH $^+$), 8.81 (br t, 3H, NH), 7.81 (s, 6H, H_{Ar}), 7.00 (br, 3H, NH), 3.72 (s, 18H, OMe), 3.52 (s, 9H, OMe), 2.55 (d, 6H, $^3J_{HH} = 5.5$, CH₂), other CH₂ obscured by H₂O signal.

The synthesis of $[(L^{16}H)_2PtCl_6]$ was not attempted as the small amount of receptor synthesised was thought to be of more use in solvent extraction studies.

3.10.2.7. Synthesis of $[(L^{17}H)_2PtCl_6]$

This compound was prepared in a similar manner to that described for $[(L^{10}H)_2PtCl_6]$ and precipitated as a yellow powder. No NMR spectra were recorded as the complex was insoluble. IR (solid, cm^{-1}): 3201 ($\nu_{(\text{N-H})}$), 1600 ($\nu_{(\text{C=C})}$), 1562 ($\nu_{(\text{C=S})}$). Anal. calc. for $C_{66}H_{92}Cl_6N_{14}O_{12}\text{PtS}_6$: C, 42.31; H, 4.95; N, 10.52. Found C, 42.01; H, 4.86 ; N, 10.43%

3.10.2.8. Synthesis of $[(L^{18}H)_2PtCl_6]$

This compound was prepared in a similar manner to that described for $[(L^{10}H)_2PtCl_6]$ and precipitated as a yellow powder. No NMR spectra were recorded as the complex was insoluble. IR (solid, cm^{-1}): 3178 ($\nu_{(\text{N-H})}$), 1598 ($\nu_{(\text{C=C})}$), 1568 ($\nu_{(\text{C=S})}$). Anal. calc. for $C_{72}H_{104}Cl_6N_{14}O_{18}\text{PtS}_6$: C, 42.10; H, 5.10; N, 9.55. Found C, 41.96; H, 5.26; N, 9.56%

3.10.2.9. Synthesis of $[(L^{19}H)_2PtCl_6]$

This compound was prepared in a similar manner to that described for $[(L^{10}H)_2PtCl_6]$. Although no precipitate was seen to form immediately, crystals of the complex formed and were characterised. ^1H NMR (300 MHz, $\text{dmso}-d_6$): δ/ppm 9.68 (br, 1H, $\underline{\text{NH}}^+$), 8.79 (t, 3H, $^3J_{\text{HH}} = 4.9$ Hz, $\underline{\text{NH}}$), 7.00 (s, 6H, $\underline{\text{H}_{\text{Ar}}}$), 6.68 (s, 3H, $\underline{\text{H}_{\text{Ar}}}$), 3.78 (s, 18H, $\underline{\text{OMe}}$), 3.70 (br, 6H, $\underline{\text{CH}_2}$), 3.50 (br, 6H, $\underline{\text{CH}_2}$). IR (solid, cm^{-1}): 3368 ($\nu_{(\text{N-H})}$), 1641 ($\nu_{(\text{C=O})}$), 1592 ($\nu_{(\text{C=C})}$), 1155 ($\nu_{(\text{C-O})}$). Anal. calc. for $C_{66}H_{86}Cl_6N_8O_{18}\text{Pt}$: C, 46.98; H, 5.14; N, 6.64. Found C, 47.05; H, 5.11; N, 6.57%. MS (ES^-): m/z 673 [$L^{19}+\text{Cl}]^-$, 936 [$(L^{19}-2\text{H})\text{PtCl}_3]^-$, 972 [$(L^{19}-\text{H})\text{PtCl}_4]^-$, 1044 [$(L^{19}\text{H})\text{PtCl}_6]^-$, 1378 [$(L^{19}\text{H})(\text{PtCl}_5)_2]^-$, 1682 [$L^{19}(L^{19}\text{H})\text{PtCl}_6]^-$. ^{195}Pt NMR (500 MHz, $\text{MeCN}-d_3$): δ/ppm 244.

3.10.2.10. Synthesis of $[(L^{20}H)_2PtCl_6]$

This compound was prepared in a similar manner to that described for $[(L^{10}H)_2PtCl_6]$ but no precipitate was seen to form and the reaction was repeated in MeCN- d_3 . 1H NMR (300 MHz, MeCN- d_3): δ /ppm 9.83 (br, 1H, NH $^+$), 7.87 (br, 3H, NH), 7.31 (d, 3H, $^3J_{HH} = 6$ Hz, H_{Ar}), 7.18 (s, 3H, H_{Ar}), 6.73 (d, 3H, $^3J_{HH} = 6$ Hz, H_{Ar}), 3.81 (s, 9H, OMe), 3.65 (s, 9H, OMe), 2.39 (br, 6H, CH₂), 2.07 (br, 6H, CH₂).

3.10.2.11. Synthesis of $[(L^{21}H)_2PtCl_6]$

This compound was prepared in a similar manner to that described for $[(L^{10}H)_2PtCl_6]$ but no precipitate was seen to form and the reaction was repeated in MeCN- d_3 . 1H NMR (300 MHz, MeCN- d_3): δ /ppm 9.96 (br, 1H, NH $^+$), 8.34 (br, 3H, NH), 7.03 (s, 6H, H_{Ar}), 4.01 (br, 6H, CH₂), 3.90 (br, 6H, CH₂), 3.73 (s, 18H, OMe), 3.72 (s, 9H, OMe). ^{13}C NMR (75 MHz, MeCN- d_3): 170, 153, 128, 117, 105, 60, 56, 55, 36.

3.10.3. Synthesis of Tetrabutylammonium Hexachloroplatinate, $(Bu_4N)_2PtCl_6$.⁴²

K₂PtCl₆ (0.12 g, 0.25 mmol) was dissolved in H₂O (*ca.* 20 cm³) to give a yellow solution to which (Bu₄N)HSO₄ (0.17 g, 0.50 mmol) in CH₂Cl₂ (*ca.* 80 cm³) was added. The resulting two-phase system was stirred at room temperature until complete decolourisation of the aqueous layer was observed. The organic layer was separated and dried over MgSO₄, the solvent was removed and the residue was dried *in vacuo* to give an orange powder. Yield: 85%. Anal. calc. for C₂₄H₅₄Cl₆N₂Pt: C, 43.05; H, 8.13; N, 3.14. Found: 42.53; H, 7.84; N, 3.04%.

3.11. References

1. Rosenqvist T., *Principles of Extractive Metallurgy*, McGraw-Hill, Tokyo, 1983.
2. Clayden J.; Green N.; Warren S.; Wothers P., *Organic Chemistry*, Oxford University Press, Oxford, 2000, pp 378.
3. Zart M. K.; Sorrell T. N.; Powell D.; Borovik A. S., *Dalton Trans.*, 2003, 1986-1992
4. Jose D. A.; Kumar D. K.; Ganguly B.; Das A., *Inorg. Chem.*, 2007, **46**, 5817-5819.
5. Zhou Y.; Yi T.; Li T.; Zhou Z.; Li F.; Huang W.; Huang C., *Chem. Mater.*, 2006, **18**, 2974-2981.
6. Clark A. J.; Geden J. V.; Thom S., *J. Org. Chem.*, 2006, **71**, 1471-1479.
7. Custelcean R.; Moyer B. A.; Hay B. P., *Chem. Commun.*, 2005, **48**, 5971-5973.
8. Liddell U.; Ramsay N. F., *J. Chem. Phys.*, 1951, **19**, 1608-1609.
9. Jeffrey G. A., *An Introduction to Hydrogen Bonding*, Oxford University Press, Oxford, 1997, 9th edition, pp 228.
10. Pregosin P.S., *Coord. Chem. Rev.*, 1982, **44**, 247-291.
11. Kovacova J.; Melnik M.; Gazo J., *Conference on Coordination Chemistry*, Slovak Tech. Univ. 1976, **6**, 143-148.
12. Bret J. M.; Castan P.; Commenges G.; Laurent J P., *Polyhedron*, 1983, **2**, 901-905.
13. Kovacova J., Gazo J., *Collection Czechoslov. Chem. Commun.*, 1980, **45**, 1331-1335.
14. For a review of S-Pt coordination chemistry being used in solvent extractions see Koch K. R., *Coord. Chem. Rev.*, 2001, **216-217**, 473-488.
15. Kurnakow N., *J. Prakt. Chem.*, 1898, **50**, 234.
16. Koenig K. H.; Schuster M.; Steinbrech B.; Schneeweis G.; Schlodder R., *Fresenius Z.*, *Anal. Chem.*, 1985, **321**, 457-460
17. Vest P.; Schuster M.; Koenig K. H.; Fresenius Z., *Anal. Chem.*, 1989, **335**, 759-763.
18. Koch K. R., *Coord. Chem. Rev.*, 2001, **216-217**, 473-488.
19. Vest P.; Schuster M.; Koenig K. H.; Fresenius Z., *Anal. Chem.*, 1991, **339**, 142-144.
20. Vest P.; Schuster M.; Koenig K. H.; Fresenius Z., *Anal. Chem.*, 1991, **341**, 566-568.

21. Koch K. R.; Bourne S.; *J. Chem. Soc. Dalton Trans.*, 1993, 2071-2072.
22. Koch K. R.; Coetzee A.; Wang Y.; *J. Chem. Soc. Dalton Trans.*, 1999, 1013-1016.
23. Koch K. R.; du Toit J.; Caira M. R.; Sacht C., *J. Chem. Soc. Dalton Trans.*, 1994, 785-786.
24. Gómez D. E.; Fabbrizzi L.; Licchelli M.; Enrico M., *Org. Biomol. Chem.*, 2005, **3**, 1495-1500.
25. Following the method of Geraldes C. F. G. C.; Brucher E.; Cortes S.; Koenig S. H.; Sherry A. D.; *J. Chem. Soc., Dalton Trans.*, 1992, 2517-2522.
26. Bulls A. R.; Pippin G.; Hahn F. E.; Raymond K. N., *J. Am. Chem. Soc.*, 1990, **112**, 2627-2632.
27. Beer P. D.; Hopkins K.; McKinney J. D., *Chem. Commun.*, 1999, **13**, 1253-1254.
28. Bulls A. R.; Pippin G.; Hahn F. E.; Raymond K. N., *J. Am. Chem. Soc.*, 1990, **112**, 2627-2632.
29. Koch K. R.; Burger M. R.; Kramer J.; Westra A. N., *Dalton Trans.*, 2006, 3277-3283.
30. Rossotti H., *Chemical Applications of Potentiometry*, van Nostrand-Reinhold, London, 1969, 1st edition.
31. Taylor P. D., *Talanta*, 1995, **42**, 845-850.
32. Connors K. A., *Binding Constants*, John Wiley and Sons, 1987, 1st edition, pp 21-31.
33. Schneider H. J.; Durr H., *Frontiers in Supramolecular Organic Chemistry and Photochemistry*, VCH, 1991, pp 129.
34. Beer P.; Gale P.; Smith D.; *Supramolecular Chemistry*, Oxford University Primer Series, Oxford University Press, 1999, pp 8-11.
35. Steed J. W., Atwood J. L., *Supramolecular Chemistry*, Wiley, 2000, pp 15-19.
36. Blanda M. T., Horner J. H., Newcomb M., *J. Org. Chem.*, 1989, **54**, 4626-4636.
37. Kavallieratos K., Bertao C. M., Crabtree R. H., *J. Org. Chem.*, 1999, **64**, 1675-1683.
38. Hynes M. J., *J. Chem. Soc., Dalton Trans.*, 1993, 311-312.
39. Frassineti C., Ghelli S., Gans P., Sabatini A., Moruzzi M. S., Vacca A., *Anal. Biochem.*, 1995, **231**, 374 - 382.
40. Frassineti C., Alderighi L., Gans P., Sabatini A., Vacca A., Ghelli S., *Anal. Bioanal. Chem.*, 2003, **376**, 1041 - 1052.

41. Iovel I. G., Goldberg Y. S., Shymanska M. V., Lukevics E., *Organometallics*, 1987, **6**, 1410-1413.
42. Miyaji H.; Collinson S. R.; Prokes I.; Tucker J., *Chem. Commun.*, 2003, 64-65.
43. Stulz E.; Scott S. M.; Bond A. D.; Otto S.; Sanders J. K. M., *Inorg. Chem.*, 2003, **42**, 3086-3096.
44. Halouani H.; Dumazet-Bonnamour I.; Perrin M.; Lamartine R., *J. Org. Chem.*, 2004, **69**, 6521-6527.

4. Solvent Extraction Studies

Following the synthesis of a series of organic soluble receptors and complexes their extraction efficiency was assessed. This Chapter describes the development of a method that has been used to analyse and compare TOA and TREN-based sulfonamide, urea and amide receptors.

4.1. Principles of Extraction

The aim of a solvent extraction process is to selectively extract the desired species from an aqueous phase into an immiscible organic phase providing a route to separation.^{1, 2} The flowchart and equations in Figure 4.1 represent the processes involved in purifying $[\text{PtCl}_6]^{2-}$. The first step is leaching in which the Pt-containing ore is dissolved in *aqua regia* to produce H_2PtCl_6 in an acidic, aqueous solution.³ Separation of $[\text{PtCl}_6]^{2-}$ is achieved by mixing an organic phase containing two equivalents of a receptor (L) with an aqueous solution of H_2PtCl_6 to form an organic soluble complex $[(\text{LH})_2\text{PtCl}_6]$. Mixing the organic phase containing $[(\text{LH})_2\text{PtCl}_6]$ with an aqueous solution of base leads to the back extraction and recovery of $[\text{PtCl}_6]^{2-}$. Finally, an electrorefining technique such as electrowinning can be employed to recover pure metallic Pt from $[\text{PtCl}_6]^{2-}$.⁴

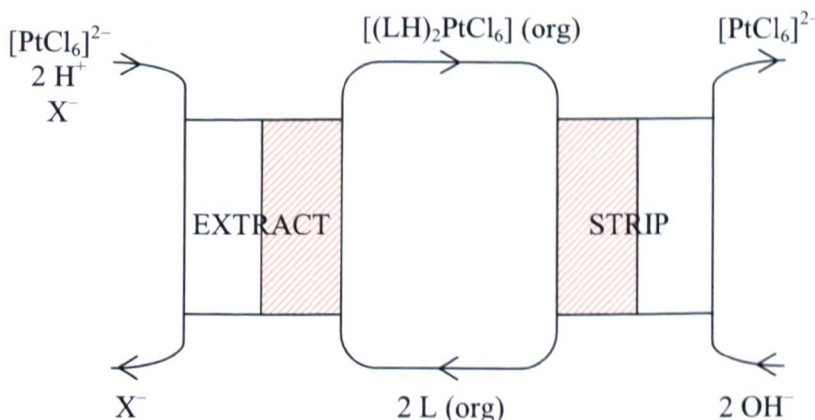


Figure 4.1a. Flowchart representing the solvent extraction of $[\text{PtCl}_6]^{2-}$

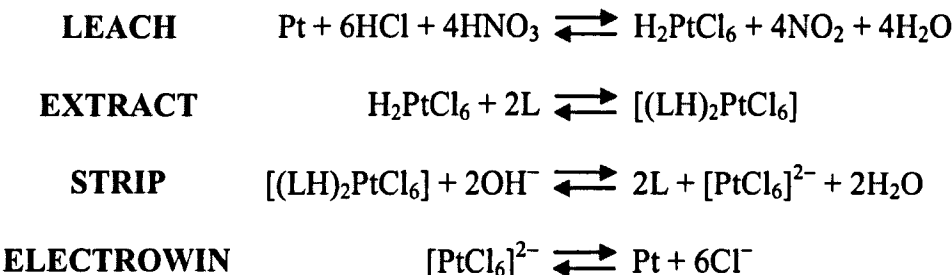


Figure 4.1b. Equations representing the solvent extraction process.

Commercially obtained $H_2PtCl_6 \cdot xH_2O$ ($x = 1$ or 6) was used throughout this work as a source of the $[PtCl_6]^{2-}$ anion. In this research the extract and strip stages were studied as these involve our synthesised receptor systems (L). Ideally, the ionophores will form an interaction with $[PtCl_6]^{2-}$ that is strong enough to extract and stabilise it in the organic phase. However, it also important that these interactions are reversible to allow recovery of free $[PtCl_6]^{2-}$.

4.2. Current Methods Used to Extract $[PtCl_6]^{2-}$

There is literature evidence suggesting that current methods to extract $[PtCl_6]^{2-}$ involve long chain alkylamines such as Alamine type reagents.⁵⁻¹¹ A variety of investigations detailing the solvent extraction of $[PtCl_6]^{2-}$ with long chain alkylamines have been reported and form the basis for developing a strategy for studying the extractive ability of our receptors.^{7, 12-14} In this work trioctylamine (TOA) has been used (Figure 4.2) as a model in order to benchmark against the new TREN-based reagents.^{13, 15-19} Extraction studies were carried out with TOA and the results are discussed in Section 4.6.1.

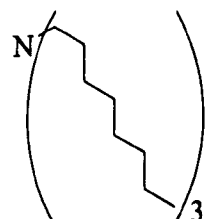


Figure 4.2. Trioctylamine (TOA).

4.3. Method Development

There are a number of factors that were considered in order to develop an optimised extraction process. These include the choice of organic solvent, the mixing time between phases and pH of extraction systems; these and other factors are discussed in the subsequent Sections.

4.3.1. Production of $[\text{PtCl}_6]^{2-}$

It is important to know the conditions under which $[\text{PtCl}_6]^{2-}$ is produced and is stable. Hydrochloric acid is an effective medium into which the PGMs in a concentrate can be brought into solution and thus, chlorometallate complexes are the most commonly encountered species.²⁰ Platinum(IV) reacts with Cl^- to form $[\text{PtCl}_6]^{2-}$ which can undergo stepwise aquation to give the diaquatetrachloro complex, $[\text{PtCl}_4(\text{H}_2\text{O})_2]$ and the aquapentachloro complex, $[\text{PtCl}_5(\text{H}_2\text{O})]^-$.^{13, 20} The proportions of the chloro-complexes formed varies with Cl^- concentration (Figure 4.3)¹³ and the aquation of $[\text{PtCl}_6]^{2-}$ is inhibited in strong chloride media. Thus, as Cl^- concentration increases the proportion of $[\text{PtCl}_6]^{2-}$ increases while the amount of $[\text{PtCl}_5(\text{H}_2\text{O})]^-$ and $[\text{PtCl}_4(\text{H}_2\text{O})_2]$ present decrease.²⁰ To ensure that Pt is present exclusively as $[\text{PtCl}_6]^{2-}$, extraction studies were undertaken using Cl^- solutions. Indeed, work published by Anuse and co-workers reports higher extraction of $[\text{PtCl}_6]^{2-}$ using TOA in HCl than in H_2SO_4 , HNO_3 , HBr or HClO_4 .¹⁴

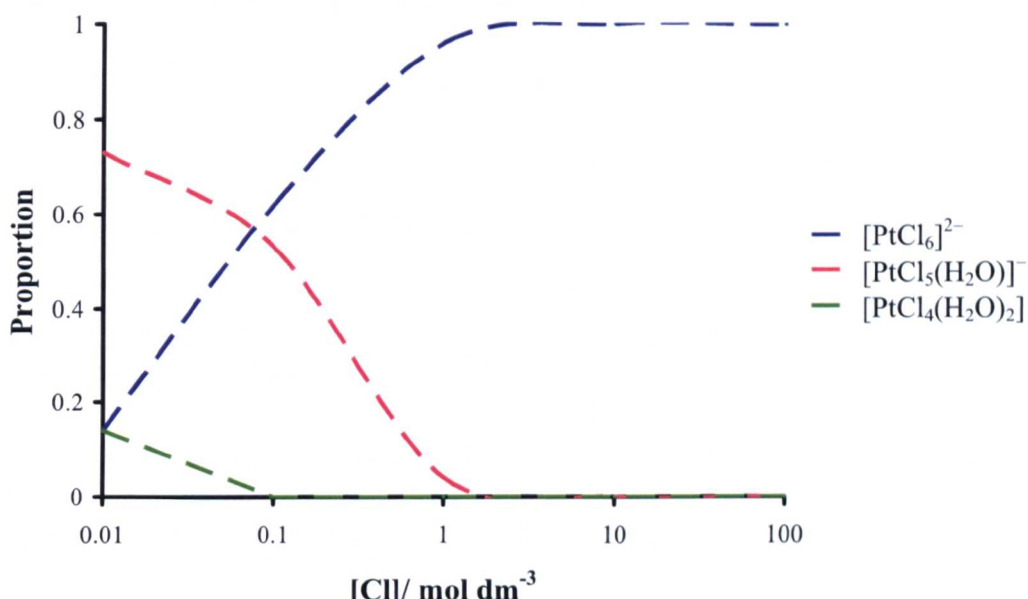


Figure 4.3. Proportion of chloro-complexes of Pt(IV) as a function of Cl^- concentration.¹³

4.3.2. Choice of Solvent

In a solvent extraction process it is critical for the receptor and its $[\text{PtCl}_6]^{2-}$ complex to be soluble in an organic solvent that is immiscible with water. If a receptor is selective for $[\text{PtCl}_6]^{2-}$ then this provides a route for separating $[\text{PtCl}_6]^{2-}$ from other species present in the aqueous phase such as Cl^- .²¹ In each of the extraction studies CHCl_3 was used as the organic phase for three reasons. Firstly, CHCl_3 is immiscible with H_2O and secondly the organic and aqueous phases separate rapidly following a period of mixing.¹³ Thirdly, our receptors and their complexes are soluble in CHCl_3 meaning that the procedure is not complicated by the formation of insoluble precipitates.

4.3.3. Measurement of Pt Extraction

Throughout this work ICP-OES and ICP-MS analysis has been used to measure the Pt content of the solution samples. These techniques are highly sensitive, reliable and a relatively quick way of analysis and was thus the method of choice for measuring

the Pt content in extraction experiments. Atomic absorption spectroscopy and flame photometry were also considered as alternatives. Trials using these methods found them to be unsuitable because there are limits as to the measurement of low levels of Pt (< 20 ppm) and the methods were also time-consuming.

4.3.4. Mixing Time Studies

Previous studies of the equilibrium time for $[\text{PtCl}_6]^{2-}$ extraction by long chain alkylamines have shown that mixing periods from several minutes (between 1-5 mins for Alamine 304 and N-n-octylaniline)^{7,14} to several hours (overnight for trioctylamine)¹³ may be necessary to achieve equilibrium. To determine the optimum mixing time a CHCl_3 phase containing L^{13} and an acidic, aqueous phase containing H_2PtCl_6 were stirred at room temperature for varying periods of time. The Pt content of the organic phase was assessed at regular intervals using ICP-MS and it was found that after four hours the maximum level of extraction was achieved suggesting that equilibrium had been established.

4.3.5. Chloride Selectivity

The presence of HCl in the processing of Pt-containing ores is necessary for the production of $[\text{PtCl}_6]^{2-}$. However, Cl^- anions may be competitive for the receptor since Cl^- is a hydrogen-bond acceptor and may form a charge-neutral complex $[(\text{LH})\text{Cl}]$.^{22, 23, 24} The selective extraction of $[\text{PtCl}_6]^{2-}$ over Cl^- , which is present in substantial excess in industrial feed streams, is essential for an efficient process and is, therefore, a key design requirement for our receptors.

To assess whether our systems will extract Cl^- , extractions using L^{13} were performed using either 0.1 M HCl or 0.6 M HCl. For both HCl concentrations studied the results showed that as the receptor concentration increased the amount of

Cl^- extracted increased. Also, more Cl^- is extracted at higher HCl concentration; thus, in the presence of 0.1 M HCl the maximum amount of Cl^- extracted was 88% compared to 100% Cl^- extraction from 0.6 M HCl (Figure 4.3). These results confirm that under certain conditions the receptor L^{13} , and potentially other tripodal receptors discussed in this thesis, can extract Cl^- to form organic soluble complexes.

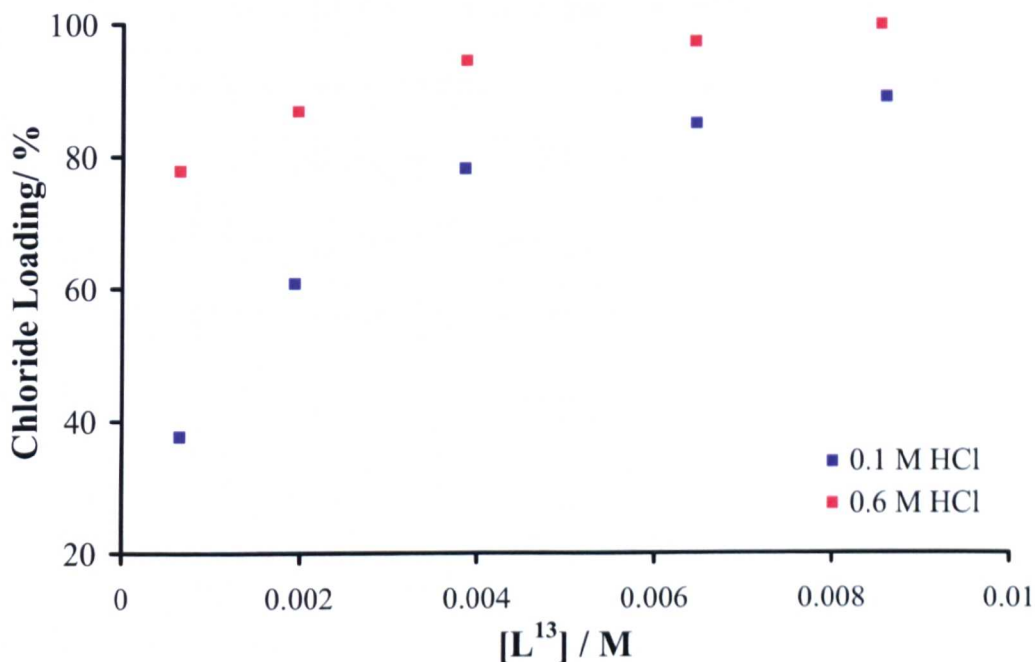


Figure 4.3. Plot of % Cl^- extracted from 0.1 M or 0.6 M HCl into CHCl_3 as a function of $[L^{13}]$.

4.3.6. pH of Extractions

It is necessary to add acid to the solvent extraction experiments to accurately represent the conditions used in the processing of Pt-containing ores.^{20, 22, 25} Despite preliminary extraction experiments showing that the TREN-based receptors can extract Cl^- , HCl was chosen because $[\text{PtCl}_6]^{2-}$ is produced and stable in this medium.^{13, 22} Experiments were performed with varying HCl concentrations to determine the effect on extraction efficiency. In each case L^{13} was used as the CHCl_3 soluble receptor and the aqueous phase contained H_2PtCl_6 dissolved in either H_2O (with no HCl added), 0.1 M HCl or 0.6 M HCl. The results are shown as a plot of

[Receptor]:[PtCl₆]²⁻ ratio against the percentage of platinum extracted and throughout this work graphs of this type have been used to make comparisons between different systems (Figure 4.4).

In each extraction it was observed that as the [Receptor]:[PtCl₆]²⁻ ratio increased, the amount of [PtCl₆]²⁻ extracted increased. Each of the plots is seen to plateau after a [Receptor]:[PtCl₆]²⁻ ratio of approximately 3:1 indicating that the system has achieved maximum loading. There is a marked difference between the results in the absence of HCl compared to samples with 0.1 M and 0.6 M HCl. For example, at an arbitrary [L¹³]:[PtCl₆]²⁻ ratio of 3:1, 63% of the anion was extracted when there was no HCl added compared to >98% extraction in 0.1 M and 0.6 M HCl (Table 4.1).

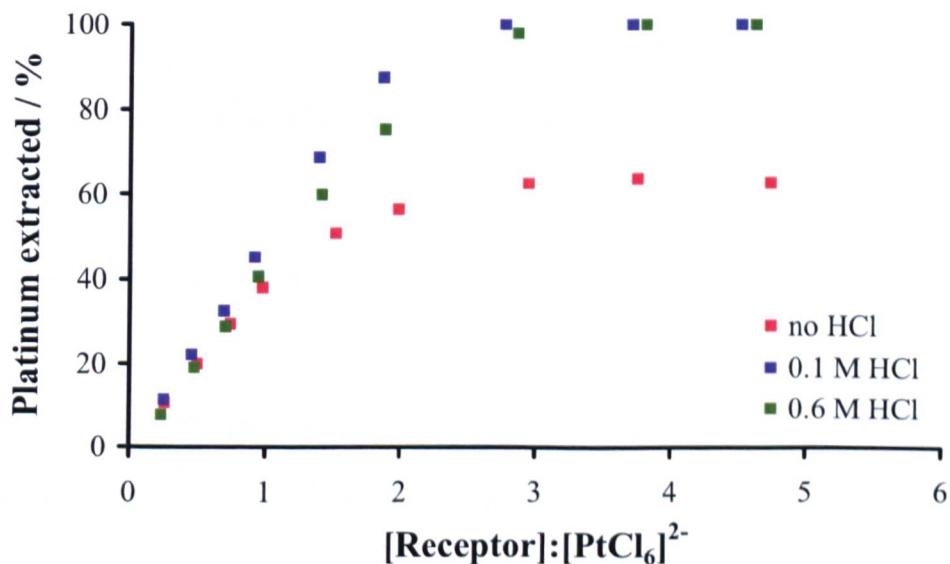


Figure 4.4. Plot of % Pt extracted as [PtCl₆]²⁻ from aqueous 0.0, 0.1 or 0.6 M HCl into CHCl₃ as a function of [Receptor]:[PtCl₆]²⁻ ratio.

Table 4.1. % of Pt extracted as [PtCl₆]²⁻ into CHCl₃ from aqueous HCl in the presence of a 3 molar excess of L

HCl concentration/ M	0.0	0.1	0.6
% Pt extracted at 3 molar excess of L	63	100	98

It was expected that as the Cl^- concentration increased the amount of $[\text{PtCl}_6]^{2-}$ extracted would decrease due to competition from Cl^- anions. Alguacil and co-workers carried out extractions of $[\text{PtCl}_6]^{2-}$ using Alamine 304 in xylene and report that as HCl concentration increases the extraction of $[\text{PtCl}_6]^{2-}$ falls which is attributed to the formation of amine HCl complexes.⁷ For L¹³, the presence of HCl *increased* the extraction efficiency presumably due to the protonated ionophores affording a greater number of electrostatic interactions with $[\text{PtCl}_6]^{2-}$. Another possible reason is that at higher Cl^- concentrations the predominant Pt species is $[\text{PtCl}_6]^{2-}$ ^{13, 20} and the receptors are designed with hydrogen-bond donor groups to target the areas of highest electron density surrounding this anion. Previous extraction experiments have shown L¹³ can extract Cl^- (Section 4.3.5) and the results presented in this Section show that extraction of $[\text{PtCl}_6]^{2-}$ is, in fact, more efficient in the presence of Cl^- . This confirms the selectivity of the receptors for $[\text{PtCl}_6]^{2-}$ over Cl^- under acidic conditions which is a significant result. All subsequent extractions were thus carried out in 0.6 M HCl; it is thought also that this most accurately represents the acidic conditions used in the processing of Pt-containing ores.^{20, 22, 25}

4.3.7. Control Experiments

A control experiment was performed to ensure that the solubility of $[\text{PtCl}_6]^{2-}$ in the organic phase remains negligible in the absence of receptor over a four hour period of mixing. It was found that the amount of $[\text{PtCl}_6]^{2-}$ extracted was 0% confirming that transfer of the anion into the organic phase only takes place only in the presence of receptor.

4.3.8. Back Extractions

Following the extraction of $[\text{PtCl}_6]^{2-}$ to form an organic-soluble complex $[(\text{LH})_2\text{PtCl}_6]$ it is necessary to recover the anion into an aqueous phase in a back extraction process (Figure 4.4). This enables Pt to be recovered from $[\text{PtCl}_6]^{2-}$ in the aqueous solution through a process such as electrowinning and regenerates the extractant for further use.⁴

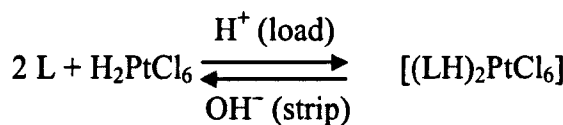


Figure 4.4. pH swing mechanism to control the uptake and release of $[\text{PtCl}_6]^{2-}$.

In this work back extractions were performed for additional reasons. Firstly, to establish the use of a pH swing mechanism to control the uptake and release of the $[\text{PtCl}_6]^{2-}$ anion. Secondly, it is not possible to directly analyse the Pt content of organic phases using ICP-OES or ICP-MS as there is no organic platinum standard to calibrate the instrument. It is, therefore, necessary to back extract the $[\text{PtCl}_6]^{2-}$ complexed in the organic phase into a “fresh” aqueous phase (that contains no Pt) to determine the amount of platinum that was present in the organic phase. Finally, although the concentration of Pt in an organic phase can be found from the difference of initial and the equilibrium aqueous phase values,^{7, 26, 27} analysis of both phases is preferable to confirm the mass balance. The amount of $[\text{PtCl}_6]^{2-}$ extracted and $[\text{PtCl}_6]^{2-}$ not extracted should sum to 100%.

Yoshizawa and co-workers have reported solvent extraction experiments with TOA and $[\text{PtCl}_6]^{2-}$ in toluene.¹³ They investigated the stripping of $[\text{PtCl}_6]^{2-}$ from an organic phase containing $[(\text{TOA}+\text{H})_2\text{PtCl}_6]$ using two different approaches. The first involved the use of aqueous HCl solution and stripping of $[\text{PtCl}_6]^{2-}$ was considered to proceed by breaking the ion-pair through the preferential binding of $(\text{TOA}+\text{H})^+$ to

Cl⁻. The second method used aqueous NaOH solution which proceeded by deprotonation of the tertiary amine in (TOA+H)⁺ removing the electrostatic attraction between receptor and anion. The stripping of [PtCl₆]²⁻ with aqueous HCl was only possible at low TOA and high HCl concentrations, whereas with aqueous NaOH solution it was found to be readily performed and complete stripping was achieved.

Experiments were performed to assess if [PtCl₆]²⁻ recovery from the organic phase containing [(LH)₂PtCl₆] was possible by addition of NaOH and to identify the volume required for such a process. A CHCl₃ phase containing [(L¹³H)₂PtCl₆] was contacted with a 0.05 M NaOH solution. This concentration of NaOH was chosen because it allowed a sensible range of volumes to be used for the test back extractions. The OH⁻: receptor ratio was varied and the amount of [PtCl₆]²⁻ recovered measured. In the presence of two equivalents of OH⁻ quantitative back extraction of [PtCl₆]²⁻ was achieved and a mixing time of 30 minutes was found to be sufficient. These experiments confirmed that complexation and decomplexation of [PtCl₆]²⁻ is reversible and pH dependent.

4.3.9. Method of Extraction

Following the development and optimisation of each step of the process an extraction method was produced which was then used to assess each of the receptors. The method is described with the full protocol and data analysis being given in Appendix E.

A stock solution of H₂PtCl₆.H₂O in 0.6 M HCl was prepared with [Pt] ~ 270 ppm (approximately 0.0332 g in 50 cm³ of 0.6 M HCl). A stock solution of the required receptor in CHCl₃ was also prepared from which nine 5 cm³ samples of varying concentration were prepared. These samples were mixed with an equivolume

of the $[PtCl_6]^{2-}$ stock solution and the two phases vigorously mixed for four hours at room temperature. The phases were then separated and 4 cm^3 aliquots of the organic phase were mixed at room temperature for 30 mins with 4 cm^3 of freshly prepared basic aqueous solutions in which the hydroxide concentration was twice the receptor concentration. The Pt content of the aqueous phases, the back extracted aqueous phases and the $[PtCl_6]^{2-}$ stock solution were determined by ICP-OES or ICP-MS (Figure 4.5).

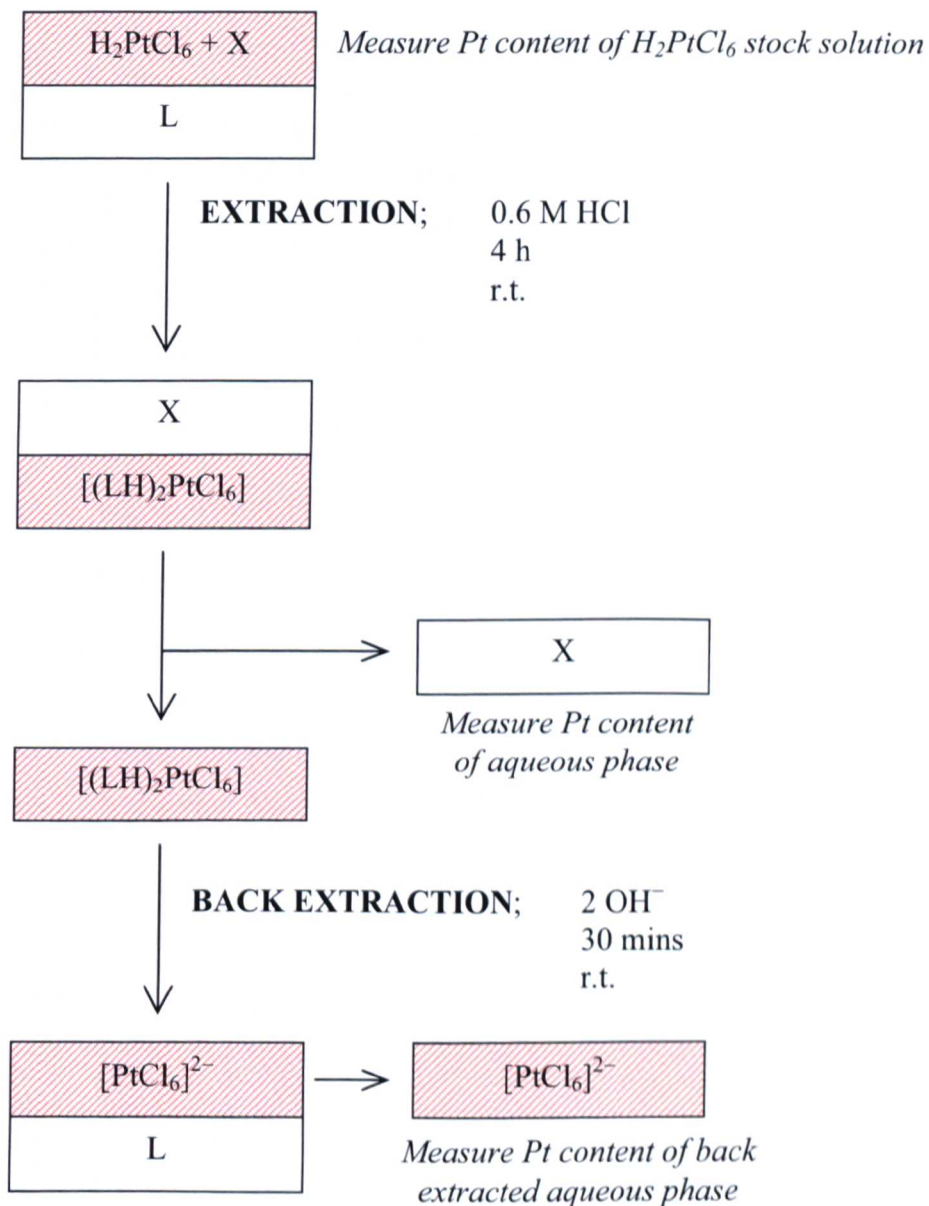


Figure 4.5. Flowchart showing the method of extraction.

4.4. Treatment of Results

4.4.1. Extraction Graph

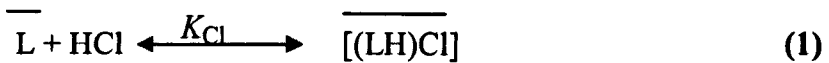
The data from the ICP-MS measurements were used to determine the amounts of $[\text{PtCl}_6]^{2-}$ extracted and the mass balance of the experiment. There was a small amount of solvent loss observed following extraction which is thought to result from either evaporation or the manual separation and transfer of phases. The extractive behaviours of the receptors are shown as graphs of [Receptor]: $[\text{PtCl}_6]^{2-}$ ratio against percentage of $[\text{PtCl}_6]^{2-}$ extracted where;

$$\% \text{ Pt extracted} = \left[\frac{\text{Amount of } [\text{PtCl}_6]^{2-} \text{ in aqueous phase following back extraction}}{\text{Amount of } [\text{PtCl}_6]^{2-} \text{ in original aqueous feed}} \right] \times 100$$

4.4.2. Confirming the Stoichiometry of the Complex

Yoshizawa made attempts to confirm the 2:1 [TOA]: $[\text{PtCl}_6]^{2-}$ stoichiometry of the complex in solution and to obtain an estimate of the equilibrium constant of the reaction.¹³ The calculations used by Yoshizawa for these analyses are outlined below.

Under acidic conditions the receptor is first presumed to form a complex with HCl as shown in Equation 1 (the overbar refers to the organic phase).



The extraction of $[\text{PtCl}_6]^{2-}$ with a receptor, L, from aqueous HCl solutions can be expressed by Equation 2.



The equilibrium constant, K_{PtCl_6} , can then be expressed as:

$$K_{\text{PtCl}_6} = \frac{\overline{[(\text{LH})_2\text{PtCl}_6]}[\text{Cl}^-]^2}{\overline{[(\text{PtCl}_6)^2]} \overline{[(\text{LH})\text{Cl}]^2}} \quad (3)$$

The distribution coefficient, D_{Pt} for the extraction process is defined in Equation 4 where $\overline{[\text{Pt}]}$ is the concentration of $[\text{PtCl}_6]^{2-}$ extracted into the organic phase and $[\text{Pt}]$ is that in the aqueous phase after equilibration.

$$D_{\text{Pt}} = \frac{\overline{[\text{Pt}]}}{[\text{Pt}]} \quad (4)$$

Substituting Equation 4 into Equation 3 and simplifying gives Equation 5 in which $[(\text{LH})\text{Cl}]$ can be estimated from the difference between the initial concentration of L and the equilibrium concentration of $[(\text{LH})_2\text{PtCl}_6]$.

$$D_{\text{Pt}} = K_{\text{PtCl}_6} \cdot \frac{\overline{[(\text{LH})\text{Cl}]^2}}{\overline{[\text{Cl}^-]^2}} \quad (5)$$

Hence;

$$\log D_{\text{Pt}} = \log K_{\text{PtCl}_6} + 2\log A \quad (6)$$

$$\text{where } A = \left(\frac{\overline{[(\text{LH})\text{Cl}]}}{\overline{[\text{Cl}^-]}} \right)$$

For a particular set of extraction data a plot of $\log A$ against $\log D_{\text{Pt}}$ should give a straight line graph with a gradient of two inferring a 2:1 L: $[\text{PtCl}_6]^{2-}$ ratio. Furthermore, a value of $\log K_{\text{PtCl}_6}$ can be determined from the y-intercept and this can be used as a measure of the strength of interaction between ligand and anion. The $\log K_{\text{PtCl}_6}$ values for a series of receptors can be compared and a relative scale of extraction efficiencies constructed.

4.5. Test Extractions

A test extraction method was developed as a quick and simple way to assess the extraction potential of the receptors. Two equivalents of the receptor were dissolved in CHCl_3 in a vial onto which an aqueous, acidic solution containing one equivalent of H_2PtCl_6 was layered. The two-phase system is shaken for a few seconds to enable the mixing of the two phases. As $[\text{PtCl}_6]^{2-}$ is orange, a colour change of the organic phase indicates extraction of the target anion (Figure 4.6). Receptors which gave rise to a colour change were subsequently studied in more detail.

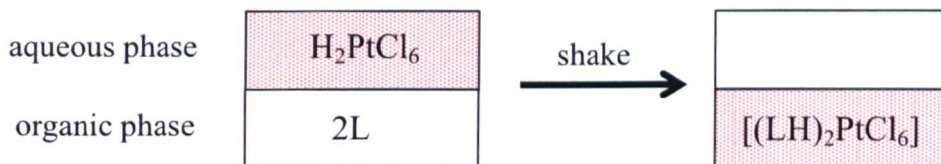
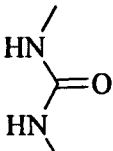
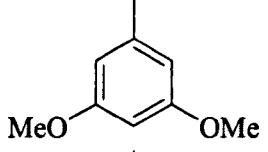
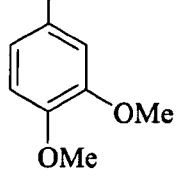
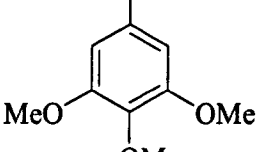
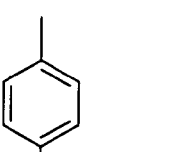


Figure 4.6. Representation of the test extraction process.

4.5.1. Test Extraction Results

Test extractions were carried out with those receptors which had good CHCl_3 solubility including urea (L^{13} , L^{14} , L^{15} and L^{16}), amide (L^{17} , L^{18} and L^{19}) and thiourea receptors (L^{20} and L^{21}). For all of the urea and amide receptors the organic phase became orange and consequently these receptors were fully investigated in solvent extraction studies. All three thiourea receptors formed insoluble precipitates of the type $[(\text{LH})_2\text{PtCl}_6]$ meaning that no solvent extraction studies were possible with these extractants (Table 4.2).

Table 4.2. Summary of the test extraction experiments.

	Urea	Amide	Thiourea
			
	✓	✓	x
	✓	✓	N/A
	✓	✓	x
	✓	N/A	N/A
			

*✓ = colour change in organic phase, x = complex is CHCl_3 insoluble, N/A = receptor was not synthesised

4.6. Extraction Results

4.6.1. TOA

Solvent extractions with TOA were performed in a range of HCl concentrations (no added HCl, 0.1 M HCl or 0.6 M HCl). The results show that extraction of $[\text{PtCl}_6]^{2-}$ with TOA is higher in 0.0 M or 0.1 M HCl than in 0.6 M HCl (Figure 4.7). An arbitrary [TOA]: $[\text{PtCl}_6]^{2-}$ ratio of 3:1 was chosen as a point at which the sets of extraction data could be compared. In 0.6 M HCl only 4% of $[\text{PtCl}_6]^{2-}$ is extracted

while the extraction efficiency in 0.0 M and 0.1 M HCl is significantly higher at 62% and 57%, respectively (Table 4.3).

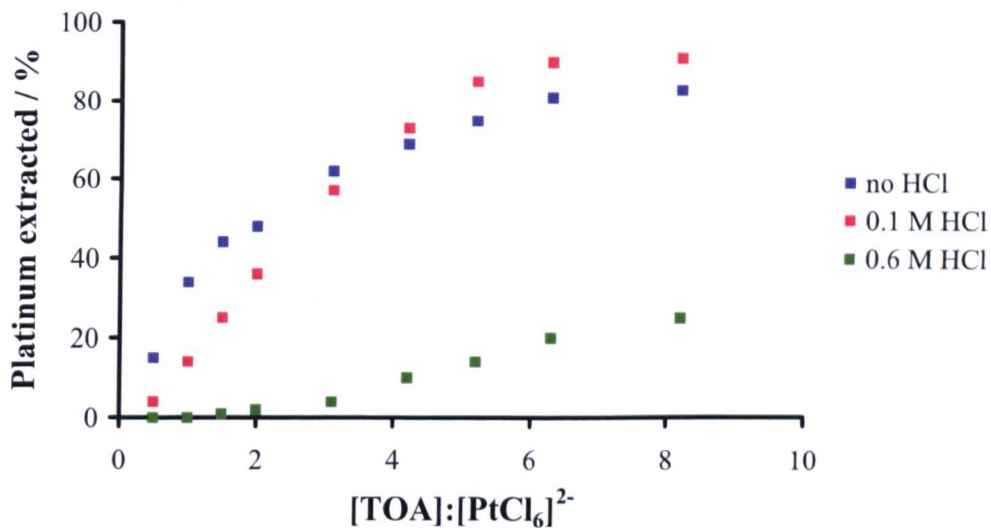


Figure 4.7. Plot of % Pt extracted as $[\text{PtCl}_6]^{2-}$ from aqueous HCl into CHCl_3 as a function of $[\text{TOA}]:[\text{PtCl}_6]^{2-}$ ratio.

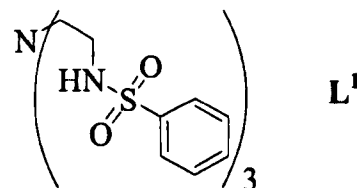
Table 4.3. % of Pt extracted as $[\text{PtCl}_6]^{2-}$ into CHCl_3 from aqueous 0.6 M HCl in the presence of a 3 molar excess of TOA

HCl concentration / M	0.0	0.1	0.6
% Pt extracted at 3 molar excess of TOA	62	57	4

As the HCl concentration increases the extraction efficiency for $[\text{PtCl}_6]^{2-}$ with TOA is observed to fall. This has been attributed to competition from Cl^- and means that TOA has optimal performance at low HCl concentrations. A similar observation was made in work carried out by Alguacil who carried out extractions of $[\text{PtCl}_6]^{2-}$ with Alamine 304.⁷ The extraction results for our receptors are presented in the subsequent Sections 4.6.2–4.6.4 and comparisons between the different types of receptor are made in Section 4.7.

4.6.2. Sulfonamide Receptor

In a test extraction with the sulfonamide receptor L^1 , no colour change was observed in the organic phase and a small amount of insoluble precipitate formed. Despite this L^1 was studied and the results show 0% extraction consistent with the lack of colour change of the organic phase in the test extraction.



The crystal structure of $[(L^1H)_2PtCl_6]$ shows that the tertiary amine position is protonated and that there is hydrogen-bonding between $[L^1H^+]$ and $[PtCl_6]^{2-}$. As this structure confirms the success of our design features some extraction of $[PtCl_6]^{2-}$ was expected. The low level of extraction displayed by L^1 can be attributed to the poor organic solubility of the resulting complex.

4.6.3. Urea Receptors

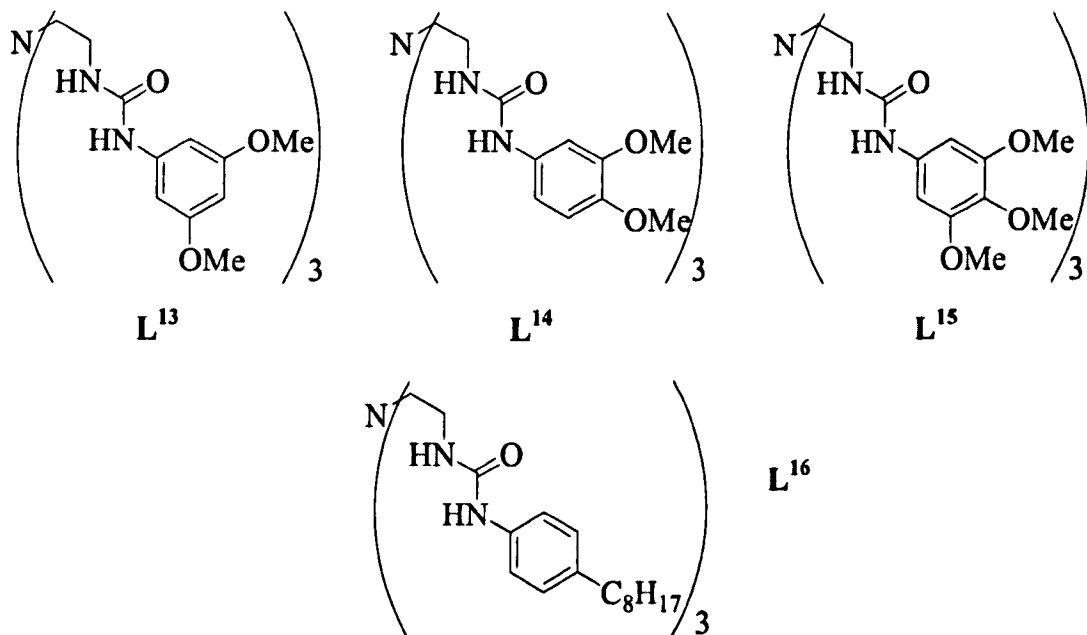
Solvent extractions were performed with the urea receptors $L^{13}-L^{16}$ for which a colour change of the organic phase was observed in a test extraction. For L^{16} , during the period of mixing a colourless emulsion formed which was attributed to the hydrophobic octyl tails of L^{16} . As the organic and aqueous phases became mixed and were inseparable this prevented ICP analysis.

For $L^{13}-L^{15}$ the aqueous and organic phases remained transparent and were separable following the period of mixing. The extractions with $L^{13}-L^{15}$ were performed twice to verify the results and for each extraction series the mass balance was found to be quantitative. The results are shown below in Figure 4.8. The results show that the maximum extraction occurs at $[Receptor]:[PtCl_6]^{2-}$ ratios greater than

or equal to three meaning a slight excess of receptor is needed which may suggest that there is a competition from Cl^- anions.

L^{15} has lower extraction efficiency than L^{13} or L^{14} and at a [Receptor]: $[\text{PtCl}_6]^{2-}$ ratio of three achieves 37% extraction while L^{13} and L^{14} extract greater than 96% (Table 4.4). The additional methoxy substituent on the phenyl groups in L^{15} may increase the aqueous solubility of the complex (compared to L^{13} and L^{14}) resulting in it having a lower extraction efficiency. As discussed previously urea receptors with terminal phenyl or *tert*-butyl substituents form insoluble complexes and L^{16} with octyl groups forms an emulsion. These results show that the nature of the substituents at the terminal position of the pendant arms of the tripodal receptor has an effect on the extraction efficiency and highlights the importance of finding a receptor system in which the organic solubility of the complex is optimised.

The extraction results for L^{13} and L^{14} suggest that the complexes have similar organic solubility and indicate that the position of methoxy substituents (3, 4-dimethoxy and 3, 5-dimethoxy, respectively) on the phenyl ring does not effect the overall extraction ability. The methoxy groups are not thought to sterically hinder the approach of the receptor to $[\text{PtCl}_6]^{2-}$ as they are located in a region of the receptor which is not involved in direct interaction with the anion.



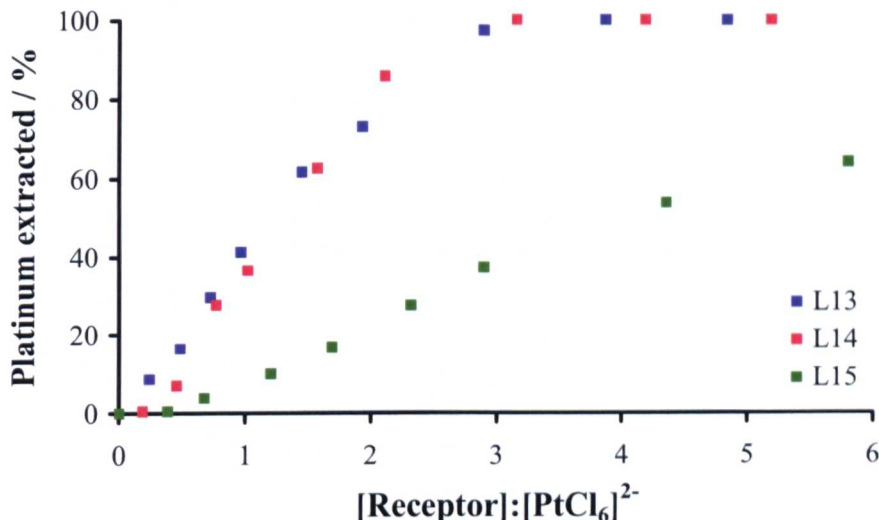


Figure 4.8. Plot of % Pt extracted as $[\text{PtCl}_6]^{2-}$ from aqueous 0.6 M HCl into CHCl_3 as a function of $[\text{Receptor}]:[\text{PtCl}_6]^{2-}$ ratio.

Table 4.4. % of Pt extracted as $[\text{PtCl}_6]^{2-}$ into CHCl_3 from aqueous 0.6 M HCl in the presence of a 3 molar excess of L

Receptor	L^{13}	L^{14}	L^{15}
% Pt extracted at 3 molar excess of L	96	97	37

Following the method of Yoshizawa, attempts were made to confirm the stoichiometry of the extracted species in solution and to obtain values for the equilibrium constant K_{PtCl_6} .¹³ For $\text{L}^{13}-\text{L}^{15}$ the data form a reasonably straight line although for both L^{13} and L^{14} there is significant deviation of the gradient from the theoretical value of two (Figure 4.9). Yoshizawa suggests that deviation of the gradient from the theoretical value of two is due to the formation of other extracted species. For our systems it is possible that $[(\text{LH})\text{Cl}]$ or $\{(\text{LH})^+[\text{PtCl}_6]^{2-}(\text{H}_3\text{O})^+\}$ complexes are also present which may effect the results of the Yoshizawa analysis. Also, in the derivation of equations, it is assumed that firstly a $[(\text{LH})\text{Cl}]$ species is formed which then participates in an anion exchange reaction with $[\text{PtCl}_6]^{2-}$ to form $[(\text{LH})_2\text{PtCl}_6]$. Each component of the extraction is in equilibrium between aqueous

and organic phases and the model postulated assumes that each component is either soluble in the aqueous or organic phase, but in reality it may be partially soluble in both. The data for L¹⁵ gives a straight line with a gradient of 2.0882 which is very close to the theoretical value. All of the receptors which produce a straight line graph with a gradient that approximates to two are compared in Chapter 7 of this thesis.

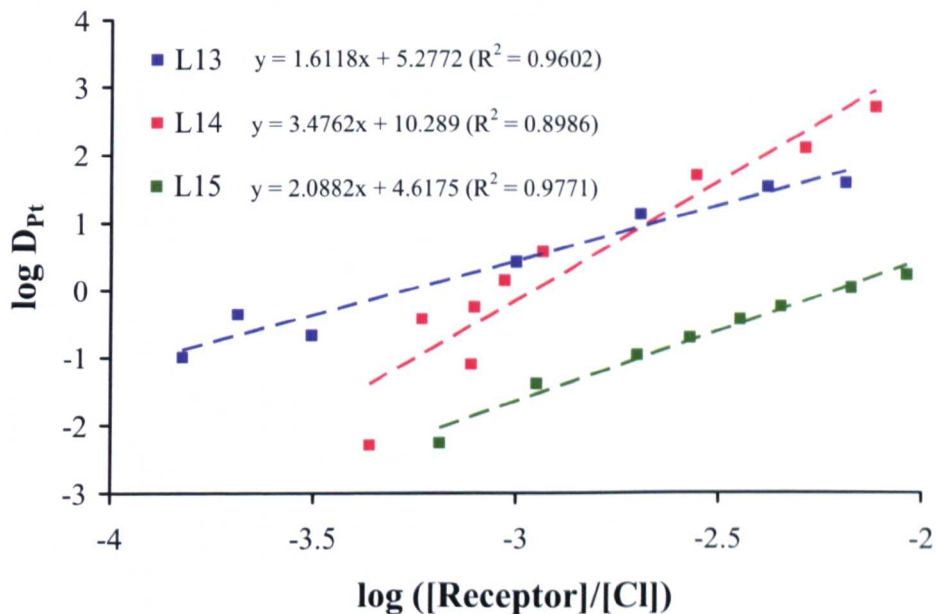


Figure 4.9. Plot of $\log ([\text{Receptor}]/[\text{Cl}])$ against $\log D$ for L¹³–L¹⁵.

4.6.4. Amide Receptors

Solvent extractions with the amide receptors L¹⁷, L¹⁸ and L¹⁹ give similar results (Figure 4.10) and at a [Receptor]:[PtCl₆]²⁻ ratio of 3:1 they extract 84%, 76% and 79%, respectively (Table 4.5). In contrast to the results obtained for the urea receptors, the number of methoxy substituents on the terminal phenyl groups does not significantly affect the extraction efficiency suggesting that all three complexes have similar organic solubility.

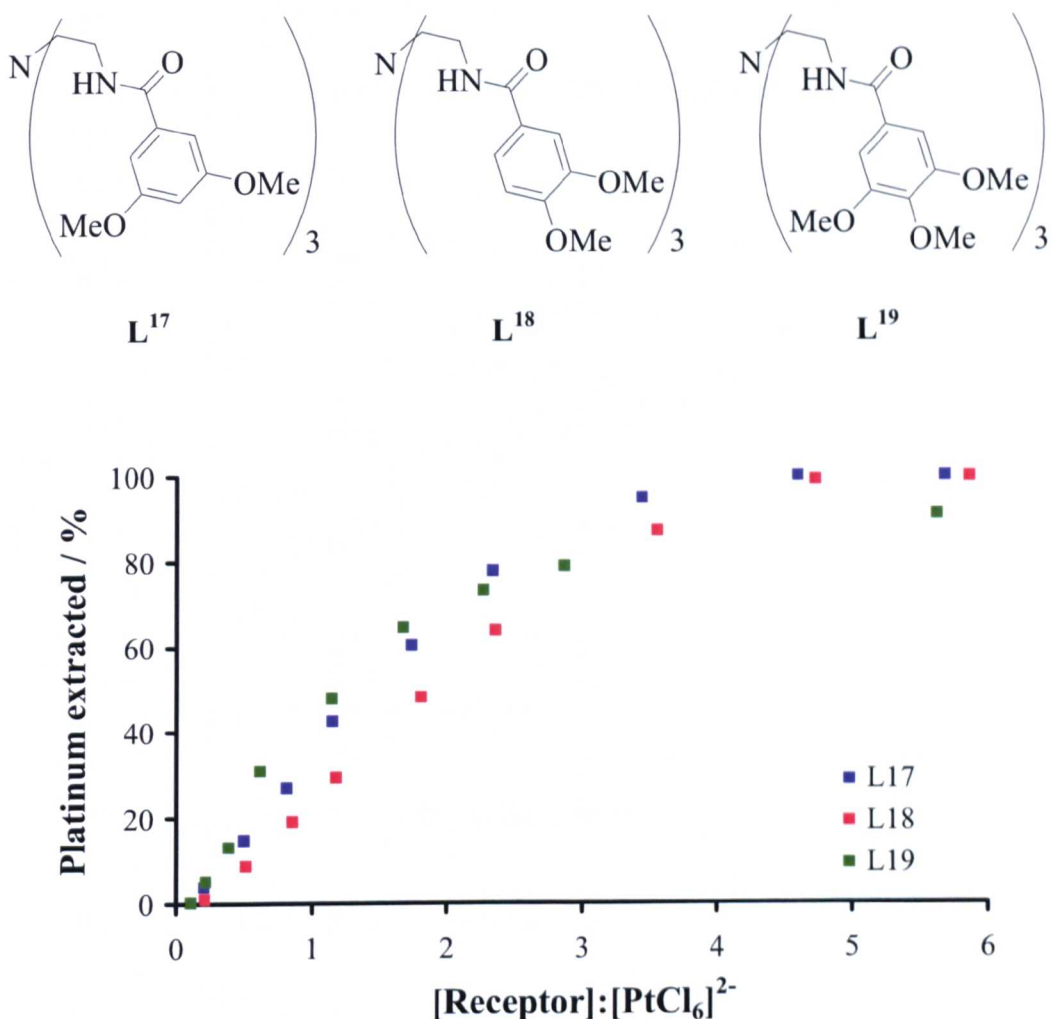


Figure 4.10. Plot of % Pt extracted as [PtCl₆]²⁻ from aqueous 0.6 M HCl into CHCl₃ as a function of [Receptor]:[PtCl₆]²⁻ ratio.

Table 4.5. % of Pt extracted as [PtCl₆]²⁻ into CHCl₃ from aqueous 0.6 M HCl in the presence of a 3 molar excess of L

Receptor	L ¹⁷	L ¹⁸	L ¹⁹
% Pt extracted at 3 molar excess of L	84	76	79

A Yoshizawa analysis was carried out on the extraction results for L¹⁷–L¹⁹ (Figure 4.11).¹³ For each receptor a straight line graph with a gradient that approximates to two and a high R² value was plotted indicating an overall 2:1 L:[PtCl₆]²⁻ stoichiometry of the extracted complex in solution. These results are consistent with previously discussed spectroscopic and crystallographic analysis of

the complexes with these ionophores. For L^{17} – L^{19} , the values of the intercepts are similar which correlates with the extraction results for these systems.

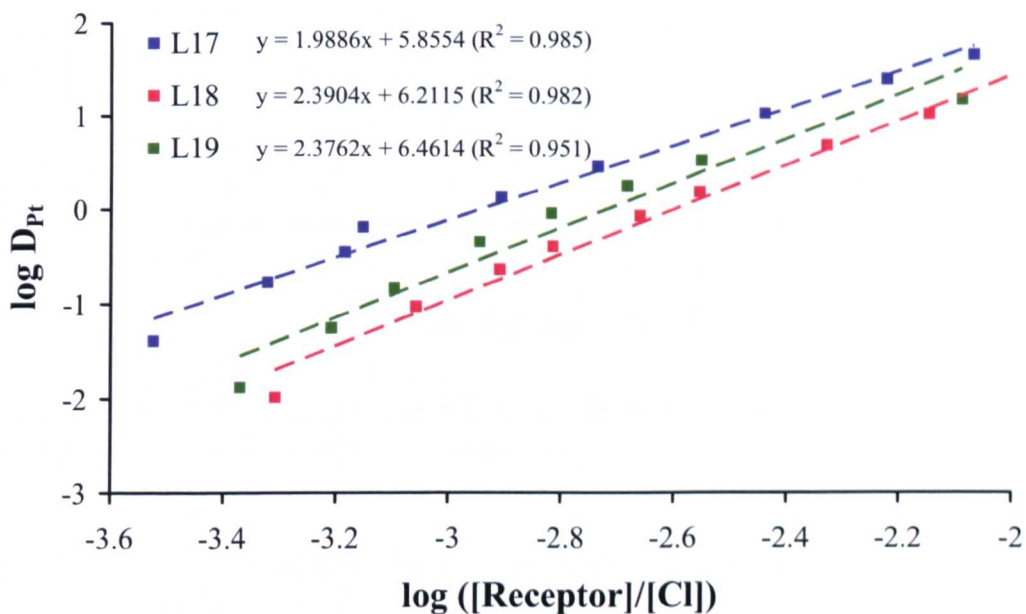
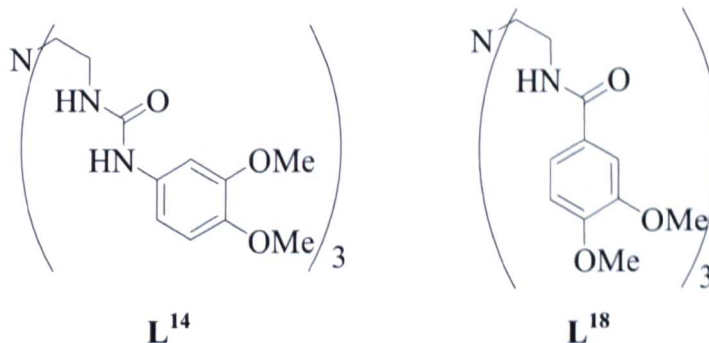


Figure 4.11. Plot of $\log ([\text{Receptor}]/[\text{Cl}])$ against $\log D$ for L^{17} – L^{19} .

4.7. Comparisons

4.7.1. Hydrogen-bond Donor Type

The data show that the urea receptor L^{14} extracts more $[\text{PtCl}_6]^{2-}$ than its analogous amide receptor L^{18} across all $[\text{Receptor}]:[\text{PtCl}_6]^{2-}$ ratios (Figure 4.12). When there is a three molar excess of L^{14} 93% of $[\text{PtCl}_6]^{2-}$ is extracted whereas for L^{18} the value is 76% (Table 4.6). The same trend is observed on comparing urea and amide receptors with 3, 5-dimethoxyphenyl terminal substituents.



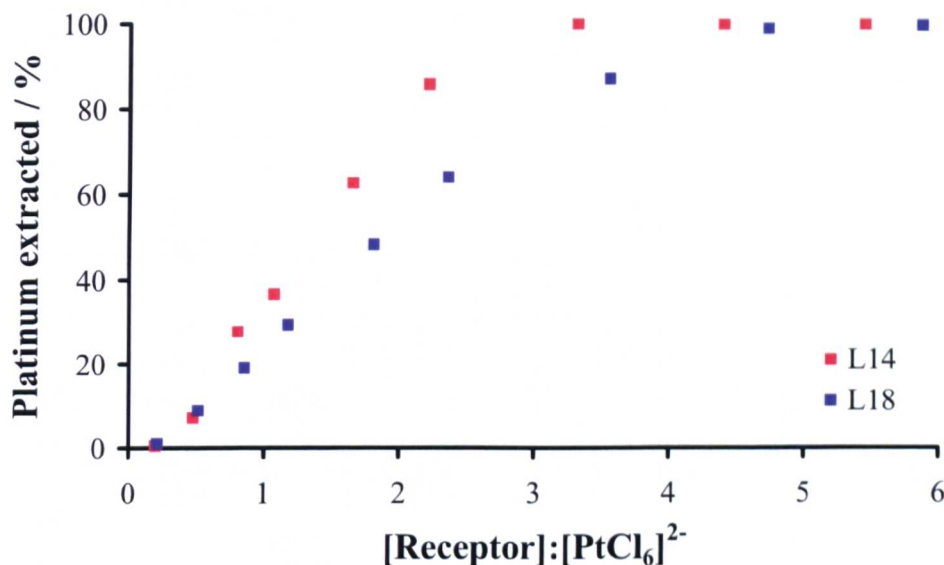


Figure 4.12. Plot of % Pt extracted as $[\text{PtCl}_6]^{2-}$ from aqueous 0.6 M HCl into CHCl_3 as a function of $[\text{Receptor}]:[\text{PtCl}_6]^{2-}$ ratio.

Table 4.6. % of Pt extracted as $[\text{PtCl}_6]^{2-}$ into CHCl_3 from aqueous 0.6 M HCl in the presence of a 3 molar excess of L

Receptor	L^{14}	L^{18}
% Pt extracted at 3 molar excess of L	93	76

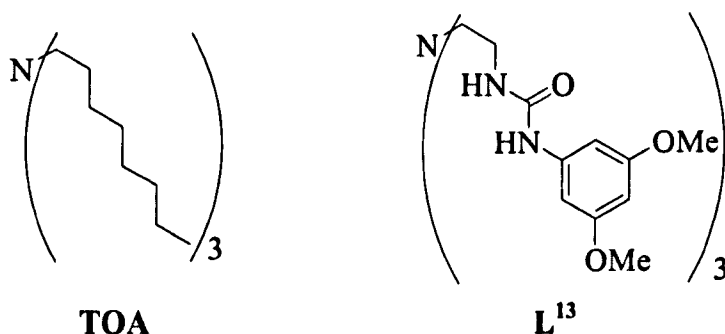
The reason for the urea-containing receptors outperforming the analogous amide systems can be attributed to there being more NH hydrogen-bond donor groups. In each molecule of TREN-based urea receptor there are six acidic NH donor units compared with three in an analogous amide receptor. As there are more NH donor groups in a urea receptor there is a higher probability they will be in a suitable location to interact with an area of high electron density on the outer sphere of $[\text{PtCl}_6]^{2-}$, leading to an enhanced interaction and improved extraction.

This is also consistent with the observations made from the complex crystal structures containing the TREN-based urea receptor $[(\text{L}^3\text{H})_2\text{PtCl}_6]$ and amide receptor $[(\text{L}^{17}\text{H})_2\text{PtCl}_6]$. There are four hydrogen-bonds from each urea receptor to $[\text{PtCl}_6]^{2-}$ anion, while in the amide complex there are only two. An increased number

of hydrogen-bonds would be expected to give stronger overall interactions and thus improved extraction.

4.7.2. Comparisons with TOA

In the presence of 0.6 M HCl all of the TREN-based urea and amide receptors that were studied show increased extraction compared to TOA confirming that the presence of hydrogen-bond donor groups leads to a more effective extraction of $[\text{PtCl}_6]^{2-}$. The results for the urea receptor L^{13} are compared with TOA in Figure 4.16 and, across all [Receptor]: $[\text{PtCl}_6]^{2-}$ ratios, L^{13} shows significantly higher extraction of $[\text{PtCl}_6]^{2-}$ (Figure 4.13). At a 3:1 [Receptor]: $[\text{PtCl}_6]^{2-}$ ratio L^{13} extracts 97% whilst TOA extracts only 4% (Table 4.7). Thus, one of the project aims has been achieved and the extraction efficiency of $[\text{PtCl}_6]^{2-}$ from acidic chloride media has been increased compared with long chain alkylamines that are thought to be currently used in the processing and refining of Pt-containing ores.^{7, 28-31} As this approach of introducing hydrogen-bonds onto the tripodal scaffold has proved successful, further work was carried out in which hydrogen-bond moieties were introduced onto other tripodal and non-tripodal scaffolds and this is discussed in Chapters 5 and 6.



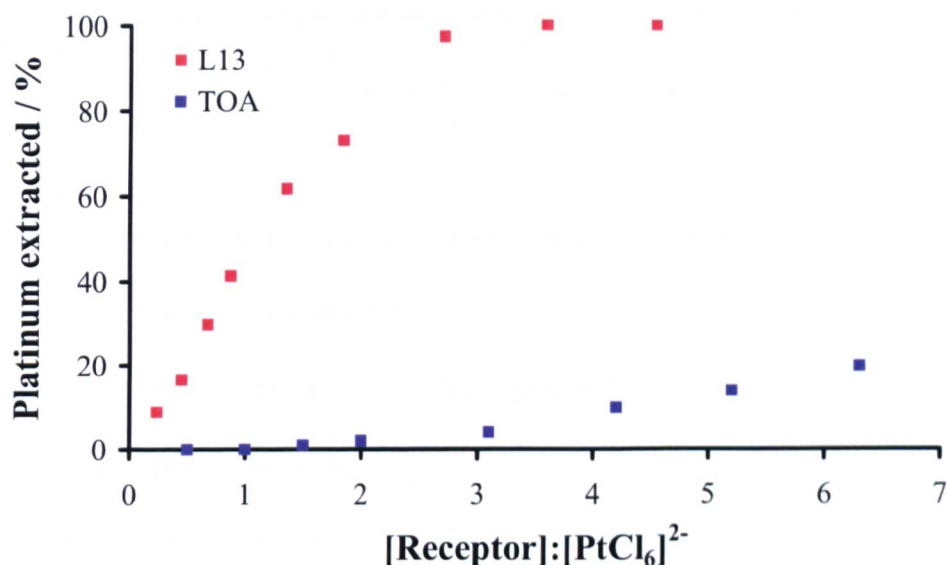


Figure 4.13. Plot of % Pt extracted as $[\text{PtCl}_6]^{2-}$ from aqueous 0.6 M HCl into CHCl_3 as a function of $[\text{Receptor}]:[\text{PtCl}_6]^{2-}$ ratio.

Table 4.7. % of Pt extracted as $[\text{PtCl}_6]^{2-}$ into CHCl_3 from aqueous 0.6 M HCl in the presence of a 3 molar excess of L

Receptor	L^{13}	TOA
% Pt extracted at 3 molar excess of L	97	4

4.8. Other Experiments

4.8.1. Receptor Selectivity

If the ores in which Pt is found contain other metals then additional chlorometallate anionic species (such as $[\text{PdCl}_4]^{2-}$ and $[\text{IrCl}_6]^{3-}$) may be produced when the ore is dissolved in *aqua regia*.^{22, 20, 25} One of the long term goals in this area of research is to be able to separate platinum and palladium chloro-anions. The preferred oxidation state for palladium is +2 and typically forms square planar $[\text{PdCl}_4]^{2-}$ species in acidic chloride media. Ideally, the different geometry between $[\text{PtCl}_6]^{2-}$ and $[\text{PdCl}_4]^{2-}$ may provide a route to the separation of the anions.

The selectivity of L^{13} for $[\text{PtCl}_6]^{2-}$ over $[\text{PdCl}_4]^{2-}$ was assessed in a solvent extraction experiment in which the aqueous phase contained both metalloanions. $[\text{PdCl}_4]^{2-}$ was introduced into the aqueous phase as K_2PdCl_4 with the relative

amounts of platinum and palladium being representative of the ratio found in a typical PGM feedstock.³² The results of the experiment are shown in Figure 4.14 and compare:

- The amount of Pt extracted when there is only H_2PtCl_6 and HCl in the aqueous phase (blue points).
- The amount of Pt extracted when there is H_2PtCl_6 , K_2PdCl_4 and HCl in the aqueous phase (red points).
- The amount of Pd extracted when there is H_2PtCl_6 , K_2PdCl_4 and HCl in the aqueous phase (green points).

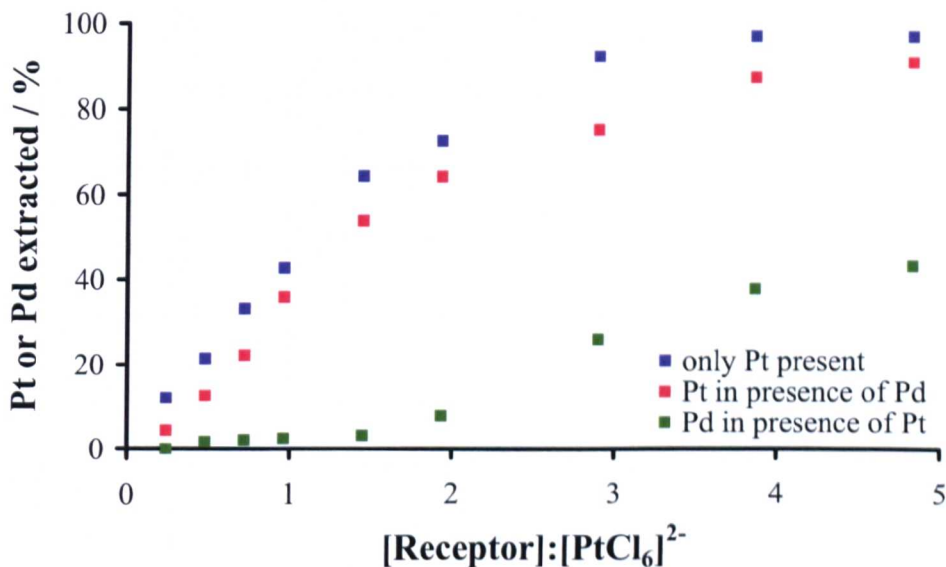


Figure 4.14. Plot of % platinum or palladium extracted (as $[\text{PtCl}_6]^{2-}$ or $[\text{PdCl}_4]^{2-}$, respectively) from aqueous 0.6 M HCl into CHCl_3 as a function of $[\text{Receptor}]:[\text{PtCl}_6]^{2-}$ ratio. The % plotted in the graph were calculated relative to the amount of H_2PtCl_6 or K_2PdCl_4 present in the initial aqueous phase of the extraction.

When $[\text{PdCl}_4]^{2-}$ is present alongside $[\text{PtCl}_6]^{2-}$ there is a decrease in the amount of Pt extracted. This suggests that some of the L¹³ molecules form complexes with $[\text{PdCl}_4]^{2-}$. At a $[\text{Receptor}]:[\text{PtCl}_6]^{2-}$ ratio of 2:1, 8% of $[\text{PdCl}_4]^{2-}$ is extracted in contrast to 64% of $[\text{PtCl}_6]^{2-}$. At $[\text{Receptor}]:[\text{PtCl}_6]^{2-}$ ratios of less than 2:1 the amount of Pd extracted is lower compared to the amount of Pt extracted, indicating

that $[\text{PtCl}_6]^{2-}$ is preferentially extracted. As the [Receptor]: $[\text{PtCl}_6]^{2-}$ ratio increases the amount of palladium extracted increases as there are more non-coordinated receptors resulting in complexes with $[\text{PdCl}_4]^{2-}$ being formed. This indicates selective extraction of $[\text{PtCl}_6]^{2-}$ before $[\text{PdCl}_4]^{2-}$ suggesting that the differences in electron density on the outer-sphere of the chlorometallate anions can be recognised by L¹³. The difference in Pt and Pd extraction at low [Receptor]: $[\text{PtCl}_6]^{2-}$ ratios may provide a route to separate these chlorometallate anions.

4.8.2. Extractions in Toluene

Throughout this work CHCl_3 was used as the immiscible, organic phase into which the complexes $[(\text{LH})_2\text{PtCl}_6]$ were extracted. As the extractions are on a small scale the toxicity and volatility of the CHCl_3 solvent has not been treated as a significant problem. In a larger, industrial scale solvent extraction process it is unlikely that CHCl_3 would be used and a cheaper, less toxic solvent may be preferred.³³

Toluene was chosen as a suitable hydrocarbon alternative in which the extractive behaviour of the receptors could be studied. The urea receptors L¹³–L¹⁶ and the amide receptors L¹⁷–L¹⁹ are all insoluble in toluene and are therefore unsuitable extractants for a toluene/ H_2O extraction. As such, the design of the sulfonamide receptor L¹ was modified to incorporate octylether substituents onto the 4 position of the terminal phenyl groups with the aim of improving the toluene solubility.

To synthesise the sulfonamide receptor L²² it was first necessary to synthesise the sulfonyl chloride precursor and this was achieved by following the method of Kajimoto and co-workers.³⁴ Octylphenyl ether **1** was reacted with sulfuric acid to form the sulfenic acid **2** which was converted to the sodium sulfonate salt **3** by reaction with NaCl. Subsequent treatment with thionyl chloride gave the sulfonyl

chloride **4** which was then reacted with TREN under basic conditions to give **L²²** in 80% yield (Figure 4.15).

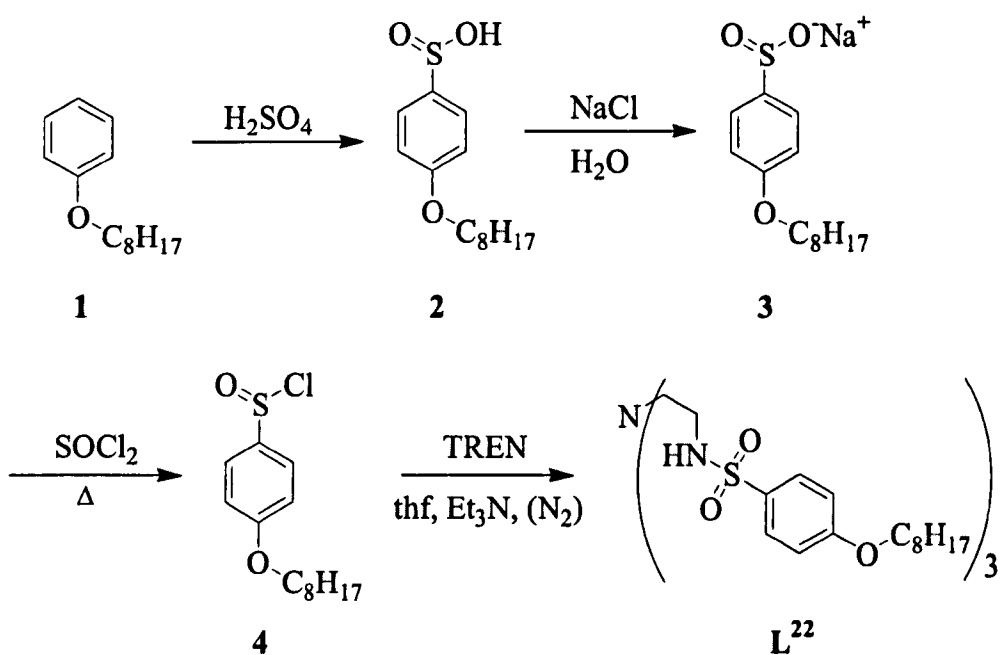


Figure 4.15. Synthesis of **L²²**

L²² was soluble in toluene and in a test extraction showed there was a colour change of the organic phase and consequently full extractions were performed. The extraction experiments were performed in duplicate to confirm the results and the mass balance was found to be quantitative confirming that back extraction with NaOH can be used in a toluene/H₂O extraction system. The maximum amount of platinum extracted is 70% which occurs at a [Receptor]:[PtCl₆]²⁻ ratio of approximately 2:1 (Figure 4.16). From the design of the receptor it was expected that the maximum extraction would occur at this ratio as it results in charge-neutral species being formed.

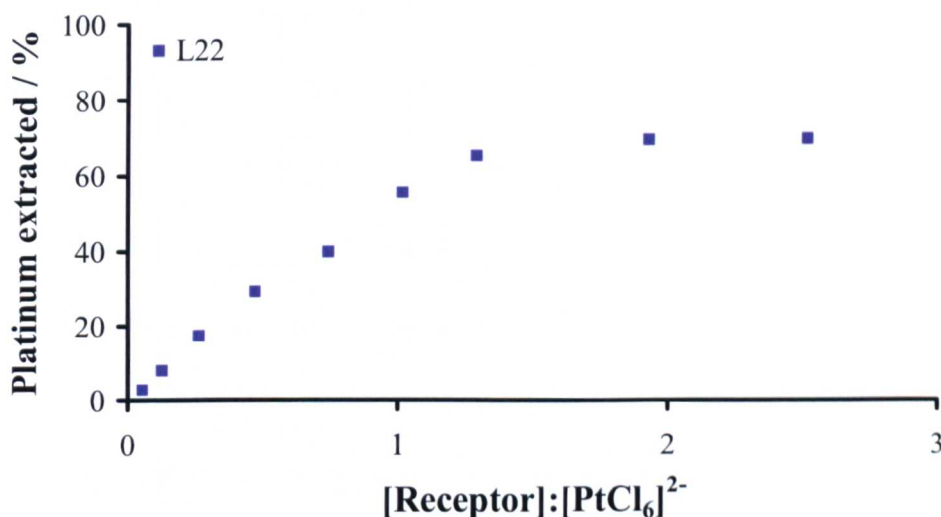


Figure 4.16. Plot of % Pt extracted as $[\text{PtCl}_6]^{2-}$ from aqueous 0.6 M HCl into toluene as a function of [Receptor]: $[\text{PtCl}_6]^{2-}$ ratio.

This result further confirms that varying the terminal R groups of a receptor can significantly affect the solubility of the extractant and its complex. It also shows that by incorporating organic solubilising moieties into the design a TREN-based sulfonamide receptor can be an effective extractant. These results also prove that the solvent extraction method is transferable between different two phase solvent systems giving this method a possible future use in similar processes.

4.8.3. Recycling Receptors

To be commercially viable, the efficiency of a receptor needs to be maintained during several repeat cycles of the extraction. The acidic and basic conditions used in a solvent extraction may degrade receptors preventing them from being recycled. To study the effect of these conditions, a solution of L¹³ in CDCl₃ was prepared and its ¹H NMR spectra recorded before, during and after extraction.

Following extraction the ¹H NMR spectra showed a signal assigned to the protonated tertiary amine nitrogen position (NH^+R_3) and there was a downfield shift in the urea NH signals indicating the formation of hydrogen-bonding interactions.³⁵,

³⁶ The ^1H NMR spectrum of the CDCl_3 phase after back extraction showed the structure of L^{13} was preserved. The back extracted CDCl_3 phase was then subsequently mixed with an acidic, aqueous solution of $[\text{PtCl}_6]^{2-}$ to represent a second ‘extraction cycle’. The organic phase became coloured indicating the extraction of $[\text{PtCl}_6]^{2-}$ and indicating that L^{13} retains its extraction efficiency for at least two extraction cycles. This gives our newly developed receptor systems the potential to be used in an industrial solvent extraction process although it would first be necessary to fully establish, amongst other factors, the lifetime of the receptors and whether the process could be scaled-up.

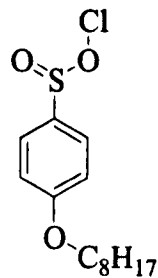
4.9. Summary of Results

Each stage in the extraction process was evaluated and developed to give an optimised methodology. The extractive ability of TOA and our TREN-based sulfonamide, urea and amide receptors were assessed. The thiourea receptors L^{20} and L^{21} formed insoluble complexes in the test extractions and therefore could not be studied.

The most significant result of this Chapter is the efficacy of the TREN-based urea and amide ligands in a pH-swing controlled process to recover platinum from acidic, chloride-containing feed solutions when compared with TOA. Receptors containing urea moieties extracted more $[\text{PtCl}_6]^{2-}$ than analogous amide receptors, which has been attributed to an increased number of NH hydrogen-bond donors. The extraction results have also highlighted the importance of optimising the organic solubility of the complexes and how seemingly slight modifications to the design can have a significant effect on the organic solubility of the resulting complex and thus the extraction efficiency.

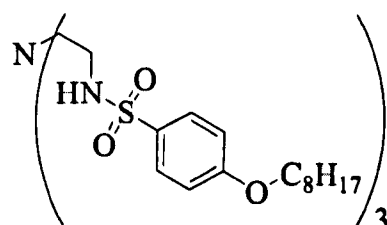
4.10. Synthesis

4.10.1. Synthesis of octylphenyl ether sulfonyl chloride³⁴



Sulfuric acid (5.0 cm³) was added to octylphenyl ether (5.0 g, 24.2 mmol) and the mixture stirred for 30 mins. The mixture was poured into a saturated aqueous solution of NaCl and the resulting precipitate collected by filtration. The solid was dried and then refluxed with thionyl chloride (11.25 cm³, 0.15 mmol) for 2 d and following cooling to r.t. the resulting colourless precipitate was collected by filtration. Yield: 0.45 g, 63%. ¹H NMR (CDCl₃, 300 MHz): 7.98 (d, 2H, ³J_{HH} = 7 Hz, H_{Ar}), 7.04 (d, 2H, ³J_{HH} = 7 Hz, H_{Ar}), 4.07 (t, 2H, ³J_{HH} = 6 Hz, OCH₂), 1.93-1.89 (m, 2H, CH₂), 1.48-1.31 (m, 10H, CH₂), 0.90 (t, 3H, ³J_{HH} = 4 Hz, CH₃).

4.10.2. Synthesis of N, N', N''-(nitrilotri-2, 1-ethanediyl)tris-octylphenyl ether sulfonamide, L²²



TREN (0.15 g, 0.99 mmol) was dissolved in dry thf (15 cm³) and flushed with N₂. A solution of the previously prepared sulfonyl chloride (1.0 g, 3.28 mmol) was also dissolved in dry thf (15 cm³) with Et₃N (0.33 g, 3.28 mmol). The two solutions were added together and stirred at room temperature overnight. The resulting precipitate was filtered and the solvent removed from the filtrate to give the crude product which was purified by column chromatography with 97% hexane/ 3% EtOAc and

then 70% hexane/ 30% EtOAc to give analytically pure L²². Yield: 0.34 g, 80%. ¹H NMR (CDCl₃, 270 MHz): 7.85 (d, 6H, ³J_{HH} = 7 Hz, H_{Ar}), 6.97 (d, 6H, ³J_{HH} = 7 Hz, H_{Ar}), 5.80 (br t, 3H, NH), 3.99 (br, 6H, OCH₂), 2.90 (br, 3H, CH₂N), 2.49 (s, 6H, CH₂N), 1.31-1.26 (m, 30H, CH₂), 0.89 (t, 9H, ³J_{HH} = 7 Hz, CH₃). ¹³C NMR (CDCl₃, 69 MHz): 163, 131, 130, 115, 69, 32, 30, 29, 28, 26, 23, 21, 20, 15. MS (ES⁺): m/z 951 [M+H]⁺. IR (solid, cm⁻¹): 3280 (ν_(N-H)), 1595(ν_(C=C, Ar)), 1150 (ν_(C-O)). Anal. calc. for C₄₈H₇₈N₄O₉S₃: C, 60.69; H, 8.28; N, 5.89. Found: C, 60.96; H, 8.30; N, 5.85%.

4.11. References

1. Rosenqvist T., *Principles of Extractive Metallurgy*, McGraw-Hill, New York, 2004, 2nd edition.
2. Charlesworth P., *Platinum Metals Rev.*, 1981, **25**, 106-112.
3. Kauffman G. B., *Inorganic Syntheses*, McGraw-Hill: New York, 1967, pp 182-4.
4. Habashi F., *A Textbook of Hydrometallurgy*, Sainte-Foye, Canada, 1999, pp 637.
5. Tasker P. A.; Plieger P. G.; West L. C., *Comp. Coord. Chem. II*, 2004, **9**, 759-808.
6. Wisniewski M.; Szymanowski J., *Polish J. App. Chem.*, 1996, **40**, 17-26.
7. Alguacil F. J.; Cobo A.; Coedo A. G.; Dorado M. T.; Sastre A., *Hydrometallurgy*, 1997, **44**, 203-212.
8. Yamamoto K.; Katoh S., *Talanta*, 1996, **43**, 61-66.
9. Sanuki S.; Matsumoto Y.; Majima H., *Metall. Mater. Trans. B*, 1999, **30B**, 197-203.
10. Rovira M.; Cortina J. L.; Arnaldos J.; Sastre A. M., *Solv. Extr. Ion Exch.* 1998, **16**, 1279-1302.
11. Charlesworth P., *Platinum Metals Rev.*, 1981, **25**, 106-112.
12. Kolekar S. S.; Anuse M. A., *Sep. Sci. Technol.*, 2003, **38**, 2597-2618.
13. Yoshizawa H.; Shiomori K.; Yamada S.; Baba Y.; Kawano Y.; Kondo K.; Ijichi K.; Hatate Y., *Solv. Extr. Res. Devel.*, Japan, 1997, **4**, 157-166.
14. Lokhande T. N.; Anuse M. A.; Chavan M. B., *Talanta*, 1998, **47**, 823-832.
15. Mirza M.Y., *Talanta*, 1980, **27**, 101-106.

16. Fu J.; Nakamura S.; Akiba K., *Sep. Sci. Technol.*, 1997, **32**, 1433-1445.
17. Fu J.; Nakamura S.; Akiba K., *Anal. Sci.*, 1995, **11**, 149-153.
18. Hasegawa Y.; Kobayashi I.; Yoshimoto S., *Solv. Extr. Ion Exch.*, 1991, **9**, 759-768.
19. Kawano Y.; Matsui T.; Kondo K.; Nakashio F., *J. Chem. Eng., Japan*, 1989, **22**, 443.
20. Cleare M. J.; Charlesworth P.; Bryson D. J., *J. Chem. Tech. Biotechnol.*, 1979, **29**, 210-214.
21. Galbraith S. G.; Tasker P. A., *Supramol. Chem.*, 2005, **17**, 191-207.
22. Bernardis F. L.; Grant R. A.; Sherrington D. C.; *React. Funct. Polym.*, 2005, **65**, 205-217.
23. Kovacs A.; Varga Z., *Coord. Chem. Rev.*, 2006, **250**, 710-727.
24. Allerhand A.; von Rague Schleyer P., *J. Am. Chem. Soc.*, 1963, **85**, 1233-1237.
25. Cleare M. J.; Grant R. A.; Charlesworth P., *Extr. Metall.*, 1981, **34**, 34-41.
26. Yordanov A. T.; Roundhill D. M., *Inorg. Chim. Acta*, 1997, **264**, 309-311.
27. Preston J. S.; du Preez A. C., *Solv. Extr. Ion Exch.*, 2002, **20**, 359-374.
28. Yamamoto K.; Katoh S., *Talanta*, 1996, **43**, 61-66.
29. Sanuki S.; Matsumoto Y.; Majima H., *Metall. Mater. Trans. B*, 1999, **30B**, 197-203.
30. Rovira M.; Cortina J. L.; Arnaldos J.; Sastre A. M., *Solv. Extr. Ion Exch.* 1998, **16**, 1279-1302.
31. Charlesworth P., *Platinum Metals Rev.*, 1981, **25**, 106-112.
32. www.matthey.com (accessed October 2007)
33. Yordanov A. T.; Roundhill D. M., *Coord. Chem. Rev.*, 1998, **170**, 93-124.
34. Kajimoto T.; Ishioka Y.; Katoh T.; Node M., *Bioorg. Med. Chem. Lett.*, 2006, **16**, 5736-5739.
35. Liddell U.; Ramsay N. F., *J. Chem. Phys.*, 1951, **19**, 1608-1609.
36. Jeffrey G. A., *An Introduction to Hydrogen Bonding*, Oxford University Press, Oxford, 9th edition, pp 228.

5. Alternative Tripodal Systems

5.1. Introduction

With the aim of improving extraction, this Chapter describes the design and synthesis of TREN-based receptors which have hydrogen- and halogen-bond donors and also tripodal systems with longer pendant arms. As the tertiary amine protonation site, hydrogen-bond donor moieties and organic solubilising groups are proven design features they have been incorporated into these new classes of receptor.

5.2. Incorporating Halogen-bonding into the Receptor Design

Halogen-bonds have been recognised as offering many of the same opportunities as hydrogen-bonds for forming reliable interactions between molecules and ions.^{1, 2} The recognition of their potential strength and directionality has led to a number of potential applications which includes anion binding.³ The use of halogen-bonds has been studied to try and enhance the interaction between the TREN-based receptors and $[\text{PtCl}_6]^{2-}$.

Halogen-bonding is a non-covalent interaction that is, in some ways, analogous to hydrogen-bonding. In the latter, a hydrogen atom is shared between an atom, group or molecule that “donates” it and another that “accepts” it. In halogen-bonding, it is a halogen atom (X) that is shared between a donor (D) and acceptor (A). Thus the two types of interaction can be defined by; D—H \cdots A and D—X \cdots A, respectively.

In hydrogen- and halogen-bonding both the donor and especially the acceptor tend to be electronegative and the acceptor is often a Lewis base with an available pair of electrons. Since hydrogen atoms are usually considered to have a partial

positive charge when bonded to an electronegative acceptor atom it is understandable that they interact attractively with electronegative atoms. However, it is surprising that halogen atoms participate in such interactions as they are typically viewed as having a partial negative charge.⁴

An important advance in understanding the non-covalent interactions of halogen atoms came through the analysis of crystal structures from the Cambridge Structural Database in which short intermolecular distances (less than the sum of the van der Waals radii of the atoms involved) were interpreted as indicating strong interactions.⁵⁻⁸ For halogens linked to carbon atoms it was observed that close contacts with nucleophiles, such as oxygen and nitrogen atoms, were formed with angles primarily between 160° and 180°. These near linear interactions between carbon bound halogens and centres of electron density is what has come to be known as halogen-bonding.⁴

The combination of C—X moieties with M—X groups has been shown to lead to a number of directional interactions in the solid state.⁹ Brammer and co-workers report a class of highly directional halogen-bonds of the type M—X···X'—C and there are several examples in the literature confirming the formation of such halogen-bonding interactions.^{2, 8, 10, 11} For example, there are published crystal structures which show C—Br···I⁻¹² and C—Cl···Cl⁻ interactions.¹³ Figure 5.1 shows part of one of these structures and in this example the halogen-bonding interaction is between the bromo substituents of 3, 5-dibromopyridine and iodide anions.

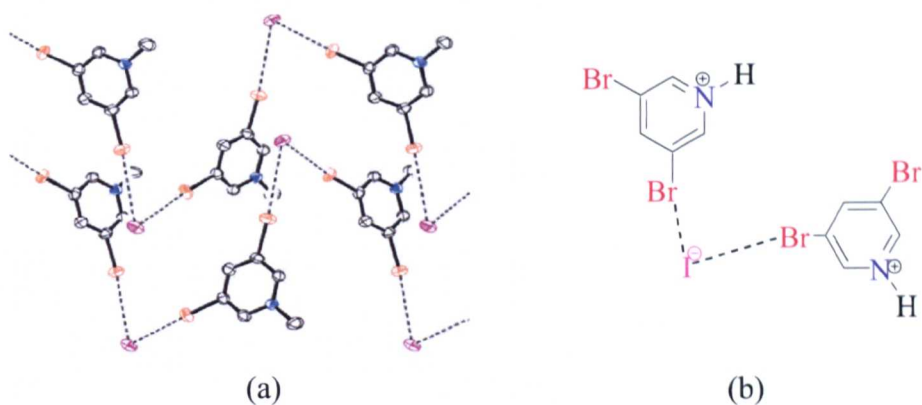


Figure 5.1. a) Structure of 3, 5-dibromopyridine interacting with I^- through halogen-bonds.¹³ and b) highlighting the nature of the halogen-bond.

Of more relevance to this work are crystal structures that show C—X \cdots Cl—Pt interactions.⁸ Figure 5.2 shows halogen-bonding interactions between the chloro substituents on 4-chloropyridine and Pt—Cl moieties.⁸

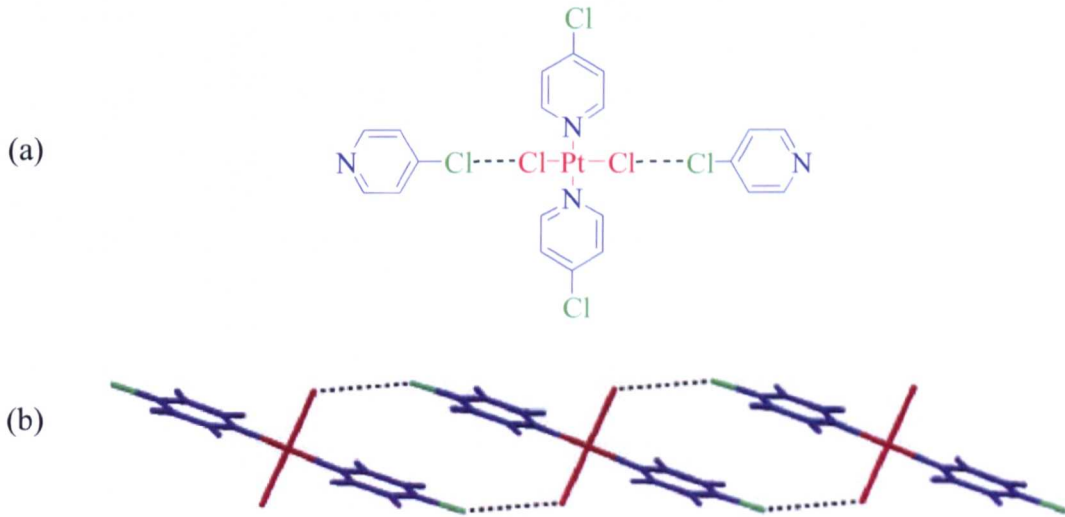


Figure 5.2. a) Structure of $\text{PtCl}_2(\text{4-chloropyridine})_2$ and b) highlighting the nature of the interaction.⁸

As the $[\text{PtCl}_6]^{2-}$ anion has metal-bound Cl^- in its inner coordination sphere it could behave as a halogen-bond acceptor. It was proposed that a Pt—Cl \cdots X—C halogen-bond could be utilised to enhance the interaction between the receptor and anion. Thus, C—X moieties were introduced into the receptor design (Figure 5.3).

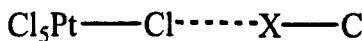


Figure 5.3. The proposed halogen-bonding interaction between $[\text{PtCl}_6]^{2-}$ and C—X.

5.2.1. Design of Receptors

Two novel TREN-based receptors were synthesised in which each of the three pendant arms was functionalised with urea or amide hydrogen-bond donor groups and bromophenyl terminal groups for halogen-bonding to $[\text{PtCl}_6]^{2-}$. Bromophenyl substituted isocyanates and acid chlorides were used to synthesise the receptors as they are commercially available and the positioning of the bromo substituents was considered. If the bromo substituent is in the ortho-position then 5-membered intramolecular hydrogen-bonded rings ($\text{N}—\text{H}\cdots\text{Br}$) may be formed reducing the possibility of the desired interactions. The para-position was also discounted as it would cause the halogen-bond and hydrogen-bond donor groups to be pointing in different directions. The optimal position is the meta-position which was chosen as, though not ideal for the urea receptor, it looked promising for an amide system (Figure 5.4).⁴

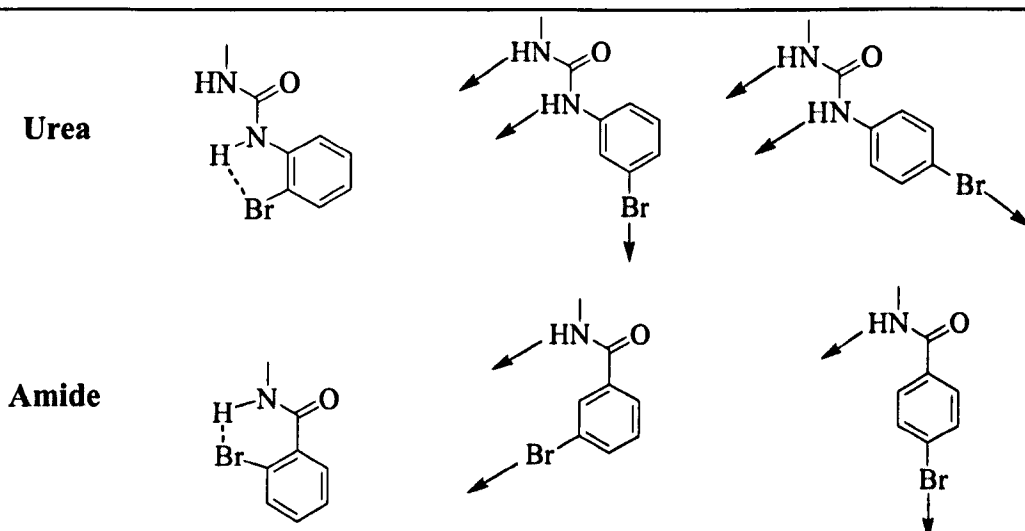
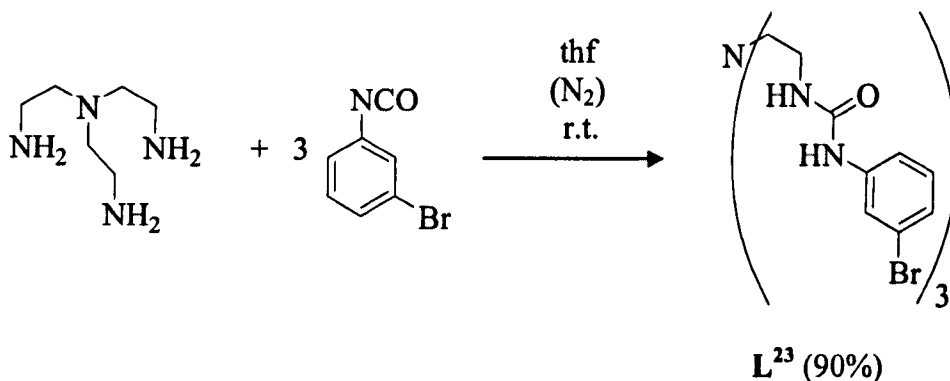


Figure 5.4. Variation in the position of bromo substituents for urea and amide receptors.

5.2.2. Synthesis of Receptors

5.2.2.1. Urea Receptor

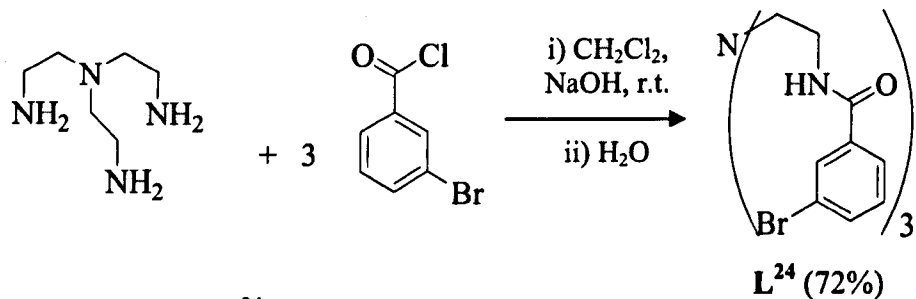
L^{23} was synthesised by the reaction of TREN with three equivalents of 3-bromophenyl isocyanate (Scheme 5.1).¹⁴ The product precipitated as a colourless solid which was collected by filtration and dried *in vacuo* to give the receptor in 90% yield. The 1H NMR spectrum of L^{23} , recorded in d_{6} -DMSO, showed a triplet and singlet signal for the two urea NH protons confirming the C_3 symmetry of the molecule in solution. Electrospray mass spectrometry showed a peak at m/z 738 assigned to $[M]^+$ whilst IR spectroscopy showed a carbonyl stretch at 1650 cm^{-1} and a band at 768 cm^{-1} assigned to the C—Br stretch. The ^{13}C NMR spectrum and elemental analytical data further confirmed the purity of the product.



Scheme 5.1. Synthesis of L^{23} .

5.2.2.2. Amide Receptor

L^{24} was synthesised by the reaction of TREN with three equivalents of 3-bromobenzoyl chloride in basic conditions (Scheme 5.2).¹⁵ In contrast to the analogous urea receptor, L^{24} was soluble in CHCl_3 . The ^1H NMR spectrum of L^{24} in CDCl_3 showed a triplet signal for the NH amide protons indicating C_3 symmetry in solution. The IR spectrum has a band at 1630 cm^{-1} assigned to the carbonyl stretch and a band at 747 cm^{-1} assigned to C—Br. Electrospray mass spectrometry on the product showed a peak at m/z 695 assigned to $[\text{M}]^+$ and elemental analytical data further confirmed the purity of the product.



Scheme 5.2. Synthesis of L^{24} .

5.2.3. Complexation Reactions

The urea receptor L^{23} was insoluble in MeCN, even when heated, thus preventing its reaction with H_2PtCl_6 . The reaction was also attempted in acetone but L^{23} remained insoluble and therefore unreactive towards H_2PtCl_6 . The insolubility of this receptor prevented the formation of complexes with $[\text{PtCl}_6]^{2-}$ and also meant that it could not be studied in solvent extraction experiments.

The amide receptor L^{24} , when heated, was soluble in MeCN and when mixed with H_2PtCl_6 a yellow precipitate formed immediately. The ^1H NMR spectrum of the product in $\text{dmso}-d_6$ has a broad signal at 9.66 ppm assigned to the protonated tertiary amine position $\text{N}^+\underline{\text{H}}\text{R}_3$ and the amide NH signal shifts downfield by 0.47 ppm

indicating the formation of hydrogen-bonding interactions. There was no evidence for halogen-bonding as the aromatic protons in the positions ortho to the bromo substituent do not shift in the ^1H NMR spectrum nor does the C—Br band in the IR spectrum. The low organic solubility of L^{24} and its complex $[(\text{L}^{24}\text{H})_2\text{PtCl}_6]$ prevents the study of the system in solvent extraction studies. Attempts were made at obtaining a crystal structure showing the interaction of L^{24} with $[\text{PtCl}_6]^{2-}$ in the solid state but proved unsuccessful.

5.2.4. Summary of Results

By introducing bromophenyl substituents into the receptors it was hoped halogen-bonds would form between the receptors and $[\text{PtCl}_6]^{2-}$ to enhance the interaction leading to improved extraction. L^{23} and L^{24} and their complexes had low organic solubility preventing the study of these systems in solvent extraction studies. In addition, there was no evidence to suggest halogen-bonding interactions had formed and therefore no further work was carried out into this area of work.

5.3. Extended Tripodal Receptors

By increasing the length of the pendant arms it was thought that the areas of highest electron density surrounding $[\text{PtCl}_6]^{2-}$ could be targeted more easily by hydrogen-bond donor groups. The additional flexibility may also allow the receptor to encapsulate the anion more leading to a stronger interaction and improved extraction. The receptors presented in this Section of work all have a tripodal scaffold in which each of the pendant arms is one carbon atom longer than in the previously presented TREN-based receptors.

5.3.1. Design of Receptors

Tris(3-aminopropyl)amine (TRPN) was chosen as the scaffold to this series of receptors because, analogous to TREN, it has a tertiary amine protonation site and three primary amine groups which can be functionalised with hydrogen-bond donor and organic solubilising groups. Whilst TREN has ethyl spacers between the tertiary nitrogen amine and the terminal primary amine positions, TRPN has propyl spacer units (Figure 5.5).

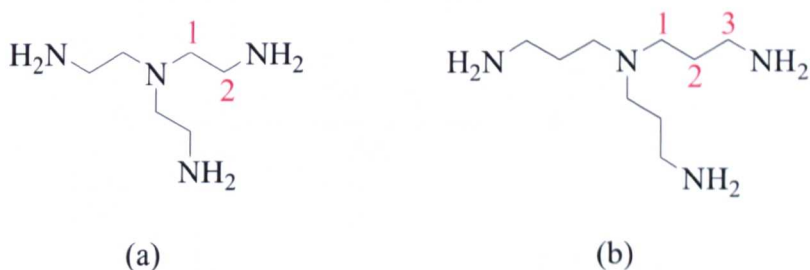
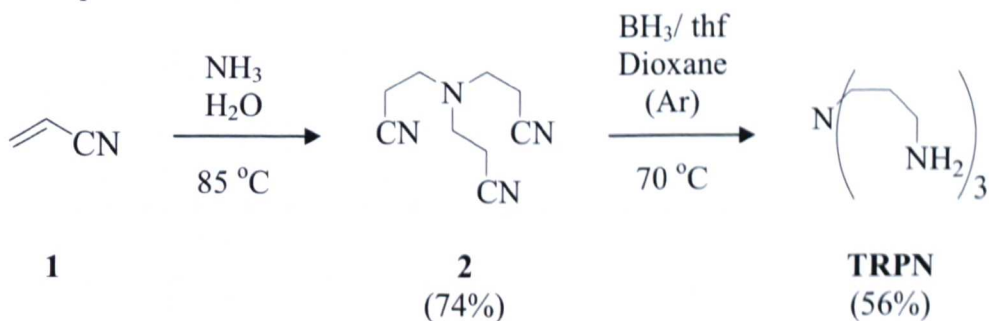


Figure 5.5. The structures of the tripodal amines a) TREN and b) TRPN.

TRPN was prepared via a two-step synthetic route (Scheme 5.3). Following the method of van Winkle and co-workers acrylonitrile **1** was reacted with NH_3 in H_2O to give the tris(cyanoethyl)amine intermediate **2**.¹⁶ Reduction of the nitrile functionality using BH_3/thf gave TRPN as a viscous oil in 56% yield.¹⁷ Characterisation of the amine by ^1H and ^{13}C NMR spectroscopy and mass spectrometry corresponded with the literature values and confirmed the formation of the desired product.^{18, 19}

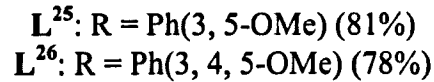
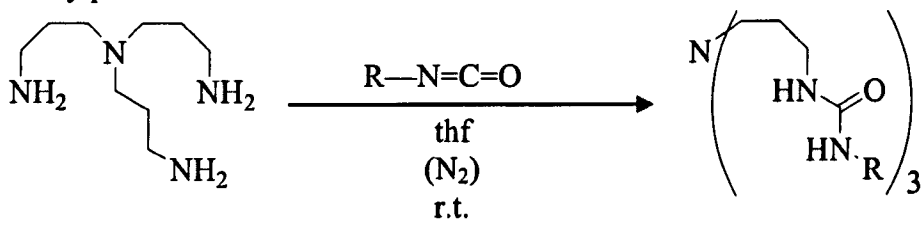


Scheme 5.3. Synthesis of tris(3-aminopropyl)amine (TRPN).

5.3.2. Synthesis of Receptors

5.3.2.1. Urea Receptors

The novel ligands L²⁵ and L²⁶ were synthesised by the reaction of TRPN with three equivalents of 3, 5-dimethoxyphenyl or 3, 4, 5-trimethoxyphenyl isocyanate, respectively (Scheme 5.4).¹⁴ Both products formed as colourless solids in yields in excess of 78% and characterisation of the products by ¹H NMR, ¹³C NMR and IR spectroscopy, mass spectrometry and elemental analytical data showed them to be analytically pure.



Scheme 5.4. Synthesis of L²⁵ and L²⁶

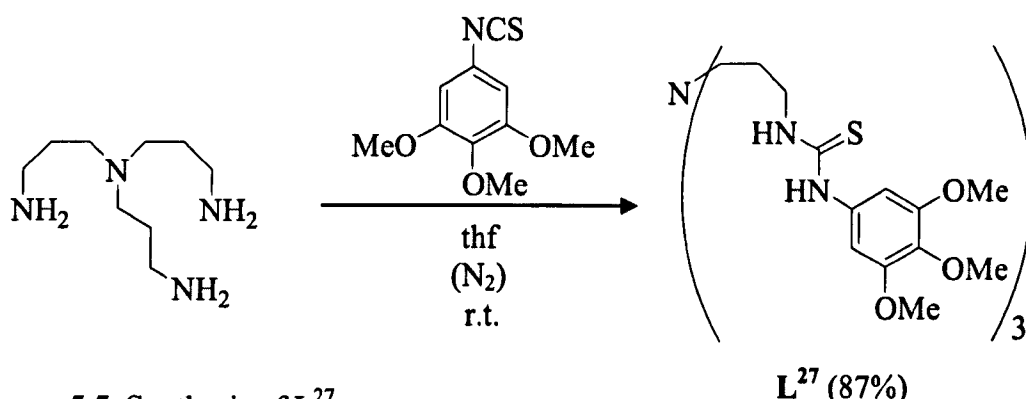
A potentiometry experiment with L²⁶ showed it to have one protonation site as described by the equilibrium L + H = LH⁺ with a log K value of 8.74(8). The tertiary amine position in L²⁶ is more basic than the tertiary amine position in the analogous TREN-based urea receptor L¹⁴ because the propyl group can donate more electron density than the ethyl group to stabilise the ammonium cation that is formed upon protonation.²⁰

5.3.2.2. Thiourea Receptor

The TREN-based thiourea receptors formed insoluble complexes with H₂PtCl₆ preventing them being studied in solvent extraction studies. Despite this result, thiourea moieties were incorporated onto a TRPN scaffold as it was thought that the

longer aliphatic chain of the scaffold may improve the organic solubility of the complexes.

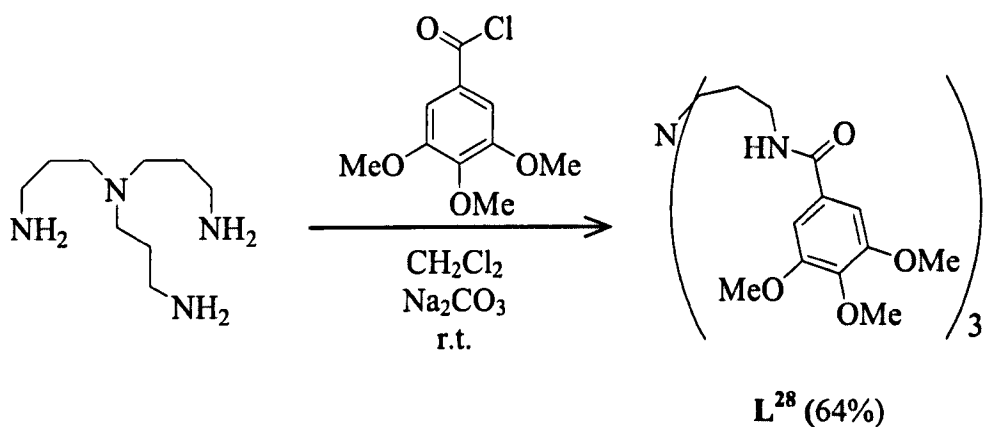
The novel receptor L^{27} was synthesised by the reaction of TRPN with three equivalents of 3, 4, 5-trimethoxyphenyl isothiocyanate (Scheme 5.5).¹⁴ The product formed as a colourless solid which was collected by filtration and dried *in vacuo* to give L^{27} in 87% yield. Characterisation of the product was achieved by ^1H NMR, ^{13}C NMR and IR spectroscopy, mass spectrometry and elemental analysis which showed it to be analytically pure.



Scheme 5.5. Synthesis of L^{27} .

5.3.2.3. Amide Receptor

The novel amide receptor L^{28} was synthesised by the reaction of TRPN with three equivalents of 3, 4, 5-trimethoxybenzoyl chloride under basic conditions (Scheme 5.6).¹⁵ The product was obtained as a colourless solid in 64% yield and characterised by ^1H NMR, ^{13}C NMR and IR spectroscopy, mass spectrometry and elemental analysis.



Scheme 5.6. Synthesis of L²⁸.

5.3.3. Complexation Reactions

5.3.3.1. Urea Complexes

L²⁵ and L²⁶ were reacted with H₂PtCl₆ in MeCN to give a transparent, orange solution. The reactions were repeated in CD₃CN and the ¹H NMR spectra of the resulting solutions recorded. In both cases a signal was observed at 9.15 or 9.12 ppm (for L²⁵ and L²⁶, respectively) which integrated in a 1:3 ratio with each of the urea NH protons and was assigned to the protonated bridgehead nitrogen position N⁺HR₃. Negative electrospray mass spectrometry on the solution resulting from the mixing of L²⁶ with H₂PtCl₆ showed a peak at *m/z* 2036 assigned to [(L²⁶H)(L²⁶)PtCl₆]⁻ suggesting the formation of the desired complex [(L²⁶H)₂PtCl₆]. Other peaks in the mass spectrum were observed at *m/z* 850, 4411 and 4480 assigned to [L²⁶+Cl]⁻, [4(L²⁶H)+2(PtCl₆)+PtCl₄+H]⁻ and [4(L²⁶H)+3(PtCl₆)]²⁻, respectively. Attempts were made at growing crystals of the complexes [(L²⁵H)₂PtCl₆] and [(L²⁶H)₂PtCl₆] but were unsuccessful possibly due to the high solubility displayed by these complexes.

5.3.3.2. Thiourea Complex

Two equivalents of L^{27} were dissolved in MeCN and added to one equivalent of H_2PtCl_6 resulting in a yellow-orange precipitate being formed. Attempts made to isolate the solid by filtration gave a small amount of insoluble waxy solid meaning characterisation was not possible in this case.

5.3.3.3. Amide Complex

Two equivalents of L^{28} were added to one equivalent of H_2PtCl_6 , dissolved in MeCN, to give a transparent, orange solution. The reaction was repeated in CD_3CN and the 1H NMR spectrum recorded. A signal at 8.96 ppm was assigned to the protonated bridgehead nitrogen position N^+HR_3 and there was a downfield shift in the signal for the amide NH proton indicating the formation of hydrogen-bonds. Negative electrospray mass spectrometry on the solution resulting from the mixing of L^{28} with H_2PtCl_6 showed a peak at m/z 805 assigned to $[L^{28}+Cl]^-$. No peak due to the 2:1 $L^{28}:[PtCl_6]^{2-}$ complex was observed in the spectrum despite the same experimental conditions being used as for the observation of $[(L^{26}H)_2PtCl_6]$. This suggests that the interaction between $[PtCl_6]^{2-}$ and L^{28} may be weaker than in $[(L^{26}H)_2PtCl_6]$. Attempts were made at growing crystals of the complex $[(L^{28}H)_2PtCl_6]$ but were unsuccessful.

5.3.4. Extraction Studies

5.3.4.1. Test Extractions

In the test extraction with the urea receptors L^{25} and L^{26} and the amide receptor L^{28} the organic layer became coloured suggesting uptake of $[PtCl_6]^{2-}$. For the thiourea receptor L^{27} an insoluble precipitate formed preventing it being studied. Solvent

extraction studies were thus undertaken with the urea receptor L²⁶ (as it was more soluble than L²⁵) and the amide extractant L²⁸.

5.3.4.2. Effect of Hydrogen-bond Donor Group

The urea receptor, L²⁶, extracts more [PtCl₆]²⁻ than its amide analogue, L²⁸, across all [Receptor]:[PtCl₆]²⁻ ratios (Figure 5.6). For example, at an arbitrary [Receptor]:[PtCl₆]²⁻ ratio of 3:1 L²⁶ extracts 74% whilst L²⁸ extracts 55% (Table 5.1). This trend is consistent with the results observed for the TREN-based extractants and is thought to be because the urea receptors have more NH donor groups enabling more hydrogen-bond interactions to form with [PtCl₆]²⁻ thus leading to enhanced extraction.

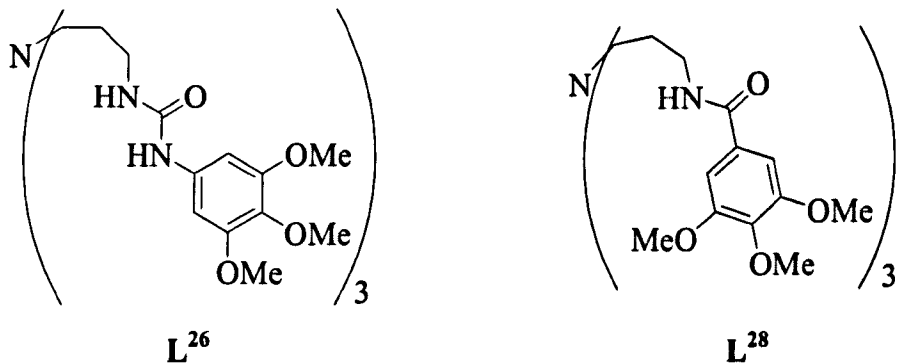


Table 5.1. % of Pt extracted as [PtCl₆]²⁻ from aqueous 0.6 M HCl into CHCl₃ in the presence of a three molar excess of L

Receptor	L^{26}	L^{28}
% Pt extracted at 3 molar excess of L	74	55

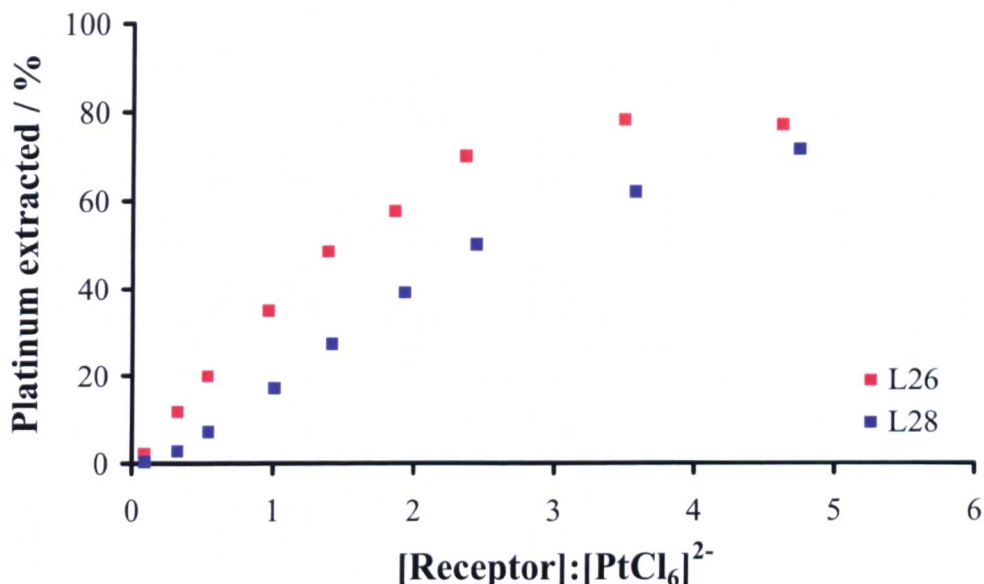


Figure 5.6. Plot of % Pt extracted as $[\text{PtCl}_6]^{2-}$ from aqueous 0.6 M HCl into CHCl_3 as a function of $[\text{Receptor}]:[\text{PtCl}_6]^{2-}$ ratio.

A Yoshizawa analysis²¹ was performed with the extraction results for L^{26} and L^{28} and in each case a straight line graph was plotted (Figure 5.7). The gradient for L^{26} is 1.0704 thus showing significant deviation from the theoretical value of two while for L^{28} the straight line has a gradient of 1.7688.

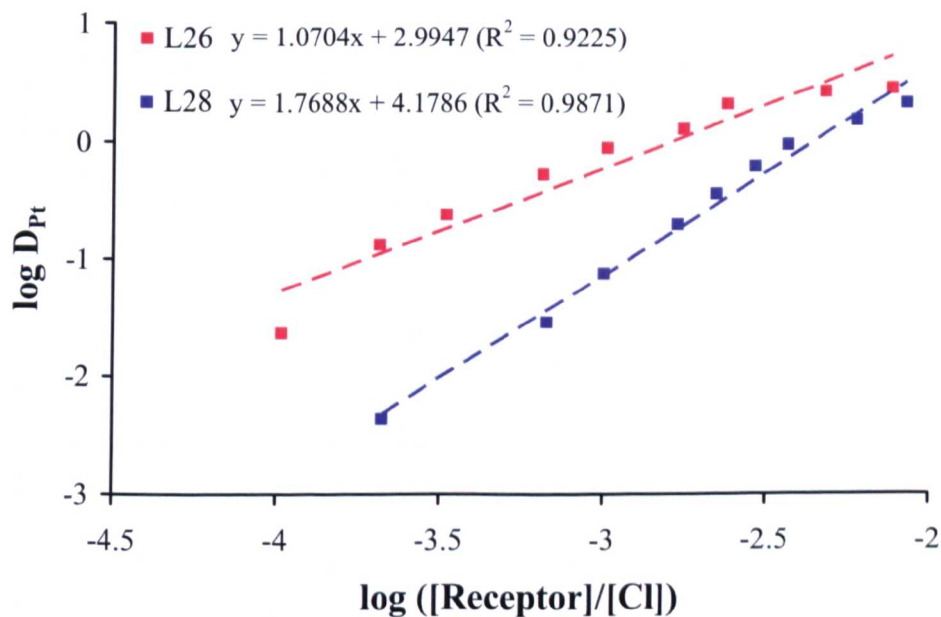


Figure 5.7. Plot of $\log ([\text{Receptor}]/[\text{Cl}])$ against $\log D$ for L^{26} and L^{28} .

5.3.4.3. Effect of Receptor Scaffold

To assess the affect of receptor scaffold the extraction results for L^{19} and L^{28} were compared. L^{19} extracts more $[PtCl_6]^{2-}$ than L^{28} across all [Receptor]: $[PtCl_6]^{2-}$ ratios and at an arbitrary ratio of three the TREN receptor L^{19} is 76% whilst the TRPN receptor L^{28} extracts 55% (Figure 5.8 and Table 5.2).

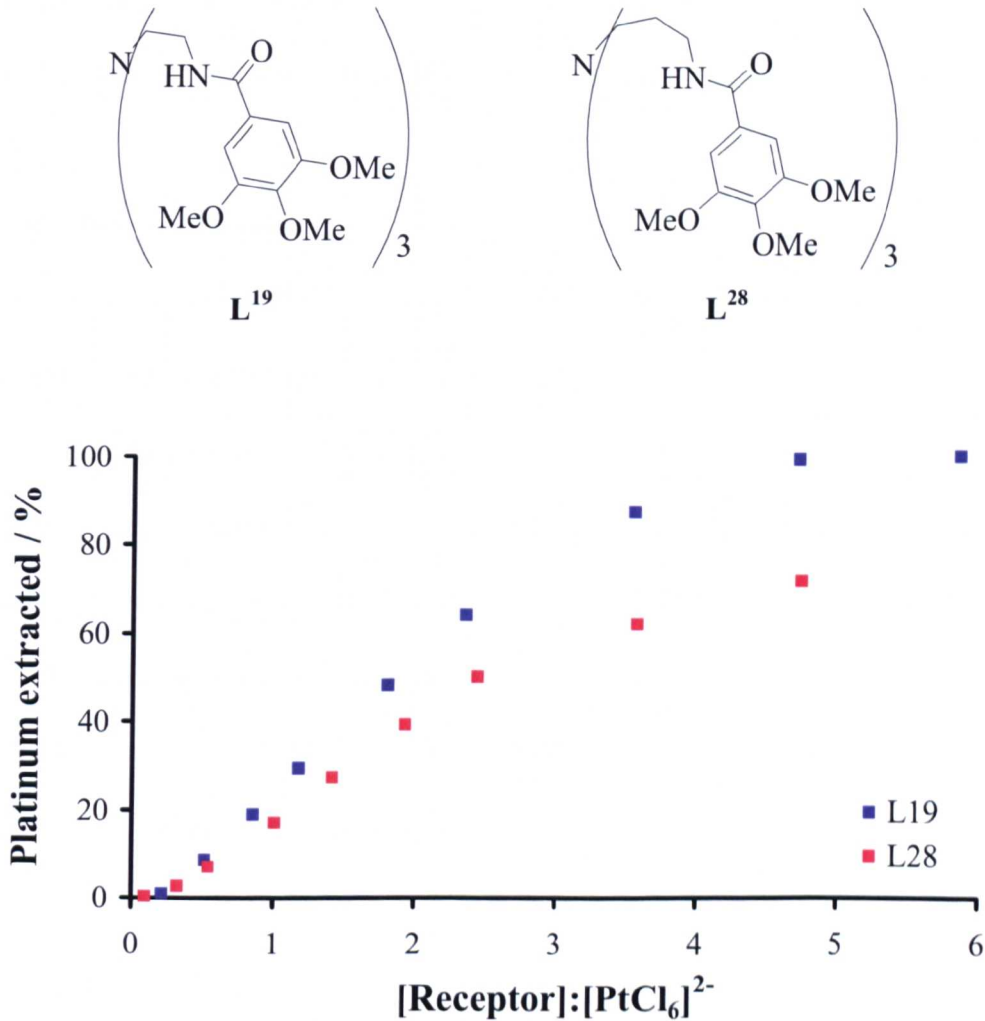


Figure 5.8. Plot of % Pt extracted as $[PtCl_6]^{2-}$ from aqueous 0.6 M HCl into $CHCl_3$ as a function of [Receptor]: $[PtCl_6]^{2-}$ ratio.

Table 5.2. % of Pt extracted as $[PtCl_6]^{2-}$ from aqueous 0.6 M HCl into $CHCl_3$ in the presence of a three molar excess of L

Receptor	L^{19}	L^{28}
% Pt extracted at 3 molar excess of L	76	55

These results show that systems with ethyl spacers give improved extraction over those with propyl units. The ethyl group is more rigid which may enforce a tripodal geometry and make the receptor more pre-organised meaning that the hydrogen-bond donor groups may already be in a position to target the areas of highest electron density on the outer-sphere of $[\text{PtCl}_6]^{2-}$. Although the TRPN systems extract less than their TREN analogues they still extract more than TOA confirming that incorporating hydrogen-bond donor groups into the design enhances extraction.

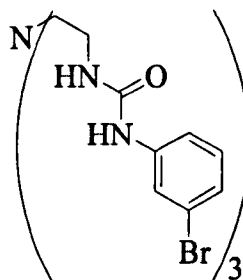
5.3.5. Summary of Results

Four receptors were synthesised which have a TRPN scaffold and either urea, thiourea or amide hydrogen-bond donor groups with terminal methoxyphenyl substituents. The complexes formed with the urea and amide systems were CHCl_3 soluble allowing them to be studied in solvent extractions whilst the thiourea receptor L^{27} formed an insoluble complex $[(L^{27}\text{H})_2\text{PtCl}_6]$. The urea receptor L^{26} was found to have higher extraction efficiency and the amide receptor L^{28} . Comparison of the extraction results for TREN and TRPN-based amides showed the TREN receptor to have higher extraction efficiency.

5.4. Experimental

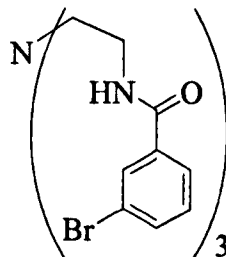
5.4.1. Synthesis of Hydrogen- and Halogen-bonding Receptors and Complexes

5.4.1.1. Synthesis of N,N'',N'''-(nitrilotri-2,1-ethanediyl)tris[N'-3-bromophenyl urea], L²³.¹⁴



To TREN (0.1 cm³, 0.68 mmol) in dry THF (20 cm³) was added 3-bromophenyl isocyanate (0.25 cm³, 2 mmol) under N₂. A colourless precipitate formed immediately and the reaction was stirred at room temperature for a further 20 h. The precipitate was collected by filtration and dried *in vacuo*. Yield: 0.45 g, 90%. ¹H NMR (270 MHz, dmsO-d₆): δ/ppm 8.77 (s, 3H, NH), 7.83 (s, 3H, H_{Ar}), 7.23 (d, 3H, ³J_{HH} = 8 Hz, H_{Ar}), 7.16 (dd, 3H, ³J_{HH} = 8 Hz, H_{Ar}), 7.06 (d, 3H, ³J_{HH} = 8 Hz, H_{Ar}), 6.26 (t, 3H, ³J_{HH} = 5 Hz, NH), 3.22–3.19 (m, 6H, CH₂), 2.62 (t, 6H, ³J_{HH} = 6 Hz, CH₂). ¹³C NMR (68 MHz, dmsO-d₆): δ/ppm 156, 143, 131, 124, 122, 120, 117, 54, 38. MS (ES⁺): calc *m/z* 738.0032 for [M+H]⁺, found *m/z* 738.0038. IR (solid, cm⁻¹): 3292(v_(NH)), 1650(v_(C=O)), 1567(v_(C=C, Ar)), 768(v_(C-Br)). Anal. calc. for C₂₇H₃₀Br₃N₇O₃: C, 43.81; H, 4.08; N, 13.24. Found: C, 43.35; H, 4.44; N, 13.14%.

5.4.1.2. Synthesis of N,N'',N'''-(nitrilotri-2,1-ethanediyil)tris[3-bromobenzamide], L^{24,15}.



To TREN (0.1 cm^3 , 0.68 mmol) in CH_2Cl_2 (20 cm^3) was added NaOH (*ca.* 0.1 g) and 3-bromobenzoyl chloride (0.26 cm^3 , 2 mmol). The reaction formed a colourless precipitate immediately and was stirred at room temperature for 20 h. H_2O (10 cm^3) was added to the reaction to dissolve the NaOH and the layers were separated and the aqueous layer washed with CH_2Cl_2 ($2 \times 15\text{ cm}^3$). The organic washings were collected, dried with MgSO_4 and the solvent removed from the filtrate to give an off-white powder. Yield: 0.34 g, 72%. ^1H NMR (270 MHz, CDCl_3): δ/ppm 7.85 (s, 3H, $\underline{\text{H}_{\text{Ar}}}$), 7.66 (d, 3H, $^3J_{\text{HH}} = 8\text{ Hz}$, $\underline{\text{H}_{\text{Ar}}}$), 7.47 (d, 3H, $^3J_{\text{HH}} = 8\text{ Hz}$, $\underline{\text{H}_{\text{Ar}}}$), 7.44 (dd, 3H, $^3J_{\text{HH}} = 8\text{ Hz}$, $\underline{\text{H}_{\text{Ar}}}$), 6.87 (t, 3H, $^3J_{\text{HH}} = 7\text{ Hz}$, $\underline{\text{NH}}$), 3.50 (br, 6H, $\underline{\text{CH}_2}$), 2.69 (br, 6H, $\underline{\text{CH}_2}$). ^{13}C NMR (68 MHz, CDCl_3): δ/ppm 167, 136, 134, 131, 130, 125, 123, 54, 38. MS (ES⁺): m/z 695 [M]⁺. IR (solid, cm^{-1}): 3305($\nu_{(\text{NH})}$), 1630($\nu_{(\text{C=O})}$), 1542($\nu_{(\text{C-C, Ar})}$), 747($\nu_{(\text{C-Br})}$). Anal. calc. for $\text{C}_{27}\text{H}_{27}\text{Br}_3\text{N}_4\text{O}_3$: C, 46.66; H, 3.92; N, 8.06. Found: C, 46.51; H, 3.79; N, 7.98%.

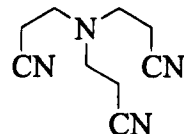
5.4.1.3. Synthesis of [(L²⁴H)₂PtCl₆]

The receptor L²⁴ (2 equivalents) was dissolved in MeCN (it was necessary to heat the solution to ensure complete solubility of the solid) and added to H_2PtCl_6 (1 equivalent) dissolved in MeCN. On the mixing of the two solutions a yellow

precipitate formed which was collected by filtration and dried *in vacuo*. ^1H NMR (270 MHz, dmso-*d*₆): δ /ppm 9.66 (br, 1H, NH⁺), 8.95 (t, 3H, $^3J_{\text{HH}} = 5$ Hz, NH), 7.95 (s, 3H, H_{Ar}), 7.82–7.74 (m, 6H, H_{Ar}), 7.43 (d, 3H, $^3J_{\text{HH}} = 8$ Hz, H_{Ar}), 3.73 (m, 6H, CH₂), other CH₂ under H₂O signal. IR (solid, cm⁻¹): 3305 ($\nu_{(\text{N-H})}$), 1637 ($\nu_{(\text{C=O})}$). Anal. calc. for C₅₄H₅₆Br₆Cl₆N₈O₆Pt: C, 36.03; H, 3.14; N, 6.22. Found: C, 35.97; H, 3.26; N, 6.23%.

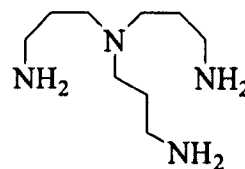
5.4.2. Synthesis of Extended Tripodal Receptors and Complexes

5.4.2.1. Synthesis of Tris(cyanoethyl)amine, 2¹⁶



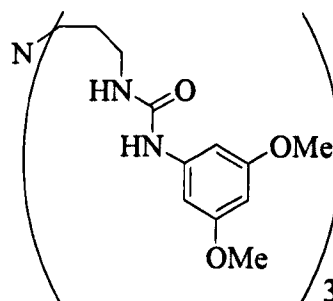
Acrylonitrile (55 g, 1.00 mol) was added dropwise to a stirred solution of 28% ammonium hydroxide at 30 °C. Stirring was continued for 2 h and then H₂O (175 cm³) and more acrylonitrile (55 g, 1.00 mol) were added. The mixture was then stirred at 75–80 °C for 48 h and then the H₂O and excess acrylonitrile removed by distillation under reduced pressure. The residual liquid formed a solid on standing which was then recrystallised from EtOH to give a colourless solid. Yield: 74%. ^1H NMR (300 MHz, CDCl₃): δ /ppm 2.94 (t, 6H, $^3J_{\text{HH}} = 6$ Hz, CH₂), 2.52 (t, 6H, $^3J_{\text{HH}} = 6$ Hz, CH₂). ^{13}C NMR (75 MHz, CDCl₃): 119, 50, 17. MS (ES⁺): *m/z* 177 [M+H]⁺.

5.4.2.2. Synthesis of Tris(3-aminopropyl)amine (TRPN)¹⁷



To a solution of tris(cyanoethyl)amine **2** (2.80 g, 15.50 mmol) in thf (100 cm³) was added BH₃/ thf (1 M, 100 cm³) under an Ar atmosphere. The reaction was heated under reflux for 16 h then cooled to room temperature. The reaction was quenched with MeOH causing a white solid to precipitate. The reaction was stirred at room temperature until the precipitate re-dissolved. The solvent was removed under reduced pressure and the residue was dissolved in 6 M HCl (125 cm³) and subsequently heated under reflux for 1 h. The H₂O was removed *in vacuo* to give the amine acid salt. The free amine was obtained by a DOWEX ion exchange column as a colourless oil. Yield: 1.64 g, 56%. ¹H NMR (300 MHz, CDCl₃): δ/ppm 2.69 (t, 6H, ³J_{HH} = 7 Hz, CH₂), 2.42–2.39 (m, 6H, CH₂), 1.60–1.50 (m, 6H, CH₂), 1.22 (br, 6H, NH₂). ¹³C NMR (75 MHz, CDCl₃): δ/ppm 51, 40, 29. MS (ES⁺): *m/z* 189 [M]⁺.

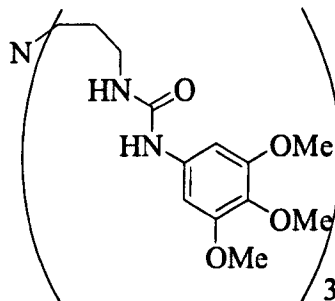
5.4.2.3. Synthesis of N,N',N''-(nitrilo-2,1-propanediyl)tris[N'-3,5-dimethoxyphenyl urea], L²⁵.¹⁴



3, 5-Dimethoxyphenyl isocyanate (0.57 g, 3.19 mmol) was dissolved in dry thf (20 cm³). TRPN (0.20 g, 1.06 mmol) was added and the reaction stirred at room

temperature for 16 h. The colourless precipitate that formed was collected by filtration and dried *in vacuo*. Yield: 0.62 g, 81%. ^1H NMR (270 MHz, CDCl_3): δ/ppm 8.11 (s, 3H, NH), 6.71 (s, 6H, H_{Ar}), 6.31 (t, 3H, $^3J_{\text{HH}} = 6$ Hz, NH), 6.08 (s, 3H, H_{Ar}), 3.72 (s, 18H, OMe), 2.52 (br, 6H, CH₂), 2.20 (br, 6H, CH₂), 1.72 (br, 6H, CH₂). ^{13}C NMR (68 MHz, CDCl_3): δ/ppm 162, 157, 141, 96, 95, 55, 51, 37, 28. MS (ES^+): calc. for $\text{C}_{36}\text{H}_{52}\text{N}_7\text{O}_9$ m/z 726.3826, found m/z 726.3809, corresponds to $[\text{M}+\text{H}]^+$. IR (solid, cm^{-1}): 3304 ($\nu_{(\text{N-H})}$), 1606 ($\nu_{(\text{C=O})}$), 1557 ($\nu_{(\text{C=C, Ar})}$), 1157 ($\nu_{(\text{C-O})}$). Anal. calc. for $\text{C}_{36}\text{H}_{51}\text{N}_7\text{O}_9$: C, 59.57; H, 7.08; N, 13.51. found: C, 59.38; H, 6.96; N, 13.17%.

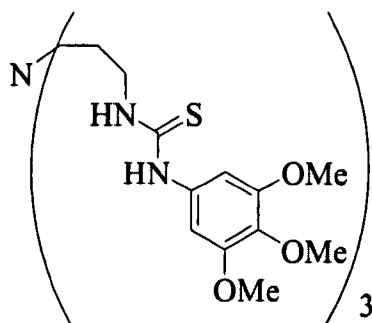
5.4.2.4. Synthesis of $\text{N,N',N''-(nitrilo-2,1-propanediyl)tris[N'-3,4,5-trimethoxyphenyl urea]}$, L^{26, 14}.



3, 4, 5-Trimethoxyphenyl isocyanate (0.66 g, 3.19 mmol) was dissolved in dry THF (20 cm³) under a N_2 atmosphere. To this was added TRPN (0.20 g, 1.06 mmol). The reaction was stirred at room temperature for 16 h. During this time a colourless precipitate formed which was collected by gravity filtration, washed with diethyl ether (2 × 5 cm³) and then dried *in vacuo*. Yield: 0.67 g, 78%. ^1H NMR (270 MHz, CDCl_3): δ/ppm 8.08 (s, 3H, NH), 6.80 (s, 6H, H_{Ar}), 6.27 (br t, 3H, NH), 3.78 (s, 18H, OMe), 3.77 (s, 9H, OMe), 2.55 (br, 6H, CH₂), 2.18 (br, 6H, CH₂), 0.97 (br, 6H, CH₂). ^{13}C NMR (68 MHz, CDCl_3): δ/ppm 157, 154, 136, 133, 94, 68, 56, 55, 51, 28.

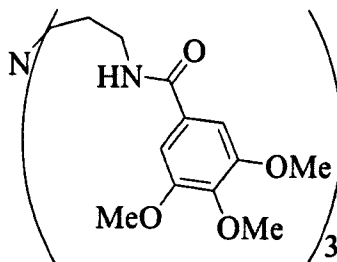
MS (ES^+): calc. For $\text{C}_{39}\text{H}_{58}\text{N}_7\text{O}_{12}$ m/z 816.4143, found m/z 816.4114, corresponds to $[\text{M}+\text{H}]^+$. IR (solid, cm^{-1}): 3318 ($\nu_{(\text{N-H})}$), 1637 ($\nu_{(\text{C=O})}$), 1604 ($\nu_{(\text{C=C, Ar})}$), 1128 ($\nu_{(\text{C-O})}$). Anal. calc. for $\text{C}_{39}\text{H}_{57}\text{N}_7\text{O}_{12}$: C, 57.41; H, 7.04; N, 12.02. Found: C, 56.98; H, 6.97; N, 11.74%.

5.4.2.5. Synthesis of $\text{N,N',N''-(nitrilo-2,1-propanediyl)tris[N'-3,4,5-trimethoxyphenyl thiourea]}$, L^{27, 14}.



3, 4, 5-Trimethoxyphenyl isothiocyanate (0.36 g, 1.59 mmol) was dissolved in dry THF (30 cm³) under N_2 . To this was added TRPN (0.10 g, 0.53 mmol) and the reaction stirred at room temperature for 16 hours. The product precipitated from solution as a colourless solid which was collected by filtration and dried *in vacuo*. Yield: 0.40 g, 87%. ^1H NMR (270 MHz, CDCl_3): δ/ppm 7.01 (br, 3H, NH), 6.75 (br, 3H, NH), 6.51 (s, 6H, H_{Ar}), 3.78 (s, 18H, OMe), 3.76 (s, 9H, OMe), 3.59–3.48 (t, 6H, ${}^3J_{\text{HH}} = 6$ Hz, CH_2), 2.33–2.22 (m, 6H, CH_2), 1.58–1.51 (m, 6H, CH_2). ^{13}C NMR (68 MHz, CDCl_3): δ/ppm 181, 154, 137, 132, 103, 61, 52, 45, 41, 29. MS (ES^+): Calc for $\text{C}_{39}\text{H}_{58}\text{N}_7\text{O}_9\text{S}_3$ m/z 864.3458, found m/z 864.3429 corresponds to $[\text{M}+\text{H}]^+$. IR (solid, cm^{-1}): 3384 ($\nu_{(\text{N-H})}$), 1587 ($\nu_{(\text{C=S})}$). Anal. calc for $\text{C}_{39}\text{H}_{57}\text{N}_7\text{S}_3\text{O}_9$: C, 54.22; H, 6.65; N, 11.35. Found: C, 53.99; H, 6.42; N, 11.31%.

5.4.2.6. Synthesis of N,N',N''-(nitrilo-2,1-propanediyl)tris[N'-3,4,5-trimethoxyphenyl benzamide], L²⁸.¹⁵



TRPN (0.20 g, 1.06 mmol) was dissolved in CH₂Cl₂ containing Na₂CO₃ (0.34 g, 3.19 mmol). 3, 4, 5-Trimethoxybenzoyl chloride (0.73 g, 3.19 mmol) was added and the reaction was stirred at room temperature for 16 h. H₂O (15 cm³) was added slowly to dissolve the Na₂CO₃ and the reaction stirred for a further hour. The layers were separated and the aqueous layer washed with CH₂Cl₂ (2 × 10 cm³). The organic fractions were collected and dried over MgSO₄. The solvent was removed to give an off-white foam which was dried *in vacuo*. Yield: 0.52 g, 64%. ¹H NMR (270 MHz, CDCl₃): δ/ppm 7.67 (br t, 3H, NH), 7.09 (s, 6H, H_{Ar}), 3.81 (s, 18H, OMe), 3.76 (s, 9H, OMe), 3.36 (br, 6H, CH₂), 2.30 (br, 6H, CH₂), 1.61 (br, 6H, CH₂). ¹³C NMR (68 MHz, CDCl₃): δ/ppm 167, 153, 141, 130, 105, 61, 52, 39, 27. MS (ES⁺): calc for C₃₉H₅₅N₄O₁₂ *m/z* 771.3811, found *m/z* 771.3778, corresponds to [M+H]⁺. Anal. calc. for C₃₉H₅₄N₄O₁₂: C, 60.77; H, 7.06; N, 7.27. Found: C, 60.39; H, 6.92; N, 7.00%.

5.4.2.7. Synthesis of [(L²⁵H)₂PtCl₆]

The receptor L²⁵ (2 equivalents) was dissolved in CD₃CN to which H₂PtCl₆ (1 equivalent) was added. A transparent orange solution was formed. ¹H NMR (300 MHz, CD₃CN): δ/ppm 9.12 (br, 1H, NH⁺), 7.79 (s, 3H, NH), 6.65 (s, 6H, H_{Ar}), 6.61

(s, 3H, H_{Ar}), 5.98 (t, 3H, $^3J_{\text{HH}} = 6$ Hz, NH), 3.68 (s, 18H, OMe), 3.26 (br, 6H, CH₂), 3.13 (br, 6H, CH₂), 1.88 (br, 6H, CH₂).

5.4.2.8. Synthesis of [(L²⁶H)₂PtCl₆]

This was prepared in an analogous manner to that described for [(L²⁵H)₂PtCl₆]. ¹H NMR (300 MHz, CD₃CN): δ / ppm 9.15 (br, 1H, NH⁺), 7.59 (br, 3H, NH), 6.78 (s, 6H, H_{Ar}), 6.30 (br, 3H, NH), 3.74 (s, 18H, OMe), 3.64 (s, 9H, OMe), 3.30 (t, 6H, $^3J_{\text{HH}} = 6$ Hz, CH₂), 3.20–3.18 (m, 6H, CH₂), 1.94–1.90 (m, 6H, CH₂). MS (ES⁺): *m/z* 850 [M+Cl][−], *m/z* 2036 [(L)(L+H)PtCl₆][−], *m/z* 4411 [4(L+H)+2(PtCl₆)+PtCl₄+H][−], *m/z* 4480 [4(L+H)+3(PtCl₆)]^{2−}.

5.4.2.9. Synthesis of [(L²⁸H)₂PtCl₆]

This was prepared in an analogous manner to that described for [(L²⁵H)₂PtCl₆]. ¹H NMR (300 MHz, CD₃CN): δ /ppm 8.96 (br, 1H, NH⁺), 7.58 (t, 3H, $^3J_{\text{HH}} = 5$ Hz, NH), 7.11 (s, 6H, H_{Ar}), 3.85 (s, 18H, OMe), 3.76 (s, 9H, OMe), 3.50 (t, 6H, $^3J_{\text{HH}} = 6$ Hz, CH₂), 3.25–3.22 (m, 6H, CH₂), 2.07 (br, 6H, CH₂). MS (ES⁺): *m/z* 805 [M+Cl][−].

5.5. References

1. Metrangolo P.; Resnati G., *Chem. Eur. J.*, 2001, **7**, 2511-2519.
2. Metrangolo P.; Neukirch H.; Pilati T.; Resnati G., *Acc. Chem. Res.*, 2005, **38**, 386-395.
3. Mele A.; Metrangolo P.; Neukirch H.; Pilati T.; Resnati G., *J. Am. Chem. Soc.*, 2005, **127**, 14972-14973.
4. Politzer P.; Lane P.; Concha M. C.; Ma Y.; Murray J. S., *J. Mol. Model.*, 2007, **13**, 305-311.
5. Murray-Rust P.; Stallings W. C.; Monti C. T.; Preston R. K.; Glusker J. P.; *J. Am. Chem. Soc.*, 1983, **105**, 3206-3214.
6. Ramasubbu N.; Parthasarathy R.; Murray-Rust P.; *J. Am. Chem. Soc.*, 1986, **108**, 4308-4314.
7. Murray-Rust P.; Motherwell W. D. S.; *J. Am. Chem. Soc.*, 1979, **101**, 4374-4376.
8. Zordan F.; Brammer L., *Cryst. Growth Des.*, 2006, **6**, 1374-1379.
9. Zordan F.; Purver S. L.; Adams H.; Brammer L., *Cryst. Eng. Comm.*, 2005, **7**, 350-354.
10. Brammer L.; Bruton E. A.; Sherwood P., *Cryst. Growth Des.*, 2001, **1**, 277-290.
11. Minguez-Espallargas G.; Brammer L.; Sherwood P., *Angew. Chem. Int. Ed.*, 2006, **45**, 435-440.
12. Logothetis T. A.; Meyer F.; Metrangolo P.; Pilati T.; Resnati G., *New J. Chem.*, 2004, **28**, 760-763.
13. Freytag M.; Jones P. G.; Ahrens B.; Fischer A. K., *New J. Chem.*, 1999, **23**, 1137-1139.
14. Zart M. K.; Sorrell T. N.; Powell D.; Borovik A. S., *Dalton Trans.*, 2003, 1986-1992.
15. Geraldes C. F. G. C.; Brucher E.; Cortes S.; Koenig S. H.; Sherry A. D., *J. Chem. Soc., Dalton Trans.*, 1992, 2517-2521.
16. van Winkle J. L.; McClare J. D.; Williams P. H., *J. Org. Chem.*, 1966, **31**, 3300-3306.
17. Hettich R.; Schneider H., *J. Am. Chem. Soc.*, 1997, **119**, 5638-5647.
18. Dittler-Klingemann, A. M.; Hahn, F. E., *Inorg. Chem.*, 1996, **35**, 1996-1999.

19. Chin J.; Banaszczyk M.; Jubian V.; Zou X., *J. Am. Chem. Soc.*, 1989, **111**, 186-190.
20. Clayden J.; Greeves N.; Warren S.; Wothers P, *Organic Chemistry*, Oxford University Press, Oxford, 2000.
21. Yoshizawa H.; Shiomori K.; Yamada S.; Baba Y.; Kawano Y.; Kondo K.; Ijichi K.; Hatake Y., *Solv. Extr. Res. Dev.*, 1997, **4**, 157-166.

6. Bipodal and Monopodal Receptors

6.1. Introduction

Although the TREN- and TRPN-based urea and amide receptors are successful extractants for $[\text{PtCl}_6]^{2-}$ the crystal structures of the complexes show that not all of the functionalised arms hydrogen-bond to the anion. To investigate whether receptors with fewer hydrogen-bond donor groups were as efficient as the tripodal extractants bipodal and monopodal systems were designed, synthesised and evaluated.

6.2. Bipodal Receptors

The amines N-methyl-2, 2'-diaminodiethylamine (Figure 6.1a) and N-methyl-3, 3'-diaminodipropylamine (Figure 6.1b) were used in the synthesis of a series of bipodal receptors as they have a tertiary amine protonation site and two primary amine positions that can be functionalised with hydrogen-bond donor and organic solubilising groups. Also, they have ethyl or propyl aliphatic linkers analogous to the tripodal TREN- and TRPN-based receptors, respectively, allowing a direct comparison between tripodal and bipodal systems.



Figure 6.1. Structures of a) N-methyl-2, 2'-diaminodiethylamine and b) 3, 3'-diamino-N-propylamine.

The success with tripodal urea and amide receptors meant these hydrogen-bond donor groups were incorporated into the bipodal ionophores. Bipodal thiourea systems were also synthesised with the aim that they would be more soluble than their tripodal analogues to allow their study in solvent extraction experiments. The

proposed interactions between bipodal urea and amide receptors and $[\text{PtCl}_6]^{2-}$ are shown in Figure 6.2 and a 2:1 L: $[\text{PtCl}_6]^{2-}$ ratio is required for the complex to be charge-neutral.

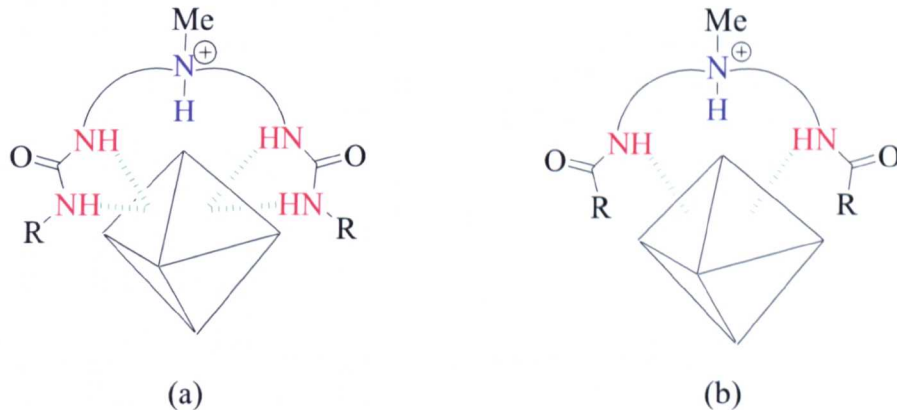
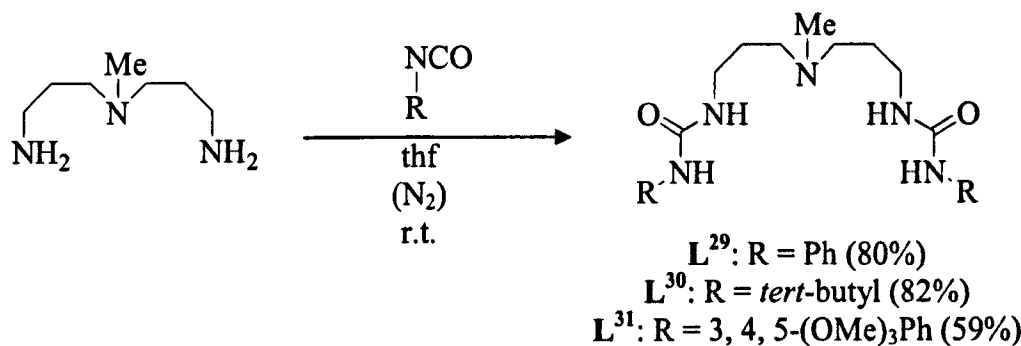


Figure 6.2. The proposed interaction of a) urea and b) amide bipodal receptors with $[\text{PtCl}_6]^{2-}$ (represented by an octahedron). The protonation sites are shown in blue and the hydrogen-bond donor groups are in red. The length of the alkyl spacer unit has not been specified in these diagrams and they are therefore applicable to receptors with an ethyl or propyl spacer.

6.2.1. Synthesis of Bipodal Receptors

6.2.1.1. Urea Receptors

The novel receptors L²⁹–L³¹ were synthesised by the reaction of 3, 3'-diamino-N-propyldiamine with three equivalents of phenyl, *tert*-butyl or 3, 4, 5-trimethoxyphenyl isocyanate, respectively (Scheme 6.1).¹ The products were obtained as colourless solids in good yields and were characterised by ¹H NMR, ¹³C NMR and IR spectroscopy, mass spectrometry and elemental analysis which confirmed them to be analytically pure.



Scheme 6.1. Synthesis of L²⁹–L³¹.

6.2.1.2. Crystal Structure of L²⁹

Single crystals of L²⁹ suitable for X-ray crystal structure analysis were grown by the vapour diffusion of Et₂O into a concentrated solution of the product in MeOH. The receptor crystallised in the monoclinic space group *P21/c* with two independent and non-interacting molecules of L²⁹ in the asymmetric unit (L^{29a} and L^{29b} in Figure 6.3). In L^{29a} there are intra-molecular bifurcated hydrogen-bonds between the urea moieties on each of the two arms between N4—H4A···O1 (H···A = 2.087 Å) and N5—H5A···O1 (H···A = 2.127 Å) (Figure 6.4). Analogous interactions are observed in L^{29b} with N10—H10A···O3 (H···A = 2.204 Å) and N9—H9A···O3 (H···A = 2.161 Å).

The extended structure shows inter-molecular hydrogen-bonding in L^{29a} with N2—H2A···O2 (H···A = 2.121 Å) and N3—H3A···O2 (H···A = 2.092 Å) (Figure 6.5). The molecules of L^{29a} have an alternating orientation and form a chain with each molecule of L^{29a} being linked to the next through bifurcated hydrogen-bonds between the urea moieties. There are analogous inter-molecular interactions between the L^{29b} molecules with N7—H7A···O4 (H···A = 2.056 Å) and N8—H8A···O4 (H···A = 2.140 Å). The full details of the hydrogen-bonding interactions present in the structure of

L^{29} are shown in Table 6.1 and the crystallographic data and structure refinement details are given in Appendix F.

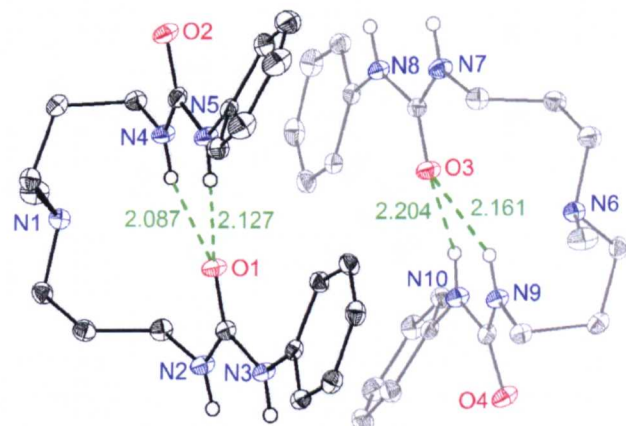


Figure 6.3. Molecular structure of L^{29} showing the two independent molecules L^{29a} and L^{29b} (shown in black and grey, respectively) in the asymmetric unit. All hydrogen atoms (except NH) are omitted for clarity. The intra-molecular hydrogen-bonds are shown in green and the $NH \cdots O$ distances are measured in Å.

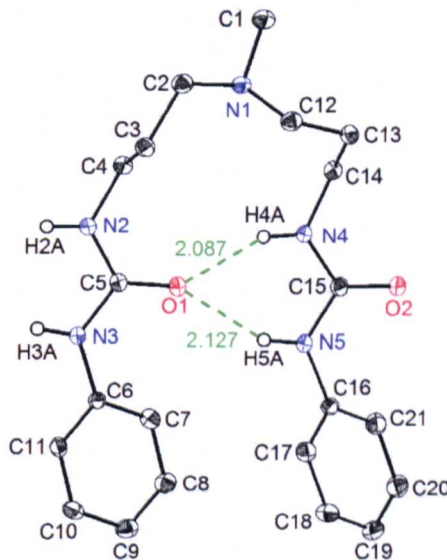


Figure 6.4. Molecular structure of L^{29a} showing intra-molecular hydrogen-bonds. All hydrogen atoms (except NH) are omitted for clarity. Ellipsoids set at 50% probability. The intra-molecular hydrogen-bonds are shown in green and the $NH \cdots O$ distances are measured in Å.

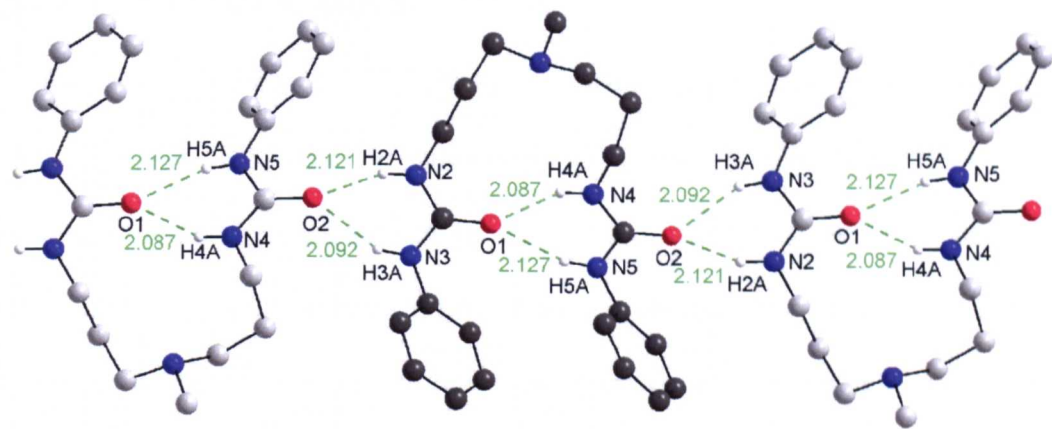


Figure 6.5. View of the structure of L^{29a} showing the intra- and inter-molecular hydrogen-bonds present in the extended structure. All hydrogen atoms (except NH) are omitted for clarity. Hydrogen-bonds are shown in green and measured in Å. The carbon atoms of the alternate molecules of L^{29a} are shown in alternating shades of light and dark grey.

Table 6.1. Intra- and inter-molecular hydrogen-bonds D—H \cdots A in L^{29} (D = donor, A = acceptor, d = distance)

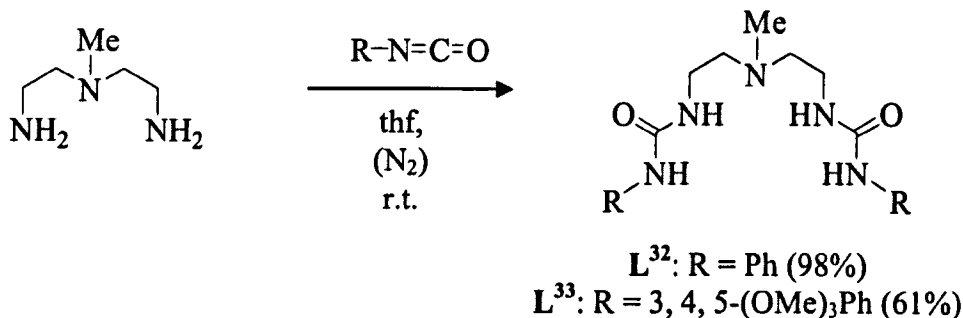
	D—H \cdots A	d(D—H)/Å	d(H \cdots A)/Å	d(D \cdots A)/Å	$\angle(DHA)/^\circ$	Symmetry Code
i	N4—H4A \cdots O1	0.86	2.087	2.8821(14)	153.5	
i	N5—H5A \cdots O1	0.86	2.127	2.9144(14)	152.1	
ii	N2—H2A \cdots O2	0.86	2.121	2.9044(14)	151.2	-x+1/2, y+1/2, -z+1/2
ii	N3—H3A \cdots O2	0.86	2.092	2.8868(14)	153.4	-x+1/2, y+1/2, -z+1/2
iii	N9—H9A \cdots O3	0.86	2.161	2.9281(14)	148.3	
iii	N10—H10A \cdots O3	0.86	2.204	2.9404(14)	143.6	
iv	N7—H7A \cdots O4	0.86	2.056	2.8583(14)	154.8	-x+3/2, y-1/2, z+1/2
iv	N8—H8A \cdots O4	0.86	2.140	2.9099(13)	148.9	-x+3/2, y-1/2, z+1/2

*Class i are intra-molecular hydrogen-bonds in L^{29a} , class ii are inter-molecular hydrogen-bonds in L^{29a} .

Class iii are intra-molecular hydrogen-bonds in L^{29b} , class iv are inter-molecular hydrogen-bonds in L^{29b} .

6.2.1.3. Urea Receptors (part 2)

L^{32} and the novel receptor L^{33} were synthesised by the reaction of N-methyl-2, 2'-diaminodiethylamine with two equivalents of phenyl or 3, 4, 5-trimethoxyphenyl isocyanate, respectively (Scheme 6.2).^{1, 2} The products of both reactions precipitated as colourless solids in yields in excess of 61% and were characterised by ^1H NMR, ^{13}C NMR and IR spectroscopy, mass spectrometry and elemental analysis which showed them to be analytically pure.



Scheme 6.2. Synthesis of L^{32} and L^{33} .

To enable a more accurate comparison between a bipodal receptor and TOA L^{34} was designed which has one octyl substituent and two urea functionalised pendant arms (Figure 6.6). In addition, the comparison of L^{34} with L^{33} will allow the effect of the alkyl substituent to be found.

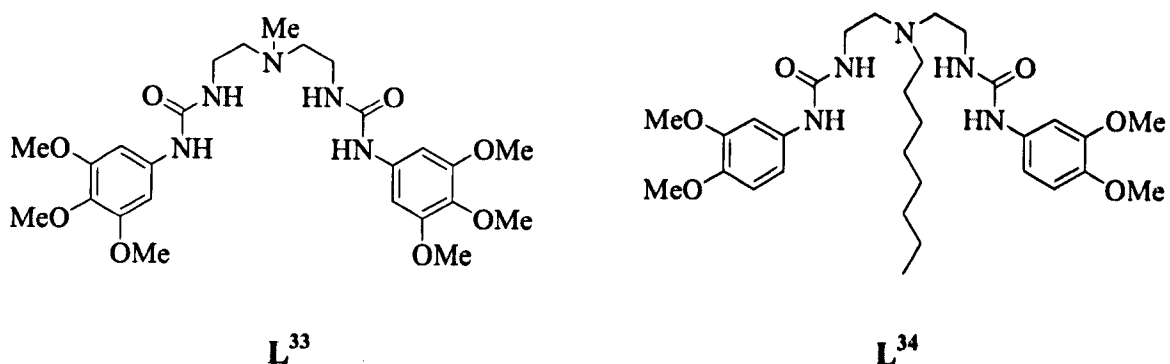
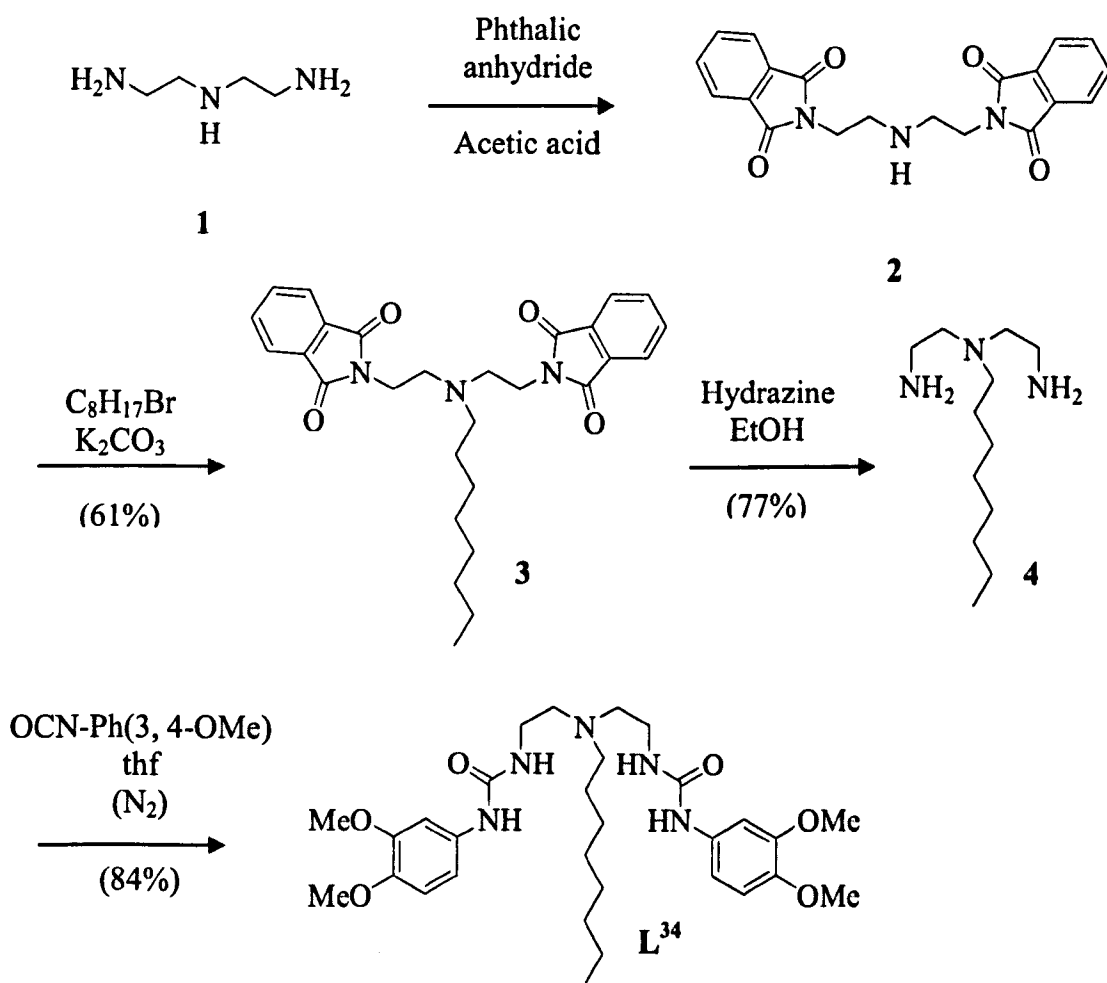


Figure 6.6. Structure of L^{33} and L^{34} .

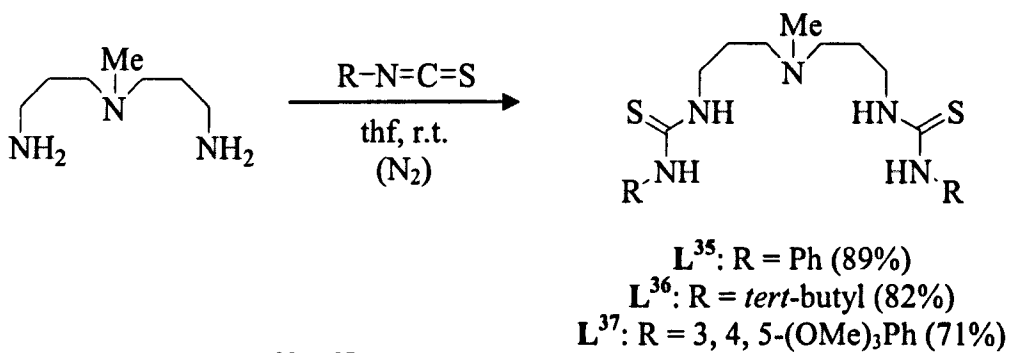
The amine precursor **4** was synthesised following the method of Miranda and co-workers (Scheme 6.3).³ The primary amine groups of diethylenetriamine **1** were protected by reacting with phthalic anhydride to give **2** which is then alkylated using octyl bromide under basic conditions. The subsequent deprotection of **3** is achieved with hydrazine to give the amine precursor **4**. Following a similar method as used for the synthesis of our other urea receptors the amine **4** was reacted with 3, 4-dimethoxyphenyl isocyanate to give the novel receptor **L**³⁴.¹ The product was obtained as an off-white powder in a moderate yield and characterisation of the product by ¹H NMR, ¹³C NMR and IR spectroscopy and mass spectrometry confirmed the formation of the desired receptor.



Scheme 6.3. Synthesis of **L**³⁴

6.2.1.4. Thiourea Receptors

The tripodal TREN- and TRPN-based thiourea receptors formed insoluble complex products which prevented them being studied in solvent extractions. With the aim of synthesising an organic soluble thiourea complex bipodal thiourea receptors were synthesised. The novel receptors L^{35} – L^{37} were synthesised by the reaction of 3, 3'-diamino-N-propylidamine with phenyl, *tert*-butyl or 3, 4, 5-trimethoxyphenyl isothiocyanate, respectively (Scheme 6.4).¹ The products were obtained as a colourless powders and characterisation by ^1H NMR, ^{13}C NMR and IR spectroscopy, mass spectrometry and elemental analysis confirmed the products to be analytically pure.



Scheme 6.4. Synthesis of L^{35} – L^{37}

6.2.1.5. Crystal Structure of L^{35}

Single crystals of L^{35} suitable for X-ray crystal structure analysis were grown by the vapour diffusion of Et_2O into a solution of the product in MeOH . L^{35} crystallises in the monoclinic space group $P21/c$ with four receptors in the unit cell. The structure of L^{35} shows a hydrogen-bond $\text{N}4\cdots\text{H}4\text{A}\cdots\text{N}1$ ($\text{H}\cdots\text{A} = 2.151 \text{ \AA}$) to form an intramolecular six membered ring (Figure 6.7). In all of our other crystal structures the NH groups of urea and thiourea moieties are orientated in the same direction and plane but this is not seen in the structure of L^{35} . The extended structure of L^{35} shows

inter-molecular hydrogen-bonds N5—H5A \cdots S1 ($H\cdots A = 2.432 \text{ \AA}$) and N3—H3A \cdots S2 ($H\cdots A = 2.554 \text{ \AA}$) giving a chain of L^{35} molecules (Figure 6.8). The details of the hydrogen-bonds present in this structure are given in Table 6.2 and the crystallographic data and structure refinement details are given in Appendix F.

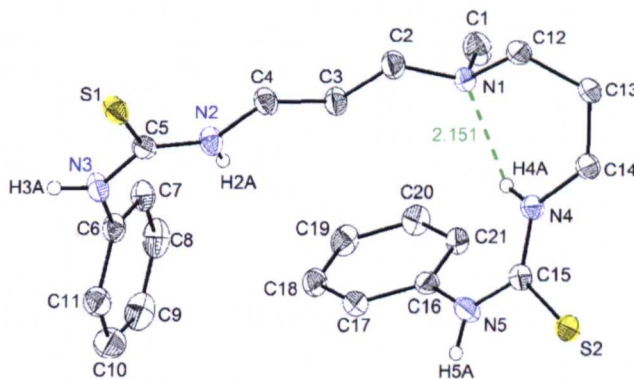


Figure 6.7. Molecular structure of L^{35} showing intra-molecular hydrogen-bonds. All hydrogen atoms (except NH) are omitted for clarity. Ellipsoids set at 50% probability. The intra-molecular hydrogen-bond is shown in green and the $NH\cdots N$ distance is measured in \AA .

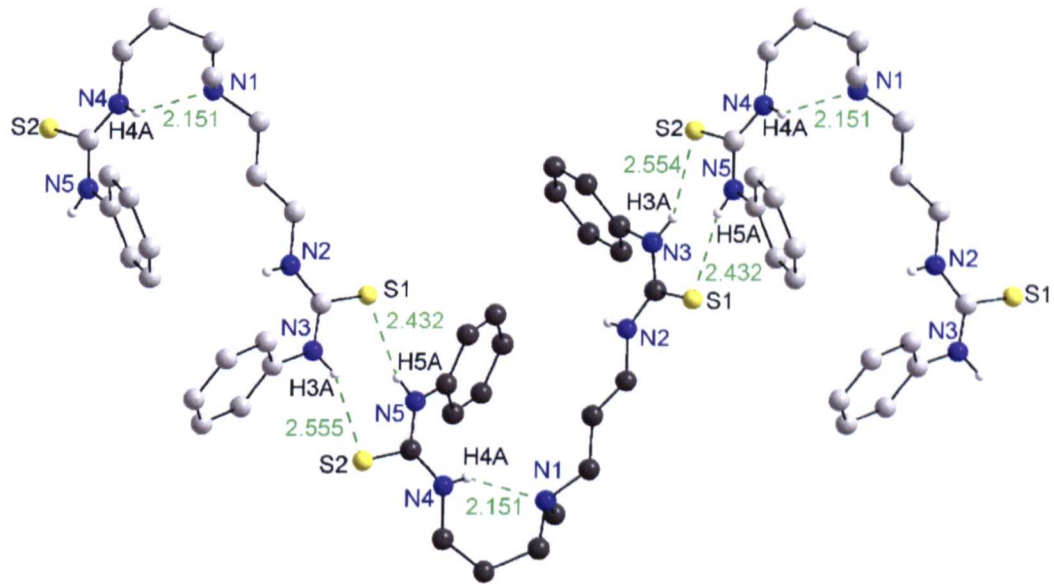


Figure 6.8. View of the structure of L^{35} showing the intra- and inter-molecular hydrogen-bonds present in the extended structure. All hydrogen-atoms (except NH) are omitted for clarity. Hydrogen-bonds are shown in green and measured in \AA . The carbon atoms of the L^{35} molecules are in different shades of light and dark grey.

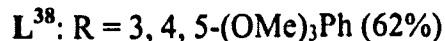
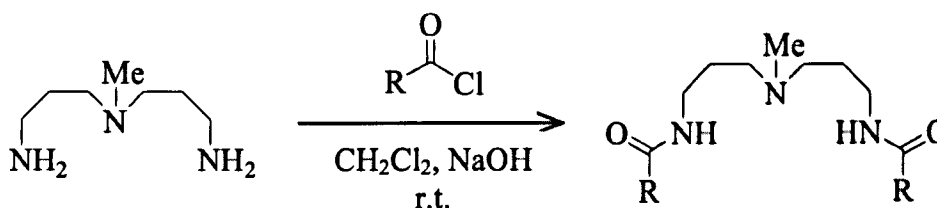
Table 6.2. Intra- and inter-molecular hydrogen-bonds D—H \cdots A in L³⁵ (D = donor, A = acceptor, d = distance)

D—H \cdots A	d(D—H) / Å	d(H \cdots A) / Å	d(D \cdots A) / Å	\angle (DHA) / °	Symmetry Code
N4—H4A \cdots N1	0.86	2.151	2.8103(13)	133	
N3—H3A \cdots S2	0.86	2.554	3.3541(10)	155	-x+2,y+1/2,-z+1/2
N5—H5A \cdots S1	0.86	2.432	3.2604(10)	162	-x+2,y-1/2,-z+1/2

*N4—H4A \cdots N1 is an intra-molecular hydrogen-bond, all other hydrogen-bonds are inter-molecular.

6.2.1.6. Amide Receptors

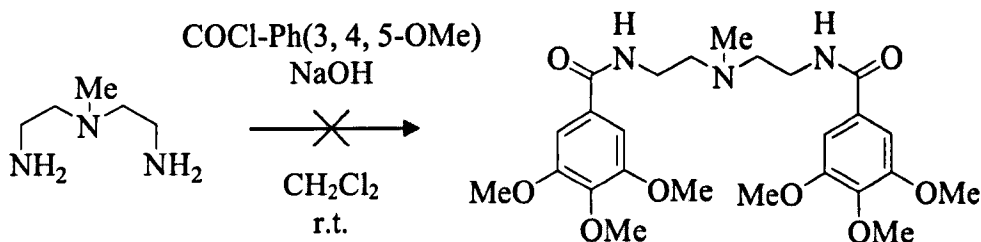
The novel receptor L³⁸ was synthesised by the reaction of 3, 3'-diamino-N-propyldiamine with two equivalents of 3, 4, 5-trimethoxybenzoyl chloride under basic conditions (Scheme 6.5).⁴ The product was obtained as a colourless solid in 62% yield and characterisation by ¹H NMR, ¹³C NMR and IR spectroscopy, mass spectrometry and elemental analysis.



Scheme 6.5. Synthesis of L³⁸.

Following a similar method N-methyl-2, 2'-diaminodiethylamine was reacted with 3, 4, 5-trimethoxybenzoyl chloride (Scheme 6.6).⁴ In previous reactions used to synthesise amide receptors H₂O was added to dissolve NaOH and the desired product was extracted into CH₂Cl₂. During the synthesis of L³⁹ after washing the aqueous phase with CH₂Cl₂ and removing the solvent no product was evident. Extraction into CHCl₃ and toluene was also tried but with no success. It is suggested that the product

is more soluble in H₂O than the organic phase or that the amide product is hydrolysed. No further work was carried out to isolate the desired product as, to be a successful extractant, it is necessary for the receptor to be soluble in an organic solvent.



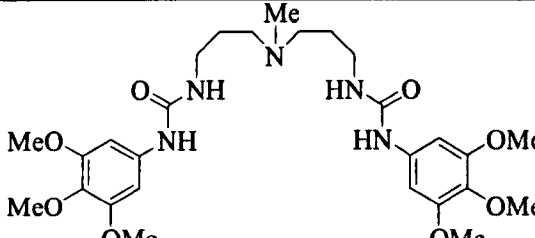
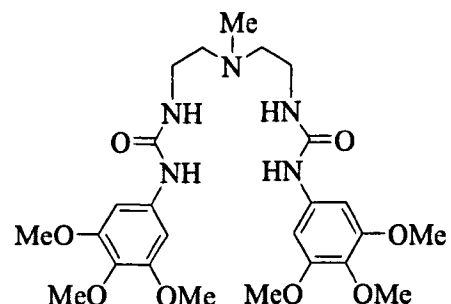
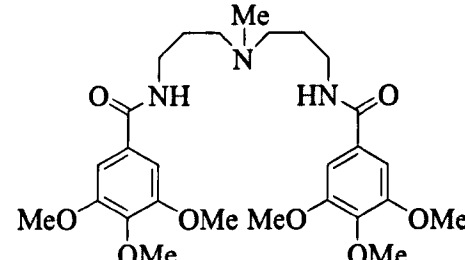
Scheme 6.6. Attempted Synthesis of L³⁹

6.2.2. Potentiometry of Bipodal Receptors*

The number of protonation sites in the bipodal receptors L³¹, L³³ and L³⁸ and the pH at which they become protonated was determined through potentiometry experiments. The results are shown in Table 6.3.

* Potentiometry experiments were carried out by Professor Antonio Bianchi and his group at the University of Florence, Italy.

Table 6.3. Protonation constants determined in MeCN/H₂O 50:50 (v/v) (0.1 M NMe₄Cl, 298.1 ± 0.1 K)

	Receptor	Equilibrium	pKa
L ³¹		$L + H^+ = LH^+$	8.56(1)
L ³³		$L + H^+ = LH^+$	7.61(1)
L ³⁸		$L + H^+ = LH^+$	8.53(1)

*Values in parentheses are the standard deviations on the last significant figure.

For each of the three receptors shown in Table 6.3 there is one protonation site as described by the equilibrium $L + H^+ = LH^+$ and the pKa values indicate that it is the tertiary amine nitrogen position that is protonated.⁵ The pKa's of the bipodal urea receptor L³¹ and the amide receptor L³⁸ differ by 0.03. This suggests that the type of hydrogen-bond donor group does not significantly affect the pH at which the tertiary amine nitrogen is protonated.

L³³ has an ethyl spacer whilst L³¹ has a propyl spacer and the difference in pKa between these bipodal urea receptors is 0.95. This suggests that the length of the

spacer unit affects the pH at which the tertiary amine position is protonated. The tertiary amine position in L^{31} is more basic than in L^{33} because the propyl substituents can more effectively stabilise the alkylammonium cation than ethyl substituents.

L^{21} and L^{38} have different numbers of amide functionalised pendant arms and the difference in pKa for these receptors is 3.6. L^{21} is more basic which suggests that having more functionalised arms bonded to a tertiary amine position increases the basicity.

6.2.3. Complexation Reactions

6.2.3.1. Urea Complexes

Two equivalents of L^{29} – L^{31} were dissolved in MeCN and added to one equivalent of H_2PtCl_6 . For L^{29} ($R = Ph$) and L^{30} ($R = tert\text{-}Bu$) a suspension of precipitate formed in solution. Attempts to isolate the solids by filtration were unsuccessful as the precipitate was very fine and in a small quantity. This also prevented analysis of the reaction solution by NMR spectroscopy or mass spectrometry.

The complexation reaction with L^{31} formed no precipitate and therefore was repeated in CD_3CN . In the 1H NMR spectrum of the resulting solution a signal at 9.12 ppm was assigned to the protonated bridgehead position (N^+HR_3) and there was a downfield shift in the urea NH resonances of 0.41 ppm and 0.30 ppm. Negative electrospray mass spectrometry showed a peak at m/z 1532 assigned to $[(L^{31}H)(L^{31})PtCl_6]^-$ suggesting the formation of the desired complex. There was also a peak at m/z 3471 assigned to $[4(L^{31}H)+3(PtCl_6)]^{2-}$ suggesting that other aggregation species formed under the conditions of the experiment.

Complexation reactions were also attempted with the urea receptors L^{32} and L^{33} . L^{32} ($R = Ph$) was only partially soluble in MeCN which hindered its reaction with H_2PtCl_6 . For L^{33} ($R = Ph(3, 4, 5\text{-OMe})$) a soluble complex $[(L^{33}H)_2PtCl_6]$ formed meaning solvent extraction studies could be performed. Due to the small amount of L^{34} that had been synthesised it was decided to use the sample in solvent extraction studies rather than in complexation reactions.

6.2.3.2. Crystal Structure of $[(L^{29}H)_2PtCl_6]$

L^{29} was dissolved in MeOH and mixed with H_2PtCl_6 dissolved in 2M HCl. The slow evaporation of the resultant solution produced yellow needle-like crystals of $[(L^{29}H)_2PtCl_6]$. The structure crystallised in the monoclinic space group $P2_1/c$ and revealed one $[PtCl_6]^{2-}$ anion lying on a centre of inversion and two receptor cations related by the inversion centre (Figure 6.9). The L^{29} molecules are protonated at the bridgehead position (N1) to give the receptor a +1 charge and for each $[PtCl_6]^{2-}$ anion present there are two $(L^{29}H)^+$ cations giving the structure a net charge of zero and confirming the expected 2:1 $(L^{29}H)^+:[PtCl_6]^{2-}$ stoichiometry of the complex. Disorder around the NMe fragment involving N1, C1 and C2 was modelled over two half-occupied sites with distance restraints and was refined with isotropic atomic displacement parameters.

The structure reveals extensive hydrogen-bonding between the urea moieties of $(L^{29}H)^+$ and $[PtCl_6]^{2-}$ and also between the $(L^{29}H)^+$ cations themselves. Each $[PtCl_6]^{2-}$ anion accepts three hydrogen-bonds from two $(L^{29}H^+)$ cations giving a total of six $NH \cdots Cl$ interactions per anion with N4—H4A \cdots Cl2 ($H \cdots A = 2.604 \text{ \AA}$), N4—H4A \cdots Cl3 ($H \cdots A = 2.745 \text{ \AA}$) and N5—H5A \cdots Cl2 ($H \cdots A = 2.729 \text{ \AA}$) (Figure 6.12).

The N4—H4A donor group is located between the Cl2 and Cl3 atoms (Figure 6.10) and the N5—H5A group is located approximately in the middle of a triangular face defined by Cl1, Cl2 and Cl3 (Figure 6.11). These correspond to areas of highest electron density surrounding $[\text{PtCl}_6]^{2-}$ and are locations predicted to be targeted by NH groups.⁶⁻⁹

There are also intra- and inter-ligand $\text{NH}\cdots\text{O}$ interactions N1—H1D $\cdots\text{O}2$ ($\text{H}\cdots\text{A} = 2.103 \text{ \AA}$), N2—H2A $\cdots\text{O}1$ ($\text{H}\cdots\text{A} = 2.069 \text{ \AA}$) and N3—H3A $\cdots\text{O}1$ ($\text{H}\cdots\text{A} = 2.141 \text{ \AA}$). The extended structure shows that one urea group in each (L^{29}H^+) cation hydrogen-bonds to $[\text{PtCl}_6]^{2-}$ while the other hydrogen-bonds to an adjacent (L^{29}H^+) molecule to give $\cdots((\text{L}^{29}\text{H}^+)\cdots[\text{PtCl}_6]^{2-}\cdots(\text{L}^{29}\text{H}^+))\cdots((\text{L}^{29}\text{H}^+)\cdots[\text{PtCl}_6]^{2-}\cdots(\text{L}^{29}\text{H}^+))\cdots$. The details of the hydrogen-bonds present in this structure are given in Table 6.4 and the crystallographic data and structure refinement details are given in Appendix F.

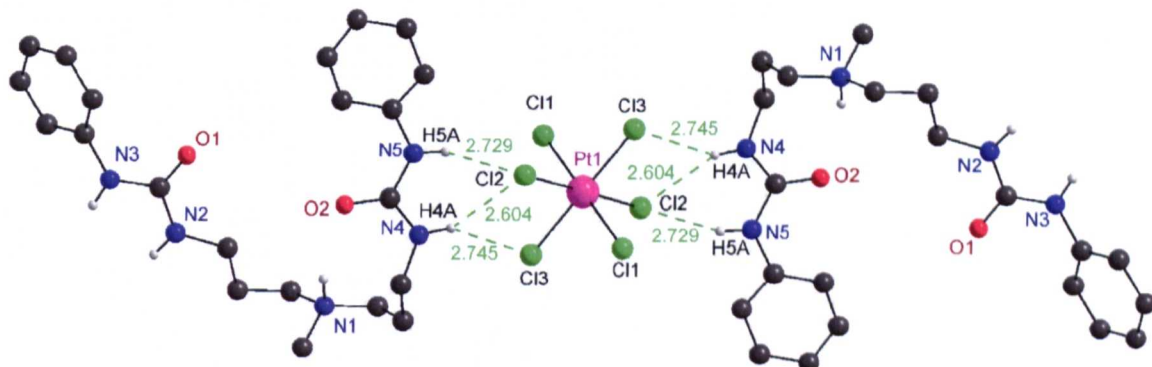


Figure 6.9. View of the structure of $(\text{L}^{29}\text{H})_2\text{PtCl}_6$ showing the $\text{N}-\text{H}\cdots\text{Cl}-\text{Pt}$ hydrogen-bonds to one $[\text{PtCl}_6]^{2-}$ anion. All hydrogen atoms (except NH) are omitted for clarity. Hydrogen-bonds are shown in green and measured the $\text{NH}\cdots\text{Cl}$ distances are measured in \AA .

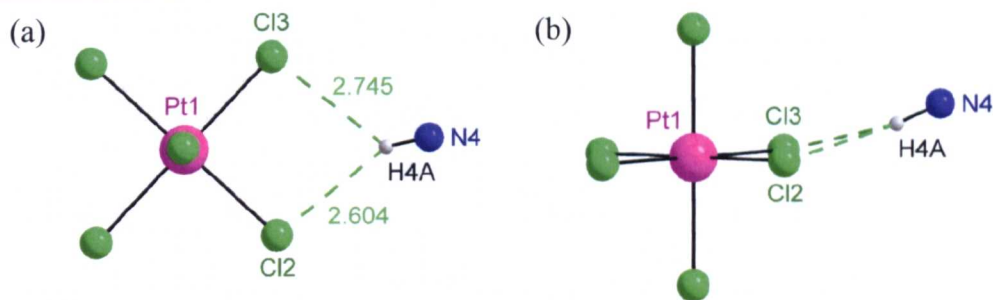


Figure 6.10. a) Highlighting the bifurcated nature of the $\text{NH}\cdots\text{Cl}$ hydrogen bonds formed from H4A and b) the H4A group is almost in the same plane as the $\text{Cl12}, \text{Cl13}$ edge.

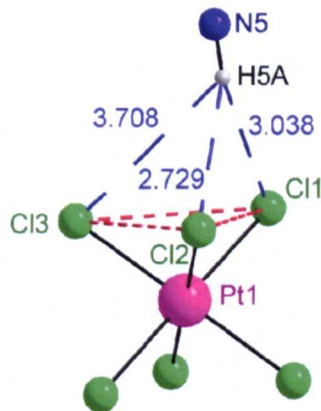


Figure 6.11. Highlighting how the H5A atom targets a triangular face (shown in red) of the octahedron.

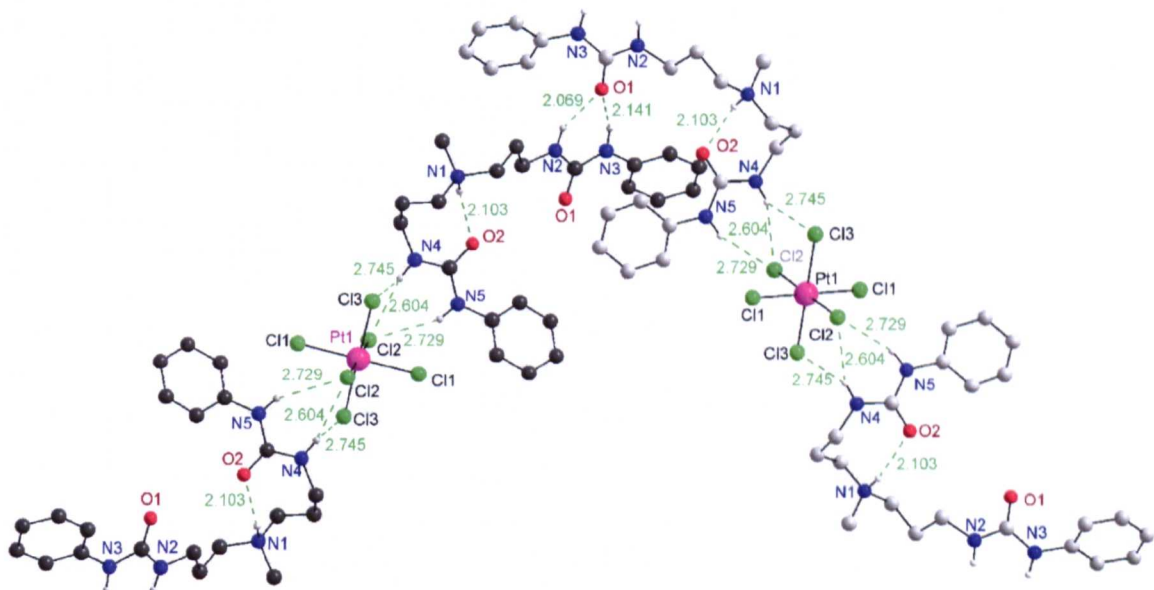


Figure 6.12. View of the structure of $[(\text{L}^{29}\text{H})_2\text{PtCl}_6]$ showing the $\text{NH}\cdots\text{Cl}$ and $\text{NH}\cdots\text{O}$ hydrogen-bonds in the structure. All hydrogen atoms (except NH) are omitted for clarity. Hydrogen-bonds are shown in green and measured the $\text{NH}\cdots\text{A}$ ($\text{A} = \text{Cl}$ or O) distances are measured in Å. The carbon atoms of each $[(\text{L}^{29}\text{H})_2\text{PtCl}_6]$ unit are shown in different shades of light and dark grey.

Table 6.4. Inter-molecular hydrogen-bonds in $[(L^{29}H)_2PtCl_6]$ (D = donor, A = acceptor, d = distance).

D—H \cdots A	d(D—H) / Å	d(H \cdots A) / Å	d(D \cdots A) / Å	\angle (DHA) / °	Symmetry Code
N1—H1D \cdots O2	0.93	2.103	2.912(13)	145	
N2—H2A \cdots O1	0.88	2.069	2.885(7)	154	x, -y+1/2, z-1/2
N3—H3A \cdots O1	0.88	2.141	2.937(7)	150	x, -y+1/2, z-1/2
N4—H4A \cdots Cl2	0.88	2.604	3.411(7)	153	-x+1, -y+1, -z+2
N4—H4A \cdots Cl3	0.88	2.745	3.386(9)	131	-x+1, -y+1, -z+2
N5—H5A \cdots Cl2	0.88	2.729	3.521(5)	151	-x+1, -y+1, -z+2

* The NH \cdots Cl and NH \cdots O interactions are separated by a horizontal line.

The conformation of the receptor changes between L²⁹ and $[(L^{29}H)_2PtCl_6]$. In the crystal structure of L²⁹ (see Section 6.2.2.2) the two pendant arms have a parallel orientation with a bifurcated intra-ligand hydrogen-bond between the urea moieties on the pendant arms. The arms are aligned less in $[(L^{29}H)_2PtCl_6]$ and there are no intra-ligand hydrogen-bonds between the urea moieties.

It was thought that a bipodal receptor would form fewer hydrogen-bonds to $[PtCl_6]^{2-}$ than a tripodal urea receptor because there are fewer NH donor groups available. The structure $[(L^{29}H)_2PtCl_6]$ shows that two out of four functionalised arms interact with the anion and there are six NH \cdots Cl hydrogen-bonds to each $[PtCl_6]^{2-}$. In contrast, the structure with the tripodal urea receptor $[(L^3H)_2PtCl_6]$ has two out of six urea groups interacting with $[PtCl_6]^{2-}$ and a total of eight NH \cdots Cl hydrogen-bonds to each $[PtCl_6]^{2-}$. This suggests that the number of functionalised pendant arms does not play a significant part in the number of hydrogen-bonds that are formed to $[PtCl_6]^{2-}$ in the solid state.

6.2.3.3. Thiourea Complexes

In the complexation reactions between L^{35} – L^{37} and H_2PtCl_6 yellow-orange precipitates formed. The products were insoluble in all common solvents meaning it was not possible to record their 1H NMR spectra. IR spectroscopy showed bands due to N—H and C=S stretches and alongside elemental analysis suggested the formation of the desired complexes $[(LH)_2PtCl_6]$. Varying the receptor scaffold of the thiourea receptors from tripodal to bipodal was unsuccessful in improving their organic solubility and prevented their analysis in solvent extractions.

6.2.3.4. Amide Complex

Two equivalents of L^{38} were reacted with H_2PtCl_6 in MeCN to give a transparent orange solution. To confirm the formation of a soluble complex the reaction was repeated in CD_3CN and the 1H NMR spectrum of the resulting solution recorded. A signal at 8.87 ppm was assigned to the protonated bridgehead nitrogen position and there was a downfield shift of 0.14 ppm for the amide NH signal.

Mass spectrometry on the reaction solution suggested fragmentation of a NH—CO bond in L^{38} to form L^{38b} (Figure 6.13). A peak at m/z 1279 was assigned to $[(L^{38}H)(L^{38b})PtCl_6]^-$ and although one of the receptor molecules has fragmented the ratio of the complex remains as 2:1 $L:[PtCl_6]^{2-}$. There were also peaks at m/z 1849 and m/z 2419 assigned to $[(L^{38}H)(L^{38})(L^{38b}H)(PtCl_6)(Cl)]^-$ and $[(L^{38}H)(L^{38})_2(L^{38b}H)(PtCl_6)(Cl)_2]^-$, respectively.

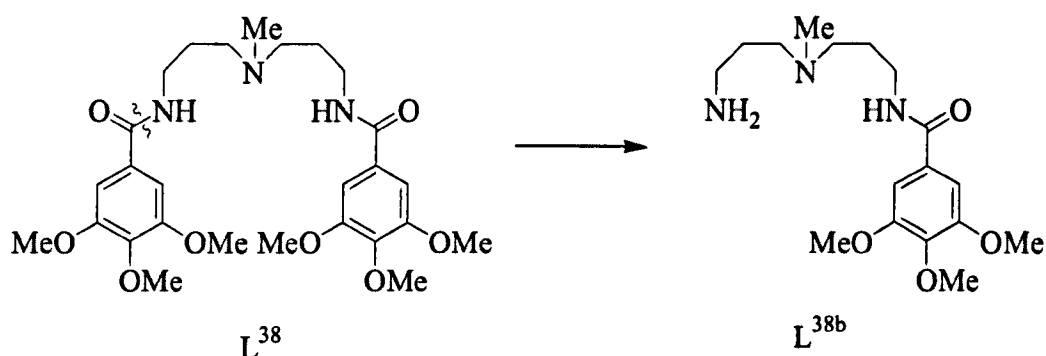


Figure 6.13. The fragmentation of L^{38} to form L^{38b} .

6.2.3.5. Crystal Structure of $[(L^{38}H)_2PtCl_6]$

Two equivalents of L^{38} were mixed with one equivalent of H_2PtCl_6 in MeCN. The solution was left at room temperature for several weeks during which time yellow needles of the complex $[(L^{38}H)_2PtCl_6]$ crystallised. The L^{38} molecules present in the structure are protonated at the tertiary amine position (N1) giving them a +1 charge and as the $(L^{38}H)^+:[PtCl_6]^{2-}$ ratio is 2:1 the crystal has a net charge of zero. The structure also contains four molecules of disordered MeCN in the unit cell however these have been omitted from the subsequent Figures.

There are N—H \cdots Cl—Pt interactions between both amide NH groups in $(L^{38}H^+)$ and two separate molecules of $[PtCl_6]^{2-}$ with N2—H2A \cdots Cl2 ($H\cdots A = 2.464 \text{ \AA}$) and N3—H3A \cdots Cl3 ($H\cdots A = 2.581 \text{ \AA}$) (Figure 6.14). There is a centre of inversion at Pt1 which means that each $[PtCl_6]^{2-}$ anion accepts one hydrogen-bond from four different $(L^{38}H^+)$ cations. The H3A atom hydrogen-bonds to Cl3 but the H3A \cdots Cl1 distance ($H\cdots A = 2.990 \text{ \AA}$) is slightly too long to be classed as a close interaction (Figure 6.15a). The H3A atom is located between the Cl1 and Cl3 atoms but slightly out of the plane defined by Pt1, Cl1 and Cl3 (Figure 6.15b). There are also inter-ligand interactions N1—H1 \cdots O5 ($H\cdots A = 2.038 \text{ \AA}$) and N1—H1 \cdots O1

($H \cdots A = 2.569 \text{ \AA}$) however, for clarity, these interactions are not shown in Figure 6.14.

Discrete $[(L^{38}\text{H})_2\text{PtCl}_6]$ entities are not present despite being observed in all other complex structures. Instead, there is an extended hydrogen-bonded network linking $(L^{38}\text{H}^+)$ cations with $[\text{PtCl}_6]^{2-}$ anions (Figure 6.16). Each $[\text{PtCl}_6]^{2-}$ anion in accepts a total of four hydrogen-bonds which is the same number as were observed in the complex structure with tripodal amide L¹⁷. This infers that the number of amide functionalised pendant arms does not effect the amount of hydrogen-bonds formed to $[\text{PtCl}_6]^{2-}$ in the solid state. The details of the hydrogen-bonds present in this structure are given in Table 6.5 and the crystallographic data and structure refinement details are given in Appendix F.

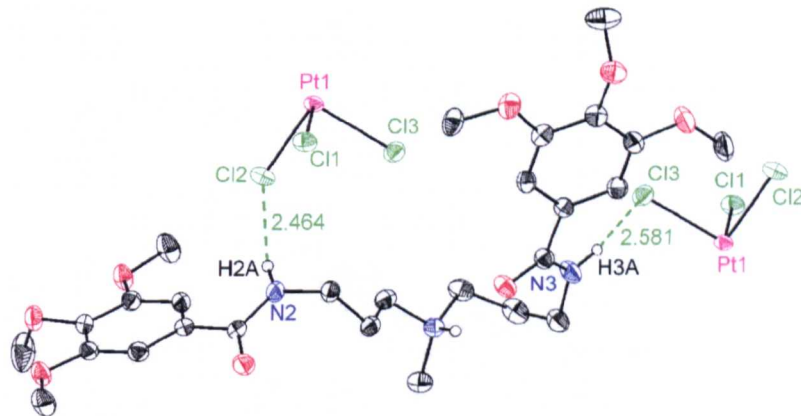


Figure 6.14. Part of the molecular structure of $[(L^{38}\text{H})_2\text{PtCl}_6]$ highlighting the $\text{N}-\text{H} \cdots \text{Cl}-\text{Pt}$ hydrogen-bonds from one $(L^{38}\text{H}^+)$ cation. All hydrogen-atoms (except NH) and solvent molecules are omitted for clarity. Ellipsoids are set at 50% probability. The hydrogen-bonds are shown in green and $\text{NH} \cdots \text{Cl}$ distances are measured in \AA .

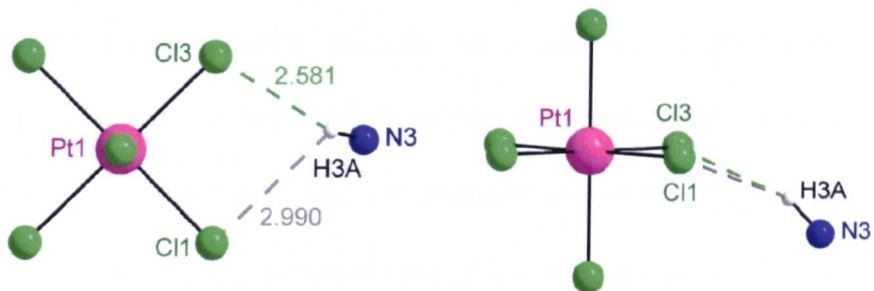


Figure 6.15. a) Highlighting the location of H3A and b) the orientation of H3A relative to the Cl1, Cl3 edge.

Table 6.5. Inter-molecular hydrogen-bonds in $[(L^{38}H)_2PtCl_6]$ (D = donor, A = acceptor, d = distance).

D—H \cdots A	d(D—H)/ \AA	d(H \cdots A)/ \AA	d(D \cdots A)/ \AA	$\angle(DHA)$ /°	Symmetry Code
N2—H2A \cdots Cl2	0.880	2.464	3.310	161.61	
N3—H3A \cdots Cl3	0.880	2.581	3.365	148.84	-x+1, -y+1, -z+1
N1—H1 \cdots O5	0.845	2.038	2.751	141.67	
N1—H1 \cdots O1	0.845	2.569	3.154	127.26	-x, -y+1, -z+2

*A horizontal line separates the NH \cdots Cl and NH \cdots O interactions

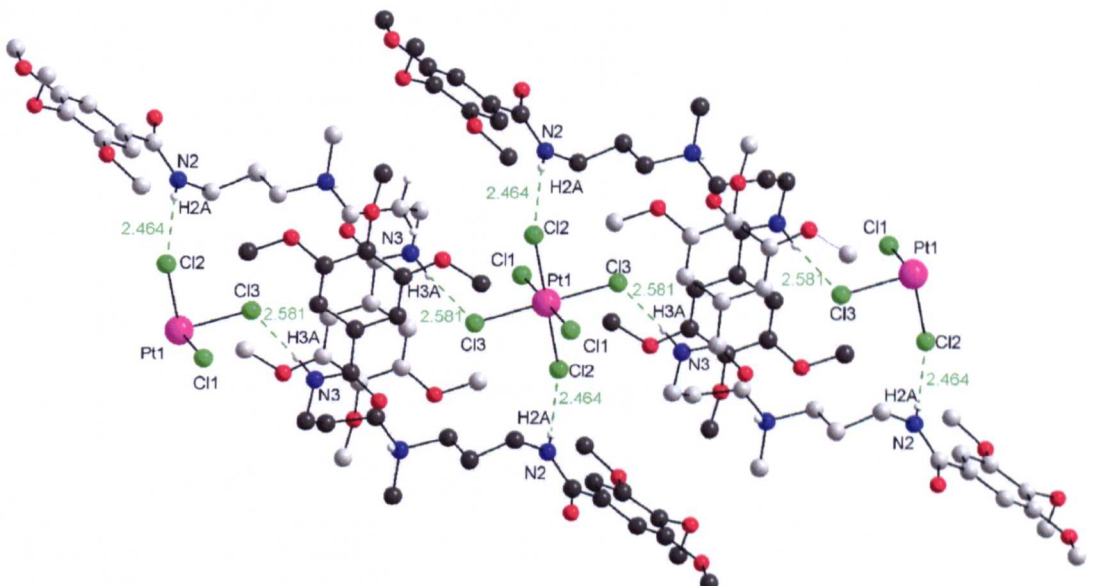


Figure 6.16. View of the structure of $[(L^{38}H)_2PtCl_6]$ showing the N—H \cdots Cl—Pt hydrogen-bonds to $[PtCl_6]^{2-}$. All hydrogen atoms (except NH) are omitted for clarity. Hydrogen-bonds are shown in green and measured the NH \cdots Cl distances are measured in \AA . The carbon atoms belonging to each $(L^{38}H^+)$ cation are shown in different shades of grey.

From the crystallographic analyses of complexes an estimated scale of extraction efficiency was constructed. Receptors which form the most hydrogen-bonds to $[\text{PtCl}_6]^{2-}$ in the solid state are assumed to form similar interactions in solution and the more hydrogen-bonds formed the stronger the interaction and the higher the extraction. Thus, the expected order of extraction is: tripodal urea > bipodal urea \approx tripodal sulfonamide > tripodal amide \approx bipodal amide.

6.2.4. Extraction Studies

6.2.4.1. Test Extractions

Test extractions with the urea receptors L^{31} and L^{34} and the amide receptor L^{38} showed a colour change of the CHCl_3 phase indicating uptake of $[\text{PtCl}_6]^{2-}$ and consequently were studied in more detail. L^{33} showed only a negligible colour change however full extraction studies were still performed to quantitatively assess the amount of $[\text{PtCl}_6]^{2-}$ extracted. In the test extraction with the thiourea receptor L^{37} an insoluble precipitate formed preventing analysis of this system.

6.2.4.2. Urea vs Amide

Extraction results for the bipodal urea receptor L^{31} and amide system L^{38} are compared in Figure 6.17. At an arbitrary [Receptor]: $[\text{PtCl}_6]^{2-}$ ratio of 3:1 L^{31} extracts 28% of $[\text{PtCl}_6]^{2-}$ while L^{38} extracts 13% (Table 6.6). This observation is consistent with previous results which show that ureas outperform analogous amide systems.

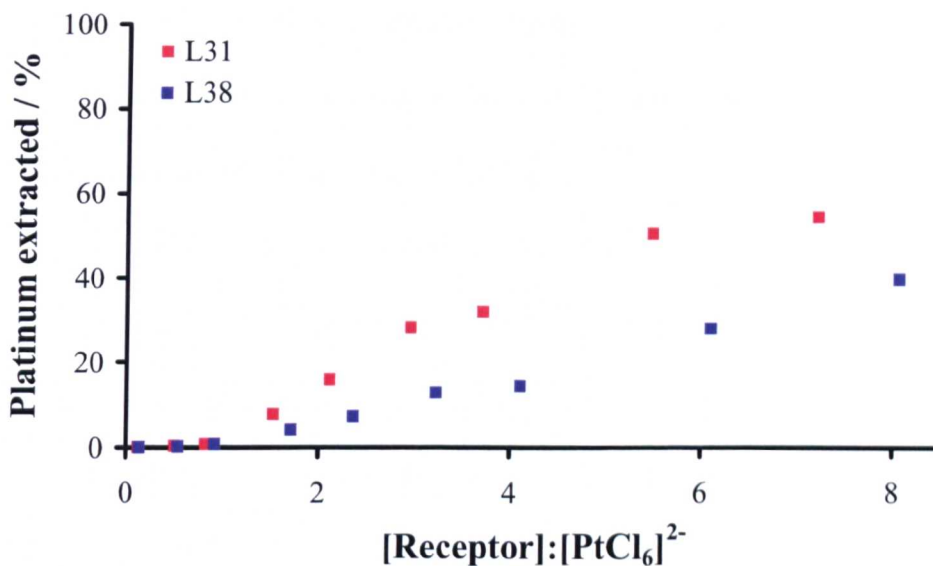
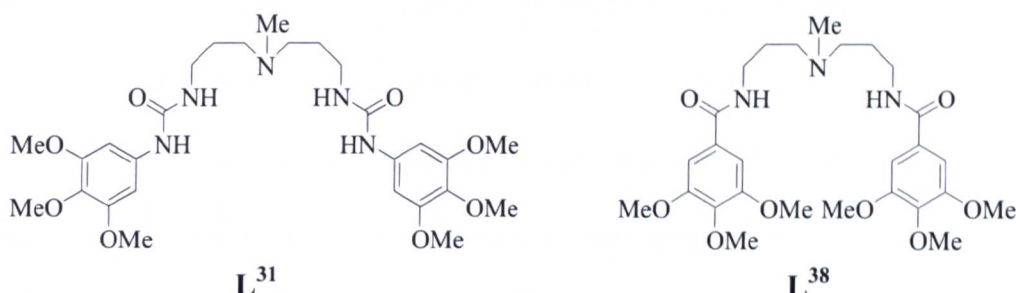


Figure 6.17. Plot of % Pt extracted as $[\text{PtCl}_6]^{2-}$ from aqueous 0.6 M HCl into CHCl_3 as a function of [Receptor]:[Pt] ratio.

Table 6.6. % of Pt extracted as $[\text{PtCl}_6]^{2-}$ into CHCl_3 from aqueous 0.6 M HCl in the presence of a 3 molar excess of L

Receptor	L ³¹	L ³⁸
% Pt extracted at 3 molar excess of L	28	13

The proposed reasons for ureas outperforming amides include the number of hydrogen-bonds, selectivity and solubility. As there are more acidic NH donor groups per arm in a urea receptor than in an amide receptor this increases the probability of the NH donor being in a suitable location to form a hydrogen-bond to $[\text{PtCl}_6]^{2-}$. This hypothesis correlates with the crystal structures of the complexes

which show that there are more hydrogen-bonds between the bipodal urea receptor L²⁹ and [PtCl₆]²⁻ than with the analogous amide receptor L³⁸.

Urea receptors may also be more selective than amide receptors for [PtCl₆]²⁻.¹⁰ Reduced selectivity means complexes with Cl⁻ may also form leading to lower extraction of [PtCl₆]²⁻. Alternatively, urea receptors may form a complex with higher organic solubility. This is supported by the attempted synthesis of the amide receptor L³⁹ which could not be isolated due to the preferred solubility of the product in H₂O rather than an immiscible organic phase.

Following the method of Yoshizawa, the extraction data for L³¹ and L³⁸ were analysed.¹¹ Both L³¹ and L³⁸ produce a straight line graph with gradients of 2.1731 and 1.7968, respectively, suggesting 2:1 (LH)⁺:[PtCl₆]²⁻ complex stoichiometries in solution (Figure 6.18). This is consistent with the spectroscopic and crystallographic data of the complexes.

Yoshizawa reports that the intercept of these graphs is representative of K_{PtCl₆} giving a measure of the strength of interaction and allowing a relative scale of extraction efficiencies to be constructed. A larger value for the intercept infers a higher value of K_{PtCl₆} and thus, a more stable complex. The urea receptor L³¹ has an intercept of 4.2808 whilst the amide receptor L³⁸ has an intercept of 3.017 which correlates with the observed extraction efficiencies.

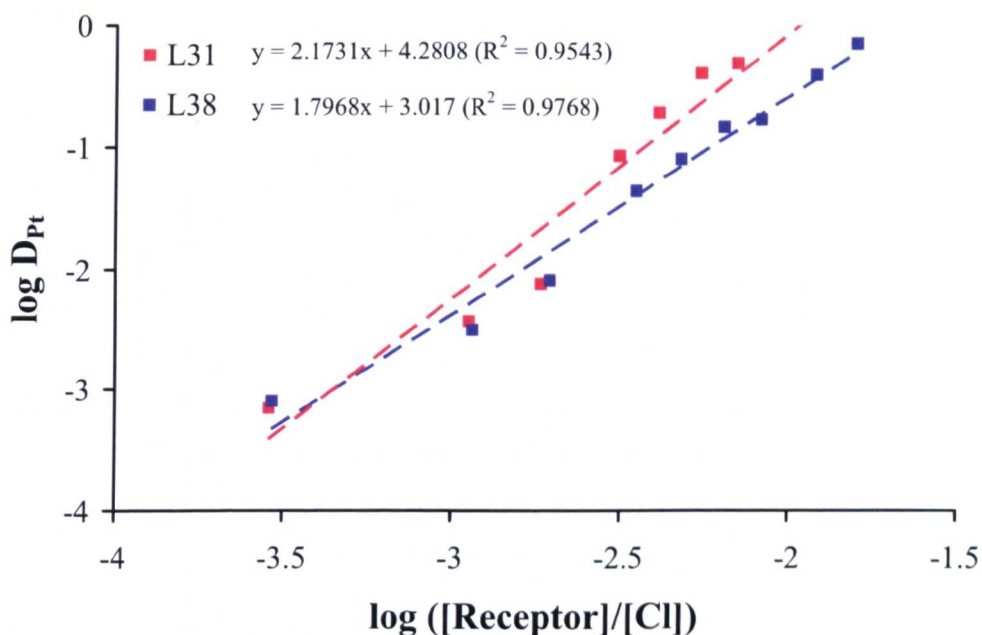
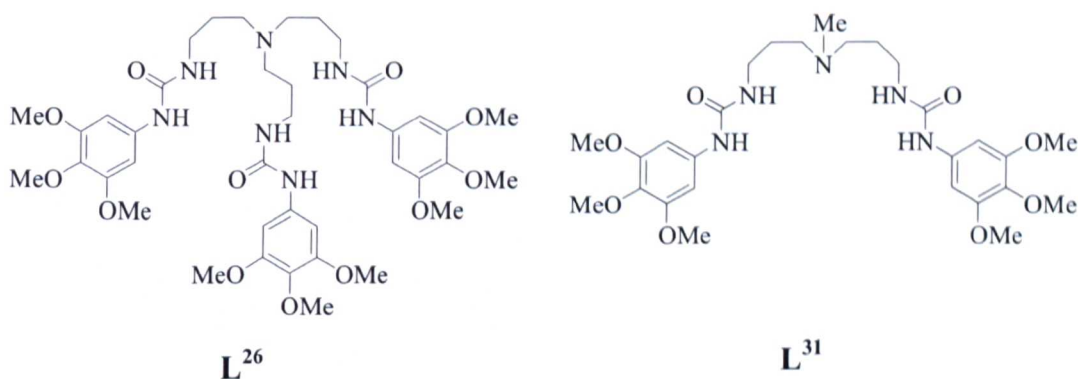


Figure 6.18. Plot of $\log D_{\text{Pt}}$ against $\log ([\text{Receptor}]/[\text{Cl}])$.

6.2.4.3. Tripodal vs Bipodal Receptors

The extraction results for tripodal urea receptor L^{26} and the bipodal analogue L^{31} are compared in Figure 6.19. Across all $[\text{Receptor}]:[\text{PtCl}_6]^{2-}$ ratios L^{26} outperforms L^{31} and at an arbitrary $[\text{Receptor}]:[\text{PtCl}_6]^{2-}$ ratio of 3:1 L^{26} extracts 74% whilst L^{31} extracts only 28% (Table 6.7).



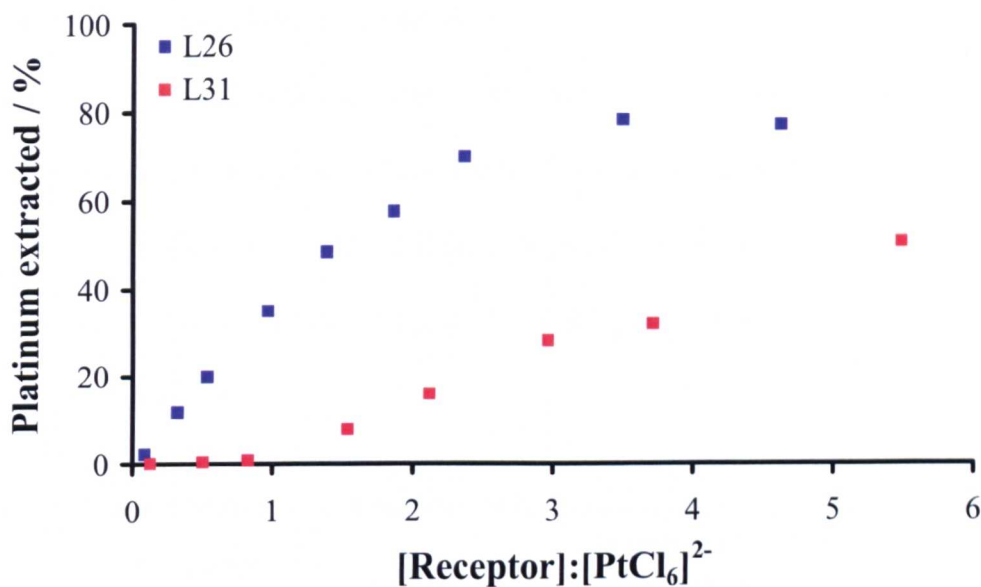


Figure 6.19. Plot of % Pt extracted as $[\text{PtCl}_6]^{2-}$ from aqueous 0.6 M HCl into CHCl_3 as a function of [Receptor]:[Pt] ratio.

Table 6.7. % of Pt extracted as $[\text{PtCl}_6]^{2-}$ into CHCl_3 from aqueous 0.6 M HCl in the presence of a 3 molar excess of L

Receptor	L^{26}	L^{31}
% Pt extracted at 3 molar excess of L	74	28

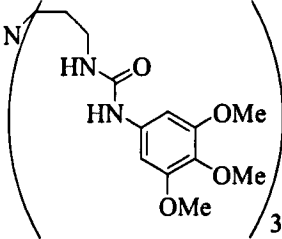
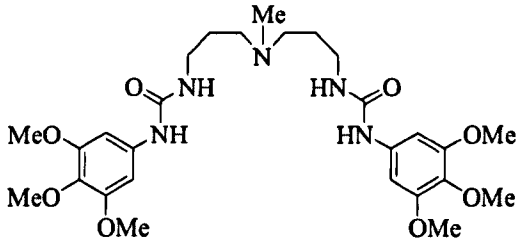
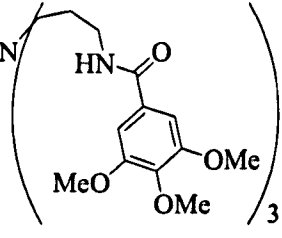
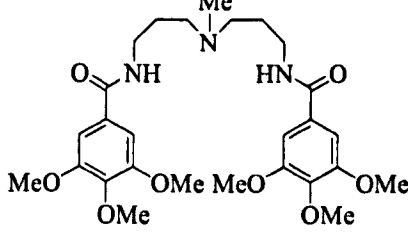
These results indicate having more hydrogen-bonds increases extraction efficiency. This correlates with the complex crystal structures which show that the tripodal urea receptor L^3 forms eight hydrogen-bonds to each $[\text{PtCl}_6]^{2-}$ anion while the bipodal urea receptor L^{29} only forms six.

Monopodal receptors were predicted to have lower extraction efficiency than tripodal and bipodal systems as they have fewer hydrogen-bond donor groups. With the aim of further improving extraction efficiency, tetrapodal systems are being synthesised and evaluated in the Schröder group.

6.2.4.4. Geometry vs Hydrogen-bonds

If the only factor affecting extraction efficiency is the number of hydrogen-bond donor groups then it would be expected that a bipodal urea receptor which has 4 NH donor groups would extract more than a tripodal amide which has 3 NH donor moieties. The extraction results for tripodal and bipodal urea and amide results are compared in Table 6.8.

Table 6.8. Relationship between number of NH donor groups and % of extraction.

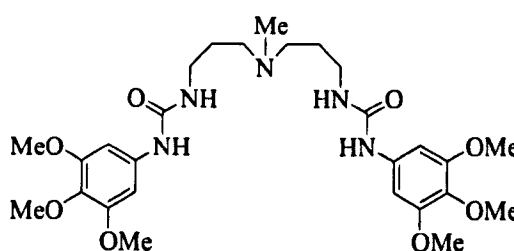
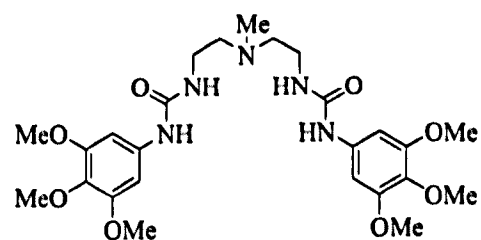
Receptor	Number of NH donor groups	% Extraction
	L ²⁶	6
	L ³¹	4
	L ²⁸	3
	L ³⁸	2

Despite L^{31} having more NH donors than L^{28} it extracts less $[PtCl_6]^{2-}$. A possible explanation for this observation is that L^{28} forms a complex that has higher organic solubility than L^{31} which leads to higher extraction efficiency. As there are more functionalised arms in L^{28} the receptor may also be more selective for the target anion.

Predicting extraction efficiency is, therefore, not as simple as counting individual NH groups in a receptor molecule. A more accurate method to predict extraction efficiency is to count the number of urea or amide moieties thus, tripodal ureas and amides both have three while bipodal ureas and amides both have two donor units. When two receptors have the same number of donor units (for example, three in tripodal systems) it is then useful to count each NH donor group and use this as a secondary indicator of extraction efficiency.

6.2.4.5. Effect of Spacer Unit

The extraction results for L^{31} and L^{33} are compared in Figure 6.20. Test extractions with L^{33} showed a negligible colour change of the organic phase suggesting little uptake of $[PtCl_6]^{2-}$ and this was verified quantitatively in the extraction studies. In the presence of a three molar excess of receptor L^{31} extracts 32% compared with only 0.7% for L^{33} (Table 6.9).

 L^{31}  L^{33}

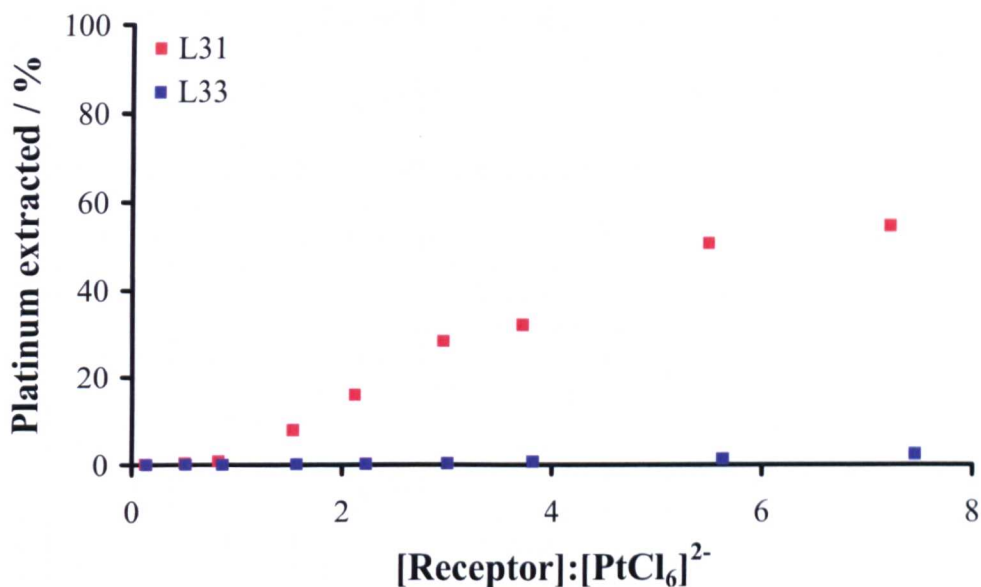


Figure 6.20. Plot of % Pt extracted as $[\text{PtCl}_6]^{2-}$ from aqueous 0.6 M HCl into CHCl_3 as a function of [Receptor]:[Pt] ratio.

Table 6.9. % of Pt extracted as $[\text{PtCl}_6]^{2-}$ into CHCl_3 from aqueous 0.6 M HCl in the presence of a 3 molar excess of L

Receptor	L^{31}	L^{33}
% Pt extracted at 3 molar excess of L	32	0.7

These results show that higher extraction is achieved with bipodal urea extractants with propyl spacers. This is in contrast to tripodal receptors which show higher extraction with ethyl spacer units. For the bipodal structures a longer and more flexible propyl backbone may be preferred because it allows the NH donor groups to target $[\text{PtCl}_6]^{2-}$ more effectively. The low extraction for L^{33} may be due to the complex being more soluble in the aqueous phase than the organic phase while the propyl spacer in L^{31} may encourage the organic solubility of the complex resulting in higher extraction.

A Yoshizawa analysis¹¹ with the extraction data for L^{33} shows poor correlation between the data points and the line of best fit; the gradient of which is

not near to the theoretical value of two (Figure 6.21). This is thought to be because the complex that forms has very low solubility in the CHCl_3 phase of the extraction and thus the calculations and assumptions used to construct the plot are invalid.

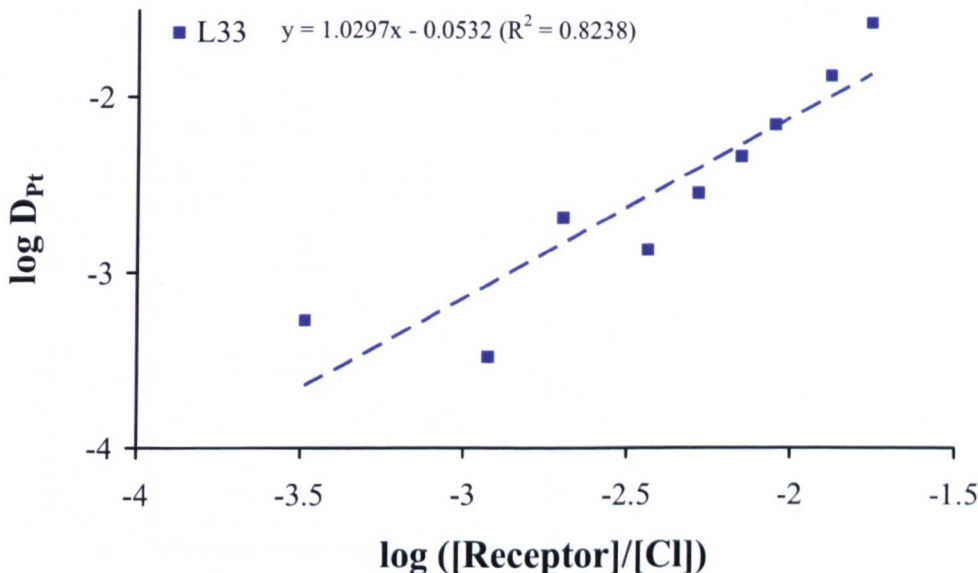


Figure 6.21. Plot of $\log D_{\text{Pt}}$ against $\log ([\text{Receptor}]/[\text{Cl}])$.

6.2.4.6. Effect of Alkyl Substituent

The extraction results for L^{33} and L^{34} are compared in Figure 6.22. These receptors differ in the type of alkyl substituent on the tertiary amine bridgehead nitrogen and the difference in the number of methoxy substituents is not thought to be significant in this case. Across all $[\text{Receptor}]:[\text{PtCl}_6]^{2-}$ ratios L^{34} significantly outperforms L^{33} and at an arbitrary ratio of 3:1 L^{33} extracts 0.3% whilst L^{34} extracts 41% (Table 6.10).

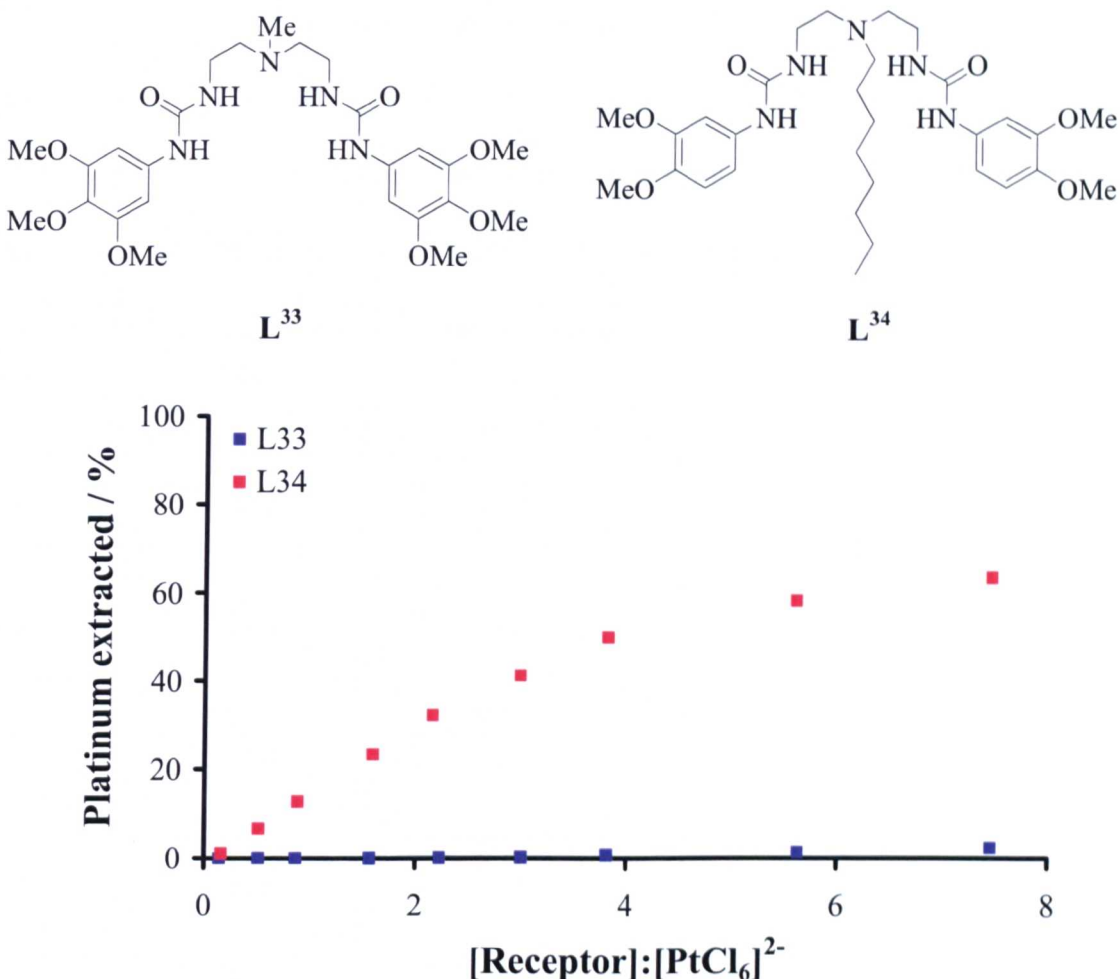


Figure 6.22. Plot of % Pt extracted as $[PtCl_6]^{2-}$ from aqueous 0.6 M HCl into $CHCl_3$ as a function of [Receptor]:[Pt] ratio.

Table 6.10. % of Pt extracted as $[PtCl_6]^{2-}$ into $CHCl_3$ from aqueous 0.6 M HCl in the presence of a 3 molar excess of L

Receptor	L^{33}	L^{34}
% Pt extracted at 3 molar excess of L	0.3	41

These results suggest that the nature of the alkyl substituent does affect extraction efficiency. It is thought that the octyl substituent in L^{34} increases the organic solubility of the resulting complex compared with L^{33} . This illustrates that slight design modifications can play a significant part in the observed extraction efficiency and that optimising the organic solubility of our complexes is vital.

A Yoshizawa analysis¹¹ was performed with the extraction data for L³⁴ and the results are shown in Figure 6.23. The data points fit well to the line of best fit ($R^2 = 0.971$) however, the gradient shows deviation from the theoretical value of two which has been attributed to other species being formed such as $[(L^{34}H)Cl]$ due to lower selectivity of bipodal receptors for $[PtCl_6]^{2-}$.

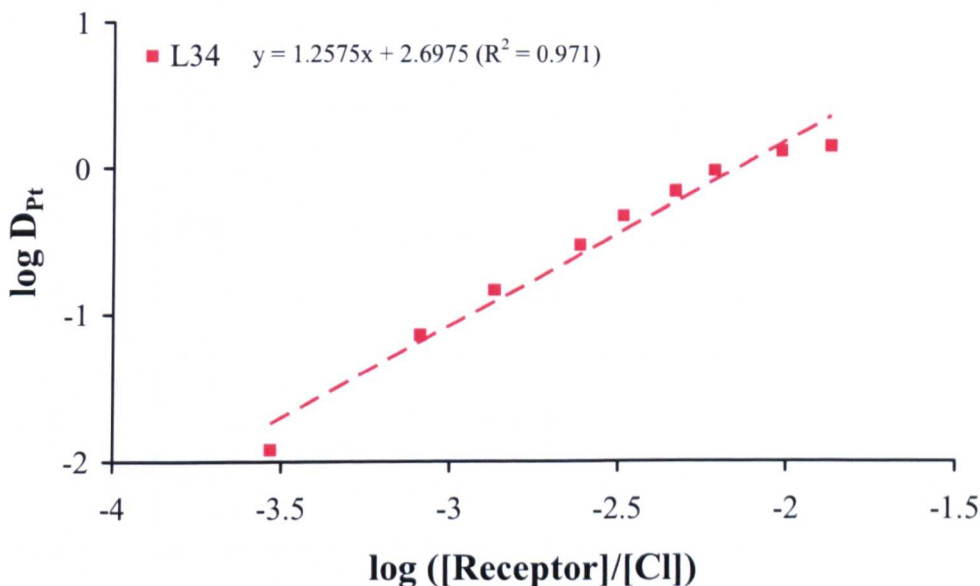


Figure 6.23. Plot of $\log D_{\text{Pt}}$ against $\log ([\text{Receptor}]/[\text{Cl}])$.

6.2.4.7. Effect of Hydrogen-bonds

The extraction results for TOA, the tripodal receptor L¹⁴ and the bipodal receptor L³⁴ are compared in Figure 6.24. The extraction efficiency increases in the order TOA < L³⁴ < L¹⁴ which correlates with the number of hydrogen-bond donor groups (Table 6.11). This result shows that pendant arms containing hydrogen-bond donor groups are better than alkyl chains for targeting $[PtCl_6]^{2-}$ and by introducing hydrogen-bond donor groups into the receptors the extraction efficiency of $[PtCl_6]^{2-}$ has been increased.

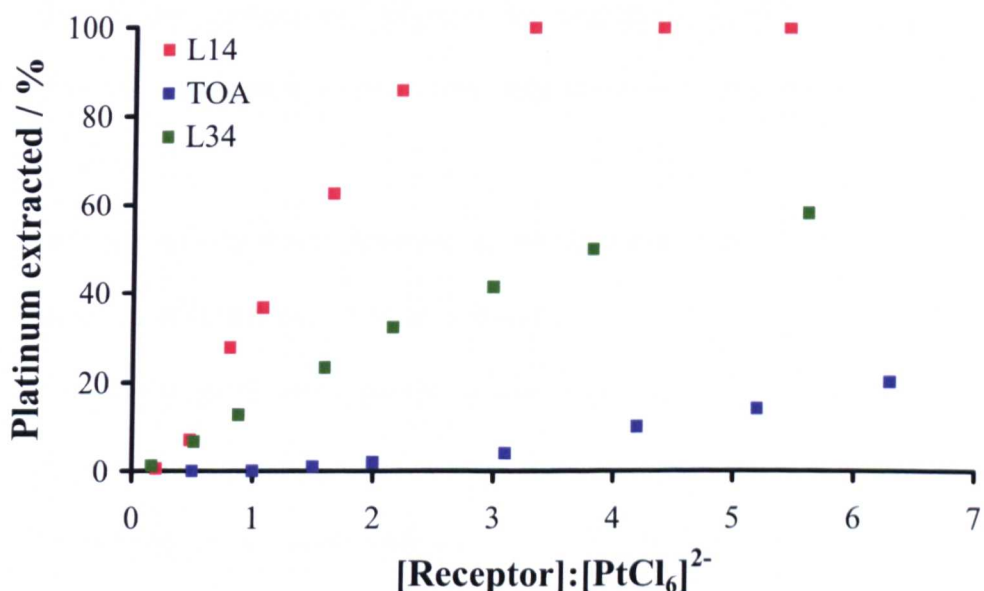
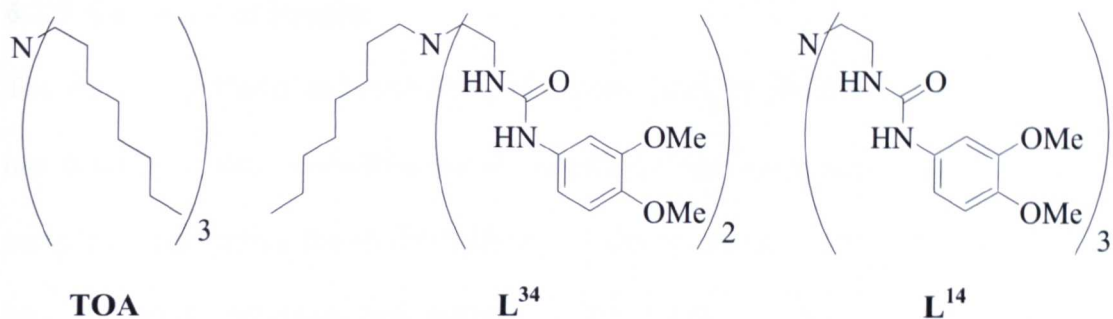


Figure 6.24. Plot of % Pt extracted as $[\text{PtCl}_6]^{2-}$ from aqueous 0.6 M HCl into CHCl_3 as a function of [Receptor]:[Pt] ratio.

Table 6.11. % of Pt extracted as $[\text{PtCl}_6]^{2-}$ into CHCl_3 from aqueous 0.6 M HCl in the presence of a 3 molar excess of L

Receptor	TOA	L^{34}	L^{14}
% Pt extracted at 3 molar excess of L	4	41	92

6.2.5. Summary of Results

The design, synthesis and evaluation of bipodal urea, thiourea and amide receptors has been presented. Unfortunately all of the thiourea receptors formed insoluble complexes preventing the study of these systems by solvent extraction. The bipodal urea and amide receptors that formed soluble complexes were studied in solvent extractions and show that:

- Bipodal urea systems extract more than analogous bipodal amide systems.
- Bipodal extractants show lower extraction than the analogous tripodal systems.

These two observations were attributed to the fact that more NH donors leads to higher extraction efficiencies. It was also found that:

- Bipodal receptors with a propyl spacer extract more than those with an ethyl spacer.
- The nature of the alkyl substituent on the tertiary amine position of the receptors affects extraction efficiency.

These two observations have been attributed to the improved organic solubility of receptors with propyl spacer units or with octyl, rather than methyl, substituents which leads to higher extraction efficiencies.

Crystal structures of $[(L^{29}H)_2PtCl_6]$ and $[(L^{38}H)_2PtCl_6]$ provide an insight into the interactions between the bipodal receptors and $[PtCl_6]^{2-}$ in the solid state. Both structures show protonation of the bridgehead nitrogen positions, a 2:1 L: $[PtCl_6]^{2-}$ ratio and hydrogen-bonds between the receptors and $[PtCl_6]^{2-}$. Although the bipodal receptors are not as successful extractants as the tripodal receptors they have

furthered our understanding of the features required to obtain high extraction efficiencies.

6.3. Monopodal Receptors

To further probe the effect of receptor scaffold on extraction efficiency the design of the receptor was modified and monopodal systems were designed, synthesised and evaluated. These receptors have a tertiary amine protonation site linked, through an aliphatic chain, to one hydrogen-bond donor group. It was hypothesised that monopodal receptors would show lower extraction than tripodal and bipodal systems as they have fewer NH hydrogen-bond donor groups. However, it was also argued that as there is less steric bulk and no pre-organised orientation the hydrogen-bond donor groups could more easily target $[\text{PtCl}_6]^{2-}$ to give a stronger interaction and improved extraction.

$\text{N}, \text{N}'\text{-dimethylethylamine}$ (Figure 6.25). was used as a scaffold in this Section of work for three reasons. Firstly, it has a tertiary amine protonation site, secondly there is one primary amine site available from which hydrogen-bond donor groups are synthetically accessible and thirdly the ethyl spacer is analogous to some of the previously described tripodal and bipodal receptors.

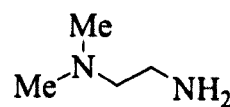


Figure 6.25. Structure of $\text{N}, \text{N}'\text{-dimethylethylamine}$.

The previous success with the urea moiety meant it was incorporated into the monopodal system and the proposed interaction with $[\text{PtCl}_6]^{2-}$ is shown in Figure

6.26. A charge-neutral complex will be formed when two protonated receptor molecules interact with $[\text{PtCl}_6]^{2-}$ to ideally give an organic soluble product.

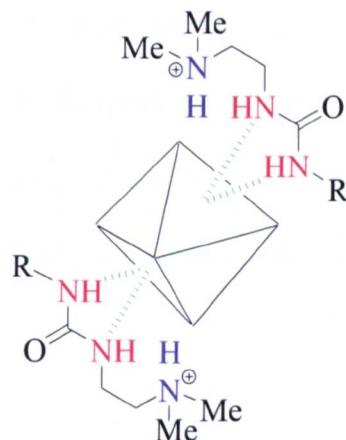
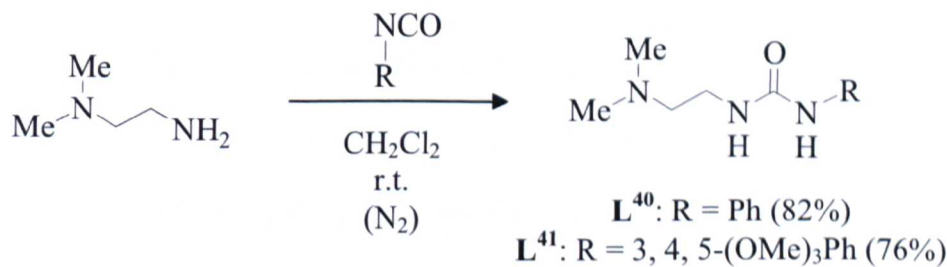


Figure 6.26. The proposed interaction of monopodal receptors with $[\text{PtCl}_6]^{2-}$.

6.3.1. Synthesis of Monopodal Receptors

L^{40} and the novel receptor L^{41} were prepared by the reaction of N, N'-dimethylethylamine with phenyl isocyanate or 3, 4, 5-trimethoxyphenyl isocyanate, respectively (Scheme 6.7).¹ The products were obtained in high yields as colourless powders and characterisation by ^1H NMR, ^{13}C NMR and IR spectroscopy, mass spectrometry and elemental analytical data showed them to be analytically pure.



Scheme 6.7. Synthesis of L^{40} and L^{41} .

6.3.2. Complexation Reactions

For L^{40} and L^{41} two equivalents of receptor were dissolved in MeCN and mixed with H_2PtCl_6 . L^{40} had very low solubility in MeCN which hindered the reaction with

H_2PtCl_6 . L^{41} was more soluble and when reacted with H_2PtCl_6 a clear orange solution formed. This reaction was repeated in CD_3CN and the ^1H NMR spectrum recorded which had a signal at 9.10 ppm which integrated in a 1:1 ratio with each of the NH urea signals and was assigned to the protonated tertiary amine nitrogen N^+HR_3 . Negative electrospray mass spectrometry on the solution showed peaks assigned to $[\text{L}^{41}-\text{H}]^-$ and $[\text{PtCl}_6]^{2-}$ but no isotope pattern due to any complexes was observed.

6.3.3. Solvent Extractions

As L^{40} had low organic solubility it could not be studied in solvent extractions. A test extraction with L^{41} showed uptake of colour in the CHCl_3 phase and as this method has been proven to be a qualitative indicator of extraction a full study was not performed.

It was initially thought that the key features needed in a receptor to extract $[\text{PtCl}_6]^{2-}$ were a protonation site, a hydrogen-bond donor group and organic solubility. Potentiometry experiments, ^1H NMR spectra and crystal structures have confirmed the protonation of the tertiary amine positions in complexes proving the success of this feature. Crystallographic analyses of complexes has confirmed that hydrogen-bonds are formed between the urea and amide NH donors of the tripodal and bipodal receptors and $[\text{PtCl}_6]^{2-}$ proving the success of this design feature.

Therefore, it is suggested that the complex $[(\text{L}^{41}\text{H})_2\text{PtCl}_6]$ has low organic solubility leading to poor extraction. To overcome this problem the methyl substituents in L^{41} could be replaced with octyl groups as for the bipodal systems the nature of the alkyl substituents affected extraction efficiency. Other explanations for the low extraction displayed by L^{41} are that inter-ligand hydrogen-bond interactions

N—H \cdots O form preferentially (Figure 6.27) or that the receptor has low selectivity for $[\text{PtCl}_6]^{2-}$.

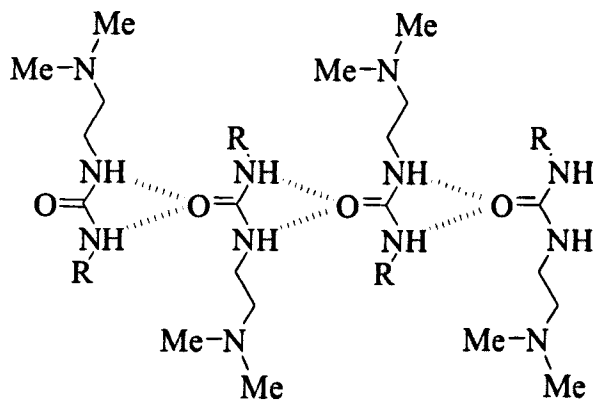


Figure 6.27. Possible inter-molecular hydrogen-bonds that may form in monopodal receptors.

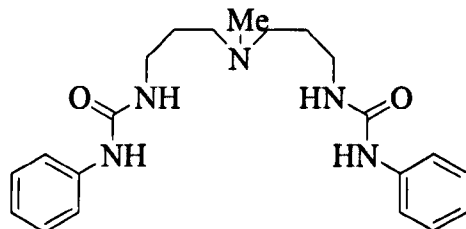
6.3.4. Summary of Results

To evaluate the effect of scaffold on extraction efficiency two monopodal urea receptors were designed, synthesised and evaluated. A complexation reaction with L^{40} was unsuccessful due to the low solubility of the receptor and L^{41} produced a soluble product $[(\text{L}^{41})_2\text{PtCl}_6]$. A test extraction with L^{41} showed no colour change of the CHCl_3 phase indicating no uptake of $[\text{PtCl}_6]^{2-}$ which has been attributed to the low organic solubility of the complex.

6.4. Experimental

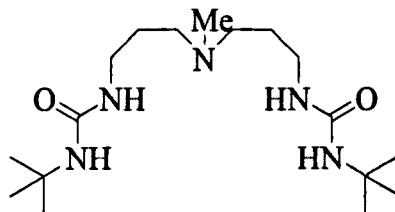
6.4.1. Receptor Synthesis

6.4.1.1. Synthesis of N,N''-[(methylimino)di-2,1-propanediyl]bis[N'-phenylurea], L²⁹.¹



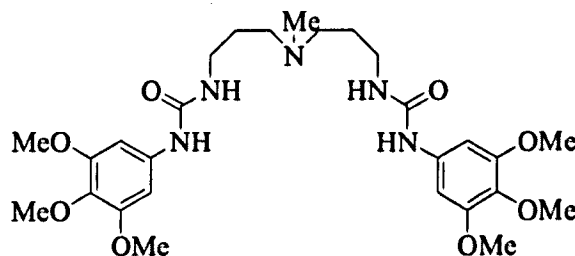
To 3, 3-diamino-N-methyldipropylamine (0.20 cm³, 1.24 mmol) in dry THF (30 cm³) was added phenyl isocyanate (0.30 g, 2.48 mmol) under N₂. The reaction stirred at r.t for 2 h and the solvent removed *in vacuo* to give an oily residue which was washed with a portion of Et₂O and MeOH to give a colourless solid which was dried *in vacuo*. Yield: 0.38 g, 80%. ¹H NMR (270 MHz, CDCl₃): δ/ppm 7.90 (br, 2H, NH), 7.31 (d, 4H, ³J_{HH} = 8 Hz, H_{Ar}), 7.16 (dd, 4H, ³J_{HH} = 8 Hz, H_{Ar}), 6.88 (t, 2H, ³J_{HH} = 8, H_{Ar}), 6.35 (br, 2H, NH), 3.20 (t, 4H, ³J_{HH} = 6 Hz, CH₂), 2.48–2.45 (m, 4H, CH₂), 2.23 (s, 3H, NCH₃), 1.60–1.56 (m, 4H, CH₂). ¹³C NMR (75 MHz, CD₃OD): δ/ppm 156, 140, 127, 122, 118, 56, 40, 36, 25. MS (ES⁺): *m/z* 384 [M+H]⁺. IR (solid cm⁻¹): 3319 (v_(N-H)), 2963 (v_(N-H)), 1637 (v_(C=O)), 1571 (v_(C=C, Ar)), 752 (v_(C-H, Ar)). Anal. calc. for C₂₁H₂₉N₅O₂: C, 65.76; H, 7.64; N, 18.26. Found: C, 65.77; H, 7.60; N, 18.18%.

6.4.1.2. Synthesis of N,N''-[(methylimino)di-2,1-propanediyl]bis[N'-*tert*-butylurea], L³⁰.¹



L³⁰ was prepared following a similar method to L²⁹ using *tert*-butyl isocyanate instead of phenyl isocyanate to give the product as a colourless solid. Yield: 0.35 g, 82%. ¹H NMR (270 MHz, CDCl₃): δ/ppm 5.75 (br, 2H, NH), 4.91 (br, 2H, NH), 3.13 (t, 4H, ³J_{HH} = 5 Hz, CH₂), 2.35–2.28 (m, 4H, CH₂), 2.11 (s, 3H, CH₃), 1.68–1.59 (m, 4H, CH₂), 1.26 (s, 18H, ^tBu). ¹³C NMR (68 MHz, CDCl₃): δ/ppm 159, 55, 50, 42, 39, 30, 28. MS (ES⁺): *m/z* 344 [M+H]⁺. IR (solid cm⁻¹): 3301 (v_(N-H)), 2945 (v_(N-H)), 1632 (v_(C=O)). Anal. calc. for C₁₇H₃₇N₅O₂: C, 59.42; H, 10.88; N, 20.39. Found: C, 59.19; H, 10.99; N, 20.18%.

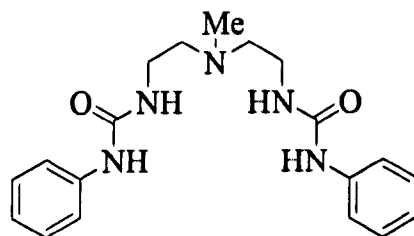
6.4.1.3. Synthesis of N,N''-[(methylimino)di-2,1-propanediyl]bis[N'-3,4,5-trimethoxyphenyl urea], L³¹.¹



3, 3-Diamino-N-methyldipropylamine (0.15 cm³, 0.96 mmol) was dissolved in CH₂Cl₂ (30 cm³) under N₂. 3, 4, 5-Trimethoxyphenyl isocyanate (0.40 g, 1.91 mmol) was added and the reaction stirred at r.t. for 24 h. H₂O (15 cm³) was added to the reaction to remove the unreacted amine and isocyanate and the aqueous layer was

washed with CH_2Cl_2 ($3 \times 10 \text{ cm}^3$). The organic fractions were collected, dried over MgSO_4 , filtered and the solvent removed to give a colourless foam. Yield: 0.32 g, 59%. ^1H NMR (270 MHz, CDCl_3): δ/ppm 8.26 (s, 2H, NH), 6.66 (t, 2H, $^3J_{\text{HH}} = 6 \text{ Hz}$, NH), 6.61 (s, 4H, H_{Ar}), 3.69 (s, 6H, OMe), 3.56 (s, 12H, OMe), 3.30 (br, 4H, CH₂), 2.31 (br, 4H, CH₂), 2.11 (s, 3H, CH₃), 1.57 (br, 4H, CH₂). ^{13}C NMR (68 MHz, CDCl_3): δ/ppm 157, 153, 136, 133, 96, 61, 56, 54, 42, 38, 27. MS (ES $^+$): calc for $\text{C}_{27}\text{H}_{42}\text{N}_5\text{O}_8 m/z$ 564.3033, found m/z 564.3032 corresponds to $[\text{M}+\text{H}]^+$. IR (solid cm^{-1}): 3328 ($\nu_{(\text{N-H})}$), 1652 ($\nu_{(\text{C=O})}$), 1603 ($\nu_{(\text{C=C, Ar})}$), 1123 ($\nu_{(\text{C-O})}$). Anal. calc for $\text{C}_{27}\text{H}_{41}\text{N}_5\text{O}_8$: C, 57.54; H, 7.33; N, 12.43. Found: C, 57.47; H, 7.18; N, 12.32%.

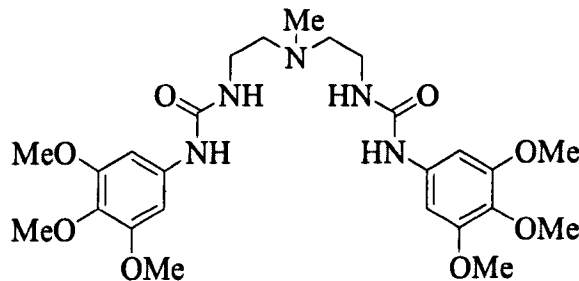
6.4.1.4. Synthesis of $\text{N,N}''$ -[(methylimino)di-2,1-ethanediyl]bis[N'-phenylurea], L³².¹



N -methyl-2, 2'-diaminodiethylamine (0.2 cm^3 , 1.55 mmol) was dissolved in THF (30 cm^3) to which phenyl isocyanate (0.34 cm^3 , 3.11 mmol) was added under N_2 and the reaction stirred at r.t. for 18 h. No precipitate formed during the reaction and the solvent was removed *in vacuo* to give a colourless solid. Yield: 0.54 g, 98%. ^1H NMR (270 MHz, $\text{dmso}-d_6$): δ/ppm 8.60 (s, 2H, NH), 7.38 (d, 4H, $^3J_{\text{HH}} = 7 \text{ Hz}$, H_{Ar}), 7.21 (dd, 4H, $^3J_{\text{HH}} = 7 \text{ Hz}$, H_{Ar}), 6.89 (t, 2H, $^3J_{\text{HH}} = 7 \text{ Hz}$, H_{Ar}), 6.16 (t, 2H, $^3J_{\text{HH}} = 5 \text{ Hz}$, NH), 3.20–3.17 (m, 4H, CH₂), 2.44 (t, 4H, $^3J_{\text{HH}} = 6 \text{ Hz}$, CH₂), 2.26 (s, 3H, Me). ^{13}C NMR (68 MHz, $\text{dmso}-d_6$): δ/ppm 156, 141, 129, 121, 118, 57, 41, 38. MS (ES $^+$): calc m/z 356.2081, found m/z 356.2098, corresponds to $[\text{M}+\text{H}]^+$. IR (solid, cm^{-1}):

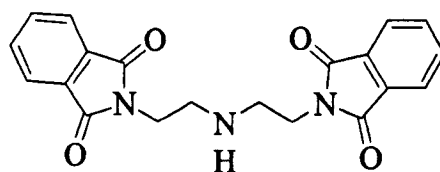
3319 ($\nu_{(N-H)}$), 1644 ($\nu_{(C=O)}$), 1601 ($\nu_{(C=C, Ar)}$). Anal. calc. for $C_{19}H_{25}N_5O_2$: C, 64.20; H, 7.09; N, 19.70. Found: C, 64.27; H, 7.13; N, 19.73%.

6.4.1.5. Synthesis of N,N'' -[(methylimino)di-2,1-ethanediyl]bis[N'-3,4,5-trimethoxyphenyl urea], L^{33,1}



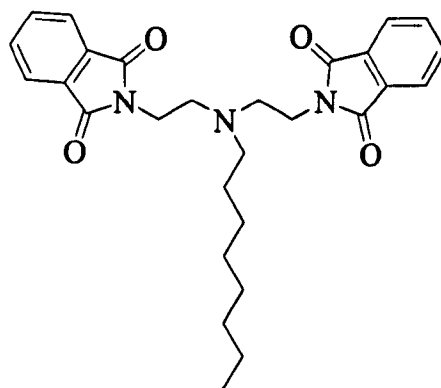
N-methyl-2, 2-diaminodiethylamine (0.2 cm³, 1.55 mmol) was dissolved in THF (30 cm³). To this was added 3, 4, 5-trimethoxyphenyl isocyanate (0.65 g, 3.11 mmol) and the flask was flushed with N₂ and the reaction stirred at room temperature for 3 h. During this time a colourless precipitate formed which was collected by filtration. Yield: 0.51 g, 61%. ¹H NMR (270 MHz, CDCl₃): δ /ppm 7.47 (s, 2H, NH), 6.63 (s, 4H, H_{Ar}), 5.83 (t, 2H, $^3J_{HH} = 5$ Hz, NH), 3.82 (s, 6H, OMe), 3.77 (s, 12H, OMe), 3.30-3.28 (m, 4H, CH₂), 2.49 (t, 4H, $^3J_{HH} = 5$ Hz, CH₂), 2.28 (s, 3H, Me). ¹³C NMR (68 MHz, dmso-*d*₆): δ /ppm 153, 135, 130, 98, 61, 58, 57, 56, 41, 38. MS (ES⁺): calc. *m/z* 536.2715, found *m/z* 536.2709, corresponds to [M+H]⁺. IR (solid, cm⁻¹): 3337 ($\nu_{(N-H)}$), 1638 ($\nu_{(C=O)}$), 1609 ($\nu_{(C=C, Ar)}$), 1127 ($\nu_{(C-O)}$). Anal. calc. for C₂₅H₃₇N₅O₈: C, 56.09; H, 6.97; N, 13.08. Found: C, 56.19; H, 7.04; N, 13.03%.

6.4.1.6.1. Synthesis of N,N'-(iminodiethylene)bisphthalimide, 2.³



Diethylenetriamine (103 g, 0.10 mmol) and phthalic anhydride (33.2 g, 0.20 mmol) were added to acetic acid (160 cm³) and heated to reflux for 4 h. The solvent was then removed under reduced pressure, hot EtOH (160 cm³) added with stirring and the solution cooled until a solid appeared. This yellow solid was collected by filtration and washed with cold EtOH, diethyl ether and then dried *in vacuo*. Yield: 0.30 g, 82%. ¹H NMR (dmso-d₆, 270 MHz): 8.12 (d, 4H, ³J_{HH} = 9 Hz, H_{Ar}), 7.49 (d, 4H, ³J_{HH} = 9 Hz, H_{Ar}), 3.74 (t, 4H, ³J_{HH} = 6 Hz, CH₂), 3.03–2.98 (m, 4H, CH₂), 2.53 (br, 1H, NH). MS (ES⁺): *m/z* 364 [M+H]⁺.

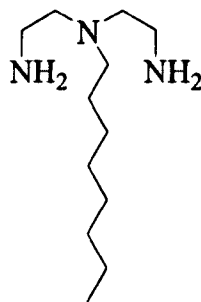
6.4.1.6.2. Synthesis of 3.³



Previously synthesised N, N'-(iminodiethylene)bisphthalimide **2** (2.90 g, 7.98 mmol), octylbromide (4.62 g, 23.94 mmol) and K₂CO₃ (3.30 g, 23.94 mmol) were heated to reflux in MeCN (120 cm³). The solvent was removed under reduced pressure and H₂O (40 cm³) added to the residue. The product was extracted with CH₂Cl₂ (3 × 20 cm³) and the organic phases were collected and dried with MgSO₄.

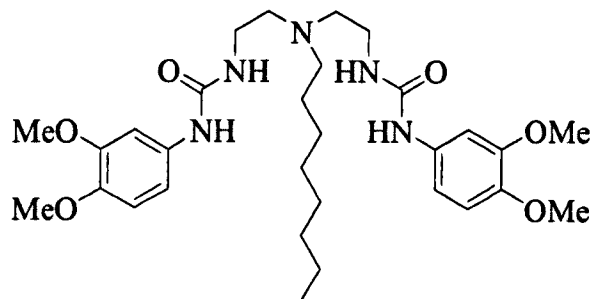
Following filtration the solvent was removed to give a colourless solid which was purified by column chromatography (75/25 hexane/EtOAc). Yield: 2.31 g, 61%. ^1H NMR (CDCl_3 , 270 MHz): 7.85 (d, 4H, $^3J_{\text{HH}} = 9$ Hz, H_{Ar}), 7.70–7.53 (d, 4H, $^3J_{\text{HH}} = 9$ Hz, H_{Ar}), 3.74 (t, 4H, $^3J_{\text{HH}} = 6$ Hz, NCH₂), 2.78–2.70 (m, 4H, NCH₂), 2.52 (t, 2H, $^3J_{\text{HH}} = 6$ Hz, NCH₂), 1.32–1.09 (m, 12H, CH₂), 0.86 (t, 3H, $^3J_{\text{HH}} = 7$ Hz, CH₃). MS (ES $^+$): *m/z* 476 [M+H] $^+$, 498 [M+Na] $^+$.

6.4.1.6.3. Synthesis of 4³



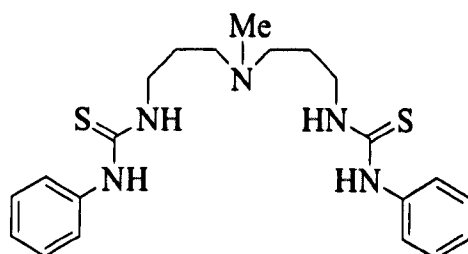
A solution of **3** (1.50 g, 3.15 mmol) and hydrazine monohydrate (3.15 g, 63 mmol) were dissolved in EtOH (131 cm^3) under an Ar atmosphere and heated at reflux for 36 h. The mixture was cooled to r.t., filtered and washed with EtOH. The solvent was removed from the filtrate and CHCl_3 (80 cm^3) added to the residue. This mixture was stirred overnight at r.t. and then the insoluble phthalhydrazine removed by filtration. The CHCl_3 was removed from the filtrate under reduced pressure to give the product as a yellow oil. Yield: 0.52 g, 77%. ^1H NMR (CDCl_3 , 270 MHz): δ/ppm 2.67 (t, 4H, $^3J_{\text{HH}} = 6$ Hz, NCH₂), 2.45–2.39 (m, 4H, NCH₂), 2.39 (t, 2H, $^3J_{\text{HH}} = 6$ Hz, CH₂), 1.24–1.18 (m, 12H, CH₂), 0.84 (t, 3H, $^3J_{\text{HH}} = 7$ Hz, CH₃). MS (ES $^+$): *m/z* 216 [M+H] $^+$

6.4.1.6.4. Synthesis of N,N''-[(octylimino)di-2,1-ethanediyl]bis[N'-3,4-dimethoxyphenylurea], L³⁴.¹



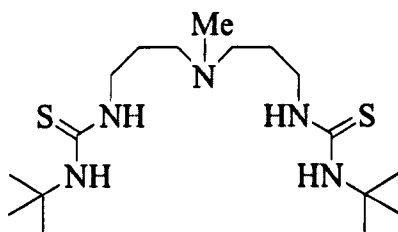
To 3, 4-dimethoxyphenyl isocyanate (0.31 g, 1.74 mmol) in THF (30 cm³) was added 4 (0.17 g, 0.79 mmol) under a N₂ atmosphere and the mixture stirred at r.t. for 18 h. The solvent was removed from the reaction under reduced pressure and the product purified by column chromatography (97/3 MeOH/CHCl₃ and then 100% MeOH). Yield: 0.34 g, 84%. ¹H NMR (CDCl₃, 270 MHz): δ/ppm 7.53 (s, 2H, NH), 7.09 (s, 2H, H_{Ar}), 6.73–6.65 (m, 4H, H_{Ar}), 6.05 (br, 2H, NH), 3.84 (br, 12H, OMe), 3.27 (br, 4H, NCH₂), 2.56 (br, 4H, NCH₂), 2.46 (t, 2H, ³J_{HH} = 6 Hz, CH₂), 1.27–1.15 (m, 12H, CH₂), 0.84 (t, 3H, ³J_{HH} = 6 Hz, CH₃). ¹³C NMR (CDCl₃, 68 MHz): 157, 149, 132, 113, 112, 106, 56, 55, 54, 38, 32, 30, 29, 27, 22, 14. MS (ES⁺): m/z 574 [M+H]⁺, 596 [M+Na]⁺. IR (solid, cm⁻¹): 3326 (ν_(N-H)), 1645 (ν_(C=O)), 1509 (ν_(C=C, Ar)), 1210 (ν_(C-O)).

6.4.1.7. Synthesis of N,N''-[(methylimino)di-2,1-propanediyl]bis[N'-phenylthiourea], L³⁵.¹



3, 3'-Diamino-N-methyldipropylamine (0.20 cm^3 , 1.24 mmol) was dissolved in THF (30 cm^3) to which phenyl isothiocyanate (0.31 cm^3 , 2.60 mmol) was added under N_2 . The reaction was stirred at r.t. for 2 h to give the product as a colourless precipitate which was collected by filtration and dried *in vacuo*. Yield: 0.46 g, 89%. ^1H NMR (270 MHz, CDCl_3): δ/ppm 7.70 (br, 2H, NH), 7.33 (d, 4H, $^3J_{\text{HH}} = 8\text{ Hz}$, H_{Ar}), 7.25 (dd, 4H, $^3J_{\text{HH}} = 8\text{ Hz}$, H_{Ar}), 7.14 (t, 2H, $^3J_{\text{HH}} = 8\text{ Hz}$, H_{Ar}), 6.86 (br, 2H, NH), 3.58 (t, 4H, $^3J_{\text{HH}} = 6.5\text{ Hz}$, CH₂), 2.21–2.15 (m, 4H, CH₂), 1.89 (s, 3H, Me), 1.47–1.40 (m, 4H, CH₂). ^{13}C NMR (68 MHz, CDCl_3): δ/ppm 180, 137, 130, 127, 125, 56, 45, 42, 25. MS (ES $^+$): *m/z* 416 corresponds to $[\text{M}+\text{H}]^+$. IR (solid cm^{-1}): 3162 ($\nu_{(\text{N-H})}$), 1597 ($\nu_{(\text{C=C, Ar})}$), 1531 ($\nu_{(\text{C=S})}$). Anal. calc. For $\text{C}_{21}\text{H}_{29}\text{N}_5\text{S}_2$: C, 60.68; H, 7.05; N, 16.85. Found: C, 60.41; H, 6.95; N, 16.11%.

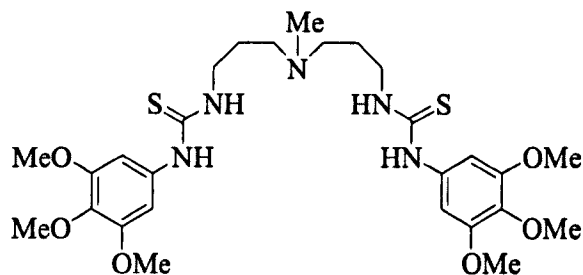
6.4.1.8. Synthesis of $\text{N,N''-[(methylimino)di-2,1-propanediyl]bis[N'-tert-butylthiourea]}$, L³⁶.¹



This was prepared in a similar way to L³⁵ using *tert*-butyl isothiocyanate to give the product as a colourless solid. Yield: 0.38 g, 82%. ^1H NMR (300 MHz, CDCl_3): δ/ppm 6.80 (br, 2H, NH), 5.95 (br, 2H, NH), 3.50 (t, 4H, $^3J_{\text{HH}} = 7\text{ Hz}$, CH₂), 2.45–2.37 (m, 4H, CH₂), 2.17 (s, 3H, Me), 1.74–1.66 (m, 4H, CH₂). ^{13}C NMR (68 MHz, CDCl_3): δ/ppm 181, 56, 54, 45, 42, 29, 25. MS (ES $^+$): *m/z* 376 corresponds to

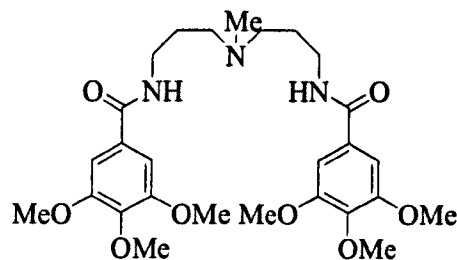
$[M+H]^+$. IR (solid cm^{-1}): 3262 ($\nu_{(\text{N-H})}$), 1542 ($\nu_{(\text{C=S})}$). Anal. calc. For $\text{C}_{17}\text{H}_{35}\text{N}_5\text{S}_2$: C, 54.34; H, 9.95; N, 18.64. Found: C, 54.20; H, 9.95; N, 18.58%.

6.4.1.9. Synthesis of N, N''-[(methylimino)di-2,1-propanediyl]bis[N'-3, 4, 5-trimethoxyphenyl thiourea], L³⁷



This was synthesised using a similar method to that used for L³⁵ using 3, 4, 5-trimethoxyphenyl isothiocyanate to give the product as a colourless solid. Yield: 0.52 g, 71 %. ¹H NMR (270 MHz, CDCl_3): δ/ppm 7.73 (br, 2H, NH), 7.21 (s, 4H, $\underline{\text{H}_{\text{Ar}}}$), 6.72 (br, 2H, NH), 3.88 (s, 6H, OMe), 3.71 (s, 12H, OMe), 3.45 (t, 4H, $^3J_{\text{HH}} = 6$ Hz, CH₂), 2.56–2.51 (m, 4H, CH₂), 1.86 (s, 3H, Me), 1.76–1.70 (m, 4H, CH₂). ¹³C NMR (68 MHz, CDCl_3): 182, 135, 132, 128, 125, 64, 62, 55, 47, 44, 24. δ/ppm MS (ES⁺): *m/z* 596 $[M+H]^+$. IR (solid cm^{-1}): 3180 ($\nu_{(\text{N-H})}$), 1607 ($\nu_{(\text{C=C, Ar})}$), 1525 ($\nu_{(\text{C=S})}$). Anal. calc. For $\text{C}_{27}\text{H}_{41}\text{N}_5\text{O}_6\text{S}_2$: C, 54.43; H, 6.94; N, 11.76. Found: C, 54.37; H, 6.88; N, 11.70%.

6.4.1.10. Synthesis of N,N'-[{(methylimino)di-2,1-ethanediyl]bis-3,4,5-trimethoxybenzamide, L³⁸.⁴

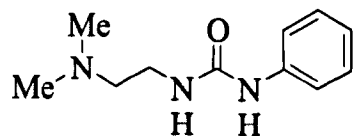


3, 3'- Diamino-N-methyldipropylamine (0.19 cm³, 1.15 mmol) was dissolved in CH₂Cl₂ containing NaOH (0.10 g, 2.30 mmol). 3, 4, 5-Trimethoxybenzoyl chloride (0.53 g, 2.29 mol) was added and the reaction was stirred at r.t. for 20 h. H₂O (20 cm³) was added to dissolve the NaOH and the reaction stirred for a further hour. The layers were separated and the aqueous layer washed with CH₂Cl₂ (3 × 10 cm³). The organic fractions were combined, dried over MgSO₄, filtered and then the solvent removed *in vacuo* to give a colourless foam. Yield: 0.38 g, 62%. ¹H NMR (270 MHz, CDCl₃): δ/ppm 7.69 (t, 2H, ³J_{HH} = 5 Hz, NH), 7.00 (s, 4H, H_{Ar}), 3.82 (s, 6H, OMe), 3.77 (s, 12H, OMe), 3.40–3.35 (m, 4H, CH₂), 2.40 (t, 4H, ³J_{HH} = 6 Hz, CH₂), 2.20 (s, 3H, CH₃), 1.74–1.66 (m, 4H, CH₂). ¹³C NMR (68 MHz, CDCl₃): δ/ppm 167, 153, 141, 130, 104, 61, 56, 55, 42, 39, 29. MS (ES⁺): calc. for C₂₇H₄₀N₃O₈ m/z 534.2822, found m/z 534.2815 corresponds to [M+H]⁺. IR (solid, cm⁻¹): 3289 (ν_(N-H)), 1630 (ν_(C=O)), 1581 (ν_(C=C, Ar)), 1123 (ν_(C-O)). Anal. calc. for C₂₇H₃₉N₃O₈: C, 60.77; H, 7.27; N, 7.87. Found: C, 60.62; H, 7.29; N, 7.81%.

6.4.1.11. Attempted Synthesis of N,N'-[(methylimino)di-2,1-ethanediyl]bis-3,4,5-trimethoxy benzamide, L³⁹.⁴

N-methyl-2, 2'-diaminodiethylamine (0.2 cm^3 , 1.55 mmol) was dissolved in CH_2Cl_2 (20 cm^3) with NaOH (0.1244 g, 3.11 mmol) to which 3, 4, 5-trimethoxybenzoyl chloride (0.716 g, 3.11 mmol) dissolved in CH_2Cl_2 (20 cm^3) was added. The reaction went cloudy suggesting the formation of product and the reaction was stirred at r.t. for 4h. H_2O (15 cm^3) was then added to the reaction and the reaction stirred at r.t. for 5 mins. The two phases were separated and the aqueous phase washed with CH_2Cl_2 (in subsequent attempts toluene and CHCl_3 were used instead). The organic phases were collected, dried over MgSO_4 , filtered and the solvent removed under reduced pressure, however, no solid was present.

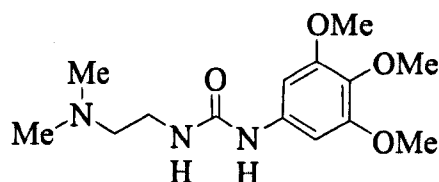
6.4.1.12. Synthesis of N-[2-dimethylamino)ethyl]-N'-phenyl urea, L⁴⁰.¹



To N, N-dimethylethylenediamine (0.20 cm^3 , 1.83 mmol) in thf (20 cm^3) was added phenyl isocyanate (0.20 g, 1.83 mmol) under N_2 . The reaction was stirred at r.t for 3 days and no precipitate formed. The solvent was removed *in vacuo* to give a colourless solid. Yield: 0.31 g, 82%. ^1H NMR (270 MHz, CDCl_3): δ/ppm 7.34–7.22 (m, 5H, H_{Ar}), 7.00 (t, 1H, $^4J_{\text{HH}} = 7\text{ Hz}$, NH), 6.08 (c, 1H, NH), 3.31–3.29 (m, 2H, CH₂), 2.47 (t, 2H, $^3J_{\text{HH}} = 5\text{ Hz}$, CH₂), 2.26 (s, 6H, 2 × Me). ^{13}C NMR (68 MHz, CDCl_3): δ/ppm 157, 140, 135, 129, 123, 60, 45, 38. MS (ES⁺): calc. for $\text{C}_{11}\text{H}_{17}\text{N}_3\text{O}$ m/z 208.1450, found m/z 208.1456, corresponds to [M+H]⁺. IR (solid cm^{-1}): 3374

($\nu_{(N-H)}$), 1687 ($\nu_{(C=O)}$), 1618 ($\nu_{(C=C, Ar)}$). Anal. calc. for $C_{11}H_{17}N_3O$: C, 63.74; H, 8.27; N, 20.27. Found: C, 63.71; H, 8.31; N, 20.38%.

6.4.1.13. Synthesis of N-[2-dimethylamino)ethyl]-N'-3,4,5-trimethoxyphenyl urea, L⁴¹.¹



This was prepared in an identical way to L⁴⁰ using 3, 4, 5-trimethoxyphenyl isocyanate instead of phenyl isocyanate to give the product as a colourless solid. Yield: 0.38 g, 69%. 1H NMR (300 MHz, CDCl₃): δ /ppm 6.68 (s, 1H, NH), 6.64 (s, 2H, H_{Ar}), 5.60 (br, 1H, NH), 3.83 (s, 9H, OMe), 3.36–3.30 (m, 2H, CH₂), 2.51 (t, 2H, $^3J_{HH} = 5$ Hz, CH₂), 2.29 (s, 3H, 2 × Me). ^{13}C NMR (68 MHz, CDCl₃): δ /ppm 157, 153, 136, 133, 97, 61, 59, 56, 45, 38. MS (ES⁺): *m/z* 298 [M+H]⁺. IR (solid, cm⁻¹): 3370 ($\nu_{(N-H)}$), 1687 ($\nu_{(C=O)}$), 1610 ($\nu_{(C=C, Ar)}$), 1126 ($\nu_{(C-O)}$). Anal. calc: C, 56.55; H, 7.80; N, 14.13. Found: C, 56.65; H, 7.68; N, 14.14%.

6.4.2. Complexation Reactions

Two equivalents of receptor (*ca.* 0.04 mmol, 2 equiv.) were dissolved in MeCN (*ca.* 2 cm³) to which one equivalent (*ca.* 0.02 mmol, 1 equiv.) also dissolved in MeCN (*ca.* 2 cm³) was also added. If a precipitate formed then this was collected by gravity filtration and characterised. If no precipitate formed the reaction was repeated using CD₃CN and the resulting solution was characterised.

6.4.2.1. Synthesis of $[(L^{29}H)_2PtCl_6]$

The receptor L^{29} was not completely soluble in MeCN preventing complex formation.

6.4.2.2. Synthesis of $[(L^{30}H)_2PtCl_6]$

No precipitate formed in the complexation reaction. 1H NMR (270 MHz, CD₃CN): δ/ppm 8.96 (br, 1H, NH⁺), 6.13 (br, 2H, NH), 5.24 (s, 2H, NH), 3.36 (t, 4H, $^3J_{HH} = 6.2$ Hz, CH₂), 2.39–2.29 (m, 4H, CH₂), 2.14 (s, 3H, Me), 1.74–1.67 (m, 4H, CH₂), 1.17 (s, 18H, 'Bu).

6.4.2.3. Synthesis of $[(L^{31}H)_2PtCl_6]$

No precipitate formed in the complexation reaction. 1H NMR (300 MHz, CD₃CN): δ/ppm 9.12 (br, 1H, NH⁺), 7.75 (s, 2H, NH), 6.78 (s, 4H, H_{Ar}), 5.95 (t, 2H, $^3J_{HH} = 6$ Hz, NH), 3.77 (s, 12H, OMe), 3.65 (s, 6H, OMe), 3.32–3.26 (m, 4H, CH₂), 3.18 (t, 4H, $^3J_{HH} = 6$ Hz, CH₂), 2.78 (s, 3H, CH₃), 1.97–1.89 (m, 4H, CH₂). MS (ES⁻): *m/z* 1532.38 [(L)(LH)PtCl₆]⁻, 3471.55 [4(LH)+3(PtCl₆)]²⁻.

6.4.2.4. Synthesis of $[(L^{32}H)_2PtCl_6]$

The receptor L^{32} was not completely soluble in MeCN preventing complex formation.

6.4.2.5. Synthesis of $[(L^{33}H)_2PtCl_6]$

No precipitate formed in the complexation reaction. 1H NMR (300 MHz, CD₃CN): δ/ppm 8.82 (br, 1H, NH⁺), 7.52 (s, 2H, NH), 6.71 (s, 4H, H_{Ar}), 5.88 (t, 2H, $^3J_{HH} = 5$ Hz, CH₂).

Hz, NH), 3.83 (s, 6H, OMe), 3.74 (s, 12H, OMe), 3.34–3.30 (m, 4H, CH₂), 2.66 (t, 4H, ³J_{HH} = 5 Hz, CH₂), 2.30 (s, 3H, Me).

6.4.2.6. Synthesis of [(L³⁴H)₂PtCl₆]

There was not sufficient receptor synthesised to perform both a complexation reaction and solvent extraction studies in duplicate and so no complexation reaction was performed.

6.4.2.7. Synthesis of [(L³⁵H)₂PtCl₆]

The complex precipitated but was insoluble hence no ¹H NMR spectrum could be recorded. IR (solid, cm⁻¹): 3273 (ν_(N-H)), 1558 (ν_(C=S)). Anal. calc. for C₄₂H₆₀N₁₀Cl₆PtS₄: C, 40.65; H, 4.87; N, 11.29. Found: C, 40.78; H, 4.79; N, 11.23%.

6.4.2.8. Synthesis of [(L³⁶H)₂PtCl₆]

The complex was insoluble hence no ¹H NMR spectrum could be recorded. IR (solid, cm⁻¹): 3328 (ν_(N-H)), 1565 (ν_(C=S)). Anal. calc. for C₃₄H₇₂N₅Cl₆PtS₂: C, 54.36; H, 9.93; N, 18.64. Found: C, 54.01; H, 9.84; N, 18.55%.

6.4.2.9. Synthesis of [(L³⁷H)₂PtCl₆]

The complex was insoluble hence no ¹H NMR spectrum could be recorded. IR (solid, cm⁻¹): 3267 (ν_(N-H)), 1550 (ν_(C=S)). Anal. calc. for C₅₄H₈₄N₅Cl₆O₆PtS₂: C, 54.43; H, 6.94; N, 11.76. Found: C, 54.21; H, 6.88; N, 11.65%.

6.4.2.10. Synthesis of $[(L^{38}H)_2PtCl_6]$

No precipitate formed in the complexation reaction. 1H NMR (300 MHz, CD₃CN): δ/ppm 8.87 (br, 1H, NH⁺), 7.56 (t, 2H, $^3J_{HH} = 5$ Hz, NH), 7.14 (s, 4H, H_{Ar}), 3.84 (s, 12H, OMe), 3.77 (s, 6H, OMe), 3.25 (br, 4H, CH₂), 3.14 (br, 4H, CH₂), 2.85 (s, 3H, CH₃), 1.95 (br, 4H, CH₂). MS (ES⁻): *m/z* 1279 $[(L^{38})(L^{38b}H)PtCl_6]^-$, 1849 $[(L^{38}H)(L^{38})(L^{38b}H)(PtCl_6)(Cl)]^-$, 2419 $[(L^{38}H)(L^{38})_2(L^{38b}H)(PtCl_6)(Cl)_2]^{2-}$.

6.4.2.11. Synthesis of $[(L^{40}H)_2PtCl_6]$

The receptor L⁴⁰ was not sufficiently soluble in MeCN preventing complexation.

6.4.2.12. Synthesis of $[(L^{41}H)_2PtCl_6]$

No precipitate formed in the complexation reaction. 1H NMR (270 MHz, CD₃CN): δ/ppm 9.10 (br, 1H, NH⁺), 6.71 (s, 1H, NH), 6.66 (s, 2H, H_{Ar}), 5.56 (br, 1H, NH), 3.90 (s, 6H, OMe), 3.81 (s, 12H, OMe), 3.42–3.35 (m, 2H, CH₂), 2.60 (br, 2H, CH₂), 2.31 (s, 6H, 2 × Me).

6.5. References

1. Following the method of Zart M. K.; Sorrell T. N.; Powell D.; Borovik A.S., *Dalton Trans.*, 2003, 1986-1992.
2. For a previous report see Nagai, T.; Hamada, K.; Sato, R.; Wakita, Y., Jpn. Kokai Tokyo Koho, 1998, JKXXAF JP10272848, A19981013, CAN129:349100, AN1998:661752.
3. Miranda C.; Escartí F.; Lamarque L.; Yunta M. J. R.; Navarro P.; García-España E.; Jimeno M. L. *J. Am Chem. Soc.*, 2004, **126**, 823-833.
4. Following the method of Geraldes C. F. G. C.; Brucher E.; Cortes S.; Koenig S. H.; Sherry A. D., *J. Chem. Soc., Dalton Trans.*, 1992, 2517-2521.
5. Taylor P. D., *Talanta*, 1995, **42**, 845-850.
6. Koch K. R.; Burger M. R.; Kramer J.; Westra A. J., *Dalton Trans.*, 2006, 3277-3284.
7. Naidoo K. J.; Klatt G.; Koch K. R.; Robinson D. J., *Inorg. Chem.*, 2002, **41**, 1845-1849.
8. Lienke A.; Klatt G.; Robisnon D. J.; Koch K.; Naidoo K. J., *Inorg. Chem.*, 2001, **40**, 2352-2357.
9. Brammer L.; Swearingen J. K.; Bruton E. A.; Sherwood P., *Proc. Nat. Acad. Sci. (USA)*, 2002, **99**, 4956-4961.
10. Bowman-James K., *Acc. Chem. Res.*, 2005, **38**, 671-678.
11. Yoshizawa H.; Shiromori K.; Yamada S.; Baba Y.; Kawano Y.; Kondo K.; Ijichi K.; Hatake Y., *Solv. Extr. Res. Dev.*, Japan, 1997, **4**, 157-166.

7. Conclusions

This thesis reports the design, synthesis and evaluation of a series of receptors for the extraction and transport of $[\text{PtCl}_6]^{2-}$. Interest in this anion arises as it contains the precious metal platinum which has low natural abundance and a wide range of technological applications. The $[\text{PtCl}_6]^{2-}$ anion is produced under acidic conditions used for the processing of platinum containing ores and, by increasing the amount of $[\text{PtCl}_6]^{2-}$ recovered from feed streams, will lead to improved materials balances.

The current methods used to extract $[\text{PtCl}_6]^{2-}$ are thought to involve long chain alkyl amines. TOA falls into this category of reagents and has been used as a benchmark in comparing our receptor systems. The aims were to increase the extraction efficiency over TOA which has low extraction efficiency in the presence of competitive Cl^- .

The key design features incorporated into the receptors include a protonation site, hydrogen-bond donor groups and organic solubilising moieties. A tertiary amine protonation site was used to provide an electrostatic attraction between the receptor and $[\text{PtCl}_6]^{2-}$ and to allow the uptake and release of the anion by a pH swing mechanism in solvent extraction processes. Protonation of receptors under acidic conditions was confirmed by ^1H NMR spectroscopy, X-ray crystal diffraction and potentiometry experiments. Upon protonation of a receptor the $[\text{PtCl}_6]^{2-}$ anion can be extracted from an aqueous phase to form an organic soluble $[(\text{LH})_2\text{PtCl}_6]$ complex. Contacting the organic phase containing $[(\text{LH})_2\text{PtCl}_6]$ with aqueous base deprotonates the receptor and results in the release of $[\text{PtCl}_6]^{2-}$.

With the aim of increasing extraction efficiency the protonation site was complemented with hydrogen-bond donor groups including sulfonamide, urea, thiourea, amide and pyrrole moieties. Evidence for hydrogen-bonding between the

NH donors of receptors and $[\text{PtCl}_6]^{2-}$ was obtained through ^1H NMR spectroscopy and X-ray crystallography.

To optimise the organic solubility of the receptors a range of terminal substituents were studied including phenyl, *tert*-butyl, *n*-butyl, methyl, 3, 5-dimethylphenyl, 4-*iso*-propylphenyl, 4-*tert*-butylphenyl, 4-octylphenyl, 3, 5-dimethoxyphenyl, 3, 4-dimethoxyphenyl and 3, 4, 5-trimethoxyphenyl. Incorporating methoxyphenyl substituents into urea and amide-based receptors gave the optimum solubility for the resultant $[(\text{LH})_2\text{PtCl}_6]$ complexes in CHCl_3 . Despite attempts to increase the organic solubility extractants with thiourea moieties remained insoluble.

The key design features were incorporated into receptors with different scaffolds. Tripodal, bipodal and monopodal systems were prepared and have hydrogen-bond donors on three, two and one pendant arm(s), respectively. Within these three groups there are also two sub-sets, that is, those with a TREN scaffold and those with a TRPN scaffold.

The receptors were mostly synthesised in a series of one-step, high yielding reactions in which the starting materials are commercially available. This is an important feature of the work as it allows the bulk synthesis of receptors. Full characterisation data for each receptor synthesised was obtained including, in most cases, single crystal structures.

Complexation reactions were performed by mixing two equivalents of receptor with H_2PtCl_6 . Characterisation of the products was achieved by a variety of techniques including X-ray crystallography, ^1H NMR and infrared spectroscopy, mass spectrometry and elemental analysis. Five different crystal structures showing how the receptors and $[\text{PtCl}_6]^{2-}$ interact in the solid state were obtained and these confirm the 2:1 L: $[\text{PtCl}_6]^{2-}$ stoichiometry of the complexes, the protonation of the

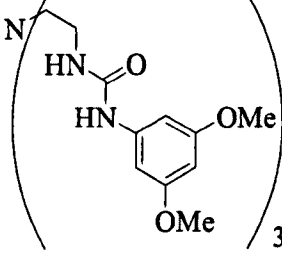
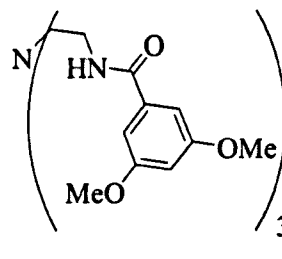
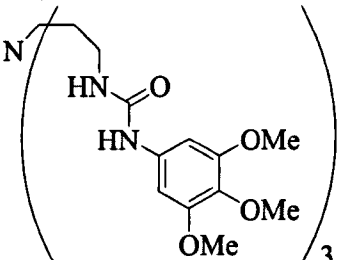
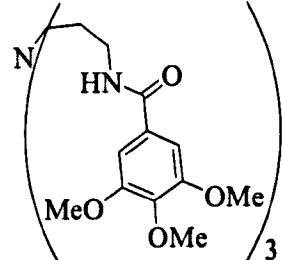
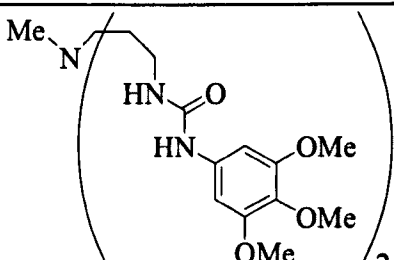
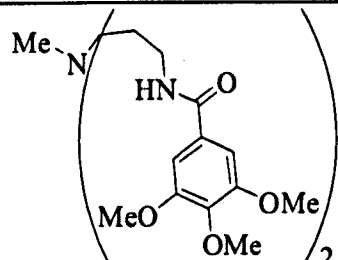
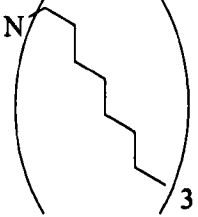
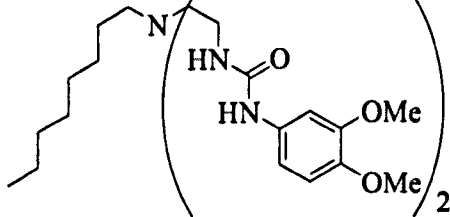
bridgehead nitrogen and the formation of hydrogen-bonds between the receptors and $[\text{PtCl}_6]^{2-}$.

The experimental procedures and protocols for solvent extractions were developed and optimised to assess the ability of the receptors to extract $[\text{PtCl}_6]^{2-}$. Only receptors that formed CHCl_3 soluble complexes could be studied in solvent extraction experiments. The graph in Figure 7.1 compares the extraction results for the different systems including:

- Tripodal TREN based urea and amide (L^{13} and L^{17} , respectively)
- Tripodal TRPN based urea and amide (L^{26} and L^{28} , respectively)
- Bipodal TRPN urea and amide (L^{31} and L^{38} , respectively)

The extraction results for TOA are provided for comparison and also the results for the receptor L^{34} which combines features of both TOA and our receptors (see Table 7.1).

Table 7.1. The structures of the receptors which have their extraction efficiency compared in Figure 7.1.

	UREAS	AMIDES
TREN-TRIPODAL	 L¹³	 L¹⁷
TRPN-TRIPODAL	 L²⁶	 L²⁸
TRPN-BIPODAL	 L³¹	 L³⁸
	 TOA	 L³⁴

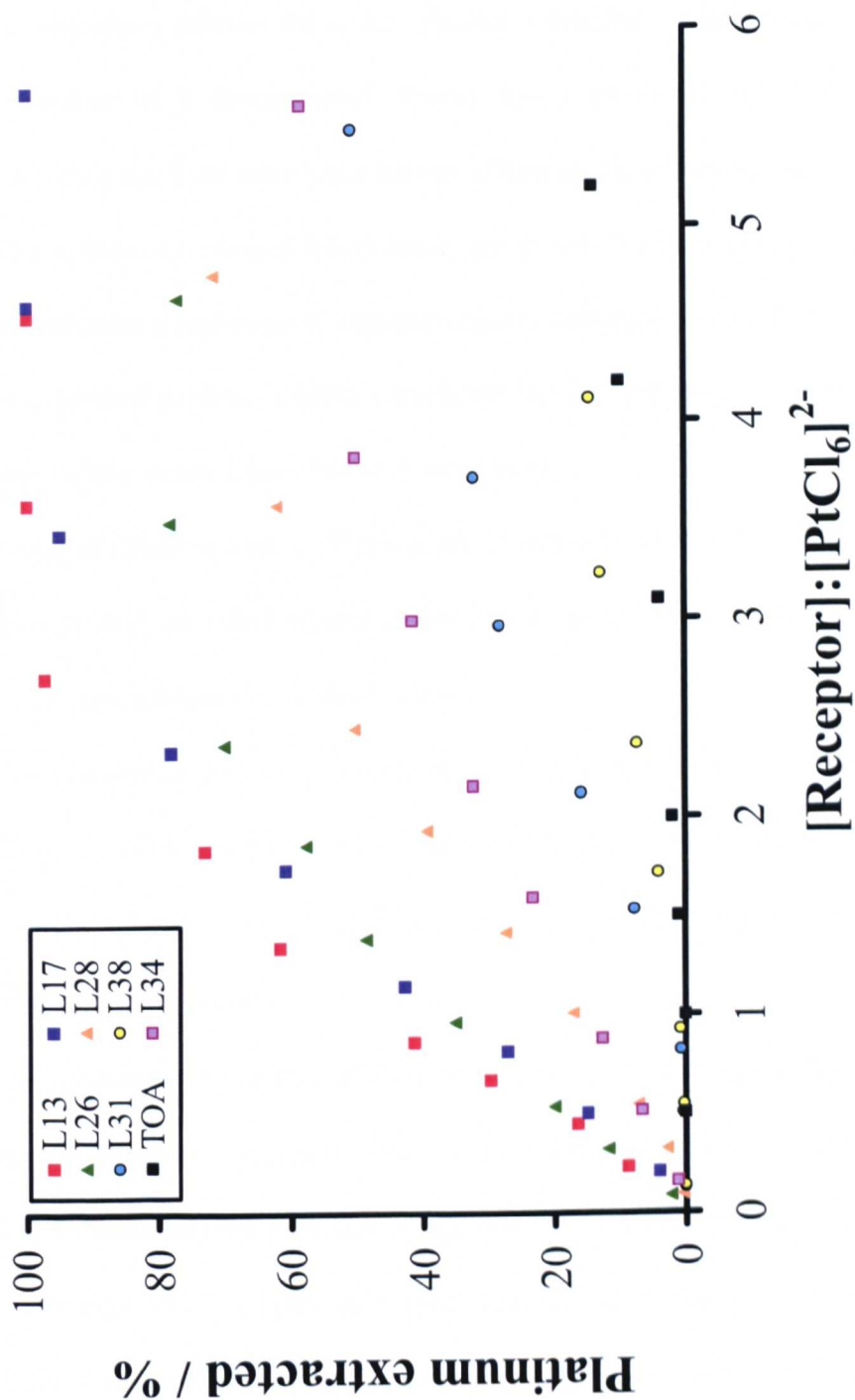


Figure 7.1. The extraction results for the receptors shown in Table 7.1

Comparison of the extraction results for these classes of receptors shows that extraction efficiency follows the order tripodal > bipodal > monopodal. This shows that the number of hydrogen-bond donors has a profound effect on extraction efficiency with more hydrogen-bond donors affording better extraction.

The optimum hydrogen-bond donor group was the urea group as it gave high extraction efficiency and formed organic soluble complexes. Receptors with amide groups also formed organic soluble complexes but in each case the amide receptors performed slightly worse than their urea analogues.

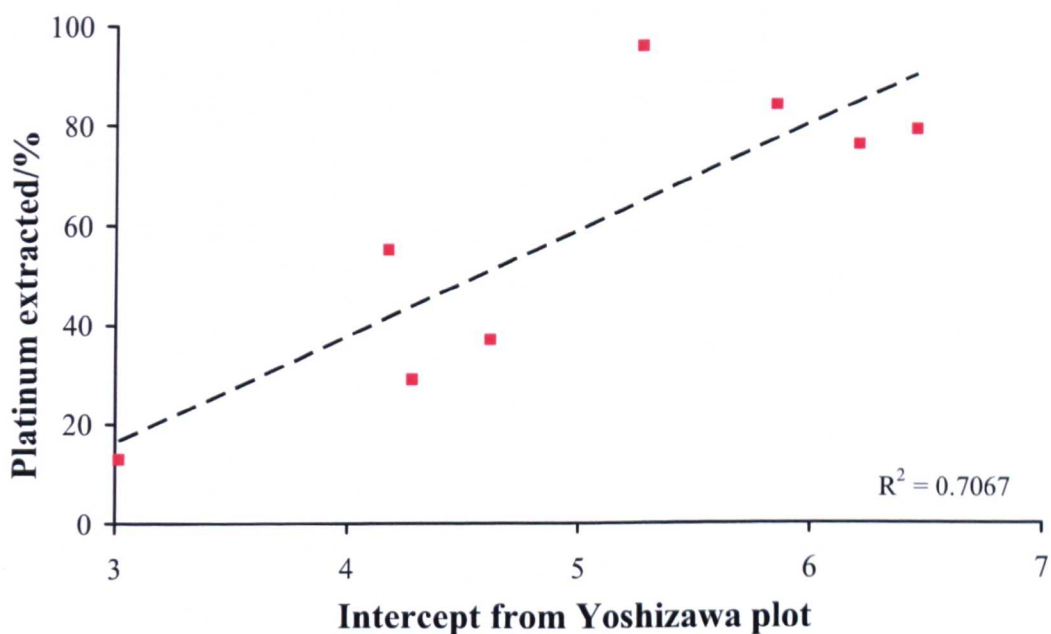
Tripodal systems with a TREN scaffold outperformed their TRPN analogues. This indicates that an ethyl spacer is preferred between the bridgehead nitrogen position and the hydrogen-bond donor sites.

Comparison of the extraction results for the receptors shown in Table 7.1 and Figure 7.1 with TOA show that all of the receptors are better than TOA. The best receptor is L¹³ and at an arbitrary [Receptor]:[PtCl₆]²⁻ ratio of three L¹³ extracts 97% whilst TOA only extracts 4%.

By following the method of Yoshizawa a plot of log A against log D_{Pt} should give a straight line with a gradient of two implying the formation of a 2:1 L:[PtCl₆]²⁻ complex in solution and the intercept being indicative of K_{PtCl₆}.¹ Table 7.2 reports the gradient, intercept and % of platinum extraction (in the presence of 3 equivalents of receptor) for a range of receptors that give a straight line graph with a gradient that approximates to two. There should be a correlation between the value of the intercept (as it represents K_{PtCl₆}) and % of platinum extracted. Although some correlation is observed there is some deviation from a straight line suggesting that Yoshizawa analyses are not a reliable indicator of extraction efficiency for our systems (Figure 7.2).

Table 7.2. The gradients, intercepts and % of Pt extracted for our receptors which have a gradient that approximated to two in a Yoshizawa plot.

Receptor	Gradient	Intercept	% Pt extracted
L^{13}	1.6118	5.2772	96
L^{15}	2.0882	4.6175	37
L^{17}	1.9886	5.8554	84
L^{18}	2.3904	6.2115	76
L^{19}	2.3762	6.4614	79
L^{28}	1.7688	4.1786	55
L^{31}	2.1731	4.2808	29
L^{38}	1.7968	3.0170	13

**Figure 7.2.** Graph comparing the intercept of Yoshizawa plots with the actual % of Pt extracted.

We have designed and synthesised a series of extractants for $[PtCl_6]^{2-}$.

Through continual design improvements an optimised receptor was developed which shows a significant improvement over TOA, the extractant thought to be currently used. The aims of the project have therefore been successfully achieved.

Suggestions for future work in this area of research include studies into the selectivity of $[PtCl_6]^{2-}$ over $[PdCl_4]^{2-}$, increasing the number of hydrogen-bond donor groups, for example, in tetrapodal or macrocyclic systems and assessing the

effect of a rigid capping group, for example pyridine, onto which pendant arms containing hydrogen-bond donor groups can be appended.

7.1. References

1. Yoshizawa H.; Shiomori K.; Yamada S.; Baba Y.; Kawano Y.; Kondo K.; Ijichi K.; Hatake Y., *Solv. Extr. Res. Devel.*, Japan, 1997, **4**, 157-166.

Reagent Preparation and Instrumentation

All solvents and reagents were commercially available from Aldrich, Fluka, Lancaster or TCI Chemicals. The reagents and solvents were used as purchased from the supplier. ^1H NMR and ^{13}C NMR spectra were recorded on a Bruker DPX 300 operating frequency 300 MHz (^1H) and 75 MHz (^{13}C) or a JEOL EX 270 operating frequency 270 MHz (^1H) and 68 MHz (^{13}C). The chemical shifts (δ) are reported in parts per million (ppm) relative to the residual solvent signal in CDCl_3 (δ_{H} 7.27 and δ_{C} 77.0), $\text{dmso}-d_6$ (δ_{H} 2.50 and δ_{C} 39.5), MeCN (δ_{H} 1.94 and δ_{C} 118.7, 1.40) or CD_3OD (δ_{H} 4.87, 3.31 and δ_{C} 49.1) at ambient temperature. All coupling constants (J) are given in Hz. ^{195}Pt NMR were recorded on a Bruker Avance DRX 500 relative to K_2PtCl_6 (1 M in D_2O) referenced at 0.0 ppm. Mass spectra were obtained on a VG Autospec instrument by Mr Tony Hollingworth and Mr Graham Coxhill at the University of Nottingham or the EPSRC National Mass Spectrometry service at the University of Wales in Swansea. IR spectra were recorded in the range 400–4000 cm^{-1} using a Nicolet Avatar 320 (solid) FT-IR spectrophotometers. Absorption spectra were recorded using a Perkin Elmer Lambda 5 spectrophotometer and using quartz cells at ambient temperature. Elemental analyses were performed using a Fisons Instruments EA 1108 CHN elemental analyser by Mr Trevor Spencer or Miss Tong Lui at the University of Nottingham or were sent to Stephen Boyer at London Metropolitan University. X-Ray diffraction data were collected on a Bruker SMART 1000 or SMART APEX CCD area diffractometer. Structure solution and refinement were carried out using the SHELX suite of programs. ICP-OES measurements at the University of Edinburgh were performed using a Perkin Elmer Optima 5300DV Spectrometer. ICP-MS measurements at the University of Nottingham were performed using a Thermo-Fisher Scientific X-Series in standard mode.

Crystallographic Details for Chapter 2

Receptor code	L ¹	L ²	L ³
Chemical formula	C ₂₄ H ₃₀ N ₄ O ₆ S ₃	C ₂₇ H ₃₃ N ₇ O ₃	C ₂₇ H ₃₃ N ₇ S ₃
M _r	566.73	503.60	551.78
Cell setting, space group	Orthorhombic, Pbc _a	Monoclinic, P2 ₁ /c	Monoclinic, C2/c
Temperature (K)	150 (2)	150 (2)	150 (2)
a, b, c (Å)	9.7652 (8), 12.7268 (10), 43.540 (3)	12.482 (2), 17.717 (3), 13.385 (2)	13.8631 (10), 14.2044 (10), 27.954 (2)
α, β, γ (°)	90.00, 90.00, 90.00	90.00, 117.501 (3), 90.00	90.00, 98.307 (1), 90.00
V (Å ³)	5411.1 (13)	2625.4 (8)	5446.9 (12)
Z	8	4	8
D _x (Mg m ⁻³)	1.391	1.274	1.346
Radiation type	Mo Kα	Mo Kα	Mo Kα
μ (mm ⁻¹)	0.32	0.09	0.30
Crystal form, colour	Block, colourless	Lath, colourless	Block, colourless
Crystal size (mm)	0.75 × 0.31 × 0.20	0.77 × 0.11 × 0.05	0.30 × 0.18 × 0.17
Diffractometer	Bruker SMART APEX CCD area detector	Bruker SMART APEX CCD area detector	Bruker SMART APEX CCD area detector
Data collection method	ω	ω	ω
Absorption correction	Multi-scan (based on symmetry-related measurements)	None	None
T _{min}	0.819	—	—
T _{max}	1.000	—	—
No. of measured, independent and observed reflections	28778, 6936, 5228	13395, 4593, 3023	15038, 6432, 4694
Criterion for observed reflections	I > 2σ(I)	I > 2σ(I)	I > 2σ(I)
R _{int}	0.028	0.007	0.051
θ _{max} (°)	27.5	25.0	27.5
Refinement on	F ²	F ²	F ²
R[F ² > 2σ(F ²)], wR(F ²), S	0.057, 0.141, 1.13	0.046, 0.116, 0.93	0.039, 0.097, 0.95
No. of reflections	6221 reflections	4593 reflections	6199 reflections
No. of parameters	388	334	334
H-atom treatment	Constrained to parent site	Constrained to parent site	Constrained to parent site
Weighting scheme	Calculated $w = 1/[\sigma^2(F_o^2) + (0.0528P)^2 + 6.3569P]$ where $P = (F_o^2 + 2F_c^2)/3$	Calculated $w = 1/[\sigma^2(F_o^2) + (0.0665P)^2]$ where $P = (F_o^2 + 2F_c^2)/3$	Calculated $w = 1/[\sigma^2(F_o^2) + (0.0532P)^2]$ where $P = (F_o^2 + 2F_c^2)/3$
(Δ/σ) _{max}	0.007	<0.0001	0.001
Δρ _{max} , Δρ _{min} (e Å ⁻³)	0.58, -0.57	0.35, -0.26	0.46, -0.26

Receptor code	L ⁸	L ⁹
Chemical formula	C ₂₇ H ₃₀ N ₄ O ₃	C ₂₁ H ₂₇ N ₇ O ₃
M _r	458.55	425.50
Cell setting, space group	Monoclinic, P2 ₁ /n	Triclinic, P-1
Temperature (K)	293 (2)	150 (2)
a, b, c (Å)	10.004 (2), 17.151 (4), 14.472 (3)	9.325 (3), 10.298 (3), 12.579 (4)
α, β, γ (°)	90.00, 101.06 (2), 90.00	76.737 (5), 88.302 (5), 68.106 (5)
V (Å ³)	2437.0 (9)	1088.8 (10)
Z	4	2
D _x (Mg m ⁻³)	1.250	1.298
Radiation type	Mo Kα	Mo Kα
μ (mm ⁻¹)	0.08	0.09
Crystal form, colour	Block, colourless	Needle, pale yellow
Crystal size (mm)	0.40 × 0.40 × 0.20	0.55 × 0.10 × 0.06
Diffractometer	Siemens P3	Bruker SMART1000 CCD area detector
Data collection method	θ–2θ	ω
Absorption correction	None	None
T _{min}	—	—
T _{max}	—	—
No. of measured, independent and observed reflections	5938, 5625, 2590	7374, 3786, 2197
Criterion for observed reflections	I > 2σ(I)	I > 2σ(I)
R _{int}	0.030	0.121
θ _{max} (°)	27.6	25.1
No. and frequency of standard reflections	3 every 300 reflections	
Intensity decay (%)	0	
Refinement on	F ²	F ²
R[F ² > 2σ(F ²)], wR(F ²), S	0.059, 0.165, 1.00	0.060, 0.163, 0.94
No. of relections	4975 reflections	3786 reflections
No. of parameters	307	280
H-atom treatment	Constrained to parent site	Constrained to parent site
Weighting scheme	Calculated w = 1/[σ ² (F _o ²) + (0.0605P) ² + 0.5052P] where P = (F _o ² + 2F _c ²)/3	Calculated w = 1/[σ ² (F _o ²) + (0.09P) ²] where P = (F _o ² + 2F _c ²)/3
(Δ/σ) _{max}	-0.001	0.001
Δρ _{max} , Δρ _{min} (e Å ⁻³)	0.16, -0.23	0.27, -0.32

	$[(\text{L}^1\text{H})_2\text{PtCl}_6]$	$[(\text{L}^3\text{H})_2\text{PtCl}_6]$
Chemical formula	$\text{C}_{48}\text{H}_{62}\text{Cl}_6\text{N}_8\text{O}_{12}\text{PtS}_6$	$2(\text{C}_{21}\text{H}_{46}\text{N}_7\text{O}_3).\text{PtCl}_6.2(\text{C}_2\text{H}_3\text{N})$
M_r	1543.21	1379.19
Cell setting, space group	Monoclinic, $P2_1/c$	Triclinic, $P-1$
Temperature (K)	150 (2)	150 (2)
a, b, c (Å)	14.140 (2), 7.3640 (13), 29.831 (5)	8.8396 (5), 13.2745 (7), 14.4379 (8)
α, β, γ (°)	90.00, 99.040 (3), 90.00	93.865 (2), 97.368 (2), 95.263 (2)
V (Å ³)	3067.6 (9)	1667.7 (3)
Z	2	1
D_x (Mg m ⁻³)	1.671	1.373
Radiation type	Mo $K\alpha$	Mo $K\alpha$
μ (mm ⁻¹)	2.82	2.40
Crystal form, colour	Lath, pale yellow	Tablet, yellow
Crystal size (mm)	0.32 × 0.14 × 0.04	0.41 × 0.34 × 0.22
Diffractometer	Bruker SMART APEX CCD area detector	Bruker SMART APEX CCD area detector
Data collection method	ω	ω
Absorption correction	Multi-scan (based on symmetry-related measurements)	Multi-scan (based on symmetry-related measurements)
T_{\min}	0.276	0.800
T_{\max}	1.000	1.000
No. of measured, independent and observed reflections	14717, 5854, 4564	14910, 7540, 7536
Criterion for observed reflections	$I > 2\sigma(I)$	$I > 2\sigma(I)$
R_{int}	0.057	0.013
θ_{\max} (°)	25.0	27.5
Refinement on	F^2	F^2
$R[F^2 > 2\sigma(F^2)], wR(F^2), S$	0.077, 0.153, 1.29	0.020, 0.054, 1.04
No. of relections	5387 reflections	7540 reflections
No. of parameters	361	333
H-atom treatment	Constrained to parent site	Constrained to parent site
Weighting scheme	Calculated $w = 1/[\sigma^2(F_o^2) + (0.0244P)^2 + 40.3792P]$ where $P = (F_o^2 + 2F_c^2)/3$	Calculated $w = 1/[\sigma^2(F_o^2) + (0.034P)^2 + 0.571P]$ where $P = (F_o^2 + 2F_c^2)/3$
$(\Delta/\sigma)_{\max}$	0.001	0.001
$\Delta\rho_{\max}, \Delta\rho_{\min}$ (e Å ⁻³)	2.66, -2.06	0.81, -0.49

Computer programs: *Bruker SMART* version 5.625 (Bruker, 2001); *Bruker SAINT* version 6.36a (Bruker, 2000); *Bruker SAINT*; *Bruker SHELXTL* (Bruker, 2001); *SHELXS-97* (Sheldrick, 1990); *SHELXS97* (Sheldrick, 1990); *SHELXL-97* (Sheldrick, 1997);; *enCIFer* (CCDC, 2003); *PLATON* (Spek, 2003); *enCIFer* (Allen et al., 2004);); *SHELXTL*; *P3-P4/PC* (Siemens, 1989); *Bruker SMART* version 5.624 (Bruker, 2001); *P3-P4/PC*; *Bruker SAINT* version 6.36a (Bruker, 2002); *XDISK* (Siemens, 1989).

Crystallographic Details for Chapter 3

	L ¹¹	L ¹²	L ¹⁹
Chemical formula	C ₃₆ H ₅₁ N ₇ O ₃	C ₃₉ H ₅₇ N ₇ O ₃	C ₃₃ H ₄₂ N ₄ O ₉
M _r	629.84	671.92	638.71
Cell setting, space group	Orthorhombic, Pbc _a	Triclinic, P-1	Triclinic, P-1
Temperature (K)	150 (2)	150 (2)	150 (2)
<i>a</i> , <i>b</i> , <i>c</i> (Å)	17.987 (2), 13.3225 (12), 29.438 (3)	11.336 (4), 12.489 (4), 14.891 (5)	9.535 (6), 13.469 (9), 13.538 (9)
α, β, γ (°)	90.00, 90.00, 90.00	88.618 (6), 88.220 (6), 66.980 (5)	74.578 (10), 89.653 (10), 73.562 (10)
<i>V</i> (Å ³)	7054 (2)	1939 (2)	1603.0 (3)
<i>Z</i>	8	2	2
D _x (Mg m ⁻³)	1.186	1.151	1.323
Radiation type	Mo K α	Mo K α	Mo K α
μ (mm ⁻¹)	0.08	0.07	0.10
Crystal form, colour	Column, colourless	Block, colourless	Block, colourless
Crystal size (mm)	0.66 × 0.08 × 0.07	0.28 × 0.16 × 0.14	0.60 × 0.51 × 0.33
Diffractometer	Bruker SMART APEX CCD area detector	Bruker SMART1000 CCD area detector	Bruker SMART APEX CCD area detector
Data collection method	ω	ω	ω
Absorption correction	None	None	None
T _{min}	–	–	–
T _{max}	–	–	–
No. of measured, independent and observed reflections	43891, 8887, 3274	17169, 8690, 3975	13578, 7120, 6114
Criterion for observed reflections	I > 2σ(I)	I > 2σ(I)	I > 2σ(I)
R _{int}	0.104	0.058	0.076
θ _{max} (°)	27.5	27.7	27.6
Refinement on	F ²	F ²	F ²
R[F ² > 2σ(F ²)], wR(F ²), S	0.043, 0.095, 0.75	0.050, 0.128, 0.85	0.051, 0.143, 1.05
No. of relections	8107 reflections	8690 reflections	7120 reflections
No. of parameters	429	440	415
H-atom treatment	Mixture of independent and constrained refinement	Constrained to parent site	Constrained to parent site
Weighting scheme	Calculated $w = 1/[\sigma^2(F_o^2) + (0.0338P)^2]$ where $P = (F_o^2 + 2F_c^2)/3$	Calculated $w = 1/[\sigma^2(F_o^2) + (0.053P)^2]$ where $P = (F_o^2 + 2F_c^2)/3$	Calculated $w = 1/[\sigma^2(F_o^2) + (0.0848P)^2 + 0.22P]$ where $P = (F_o^2 + 2F_c^2)/3$
(Δ/σ) _{max}	0.001	<0.0001	0.001
Δρ _{max} , Δρ _{min} (e Å ⁻³)	0.37, -0.25	0.40, -0.28	0.44, -0.41
Extinction method	None	SHELXL	None
Extinction coefficient		0.0065 (12)	

$[(L^{19}H)_2PtCl_6]$	
Chemical formula	$C_{70}H_{92}Cl_6N_{10}O_{18}Pt$
M_r	1769.33
Cell setting, space group	Triclinic, $P\bar{1}$
Temperature (K)	150 (2)
a, b, c (Å)	9.1959 (7), 14.6947 (11), 14.7245 (11)
α, β, γ (°)	93.921 (2), 98.260 (2), 101.795 (2)
V (Å ³)	1917.7 (4)
Z	1
D_x (Mg m ⁻³)	1.532
Radiation type	Mo $K\alpha$
μ (mm ⁻¹)	2.113
Crystal form, colour	Column, pale yellow
Crystal size (mm)	0.35 × 0.19 × 0.13
Diffractometer	Bruker SMART1000 CCD area detector
Data collection method	ω
Absorption correction	Multi-scan (based on symmetry-related measurements)
T_{\min}	0.823
T_{\max}	1.000
No. of measured, independent and observed reflections	17129, 8568, 7816
Criterion for observed reflections	$I > 2\sigma(I)$
R_{int}	0.028
Θ_{\max} (°)	27.5
Refinement on	F^2
$R[F^2 > 2\sigma(F^2)], wR(F^2), S$	0.034, 0.078, 1.105
No. of relections	8566
No. of parameters	477
H-atom treatment	Constrained to parent site
Weighting scheme	Calculated $w = 1/[\sigma^2(F_o^2) + (0.0408P)^2 + 0.4771P]$ where $P = (F_o^2 + 2F_c^2)/3$
$(\Delta/\sigma)_{\max}$	0.008
$\Delta\rho_{\max}, \Delta\rho_{\min}$ (e Å ⁻³)	0.85, -0.50

Computer programs: *Bruker SMART version 5.625* (Bruker, 2001); *Bruker SMART version 5.624* (Bruker, 2001); *Bruker SAINT version 6.36a* (Bruker, 2000); *Bruker SAINT version 6.36a* (Bruker, 2002); *Bruker SAINT*; *Bruker SHELXTL* (Bruker, 2001); *SHELXS97* (Sheldrick, 1990); *SHELXS-97* (Sheldrick, 1990); *SHELXL97* (Sheldrick, 1997); *SHELXL-97* (Sheldrick, 1997); *enCIFer* (Allen et al., 2004); *PLATON* (Spek, 2003);

Potentiometry Experiments

All pH-metric measurements ($\text{pH} = -\log[\text{H}^+]$) employed for the determination of protonation constants were carried out in solutions in MeCN/ H₂O 50:50 (v:v) mixture containing 0.10 M NMe₄Cl at 298.1 ± 0.1 K under a nitrogen atmosphere. A Hamilton glass electrode was calibrated as a hydrogen concentration probe by titrating known amounts of HCl with CO₂-free NaOH solutions and determining the equivalent point by Gran's method which allows one to determine the standard potential E^o and the ionic product of H₂O ($\text{pK}_w = 14.99(1)$). At least three measurements were performed for each system in the pH range 2.5 -11.0. In all experiments the ligand concentration was approximately 1×10^{-4} M. The computer program HYPERQUAD was used to calculate the equilibrium constants from e.m.f data.

Solvent Extraction Protocol**1a) Make up $[PtCl_6]^{2-}$ stock solution**

Weigh out of $H_2PtCl_6 \cdot H_2O$ 1.28 mmol (0.0332 g) (record the weight of the H_2PtCl_6 in spreadsheet) and dissolve in 0.6 M HCl (50 cm^3) in a volumetric flask to give the $[PtCl_6]^{2-}$ stock solution (0.6 M HCl = 5 cm^3 of 6 M HCl and 45 cm^3 deionised H_2O)

b) Using a variable pipettor measure 5 cm^3 portions of the $[PtCl_6]^{2-}$ stock solution into nine 25 cm^3 Schott flasks (check by weight that the first decimal place is zero i.e. 5.0xxx).

2a) Make up stock solution of ligand

Weigh the receptor (10.26 mmol) and record the weight in the spreadsheet then dissolve this in $CHCl_3$ (25 cm^3) in a volumetric flask to give the ligand stock solution. N.B. This can be scaled down so that you have 5.13 mmol of receptor in 12.5 cm^3 of $CHCl_3$ and eliminating sample one from the extraction series).

b) From the ligand stock solution prepare dilutions for each of the nine extraction experiments. The standard volumes are provided in the spreadsheet and cover a range of [Receptor]: $[PtCl_6]^{2-}$ ratios. Use a variable pipettor to add the required aliquots of the stock solution into the respective flask and record the weight of each aliquot in the spreadsheet then dilute each flask to 5 cm^3 with $CHCl_3$.

3) Extraction

Add the receptor solutions into each of the $9 \times 25\text{cm}^3$ Schott flasks which contain aqueous $[PtCl_6]^{2-}$ and add lids to prevent evaporation of the solvents. Stir the samples vigorously at r.t. for 4 h.

4a) Whilst the extraction is taking place input the weights of H_2PtCl_6 , receptor and 9 receptor aliquots into the spreadsheet. The required amounts of H_2O and NaOH (0.05502 M) for the back extraction are calculated through the spreadsheet (2:1 NaOH:L).

b) Use a variable pipettor to prepare the back extraction solutions. In nine large vials add the required amount of deionised H_2O then NaOH and record the weights of the aliquots added. The volume of each back extraction solution totals 4cm^3 .

5) Following the 4h extraction stop the extractions stirring and allow the layers to separate. Use a Pasteur pipette to separate the aqueous and organic phases of the 9 extractions into 18 ICP tubes labelled 1a–9a and 1o–9o (a and o refer to aqueous and organic phases, respectively).

6) Back Extraction

Using a variable pipettor add 4 cm^3 of the organic phase into the respective back extraction solutions. Add lids to the vials, secure the lids with parafilm and stir the phases at r.t. for 30 mins.

7) Whilst the back extractions are stirring use a variable pipettor to measure 2 cm^3 aliquots of the aqueous samples (1a–9a) into nine 5 cm^3 volumetric flasks. Record the weight of the 2 cm^3 aliquots in the spreadsheet and then dilute to 5 cm^3 with deionised H_2O . Transfer the samples into ICP tubes.

8) After 30 mins stop the back extraction stirring and allow the layers to separate. Use a Pasteur pipette to measure 2.0 g aliquots of each aqueous phase into nine 5 cm^3

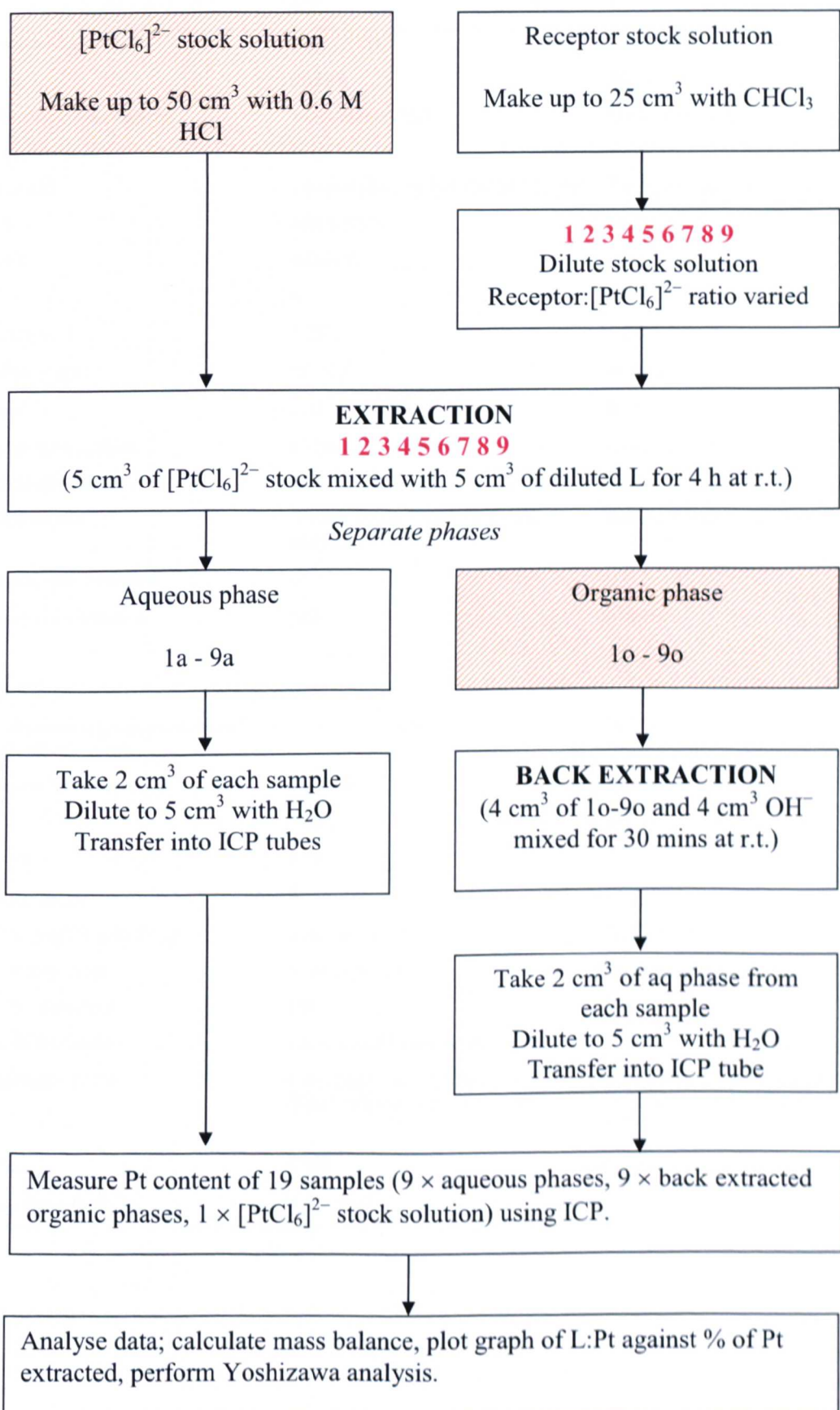
volumetric flasks taking care that no CHCl₃ is transferred. Record the weights of the aliquots in the spreadsheet. Dilute the samples to 5 cm³ with deionised H₂O and transfer the samples into ICP tubes.

9) Using a variable pipettor measure 2cm³ of the [PtCl₆]²⁻ stock solution into a 5 cm³ volumetric flask and record the weight of the aliquot in the spreadsheet. Dilute to 5 cm³ with deionised H₂O and transfer the solution into an ICP tube.

10) ICP measurements

For an extraction series consisting of 9 samples there will be 19 samples for analysis by ICP-MS; 9 aqueous phases, 9 back extracted aqueous phases and 1 platinum stock solution. To get the concentration of Pt into the working range of the spectrometer for ICP-MS it is necessary to dilute the solutions by a factor of 1000 using 2% HCl (made with analytical grade HCl and ΩQ H₂O).

Solvent Extraction Flowsheet*



* 'a' denotes aqueous phase from original separation

'o' denotes the back extracted aqueous phases that originate from the organic phase in the initial separation

Crystallographic Details for Chapter 6

	L²⁹	L³⁸
Chemical formula	C ₂₁ H ₂₉ N ₅ O ₂	C ₂₁ H ₂₉ N ₅ S ₂
M _r	383.49	415.61
Cell setting, space group	Monoclinic, P2 ₁ /n	Monoclinic, P2 ₁ /c
Temperature (K)	150 (2)	150 (2)
a, b, c (Å)	10.4804 (14), 18.205 (2), 21.775 (3)	7.5271 (4), 16.7186 (9), 18.0355 (9)
β (°)	103.123 (2)	92.666 (2)
V (Å ³)	4046 (2)	2267.2 (3)
Z	8	4
D _x (Mg m ⁻³)	1.259	1.218
Radiation type	Mo Kα	Mo Kα
μ (mm ⁻¹)	0.08	0.25
Crystal form, colour	Column, colourless	Cube, colourless
Crystal size (mm)	0.80 × 0.21 × 0.18	0.60 × 0.60 × 0.56
Diffractometer	Bruker SMART1000 CCD area detector	Bruker SMART APEX CCD area detector
Data collection method	ω	ω
Absorption correction	None	None
T _{min}	—	—
T _{max}	—	—
No. of measured, independent and observed reflections	25431, 9164, 6501	14294, 5219, 4615
Criterion for observed reflections	I > 2σ(I)	I > 2σ(I)
R _{int}	0.066	0.037
θ _{max} (°)	27.6	27.5
Refinement on	F ²	F ²
R[F ² > 2σ(F ²)], wR(F ²), S	0.042, 0.119, 0.99	0.033, 0.097, 1.05
No. of reflections	9164 reflections	5219 reflections
No. of parameters	505	253
H-atom treatment	Constrained to parent site	Constrained to parent site
Weighting scheme	Calculated $w = 1/[\sigma^2(F_o^2) + (0.062P)^2]$ where $P = (F_o^2 + 2F_c^2)/3$	Calculated $w = 1/[\sigma^2(F_o^2) + (0.0574P)^2 + 0.320P]$ where $P = (F_o^2 + 2F_c^2)/3$
(Δ/σ) _{max}	0.001	0.001
Δρ _{max} , Δρ _{min} (e Å ⁻³)	0.31, -0.25	0.30, -0.26

	$[(\text{L}^{29}\text{H})_2\text{PtCl}_6]$	$[(\text{L}^{38}\text{H})_2\text{PtCl}_6]$
Chemical formula	$2(\text{C}_{21}\text{H}_{30}\text{N}_5\text{O}_2).\text{PtCl}_6$	$2(\text{C}_{27}\text{H}_{40}\text{N}_3\text{O}_8).\text{Cl}_6\text{Pt}.2(\text{C}_2\text{H}_3\text{N})$
M_r	1176.79	1641.25
Cell setting, space group	Monoclinic, $P2_1/c$	Triclinic, $P-1$
Temperature (K)	150 (2)	150 (2)
a, b, c (Å)	9.1802 (8), 32.097 (3), 9.2877 (8)	11.2141 (6), 13.1967 (7), 14.3580 (8)
α, β, γ (°)	90.00, 116.521 (1), 90.00	81.647 (1), 68.232 (1), 68.534 (1)
V (Å ³)	2448.7 (6)	1836.3 (3)
Z	2	1
D_x (Mg m ⁻³)	1.596	1.484
Radiation type	Mo $K\alpha$	Mo $K\alpha$
μ (mm ⁻¹)	3.24	2.20
Crystal form, colour	Tablet, yellow	Block, yellow
Crystal size (mm)	0.31 × 0.12 × 0.02	0.59 × 0.32 × 0.17
Diffractometer	Bruker SMART APEX CCD area detector	Bruker SMART APEX CCD area detector
Data collection method	ω	ω
Absorption correction	Multi-scan (based on symmetry-related measurements)	Multi-scan (based on symmetry-related measurements)
T_{\min}	0.513	0.717
T_{\max}	1.000	1.000
No. of measured, independent and observed reflections	12625, 5737, 4444	15883, 8348, 8212
Criterion for observed reflections	$I > 2\sigma(I)$	$I > 2\sigma(I)$
R_{int}	0.029	0.018
θ_{\max} (°)	27.5	27.6
Refinement on	F^2	F^2
$R[F^2 > 2\sigma(F^2)], wR(F^2), S$	0.064, 0.128, 1.17	0.025, 0.063, 1.04
No. of relections	5615 reflections	8346 reflections
No. of parameters	277	440
H-atom treatment	Constrained to parent site	Rigid rotor; riding model
Weighting scheme	Calculated $w = 1/[\sigma^2(F_o^2) + (0.029P)^2 + 14.16P]$ where $P = (F_o^2 + 2F_c^2)/3$	Calculated $w = 1/[\sigma^2(F_o^2) + (0.037P)^2 + 0.726P]$ where $P = (F_o^2 + 2F_c^2)/3$
$(\Delta/\sigma)_{\max}$	0.001	0.001
$\Delta\rho_{\max}, \Delta\rho_{\min}$ (e Å ⁻³)	1.64, -1.24	1.09, -0.61

Computer programs: Bruker SMART version 5.625 (Bruker, 2001); Bruker SAINT version 6.36A (Bruker, 2000); Bruker SAINT version 6.36a (Bruker, 2000); Bruker SAINT; Bruker SHELXTL (Bruker, 2001); SHELXS97 (Sheldrick, 1990); SHELXL97 (Sheldrick, 1997); SIR92 (Altomare et al., 1994); enCIFer (Allen et al., 2004); PLATON (Spek, 2003).

TEXT BOUND CLOSE TO THE SPINE IN
THE ORIGINAL THESIS

Outer-Sphere Coordination Chemistry: Selective Extraction and Transport of the $[\text{PtCl}_6]^{2-}$ Anion**

Katherine J. Bell, Arjan N. Westra, Rebecca J. Warr, Jy Chartres, Ross Ellis, Christine C. Tong, Alexander J. Blake, Peter A. Tasker,* and Martin Schröder*

Selectivity in the transport of platinum group metal ions by solvent extraction in industrial processes depends critically upon control of the metal coordination chemistry through the formation of either inner-sphere complexes with dialkyl sulfides or hydroxyoximes,^[1] or through formation of outer-sphere organic-soluble salts with hydrophobic trialkylamine and related reagents of the Alamine type.^[1,2] The latter rely upon control of partition coefficients and solubilities such that anion exchange can be used to transfer the chlorometallate to a water-immiscible solvent in a pH-dependent equilibrium [Eq. (1)].^[2]



Although the solvent extraction of base metals such as Cu and Zn usually involves the formation of inner-sphere coordination complexes,^[3] the very slow ligand exchange for the $[\text{PtCl}_6]^{2-}$ ion^[4] makes it necessary to address and recognise the outer coordination sphere of this species to form neutral anion-ligand packages. Selectivity continues to be a challenge in the development of supramolecular recognition of anions^[5] and is a pervasive problem in extractive metallurgy because the generation of electrolytes of high purity is essential for efficient electrolytic reduction to produce metals.^[6] Thus, an understanding of the nature and disposition of electrostatic and supramolecular hydrogen-bonding interactions to chlorometallates is essential to the design of selective extractants for these anions. DFT calculations and NMR spectroscopic

studies of the solvation and ion pairing of $[\text{PtCl}_6]^{2-}$ suggest that hydrogen-bonding solvate molecules, such as methanol, address the triangular faces of the hexachloro octahedron,^[7] whereas formation of trifurcated hydrogen-bonds to faces or bifurcated hydrogen-bonding to edges of the hexachloro octahedron has been predicted on the basis of the location of maximum electron density in the anion;^[8] such interactions have indeed been observed in solid-state structures of chlorometallates.^[9]

We report herein a new approach to the selective complexation and extraction of hexachlorometallates in the presence of chloride ions using tripodal ionophores incorporating multiple hydrogen-bond donors linked to a protonatable bridgehead N center. Such a design can not only address the threefold symmetry of the outer coordination sphere of $[\text{PtCl}_6]^{2-}$ by presenting neutral hydrogen-bond donors to the faces or edges of the hexachloro octahedron (Figure 1), but

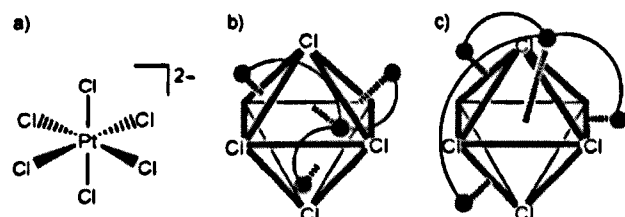
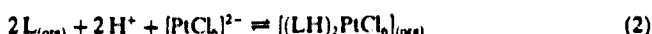


Figure 1. The structure of $[\text{PtCl}_6]^{2-}$ (a) and proposed modes of binding to tripodal multiple hydrogen-bond ionophores through interactions with the faces (b) or the edges (c) of the hexachloro octahedron. The protonated amine of the receptor is shown as a black sphere and the neutral hydrogen-bond donors as gray spheres.

also provides a positive charge to ensure the solubility of a neutral 2:1 $[\text{LH}^+] : [\text{PtCl}_6]^{2-}$ complex in water-immiscible solvents. Our target in this work was to design useful solvent extractants for the recovery of Pt^{IV} from acidic chloride streams, whereby loading and stripping of the organic phase are controlled by a "pH-swing" mechanism [Eqs. (2) and (3)].



Such a protocol could then be implemented for the recovery of platinum metal anions from the highly acidic chloride streams currently used in industry. Furthermore, selective extraction of $[\text{PtCl}_6]^{2-}$ over Cl^- , which is present in substantial excess in industrial feed streams, is essential for an efficient process, and is, therefore, a key design requirement for our

[*] K. J. Bell, Dr. R. J. Warr, Prof. Dr. A. J. Blake, Prof. Dr. M. Schröder

School of Chemistry

University Park

University of Nottingham

Nottingham, NG7 2RD (UK)

Fax: (+44) 115-951-3563

E-mail: M.Schroeder@nottingham.ac.uk

Dr. A. N. Westra, Dr. J. Chartres, R. Ellis, Dr. C. C. Tong, Prof. Dr. P. A. Tasker

School of Chemistry

University of Edinburgh

West Main Road, Edinburgh, EH9 3JJ (UK)

Fax: (+44) 131-650-6453

E-mail: P.Tasker@ed.ac.uk

[**] We thank the EPSRC, the Chemistry Innovation Programme, and the National Research Foundation of South Africa for funding, and the EPSRC National Mass Spectrometry Service at the University of Wales, Swansea (UK) for mass spectra. M.S. gratefully acknowledges receipt of a Royal Society Wolfson Merit Award and of a Royal Society Leverhulme Trust Senior Research Fellowship.

Supporting information for this article is available on the WWW under <http://www.angewandte.org> or from the author.

receptors. Significantly, the simple trialkylamine reagents of the Alamine type [Eq. (1)] are known to exhibit poor selectivity for $[\text{PtCl}_6]^{2-}$ over Cl^- (see below), particularly at high acid concentrations.^[10] In this work we have used trioctylamine (TOA) as a model for the Alamines^[10,11] to benchmark against our new reagents.

A range of amide and urea tripodal ligands L^{1-10} derived from tris(2-aminoethyl)amine (tren) were prepared and characterized (Scheme 1; see also the Supporting Information). Ligand L^1 was designed with a long spacer between the protonatable amine bridgehead and the neutral hydrogen-bond donors to allow these to address three faces of the $[\text{PtCl}_6]^{2-}$ octahedron (Figure 2). The urea ligands L^{2-5} and L^{10} and amide ligands L^{6-9} were synthesized to access potential tri- and bifurcating hydrogen-bonding to the $[\text{PtCl}_6]^{2-}$ ion (Figure 2).

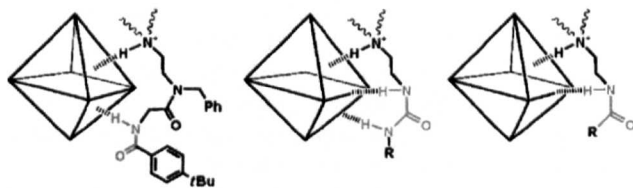


Figure 2. Binding modes of the arms of tren-based urea and amide receptors that preserve pseudo threefold symmetry (only one arm is shown for clarity).

Equilibration to form the outer-sphere complexes $(\text{LH}_2\text{PtCl}_6)$ [Eq. (2)] was achieved within minutes of mixing $\text{H}_2[\text{PtCl}_6]$ in aqueous 0.6 M HCl with a solution of L in CHCl_3 at room temperature. Prolonged mixing (> 16 h) led to a slight drop in the content of platinum in the CHCl_3 layer, and this observation is attributed to inner-sphere substitution processes to form insoluble complexes. Quantitative back-

extraction of $[\text{PtCl}_6]^{2-}$ from the organic layer into an aqueous solution was achieved by contacting the loaded CHCl_3 layer with an aqueous solution containing a twofold excess of NaOH over ligand [Eq. (3)]. Results for the extraction of $[\text{PtCl}_6]^{2-}$ by the receptors are summarized in Figure 3 along with data for TOA for comparison. Ligands L^2 and L^6 afforded metal complex salts that precipitated out of solution and are therefore not discussed.

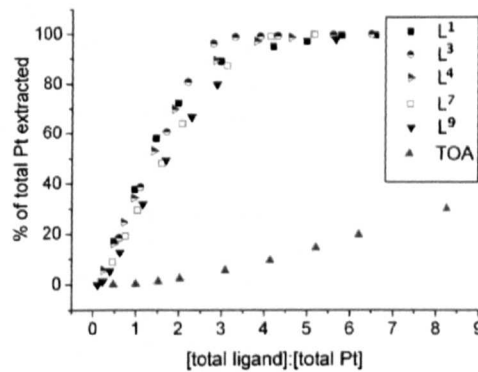
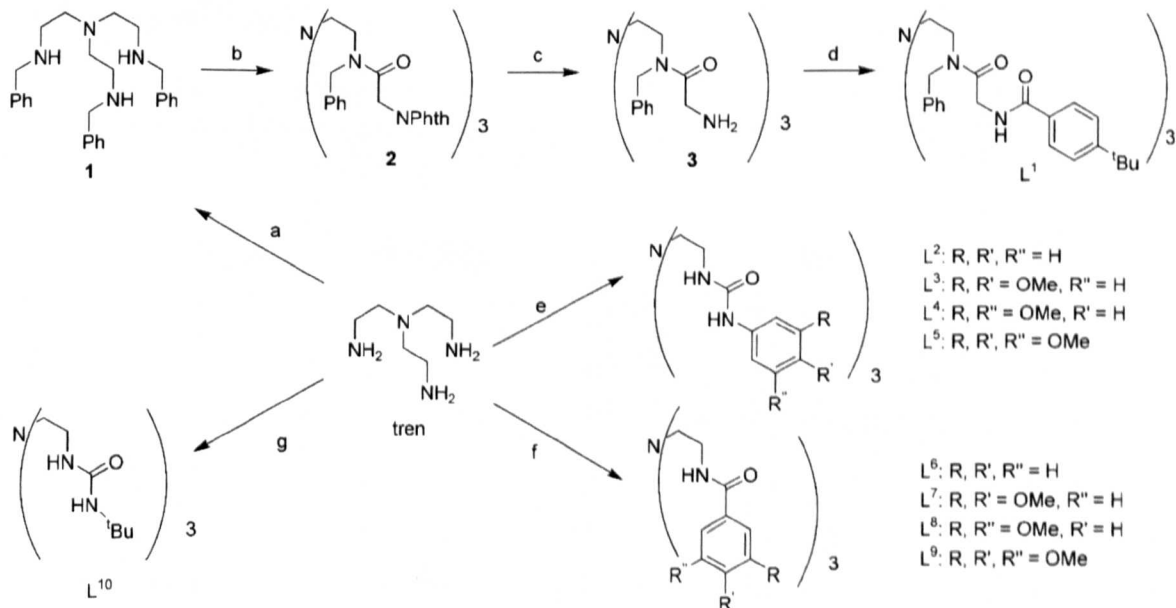


Figure 3. Plot of percentage of the total platinum extracted as $[\text{PtCl}_6]^{2-}$ from aqueous 0.6 M HCl into CHCl_3 as a function of the [L]:[Pt] ratio.

TOA is not an effective extractant at high concentrations of HCl. Although platinum uptake by a threefold excess of TOA from an aqueous solution of $\text{H}_2[\text{PtCl}_6]$ with no added HCl is around 80% of the theoretical value, it drops to around only 20% when the aqueous feed solution contains 0.6 M HCl, suggesting strong transfer of Cl^- instead of $[\text{PtCl}_6]^{2-}$ under these conditions (see the Supporting Information). As a consequence, the transport efficiency of platinum from acidic feeds in a flow sheet will be low using TOA, and chloride concentrations will build up downstream. Significantly, the



Scheme 1. Synthesis of the receptors L^1-L^{10} : a) benzaldehyde, MeOH, RT then NaBH_4 ,^[12] b) 2-phthalimidoacetyl chloride, Et_3N , CHCl_3 , 0°C then RT; c) $\text{NH}_2\text{NH}_2 \cdot \text{H}_2\text{O}$, EtOH , CHCl_3 , reflux; d) *tert*-butylbenzoyl chloride, Et_3N , CHCl_3 , 0°C then RT; e) phenyl, 3,4-dimethoxyphenyl, 3,5-dimethoxyphenyl, or 3,4,5-trimethoxyphenyl isocyanate, THF, RT;^[13] f) benzoyl, 3,4-dimethoxybenzoyl, 3,5-dimethoxybenzoyl, or 3,4,5-trimethoxybenzoyl chloride, NaOH , H_2O , CH_2Cl_2 , or Et_2O , RT;^[14,15] g) *tert*-butyl isocyanate, THF, RT. Full details of preparations are given in the Supporting Information.

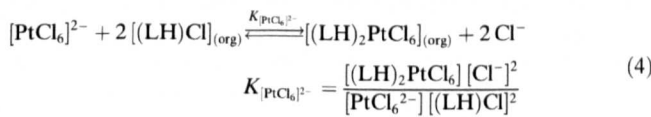
tripodal hydrogen-bond donor ligands described herein are much more effective than the Alamine model TOA^[10] in recovering $[\text{PtCl}_6]^{2-}$ in the presence of excess HCl (Figure 3 and Table 1). We note that L^3 is especially effective in this system. Loadings of greater than 90% imply that the

Table 1: Percentage of Pt extracted as $[\text{PtCl}_6]^{2-}$ into CHCl_3 from aqueous 0.6 M HCl in the presence of 3 molar excess of L.

Ligand	TOA	L^1	L^3	L^4	L^7	L^9
% Pt extracted	5	89	98	90	85	80

triamide/urea ligands show high selectivity for $[\text{PtCl}_6]^{2-}$ over Cl^- because the latter is present in a 60-fold excess in the aqueous feed solution. Generally, extractant strengths are observed to be greater for the urea-containing ligands than their amido analogues (Table 1).

We used a procedure similar to that described by Yoshizawa and co-workers^[11] to determine the stoichiometry of the platinum-containing complex formed in the water-immiscible phase and to probe further the selectivity of $[\text{PtCl}_6]^{2-}$ over Cl^- . At low pH values, where it can be assumed that the ligand is fully protonated, the extraction of $[\text{PtCl}_6]^{2-}$ is a competitive process, as shown by Equation (4).



Assuming no inner-sphere substitution on the timescale of the extraction, the distribution coefficient for platinum is $D_{\text{Pt}} = [(\text{LH})_2\text{PtCl}_6]/[\text{PtCl}_6^{2-}]$, and from Equation (4), $\log D_{\text{Pt}}$ has values defined by Equation (5).

$$\log D_{\text{Pt}} = \log K_{[\text{PtCl}_6]^{2-}} + 2 \log \left[\frac{[(\text{LH})\text{Cl}]}{[\text{Cl}^-]} \right] \quad (5)$$

Plots of $\log D_{\text{Pt}}$ versus $\log \{[(\text{LH})\text{Cl}]/[\text{Cl}^-]\}$ (Figure 4) for TOA, L^1 , and L^4 show slopes close to 2, which is in line with formation of the anticipated 2:1 $[\text{LH}]^+:[\text{PtCl}_6]^{2-}$ assemblies in

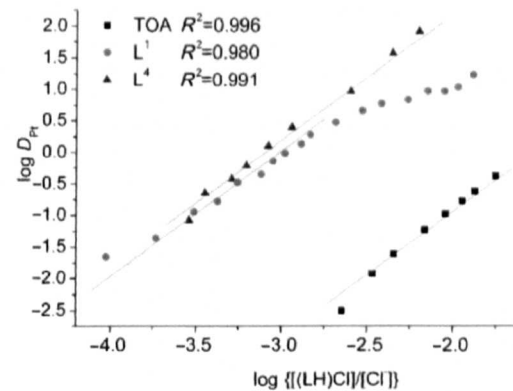


Figure 4: Plot of $\log D_{\text{Pt}}$ vs. $\log \{[(\text{LH})\text{Cl}]/[\text{Cl}^-]\}$.

CHCl_3 . Whilst the data for these ligands are consistent with the formation of $[(\text{LH})_2\text{PtCl}_6]$ complexes as the extracted species, for other ligands, L^3 , L^5 , L^7 , and L^9 in this work, and for TOA at high ligand concentrations,^[11] the Yoshizawa plots show some deviation from linearity (see the Supporting Information). Such deviations may be due to the formation of outer-sphere complexes with alternative stoichiometries such as 3:1:1 $[\text{LH}]^+:[\text{PtCl}_6]^{2-}:\text{Cl}^-$ at high ligand concentrations or may involve the incorporation of a hydroxonium ion into the outer-sphere complex giving a 1:1:1 assembly $[\text{LH}]^+:\text{H}_3\text{O}^+:[\text{PtCl}_6]^{2-}$, which would be favored at low ligand concentrations. Alternatively, the receptors, their hydrochloride salts, and/or their platinum complexes with some solubility in the aqueous phase cannot be discounted at this stage. These caveats notwithstanding, the triamide/urea ligands L^1 and L^4 show very high selectivity for $[\text{PtCl}_6]^{2-}$ over Cl^- , the latter being present in a 60-fold excess.

The formation of a 2:1 $[\text{LH}]^+:[\text{PtCl}_6]^{2-}$ package in organic media was supported further by a single-crystal X-ray structure determination of $[(\text{L}^{10}\text{H})_2\text{PtCl}_6]$.^[16] The structure determination confirms the presence of significant hydrogen-bonding between the urea moieties of $[\text{L}^{10}\text{H}]^+$ and the $[\text{PtCl}_6]^{2-}$ ion, and, as anticipated, the bridgehead N atom in L^{10} is protonated to afford a complex with a net neutral charge (Figure 5). A bifurcated hydrogen bond is observed between

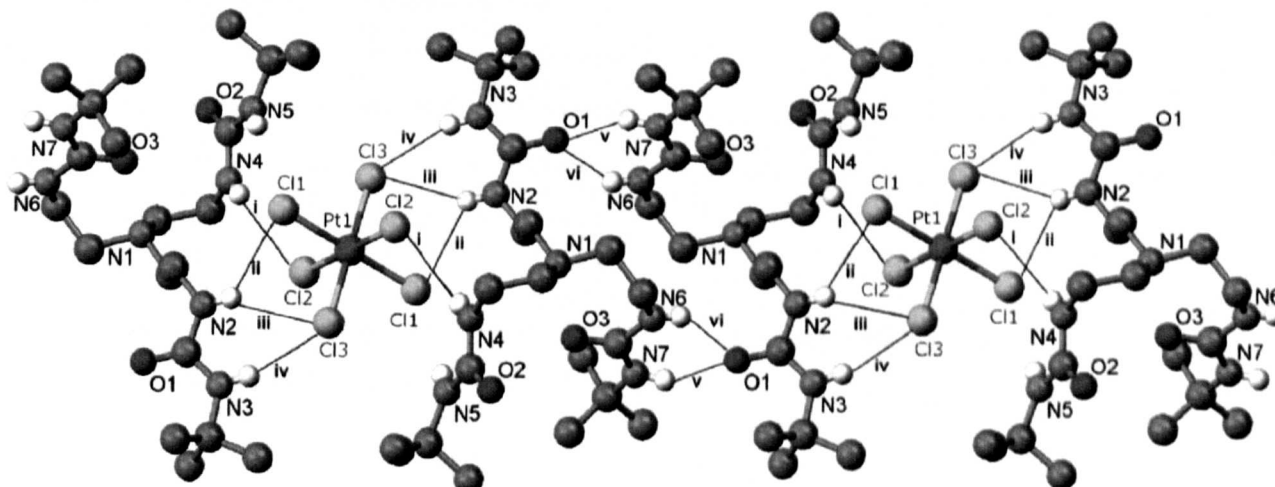


Figure 5: View of the structure of $[(\text{L}^{10}\text{H})_2\text{PtCl}_6]$. Hydrogen-bond lengths: i) 2.791, ii) 2.799, iii) 2.805, iv) 2.664, v) 2.180, vi) 2.096 Å.

N2–H2A···Cl1 [2.799 Å] and N2–H2A···Cl3 [2.805 Å] with further hydrogen-bond interactions between N3–H3A···Cl3 [2.664 Å] and N4–H4A···Cl2 [2.791 Å]. Although there are extensive hydrogen-bonding interactions between $[L^{10}H]^+$ and $[PtCl_6]^{2-}$, only two of the three arms of the receptor interact with one $[PtCl_6]^{2-}$ ion; the third arm participates in hydrogen-bonding with an adjacent molecule of $[L^{10}H]^+$ to form an extended ribbon structure (Figure 5). This ribbon structure accounts for the low solubility of this complex in chloroform, which excluded this ligand from the extraction experiments. Although the results for the solid-state structure cannot be translated directly to the structure in solution, they do confirm the success of our strategy and illustrate many of the design features that we sought in addressing the molecular recognition and selectivity of hexachlorometallate anions through coordination at the outer sphere.

Significantly, the efficacy of our tripodal amide and urea ligands in a “pH-swing” controlled process to recover platinum from acid chloride feed solutions has been established. The very high $[PtCl_6]^{2-}$ loading from acidic chloride solutions for the new receptors reported herein, coupled with the quantitative stripping and release of metallate anion by base, provides the basis for a very efficient process for the separation and concentration of platinum with minimal reagent consumption (2 equivalents of NaOH) and generation of 2 mol equivalents of NaCl as a by-product. Variation of the disposition and nature of hydrogen-bonding groups in the pendant arms of the reagents should allow the selectivity of receptors to be tuned to accomplish the separation of chlorometallates having second coordination spheres with different geometries (e.g., $[PtCl_6]^{2-}$ and $[PdCl_4]^{2-}$), sizes (e.g., $[PdCl_4]^{2-}$ and $[PtCl_4]^{2-}$), or net charges (e.g., $[PtCl_6]^{2-}$ and $[IrCl_6]^{3-}$).

Received: July 21, 2007

Revised: November 21, 2007

Published online: January 22, 2008

Keywords: anions · ionophores · metal extraction · metal transport · platinum

- [1] F. Bernardis, R. A. Grant, D. C. Sherrington, *React. Funct. Polym.* **2005**, *65*, 205–217, and references therein.
- [2] P. A. Tasker, P. G. Plieger, L. C. West in *Comprehensive Coordination Chemistry II*, Vol. 9 (Eds.: J. A. McCleverty, T. J. Meyer), Elsevier Ltd., Oxford, **2004**, pp. 759–808, and references therein.
- [3] S. G. Galbraith, Q. Wang, L. Li, P. G. Plieger, A. J. Blake, C. Wilson, S. R. Collinson, L. F. Lindoy, M. Schröder, P. A. Tasker, *Chem. Eur. J.* **2007**, *13*, 6091–6107, and references therein; S. G. Galbraith, L. F. Lindoy, P. A. Tasker, P. G. Plieger, *Dalton Trans.* **2006**, 1134–1136, and references therein.
- [4] B. K. O. Leung, M. J. Hudson, *Solvent Extr. Ion Exch.* **1992**, *10*, 173–190; E. Benguerel, G. P. Demopoulos, G. B. Harris, *Hydrometallurgy* **1996**, *40*, 135–152.
- [5] M. J. Deetz, M. Shang, B. D. Smith, *J. Am. Chem. Soc.* **2000**, *122*, 6201–6207; P. D. Beer, P. A. Gale, *Angew. Chem.* **2001**, *113*,

502–532; *Angew. Chem. Int. Ed.* **2001**, *40*, 486–516; K. Choi, A. D. Hamilton, *Coord. Chem. Rev.* **2003**, *240*, 101–110; P. A. Gale, *Coord. Chem. Rev.* **2003**, *240*, 191; F. P. Schmidtchen, *Coord. Chem. Rev.* **2006**, *250*, 2918–2928; K. Wichmann, B. Antonioli, T. Söhnle, M. Wenzel, K. Gloe, K. Gloe, J. R. Price, L. F. Lindoy, A. J. Blake, M. Schröder, *Coord. Chem. Rev.* **2006**, *250*, 2987–3003; R. Custelcean, L. H. Delmau, B. A. Moyer, J. L. Sessler, W.-S. Cho, D. Gross, G. W. Bates, S. J. Brooks, M. E. Light, P. A. Gale, *Angew. Chem.* **2005**, *117*, 2593–2598; *Angew. Chem. Int. Ed.* **2005**, *44*, 2537–2542; J. L. Sessler, P. A. Gale, W. S. Cho, *Anion Receptor Chemistry*, Royal Society of Chemistry, Cambridge UK, **2006**.

- [6] K. Gloe, H. Stephan, M. Grotjahn, *Chem. Eng. Technol.* **2003**, *26*, 1107–1117; B. A. Moyer, P. V. Bonnesen, R. Custelcean, L. H. Delmau, B. P. Hay, *Kem. Ind.* **2005**, *54*, 65–87; P. A. Tasker, C. C. Tong, A. N. Westra, *Coord. Chem. Rev.* **2007**, *251*, 1868–1877.
- [7] K. J. Naidoo, A. S. Lopis, A. N. Westra, D. J. Robinson, K. R. Koch, *J. Am. Chem. Soc.* **2003**, *125*, 13330–13331.
- [8] L. Brammer, J. K. Swearingen, E. A. Bruton, *Proc. Natl. Acad. Sci. USA* **2002**, *99*, 4956–4961.
- [9] L. Brammer, E. A. Bruton, P. Sherwood, *Cryst. Growth Des.* **2001**, *1*, 277–290; see also: J. C. Mareque Rivas, L. Brammer, *Inorg. Chem.* **1998**, *37*, 4756–4757; B. Dolling, A. G. Orpen, J. Starbuck, X.-M. Wang, *Chem. Commun.* **2001**, 567–568; M. Felloni, P. Hubberstey, C. Wilson, M. Schröder, *CrystEngComm* **2004**, *6*, 87–95.
- [10] The compositions of Alamines are proprietary but are thought to be mixtures of octyl and decyl tertiary amines.^[2]
- [11] H. Yoshizawa, K. Shiomori, S. Yamada, Y. Baba, Y. Kawano, K. Kondo, I. Kazuo, K. Ijichi, Y. Hatake, *Solvent Extr. Res. Dev. Jpn.* **1997**, *4*, 157–166.
- [12] A. A. Naiini, W. M. P. B. Menge, J. G. Verkade, *Inorg. Chem.* **1991**, *30*, 5009–5012; Md. A. Hossain, J. A. Liljegegren, D. Powell, K. Bowman-James, *Inorg. Chem.* **2004**, *43*, 3751–3755.
- [13] C. Raposo, M. Almaraz, M. Martín, V. Weinrich, L. Mussóns, V. Alcázar, C. Caballero, J. R. Morán, *Chem. Lett.* **1995**, 759–760.
- [14] S. Valiyaveettil, J. F. J. Engbersen, W. Verboom, D. N. Reinhoudt, *Angew. Chem.* **1993**, *105*, 942–944; *Angew. Chem. Int. Ed. Engl.* **1993**, *32*, 900–901.
- [15] P. D. Beer, P. Hopkins, J. D. McKinney, *Chem. Commun.* **1999**, 1253–1254.
- [16] Crystal data for $[(L^{10}H)_2PtCl_6]$: $M_r = 1379.2$, triclinic, $a = 8.8396(5)$, $b = 13.2745(7)$, $c = 14.4379(8)$ Å, $\alpha = 93.865(2)$, $\beta = 97.368(2)$, $\gamma = 95.263(2)^\circ$, $V = 1667.7(3)$ Å³, $T = 150(2)$ K, space group $P\bar{1}$, $Z = 1$, $\rho_{\text{calcd}} = 1.373 \text{ g cm}^{-3}$, $\mu(\text{MoK}\alpha) = 2.397 \text{ mm}^{-1}$, 7540 unique reflections ($R_{\text{int}} = 0.013$) used in all calculations. Final R_1 [$7536 F \geq 4\sigma(F)$] = 0.0202 and $wR_2(\text{all } F^2)$ was 0.0536. The dataset for $[(L^{10}H)_2PtCl_6]$ was collected on a Bruker APEX CCD diffractometer. The structure was solved by direct methods using SHELXS97^[18] and refined by full-matrix least-squares on F^2 using SHELXL97.^[19] CCDC-653924 contains the supplementary crystallographic data for this paper. These data can be obtained free of charge from The Cambridge Crystallographic Data Centre via www.ccdc.cam.ac.uk/data_request/cif.
- [17] N. Ullah, C. N. Fali, I. D. Spenser, *Can. J. Chem.* **2004**, *82*, 579–582.
- [18] G. M. Sheldrick, *SHELXS97*. University of Göttingen, Göttingen, Germany, **1997**.
- [19] G. M. Sheldrick, *SHELXL97*. University of Göttingen, Göttingen, Germany, **1997**.